NASA CR-145192

STUDY OF ADVANCED COMPOSITE STRUCTURAL DESIGN CONCEPTS FOR AN ARROW WING SUPERSONIC CRUISE CONFIGURATION

Task III Final Report

Boeing Commercial Airplane Company

Preliminary Design Department

January 1978



Prepared under contract NAS1-12287

for

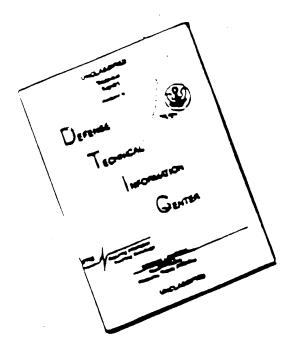
Langley Research Center
NATIONAL AERONAUTICS AND SPACE ADMINISTRATION
Hampton, Virginia 23665

DIMO QUALITY INSPECTED 1

19960228 001



DISCLAIMER NOTICE



THIS DOCUMENT IS BEST QUALITY AVAILABLE. THE COPY FURNISHED TO DTIC CONTAINED A SIGNIFICANT NUMBER OF PAGES WHICH DO NOT REPRODUCE LEGIBLY.

1 Report No. NASA CR-145192	2. Government Accession No.	3. Recipient's Catal	3. Recipient's Catalog No.								
4. Title and Subtitle STUDY OF ADVANCED CONCEPTS FOR AN ARROV TRANSPORT CONFIGURAT		5. Report Date January 6. Performing Organ D6-42438-4	ızation Code								
7. Author(s)		8. Performing Organ									
Preliminary Design Departmen	t	10. Work Unit No.									
9. Performing Organization Name and Address Boeing Commercial Airplane C	Company										
P.O. Box 3707 Seattle, Washington 98124	1 1111	NAS1-1228	7								
12. Sponsoring Agency Name and Address National Aeronautics and Space	re Administration	13. Type of Report at Task III Fin									
Langley Research Center Hampton, Virginia 23665	14. Sponsoring Agenc	 									
15. Supplementary Notes Contract Monitors: James C. I NASA Langley Research Center	Robinson and E. Carson Yates, Jr er, Hampton, Virginia	•									
NASA Langley Research Center, Hampton, Virginia 16. Abstract A structural design study was conducted to assess the relative merits of structural concepts using advanced composite materials for an advanced supersonic aircraft cruising at Mach 2.7. The configuration and structural arrangement developed during Task I and II of the study, previously reported in NASA CR-132576, was used as the baseline configuration. Allowable stresses and strains were established for boron and advanced graphite fibers based on projected fiber properties available in the next decade. Structural concepts were designed and analyzed using graphite polyimide and boron polyimide, applied to stiffened panels and conventional sandwich panels. The conventional sandwich panels were selected as the structural concept to be used on the wing structure. The upper and lower surface panels of the Task I arrow wing were redesigned using high-strength graphite polyimide sandwich panels over the titanium spars and ribs. The ATLAS computer system was used as the basis for stress analysis and resizing the surface panels using the loads from the Task II study, without adjustment for change in aeroelastic deformation. The flutter analysis indicated a decrease in the flutter speed compared to the baseline titanium wing design. The flutter speed was increased to that of the titanium wing, with a weight penalty less than that of the metallic airplane.											
17. Key Words (Suggested by Author(s)) Arrow Wing, Supersonic Cruise SCAR Technology NASA SCAT 15-F Advanced Composites		18. Distribution Statement Unclassified - Unlimited									
19. Security Classif. (of this report) Unclassified	20. Security Classif. (of this page) Unclassified	21. No. of Pages 383	22. Price*								

CONTENTS

	Fage
	INTRODUCTION
1	MATERIAL PROPERTIES
2	ALLOWABLES
3	CONCEPT DESIGN AND MATERIAL SELECTION
4	PANEL DESIGN
5	THEORETICAL-TO-ACTUAL MASS FACTORS
6	COMPOSITE ANALYSIS AND DESIGN
7	REVISION OF MATHEMATICAL MODEL
8	FLUTTER ANALYSIS
9	FINAL WEIGHT ANALYSIS
10	AERODYNAMIC HEATING ANALYSIS

INTRODUCTION

This document presents a detailed account of Task III of a study conducted by the Boeing Commercial Airplane Company as a part of the NASA Supersonic Cruise Aircraft Research program. The principal overall objectives of the study were to assess the relative merits of various concepts and materials suitable for an advanced supersonic aircraft cruising at Mach 2.7, to select the structural approaches best suited for the Mach 2.7 environment, and to provide construction details and structural mass estimates based on in-depth structural design studies of representative wing and fuselage structures. Earlier work in Tasks I and II of this study comprised the following activities: (1) detailed analysis and refinement of the aircraft configuration; (2) evaluation of alternate structural arrangements and selection of an arrangement for detailed analysis and design studies; (3) evaluation and selection of materials and concepts representative of a 1975 technology level; (4) detailed structural analysis and design and structural mass analysis utilizing the 1975 materials and concepts. In Task III the detailed structural analysis and the design and mass analysis have been repeated with advanced concepts and materials that are expected to be available in the 1986 time period.

The airplane configuration on which the structural analysis was conducted is an arrow-wing concept representative of a 1975 technology level. It was derived from a configuration presented by NASA (see reference I-1), and is similar to the Model 969-336C that was studied during the National SST Program (ref. I-2). A detailed multidisciplinary analysis of the configuration was conducted during Task I of the study, and further modifications and refinements were introduced. The resulting configuration, designated as Model 969-512B is shown in figure -1. Geometric data and other characteristics are listed in table -1. The wing structure that was selected for detailed analysis and design in Task II consisted of a multispar internal structure with aluminum brazed titanium sandwich panels for the wing surfaces, except for a machined skin concept on the lower surface of the main wing box. The fuselage structure consisted of skin stringer construction. Ti-6Al-4V alloy was used as the primary structural material throughout.

A single basic finite element model of the structure was developed for aeroelastic loads, stress and flutter analyses, containing approximately 2000 nodes, 4200 elements and 8500 active degrees of freedom. Analyses were performed by an integrated structural analysis and design system interfaced with loads and flutter analysis systems. The elements in the wing covers were resized using an automated resizing module in the integrated system, with convergence, measured in terms of total mass change, occurring in three cycles. Nine flutter analyses were conducted to evaluate a series of stiffness changes to remedy a flutter deficiency in the strength design. Stiffness changes were based on engineering judgment and experience from the National SST Program.

The resulting configuration has a maximum taxi gross mass of 340 200 kg (750 000 lbm) and a payload of 22 200 kg (49 000 lbm), representing 234 passengers in tourist accommodations, and a cruise Mach number of 2.7. The structure, stability and control characteristics, and systems meet the appropriate requirements of Federal Aviation Regulations, Part 25, and the Tentative Airworthiness Requirements for Supersonic Transports.

A detailed account of the work performed in Tasks I and II is presented in reference I-1; for a more condensed summary see reference I-3.

The configuration and structural arrangement developed for the titanium structure were used without modification in the subsequent investigation discussed in this report. Allowable stresses and strains, based on estimated fiber properties to be available in the next decade, were established for advanced composite materials using boron and graphite fibers. Stiffened panel and conventional sandwich panel concepts were designed and analyzed, using graphite/polyimide and boron/polyimide materials, and the conventional sandwich panel was selected as the structural concept to be used in the modified wing structure.

Upper and lower surface panels of the arrow wing structure were then redesigned, using high strength graphite/polyimide sandwich panels, retaining the titanium spars and ribs that had been designed in the prior study. The ATLAS integrated analysis and design system was used for stress analysis and automated resizing of surface panels, using the design loads that were developed in the prior study of the metallic structure.

For the present study properties of candidate advance composite materials were estimated for a 1986 time period, based on assumptions regarding development work to be accomplished in the intervening time period. Estimated material properties were then used in structural concept design studies, and in concept and material evaluation and selection. Following material and concept selection, a finite element model of the complete structure was defined retaining the structural arrangement and finite element geometry from the prior study of the metallic structure.

Since supersonic cruise aircraft tend to be large and flexible, aeroelasticity is a major design consideration, and realistic aeroelastic considerations based on analysis of finite element structural models and sophisticated aerodynamic loading analysis are required, even in a preliminary design study of such a vehicle. Strong interaction of the various technical disciplines in aeroelastic analysis requires the use of computer-aided design methods to organize and expedite the aeroelastic and structural resizing cycle. Computer-aided design methods are also required to handle the large number of material parameters that must be accommodated in designing a composite structure.

Flutter analysis of the hybrid structure showed a significant decrease in flutter speed relative to the baseline strength designed titanium wing structure. The flutter speed was increased to that of the final titanium design by selective increase in thickness of wing panel laminates and by substituting a graphite/polyimide material with properties intermediate between high strength and high modulus materials. The final mass of the hybrid wing structure was significantly less than that of the titanium wing with equal flutter speed.

The following sections of the report present a detailed account of design and analytical work, resizing of the wing shell to satisfy strength and flutter criteria, and evaluation of the reduction in structural wing mass relative to the all titanium wing. Recommendations are also presented relating to further research and development work that will be needed to achieve the anticipated benefits from application of advanced composite materials in primary structure of large supersonic cruise aircraft.

Table I.—Configuration Characterististics, Model 969-512B

Geometry	-		Wing	Wing vert. stabilizer	Vertical stabilizer	Horizontal stabilizer
Area	m ²	(sq ft)	915 (9,848)*	26.7 (287)/side	41.7 (449)	55.7 (600) exposed
Aspect ratio,	AR		1.78	0.493	0.848	1.32
Taper ratio,	λ			0.135	0.24	0.247
Sweep at LE	Rad	(deg)	1.29/1.23/1.05 (74/70.5/60)	1.30 (74.5)	0.89 (51)	.94 54
Incidence	Rad	(deg)	_	_	_	-0.26/0.52 + 0.26/0.44 (-15/30 + 15/25)
Dihedral	Rad	(deg)	_	_	_	0
Root t/c	%		_	3	3	3
Tip t/c	%		_	3	3	3
Root chord	m	(in.)	47.8 (1881.1)	13.0 (510)	11.30 (445)	10.52 (414)
Tip chord	m	(in.)	5.18 (204	1.75 (69)	2.72 (107)	2.59 (102)
MAC	m	(in.)	30.1 (1187)	8.79 (346)	7.90 (311)	7.34 (289)
Span	m	(in.)	40.4 (1590)	3.63 (143)	-	8.59 (338)
Tail arm	m	(in.)	_	17.70 (697)	24.82 (977)	26.97 (1062)
Tail vol coeff,	v		_	0.013	0.028	0.0545

^{*} Reference area. Total wing area ABCDEFGH = 1045 m² (11 244 sq ft)

Gross mass: 340 200 kg (750 000 lbm)

	Length, m (in.)	Max dia, m (in.)	Accommodation					
Body	92.4 (3640)	3.87 (152.2)	234 pass.	4/5 AB				
	Number	Type	Airflow	Inlet				
Powerplants	4	ATAT-1	287 kg/sec (633 lbm/sec)	Axisym				
	Nose	Main	Loc % MAC					
Landing gear wheels	2-86 x 41 cm (34 x 16 in.)	24-103 x 36 cm (40.7 x 14 in.)	57.7 (pivot)					
	Wing	Body	Total					
Fuel capacity, kg (lbm)	143 970 (317 400)	32 660 (72 000)	176 450 (389 000)					
cg limits	Takeoff	Cruise	Landing					
Fwd			49.7					
% MAC Aft		55.5	53.0					

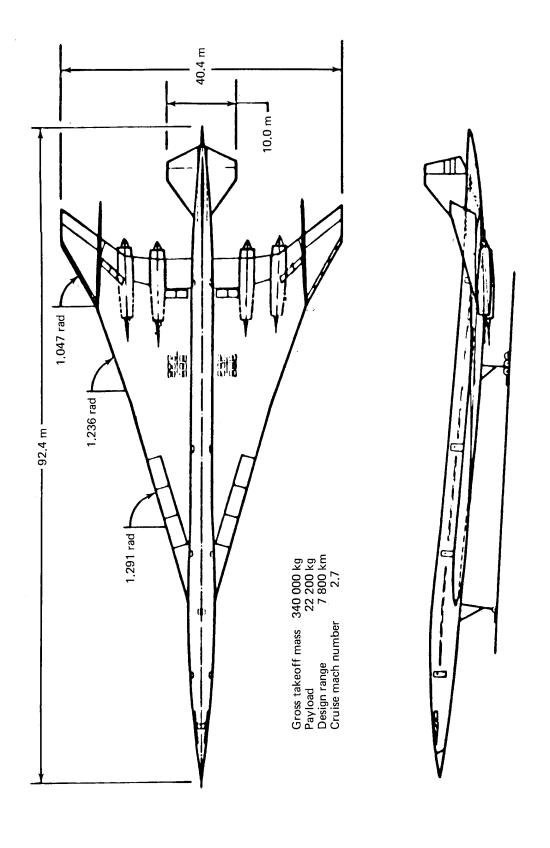


Figure I.—Configuration for Structural Analysis, Model 969-512B

REFERENCES

- I-1 Boeing Staff: Study of Structural Design Concepts for an Arrow Wing Supersonic Transport Configuration. NASA CR 132576-1 and -2, 1976.
- I-2 Boeing Staff: Mach 2.7 Fixed Wing SST Model 969-336C (SCAT 15F). D6A11666-1, The Boeing Company, 1969.
- I-3 Turner, M. J.; and Grande, D. L.: Study of Metallic Structural Design Concepts for an Arrow Wing Supersonic Cruise Configuration. NASA CR-2743, 1976.

SECTION 1

MATERIAL PROPERTIES

by

C. L. HENDRICKS

CONTENTS

P	Page
INTRODUCTION	6
LITERATURE SEARCH	6
975 COMPOSITE PROPERTIES	8
986 COMPOSITE PROPERTIES	10
RECOMMENDED IMPROVEMENTS IN DATA BASE	1.1
REFERENCES	13

TABLES

No.		Page
1-1	Basic Graphite/Polyimide Laminate Unidirectional [0] Properties	14
1-2	Basic Graphite/Polyimide Unidirectional Laminate [90] Properties	15
1-3	Basic Graphite/Polyimide Laminate [±45] Properties	
1-4	Normalized Graphite/Polyimide Laminate [0] Properties Normalized to	
	60% Fiber Volume	17
1-5	Normalized Graphite/Polyimide Laminate [90] Properties Normalized to	
	60% Fiber Volume	18
1-6	Normalized Graphite/Polyimide Laminate [±45] _S Properties Normalized	
	to 60% Fiber Volume	19
1-7	"B" Allowables, Graphite/Polyimide Laminate Normalized to 60% Fiber	
	Volume, 1975	20
1-8	"B" Allowables, Graphite/Polyimide Laminate Normalized to 60% Fiber	
	Volume, 1986	21
1-9	"B" Allowables, Boron/Polyimide Laminate Normalized to 50% Fiber Volume, 1986	22

FIGURES

No.		Page
1-1	Temperature Dependence of Material Properties for Advanced Composite	
	Wing Cover Panels	 23
1-2	Strength and Moduli of Various Materials	

SYMBOLS

 $\begin{array}{ll} E_c & \mbox{Modulus of elasticity in compression} \\ E_t & \mbox{Modulus of elasticity in tension} \\ F_{cu} & \mbox{Ultimate compressive stress} \\ F_{tu} & \mbox{Ultimate tensile stress} \\ RT & \mbox{Room temperature} \\ H/M & \mbox{High modulus} \\ H/S & \mbox{High strength} \end{array}$

INTRODUCTION

The incorporation of high-strength low density fibers into a compatible matrix presents a composite material that offers the potential for a major breakthrough in airframe design. The most common composite materials that have been studied and put into limited use are boron-epoxy and graphite-epoxy. These materials are limited to a maximum service temperature of 450K (350°F) continuous and 489K (420°F) for intermittent service. For higher temperatures than that, the matrix material must be either metallic such as aluminum, or a high temperature organic material such as polyimide (PI). Either of these materials is suitable for operation at Mach 2.7 involving temperatures of 559K (490°F).

Figure 1-1 presents a comparison of the ultimate tension stress of several composite laminates with titanium for temperatures up to 506K (450°F). Figure 1-2 compares the ultimate tension stress and the Young's modulus of representative metals and composite materials.

The use of advanced composites on a supersonic cruise aircraft assumes that the earliest flight of the airplane will be about 1990, and the engineering freeze on the design will be about four years preceding that time; thus, 1986 is the year in which the engineering properties for the composite material would have to be known to be of use on such a program. This date is also consistent from the standpoint that it will require about that amount of time to develop the material systems and the necessary manufacturing techniques and mechanical properties to utilize the material.

The objective of this subtask is to project the allowables for the advanced composite materials to values that would be available in 1986 for application to the structure of a supersonic aircraft. In selecting the fibers to be considered, it has been noted that both the boron and graphite fibers are currently available and under development. The graphite technology seems to be advancing much more rapidly than the boron technology, however, as reflected in the reduction in price and increase in production volume. The dramatic increase in the use of the graphite fibers seems to be associated with athletic equipment such as golf club shafts, bows, tennis rachets and the like. Boron, on the other hand, does not seem to be enjoying this popularity in the common market, and thus has not attained that level of funding in research and development. Because of this, major emphasis was placed on graphite/polyimide properties. Boron/polyimide data were also compiled. Boron/aluminum data acquisition effort was limited since a significant amount of work on this material was already completed in Task II.

The steps used to obtain projected composite properties included research of past and current program efforts, compilation of applicable data, estimation of 1975 allowables and projection of estimated 1986 allowables.

LITERATURE SEARCH

A literature search was conducted to determine the state-of-development of high temperature stable advanced composites. The state-of-the-art to date provides limited design data for composites exposed to long time simulated arrow wing service environment. The level and objectives of current programs and future efforts may provide this vital information.

The data base for estimation of composite mechanical properties is taken from the following sources:

• Development of Design Data for Graphite Reinforced Epoxy and Polyimide Composites.

This report, reference 1-1, presents basic design data for HM-S and HT-S/polyimide composites at room temperature and 588K (600°F).

• Time-Temperature-Stress Capabilities of Composite Materials for Advanced Supersonic Technology Applications.

This report, reference 1-2, presents work currently being conducted to determine the effects of supersonic airplane environments upon composite properties. Composite exposure time to 1000 hours at 506K (450°F) has been reached. Limited design data was taken from this work.

• Develop Fabrication/Processing Techniques for High Temperature Advanced Composites for Use in Aircraft Structures.

The composite design data in this report, reference 1-3, were the most complete of the various applicable sources. A comparison of coupon and sandwich beam test properties contained in this report provided a correlation for other programs which conducted only coupon tests. Elevated temperature tests were performed at 560K (550°F).

• Development and Fabrication of a Graphite/Polyimide Box Beam.

The data from this program were compiled in reference 1-4 with that derived from other sources. It evaluated and used Gemon polyimide matrix.

Resin/Graphite Fiber Composites.

This report, reference 1-5, was used to illustrate the kind of research in polyimide resins that could produce high quality, thermally stable composite systems applicable to supersonic transport primary structure.

• Effects of Thermal and Environmental Exposure on the Mechanical Properties of Graphite/Polyimide Composites.

This report, reference 1-6, contains long-time elevated-temperature exposure data on graphite/polyimide composites which indicates some degradation at service temperatures. However, the resin matrix used in the tested composites is not one of the more thermally stable polyimide systems. A major part of the data is presented as interlaminar shear not directly translated to other design properties.

• Effect of 450°F and 600°F Exposures on the Mechanical Properties of Polyimide/Glass-Fiber Honeycomb Sandwiches and Laminated Beams.

This report, reference 1-7, contains data on long-time elevated-temperature exposure of glass/polyimide structure. Data to 4000 hours at 506K (450°F) with reduced pressure (simulating flight altitude) shows no significant degradation of mechanical properties. This data was used for rationale to assume that polyimide composites are subject to only minor degradation at 506K (450°F) when combined with reduced atmospheric pressure and covered with a protective or decorative coating.

• Elevated Temperature Laminates.

The data in this report, reference 1-8, includes exposure of glass/polyimide laminates to elevated temperatures for up to 30 000 hours. Degradation of mechanical properties at 506K (450°F) had stabilized at 2-3000 hours even when exposed to continuous atmospheric pressure and no protection. Aging at this temperature was discontinued at 5000 hours. Test results after exposure to 477K (400°F) indicated no significant degradation between 10 000 and 30 000 hours.

 Development of Engineering Data on the Mechanical and Physical Properties of Advanced Composite Materials.

The data in this report, reference 1-9, covered boron/aluminum, AVCO 5505 boron/epoxy, and graphite/epoxy composites. It was used as a base of comparison from epoxy to polyimide composites design data.

• Crack Propagation in Fiber Reinforced Plastic Composites. Fundamental Aspects of Fiber Reinforced Plastic Composites.

This report, reference 1-10, was used to illustrate the kind of resin modification which can be successful in elimination of micro cracking in tension stressed advanced composite systems.

1975 COMPOSITE PROPERTIES

The data published in the reports listed previously are organized and compiled according to the test laminate orientations [0], [90], and [±45] (tables 1-1, 1-2, and 1-3). Much of the data was subject to variables such as sandwich beam versus coupon test methods, differences in composite fiber fractions, resin systems, test temperatures and exposure times.

Each mechanical property value was normalized to represent a 60% fiber volume for graphite and a 50% fiber volume for boron. These normalized test values were determined by multiplying the graphite test values by the ratio:

60 volume percent fiber fiber volume percent of specimen

and by multiplying the boron composite test values by the ratio:

50 volume percent fiber fiber volume percent of specimen

The normalized test coupon values were subsequently factored to sandwich beam values. These factors (from ref. 1-3) are listed below:

Lam	inated Orientation	Factor
[0]	Tension, Strength Modulus	1.21 NF*
[0]	Compression, Strength Modulus	1.74 NF
[90]	Tension, Strength Modulus	3.90 2.0
[90]	Compression, Strength Modulus	NF NF

^{*}NF = not factored

The [±45] laminate tension and compression properties were assumed equal to values for epoxy as published in the Air Force Advanced Composites Design Guide because the polyimide data generated in the various reports were inferior to that for epoxy. This was done on the assumption that a good quality dense polyimide matrix composite should perform at least as well as a good quality epoxy matrix composite.

Normalized and factored numbers (tables 1-4, 1-5, and 1-6) were averaged and used to derive the 1975 "B" allowables for graphite/polyimide allowables (table 1-7). It should be noted that the data in reference 1-5 contained significantly lower values when compared to the other data sources and was not included when computing the average value.

The allowables were calculated using an assumed 30 specimen population and 8% coefficient of variation which results in a K factor of 1.777. An illustration of the method of calculating "B" allowables is as follows:

"B" Allowable =
$$\overline{X}$$
 - K_BS

where
$$\overline{X} = \text{calculated average value}$$

$$K_B = \text{one-sided tolerance limit factor for normal distribution and sample size}$$

$$\text{at } P = 0.90$$

$$S = \text{standard deviation}$$

$$S = (C_V) (\overline{X})$$

$$\text{where } C_V = \text{coefficient of variation}$$

Example:

```
HT-S 0° Tension Ultimate Strength (UTS) average = 200 KSI (see table 1-4) K_B = 1.777 \ (30 \ \text{specimen population - minimum allowed for "B" allowable calculation}) C_V = 0.08 \ (\text{assumed value}) S_B = (0.08) \ (200 \ \text{KSI}) = 16 \ \text{KSI} "B" allowable = 200 KSI - (1.777) (16 KSI)
```

= 172 KSI (see table 1-7)

1986 COMPOSITE PROPERTIES

Properties of the composite materials are projected to 1986 based on assumptions on the amount of development work that will likely be accomplished in the intervening time period. These assumptions have been arrived at through conversations and communications with the manufacturers who are currently involved in research in the advanced composite field. The allowables presented in table 1-8 for graphite/polyimide are based on these assumptions and have been adjusted to represent a 60% fiber volume. The allowables in table 1-9 for the boron/polyimide are adjusted in a similar manner to represent a 50% fiber volume.

GRAPHITE/POLYIMIDE

Polyimide resins have, for the past several years, undergone development to improve processing characteristics and thermal stability. The various programs currently being funded and future work on this material can be expected to yield a moderate degree of success to achieve these objectives and result in a dense polyimide matrix capable of performance under the supersonic environmental conditions.

The manufacturers of graphite fibers are continuing to develop fibers with improved properties. They currently have in the laboratory high strength and high modulus fibers that can be expected to be available on the market by the 1986 time period. These fibers range from a high strength version having a 4136 MN/m^2 (600 ksi) strength to a high modulus version having a Young's modulus of 620 GN/m^2 (90 x 10⁶ psi).

The coefficient of variation for graphite composites, typically in the range of 12%, is expected to drop to a value no more than 8% through improved quality control in the manufacture of the fiber and the processing of the composite.

BORON/POLYIMIDE

The development of superior polyimide resin matrices for boron composites can be expected by 1986 through continuing programs as discussed previously for graphite/polyimide composites.

Research directed to improve boron filament properties have not been successful. The basic process with boron deposition on tungsten wire core has reached the upper limits of optimization. Attempts at depositing Boron silicon on graphite cores are not expected to result in higher fiber mechanical properties.

Continued close quality control of fiber production, and of the processing and prestressing of fiber tapes can be expected to reduce the coefficient of variation to the range of 8%.

BORSIC/ALUMINUM

No improvements in basic borsic fiber are expected for 1986 composite technology. The elastic allowables developed in Task II are used for Task III design considerations. "B" allowable fiber strains for borsic aluminum are assumed to be identical to "B" allowable strains used for boron/polyimide composites.

There are not allowables shown in the tables for borsic/aluminum since the material properties and allowables were developed during the Task II studies. These allowables and material properties can be found in Section 14 of reference 1-11.

RECOMMENDED IMPROVEMENTS IN DATA BASE

The survey of high temperature stable advanced composite systems programs indicated major areas which lack sufficient technical information to accurately predict performance of these materials in a commercial SST environment.

Time-temperature-stress relationships simulating future supersonic transport requirements for more than 5000 hours are non-existent for composite materials. Many of the polyimide systems used are not sufficiently thermally stable, or process with difficulty in the manufacture of high quality, uniform, reproducible composites; much of the data generated in past programs emphasized interlaminar shear and/or flexure properties for materials evaluation. This data is not directly translatable to other design properties. The test programs which have generated design data used a combination of test coupons and sandwich beam methods which require factors for correlation between the test methods and test programs.

One of the basic problems associated with advanced composites utilizing organic matrices is localized cracking of the matrix produced by externally applied tensile loads. Matrix cracking results primarily from a combination of resin brittleness, fiber-to-fiber contact or proximity and tensile stress components acting perpendicular to the fibers. This problem was recognized several years ago in fiberglass/epoxy systems (ref. 1-10). Attempts to eliminate micro cracking have been successful through blending of low percentages ($\leq 10\%$) of elastomeric polymers into the matrix. The addition of elastomers is thought to greatly increase the fracture surface work in the matrix preventing the initiation of micro cracks. This same kind of modification appears feasible and practical for polyimide matrix composites by 1986.

The technical personnel of Narmco, a major supplier of prepreg tapes, have stated that they also foresee the application of high temperature stable elastomers to polyimide or similar resin matrices to eliminate the micro cracking problem.

It should be noted that the ten most significant reports, used as the basis for projection of composite properties to 1986, required the application of several basic assumptions discussed previously to reduce the data to usable design information. Reference 1-2 was the only effort whose objectives closely matched the data requirements to obtain advanced composites design information for the arrow wing supersonic cruise vehicle.

Improvements in the data base should be directed toward (1) continued research on polyimide systems with improved thermal stability and processing characteristics, (2) improvement in graphite fiber properties similar to that being attempted by Union Carbide under contract to the Air Force, (3) research to eliminate tension strain micro cracking problems, through addition of elastomeric polymer to the matrix, (4) continuation of composite aging studies using time-temperature-stress combination effects, (5) standardization of composite test methods which reflect actual load parameters, and (6) establishment of design allowables applicable in design of supersonic cruise aircraft.

REFERENCES

- 1-1 Scheck, W. G.: Development of Design Data for Graphite Reinforced Epoxy and Polyimide Composites. NASA CR 120413, General Dynamics Convair Aerospace.
- 1-2 Haskins, J. F.; Kerr, J. R.; and Stein, B. A.: Time-Temperature-Stress Capabilities of Composite Materials for Advanced Supersonic Technology Applications. Proceedings of the SCAR Conference, NASA CP-001, 1976.
- 1-3 E. B. Birchfield and R. Kollmansberger: Develop Fabrication/Processing Techniques for High Temperature Advanced Composites for Use in Aircraft Structures. AFML TR-72-91, McDonnell Aircraft Company, 1972.
- 1-4 Nadler, M. A.; and Darms, F. J.: Development and Fabrication of a Graphite/Polyimide Box Beam. NASA CR 123959, North American Rockwell Space Division, 1972.
- 1-5 Cavano, P. J.: Resin/Graphite Fiber Composites. NASA CR 121275, TRW Incorporated, 1974.
- 1-6 Hanson, M. P.; and Serafini, T. T.: Effects of Thermal and Environmental Exposure on the Mechanical Properties of Graphite/Polyimide Composites. NASA TN D-6604, 1971.
- 1-7 Stein, B. A.; and Pride, Richard A.: Effect of 450°F and 600°F Exposures on the Mechanical Properties of Polyimide/Glass-Fiber Honeycomb Sandwiches and Laminated Beams. Journal of Aircraft, Vol. V., No. 1, January-February 1968.
- 1-8 Elton, J.: Elevated Temperature Laminates. Document No. D6A-10737-1, The Boeing Company, 1971.
- 1-9 Hofer, Jr., K. E.; Rao, N.; and Larson, D.: Development of Engineering Data on the Mechanical and Physical Properties of Advanced Composite Materials. AFML TR-72-205, 1974.
- 1-10 McGarry, Frederick J.: Crack Propagation in Fiber Reinforced Plastic Composites. Fundamental Aspects of Fiber Reinforced Plastic Composites. R. T. Schwartz and H. S. Schwartz, eds., Inter Science Publishers, 1968
- 1-11 Boeing Staff: Study of Structural Design Concepts for an Arrow Wing Supersonic Transport Configuration. NASA CR 132576-1 and -2, 1976.

Table 1-1.—Basic Graphite/Polyimide Laminate Unidirectional [0] Properties

Source		?				_ `	- 							-	7	- (-	_				-	f 1.2			10.	. ~			¥ Ref. 1-5
		. <u>-</u>		•		٥	B. C.) :							ά	B. G.						ם לם	ב ב ב	ב ב ב	B. C.	. α σ	E G	<u>}</u>	B.
Thermal expansion μ in./in./°F																											9	9 0	
Poisson's ratio																							0.37	0.5	5		0 29	7.0	
Strain,	9034))		6237	2838	2658	5316	5394				2950													7610	4300	2		
E _c , 10 ⁶ lb/in ²	22.0	i		19.1	22.5	20.0	19.7	19.6				27.3											17.3	17.5	19.6	24.6	2		
F _{cu,}	178.0			102.0	64.0	50.0	102.0	54.5				51.1	37.2	46.1	37.0								138.0	57.0	1410	1000	147.0	133.0	130.0
Strain	8692	7429	7867	9370			6741	0069				5380	4532	8180	4875						•				6920	3360	3300) 	
E _t , 10 ⁶ lb/in ²	23.2	23.6	20.7	17.7			22.7	21.6				26.0	25.6	23.7	28.6								19.3		22.5	26.9	23.9		
F _{tu} ,	213.0	169.0	162.0	176.0			163.0	162.0	165.0	154.0	150.0	131.0	129.0	129.0	123.0	176.0	113.0	172.0	191.0	189.0	178.0	167.0	170.0	154.0	161.0	0.86	78.8		
Test specimen	SW beam	-	SW beam	Coupon	_									•														-	Coupon
Exposure time, hr	0	0.5	100.0	0	0.5	100.0	0.7	0.5	100.0	200.0	400.0	0	0	200.0	200.0	0	500.0	1000.0	0	200.0	500.0	1000.0	0	0.5	0	0	0	0.5	500.0
Exposure temp. °F	RT	220	220	RT	220	220	R	009	009	009	009	RT	009	009	009	RT	450	450	RT	550	550	550	RT	200	RT	RT	RT	200	550
Test temp. °F	RT	550	220	RT	220	550	R	009	009	009	009	RT	009	RT	009	RT	450	450	RT	220									200
Resin	Skybond 703				> ,	Skybond 703	Skybond 710					_					-				-	Skybond 710	Gemonl	Gemonl	5206	3002M	PMR-15	→	PMR-15
Fiber	Polyimide Mod II				-	Mod II	S-TH			-	HT-S	S-WH		→	S-MH	HT-S					>	HT-S				S-MH	de	→	de HM-S
i	Polyimi	_											•										→	Polyimi	Epoxy	Epoxy	Polyimide	→	Polyimide

Table 1-2.—Basic Graphite/Polyimide Unidirectional Laminate [90] Properties

Source	Ref, 1-3				-	Ref. 1-3			-	•			•	Ref. 1-9	
Thermal expansion μ in./in. $^{\circ}$ F											25.0				
Strain \$\mu\$ in./in.	11 536			18 850	14 630	17 810	2 285	2 500		1 695				20 340	19 670
E _c , 10 ⁶ lb/in ²	1.16			0.68	0.84	0.82	1.22	0.99	2.02	1.02				1.71	1.25
F _{cu} ,	18.99			21.2	10.2	9.83	12.4	11.4	8.94	7.35				24.7	21.4
Strain,	4535	2000	4708	1880	-		2859	2625	2420	2680			7200	4050	2260
E _t , 10 ⁶ lb/in ²	2.02	1.15	1.20	0.99			1.37	1.17	1.44	1.44	1.32	9.0	98.0	1.28	96.0
r, ksi	9.89	4.34	4.34	2.53			2.32	1.72	1.77	1.70	2.39	96.0	7.0	5.2	2.3
Test	SW beam	→	SW beam	Coupon	_									-	Conpon
Exposure time, hr	0	0.5	100.0	0	0.5	100.0	0	0.5	0	0.5	0	0.5	0	0	0
Exposure temp, °F	RT	550	550	RT	550	550	RT	009	RT	009	RT	200	RT	RT	RT
Test temp, °F	RT	220	220	RT	550	550	RT	009	RT	009	RT	200	RT	RT	RT
Resin	Skybond 703				>	Skybond 703	Skybond 710			Skybond 710	Gemonl	Gemont	PMR-15	5206	3002M
Fiber	Polvimide Mod II				->	Mod	HT-S	S-TH	S-MH	HM-S	Mod II	II poW	Polyimide HM-S		Epoxy HM-S

Table 1-3. Basic Graphite/Polyimide Laminate $[\pm 45]_{\rm S}$ Properties

Source	Ref. 1-1 Ref. 1-1 Ref. 1-1 Ref. 1-4
Poisson's Ratio	0.80
Strain	11 900 11 900 9 670 13 712
E _c , 10 ⁶ lb/in ²	4.63 2.19 3.77 2.47
F _{cu} ,	28.5 20.5 15.1 11.6
Strain μ in./in.	10 500 15 700 7 880 12 800
E _t , 10 ⁶ lb/in ²	2.6 1.7 2.0 1.7 2.96 2.30
F _{tu} ,	16.2 10.8 10.7 8.3 17.9
Test	Coupon
Exposure time, hr.	0.5 0.5 0.5 0.5
Exposure temp., °F	FRT 600 RT 600 RT 500
Test temp., °F	RT 600 RT 600 RT 500
Resin	Skybond 710 Skybond 710 Gemonl
Fiber	HT-S HT-S HM-S HM-S Mod II

Note: Tensile test specimens had a 64.8% volume fraction. Compression test specimens had a 61.1% volume fraction.

Table 1-4.—Normalized Graphite/Polyimide Laminate [0] Properties Normalized to 60% Fiber Volume

Source	Ref. 1-3		•		Ref. 1-5		Ref. 1-3 Ref. 1-1 Ref. 1-2 Ref. 1-4			Ref. 1-1 Ref. 1-5		
No. of specimens	10	9	7	က	ო							
Poisson's ratio				0.37								
Strain	9034	5210	<u>:</u>			lues (F $_{ m tu}$ and F $_{ m cu}$) corrected by multipication to sandwich beam 1.21 tension, 1.74 compression		8700	7450		5650	4850
E _c ,	22.0	- 82)			sion, 1.74		20.0	20.0	27.3	26.0	20.0
F _{cu} , ksi	178.0	02.0)			n 1.21 ten	178.0	174.0	149.0	147.0	147.0	126.0
Strain µ in./in.	8692	7190	9590	8880	6730	ndwich bean		9850	8430	0989	0989	5870
E _t ,	23.2	10.7	17.2	19.7	20.8	ation to sa		19.7	19.7	25.2	25.2	25.2
F _{tu} , ksi	213.0	144.0	165.0	175.0	140.0a	/ multipic	213.0 174.0 200.0 211.0 170.0a	200.0	172.0	173.0	173.0	148.0
Test specimen	SW beam	uodnon		>	Coupon	corrected by						
Exposure time, hr	00	-	0	0	0	and F _{CU}) o			tion)			ion)
Exposure temp., °F	RT-				R	h values (F _{tı}			 of calculation)			 of calculation)
Test temp., °F	TH_			→	RT	Above strength va			or methoc			or method
Resin	Skybond 703	Skybond /U3	Skybond 710	Gemont	PMR-15	Ab			"B" allowables (see text for method of	Skybond 710		"B" allowable (see text for method of
Fiber	Mod II	Mod	Ç L	Mod II	HT-S			Average	"B" allo	S-MH	Average	"B" allo
	drgnartz dgiH											ЧвіН

^aNot used for averaging.

Table 1-5.—Normalized Graphite/Polyimide Laminate [90] Properties Normalized to 60% Fiber Volume

		1							T	
Source	Ref. 1-3 Ref. 1-1 Ref. 1-1 Ref. 1-2 Ref. 1-4		Ref. 1-3 Ref. 1-1	Ref. 1-4 Ref. 1-3			Ref. 1-1 Ref. 1-5		Ref. 1-1	
No. of specimen	01 01 8									
Strain, \$\mu\$ in./in.	11 536 18 850 2 285 9 290					12 320	4 430	_		3 790
E _c ,	1.16 0.68 1.22 1.70	on strength nodulus	1.16	1.70	1.19	1.19	2.02	on strength, nodulus	2.02	2.02
F _{cu} , ksi	18.99 21.20 12.4 15.79	.90) tensid	18.99	15.79	17.09	14.66	8.94	90), tensic	8.94	7.66
Strain, μ in./in.	4535 1880 2859 4240 1810	Above data (F_{tu} , E_t , F_{cu} , and E_c) corrected to sandwich beam (3.90) tension strength, (2.0) tension modulus, (1.0) compression strength, (1.0) compression modulus				3940	2420 7200a	Above data (F _{tu} , E _t , F _{cu} , and E _c) corrected to sandwich beam (3.90), tension strength, (2.0) tension modulus, (1.0) compression strength, (1.0) compression modulus		2055
E _t , 10 ⁶ 1b/in ²	2.02 0.99 1.37 0.75 1.32	ed to sandv sion streng	2.02 2.74	2.64	2.22	2.22	1.44 0.86 ^a	d to sandw sion streng	2.88	2.88
F _{tu} , ksi	9.89 2.53 2.32 3.18 2.39) correcte	9.89	9.32	10.2	8.75	1.77 7.0a	correcte	6.90	5.92
Test	SW beam Coupon Coupon	F _{cu} , and E _c					Coupon	cu, and E _c) odulus, (1.0)		
Exposure time, hr	0000	a (F _{tu} , E _t , tension mo				(-	0	ı (F _{tu} , E _t , I tension mo		<u>_</u>
Exposure temp., ^o F	FR FR	Above dat (2.0)				 of calculation) 	RT	Above data (2.0)		 of calculation)
Test temp., °F	ж 						RT RT			for method
Resin	703 703 710 710 Gemonl		703 710 710	Gemonl		"B" allowable (see text for method	710 PMR-15		Corrected data values	"B" allowable (see text for method
Fiber	Mod II Mod II HT-S HT-S Mod II		Mod II HT-S HT-S	Mod	Average	"B" allows	HM-S HM-S		Corrected	"B" allowe
		Կ դճս	High stre				sn	iubom di	giH	

^aData not used for "B" allowable

Table 1-6. Normalized Graphite/Polyimide Laminate $[\pm 45]_S$ Properties Normalized to 60% Fiber Volume

	i i	C. C	Test, E	Exposure	Exposure Exposure	F tu,	E _t , 8	Strain,	F Cu',	Ec, 5	Strain,	Cource
	Incl	nesill	leilip., r	reilip.,	רוווובי ווו			K III./ III.	2	111/01 01	r/	23 1000
дұр	S-TH	710	RT	RT	ó	15.0	2.18	088 9	28.0	4.55	6 150	Ref. 1-1
	Mod II	Gemonl	RT	RT	0	22.6	3.73	0909				Ref. 1-4
20	S-TH	Epoxy	R	RT	0	30.0	2.34	2 000	38.0	2.34	4 300	AFDG
	Average HT-S				0	30.0b	2.75	5 000a	38.0b	3.44	4 300a	
	"B" allowable HT-S				0	25.7	2.75	2 500a	32.6	3,44	3 000a	
Γ,	S-MH	710	RT	RT	0	11.5	2.14	8 000a	16.2	4.03	10 000a	Ref. 1-1
njr		Epoxy	RT	RT	0	21.0	2.38	14 500	27.0a	2,38a		AFDG
200	Average				0	21.0	3.80a	13 000a	27.0a	3.80a	15 000a	
	"B," allowable HM-S				0	18.0	3.80a	10 000a	23.2	3.80a	11 000a	

^aEstimated

^bBased on Air Force Design Guide data, polyimide data inferior

Table 1-7.—"B" Allowables, Graphite/Polyimide Laminate Normalized to 60% Fiber Volume, 1975

								:						
Absorptivity	0.85											->-	0,85	
Thermal expansion μ in./in.ºF	-0.17		9.45					-0.4		17.0				
Thermal cond. Btu in.	160		16					370		20				
Poisson's ratio	0.31	0.31			0.80	0.84		0.29	0.29			0.79	0.83	
Strain, μ in./in.	8 600	7 800	12.400	13 000	13 000a	14 000a		4 800	4 300	8 800 ^a	10 000a	7 600a	6 400a	
E _c ,	20.0	20.0	1.19	1.0	3.44	1.7		26.0	26.0	2.02	1.6	3.80	3.2	
F _{cu} ,	172.0	155.0	14.7	13.0	32.6	19.8		126.0	113.0	16.0	14.5	23.2	18.0	
Strain,	8 730	7 900	4 000	3 400	12 000a	12 000a		2 900	5 300	2 100	1,900	5 800a	5 200a	
E _t , 10 ⁶ lb/in ²	19.7		2.22		2.75	1.8		25.2		2.88	2.7	3.80a	3.2	
F tu,	172.0	155.0	8.75	6.5	25.7	17.5		148.0	133.0	5.92	5.0	18.0	14.0	
Test temp, °F	RT	450	RT	450	RT	450		RT	450	RT	450	RT	450	
Fiber type	High				-	High	strength	High modulus				-	High	modulus
Fiber	[0]	[0]	[06]	[06]	[+45]	[1 45]		[0]	[0]	[06]	[06]	[‡ 45]	[± 45]	

^aEstimated

Table 1-8.—"B" Allowables, Graphite/Polyimide Laminate Normalized to 60% Fiber Volume, 1986

Absorptivity	0.85							-			~	0.85
Thermal expansion, μ in./in. °F	-0.17		9.45				-0.40	-	17.0			
Thermal cond, Btu in. hr ft ^{2 °} F	160		16				370		20			
Poisson's ratio	0.31	0.31			0.80	0.84	0.29	0.29			0.79	0.83
Strain, µ in./in.	14 500	13 000 ^b	15 000	15 500	25 000	23 000	3 150	2 825	12 000	12 400	10 000	8 500
E _c ′ 10 ⁶ lb/in ²	20.0	20.0	1.8	1.7	2.8	1.8	40.0	40.0	1.8	1.7	3.8	3.2
F _{cu} ,	290.0	260.0	23.0	21.0	26.0	34.0	126.0	113.0	18.0	16.5	23.0	18.0
E _τ , Strain, 106 _{lb/in} 2 μ in./in.	14 750	13 250	2 000	3 900	19 000	19 000	3 700	3 305	4 000	3 100	2 200	009 9
E _t , 10 ⁶ lb/in ²	20.0		2.0									
F _{tu} , ksi	295.0	265.0	8.8	6.5	44.0	30.0	148.0	133.0	7.0	2.0	18.0	14.0
Test temp., °F	RT	450	RT	450	RT	450	RT	450	RT	450	RT	450
Fiber	T600ª	T600a	T600a	T600a	T600a	T600a	790°C		T90c	T90c	_061	T90c
Fiber	[0]	[0]	[06]	[06]	[±45] c	[±45]	, [0]	[0]	[06]	[06]	[±45] c	[±45]S

 $^{a}
ho_{T600} = 0.056 \text{ lb/in}^{3}$

^bEstimated

 $^{\rm c}
ho_{\rm T90}$ = 0.058 lb/in³

Table 1-9.—"B" Allowables, Boron/Polyimide Laminate^a Normalized to 50% Fiber Volume, 1986

Thermal expansion μ in./in. °F.	2.3	3.0	10.6	19.6		
Thermal cond. Btu in. hr ft ^{2 °} F	16	16	∞	ω		
Poisson's ratio	0.21	0.21			0.85	0.91
Strain, \$\mu\$ in./in.	11 000	10 500	14 000	15 000	16 000	15 500
E _c , Strain, 10 ⁶ lb/in2 μ in./in.	32.0	30.0	3.6	3.0	2.5	2.3
F cu', ksi	350	315	38	34	35	32
Strain, F _{cu} '	6100	5900	3500	3600	9500	9500
Ε _τ , (10 ⁶ lb/in ² μ	32.0	30.0	2.8	2.5	2.5	2.3
F tu, ksi	195.0	175.0	7.8	7.0	22.0	20.0
Test temp, °F	RT	450	RT	450	RT	450
Fiber Orientation	[0]	[0]	[06]	[06]	[1 45]	[±45]

 $^{a}\rho = 0.0725 \text{ lb/in}^{3}$

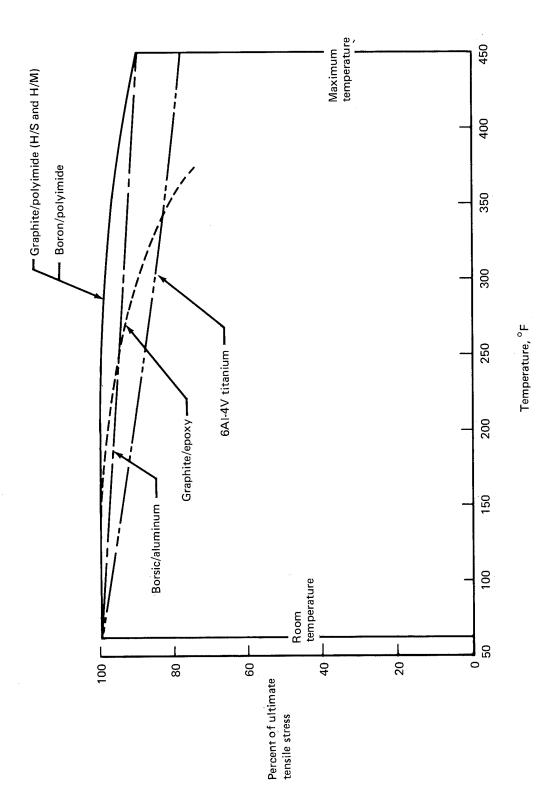


Figure 1-1.—Temperature Dependence of Material Properties for Advanced Composite Wing Cover Panels

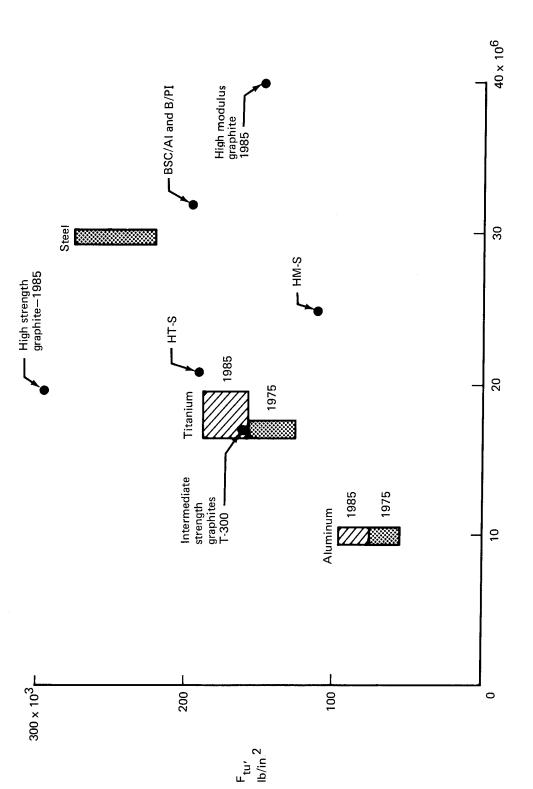


Figure 1-2.—Strength and Moduli of Various Materials

Modulus of elasticity in tension, $\mathrm{lb/in}^{\,2}$

SECTION 2

ALLOWABLES

by

V. D. BESS

F. D. FLOOD

CONTENTS

	Page
INTRODUCTION	30
STRESS-STRAIN RELATIONSHIPS	
THERMAL EFFECTS	35
MATERIAL ALLOWABLES	35
REFERENCES	. 36

TABLES

No.									Page
2-1	High Strength Graphite/Polyimide Mechanical Properties								37
2-2	High Modulus Graphite/Polyimide Mechanical Properties								38
2-3	Boron/Polyimide Mechanical Properties								39
2-4	5.7-Mil Borsic/Aluminum Mechanical Properties	.•		•		•		•	40

FIGURES

No.					Page
2-1	Graphite/Polyimide Stress-Strain, Tension and Compression, [0] Orientation .				41
2-2	Graphite/Polyimide Stress-Strain, Tension, [90] Orientation				42
2-2 2-3	Graphite/Polyimide Stress-Strain, Compression, [90] Orientation	•	•	•	43
2-4	Graphite/Polyimide Stress-Strain, Tension and Compression, [90] Orientation.	٠	•	•	44
2-5	Graphite/Polyimide Stress-Strain, Tension, [±45] Orientation	٠	•	•	45
2 - 6	Graphite/Polyimide Stress-Strain, Compression, [±45] Orientation		•	•	46
2-7	Graphite/Polyimide Stress-Strain, Tension and Compression, [±45] Orientation	٠	•	•	47

SYMBOLS

	CLT	Classical lamination theory
	E	Modulus of elasticity
	E_s	Secant modulus
	G	Modulus of rigidity (shear)
	N	Load per inch of edge length
	t	Skin thickness
	γ	Shear strain
	ϵ	Axial strain
	μ	Poisson's ratio
	σ	Axial stress
	au	Shear stress
Subscri	ipts	
	L	Longitudinal
	T	Transverse

INTRODUCTION

In the next decade development of polyimide matrix systems is expected to permit design and fabrication of advanced composite material systems that are truly fiber critical. The problem that must be addressed is that of increasing the matrix strain capability to equal or exceed that of the fiber. Strains of this magnitude must not induce micro-cracks, and the matrix modulus must be sufficiently large to develop acceptable fiber strengths in compressive loading. Research toward achieving these goals for epoxy matrices is reported in references 1-10 and 2-1. In the development of allowables reported below it is assumed that the composite material system is fiber critical.

When developing elastic property values for use with the ATLAS system it was a requisite that the values be constant throughout the total range of loading at any given temperature. Thus, for example, a modulus of elasticity for tensile loads should equal that for compressive loads. The approach used to establish elastic and mechanical properties is outlined below using the high-strength graphite/polyimide room temperature (R.T.) values for illustrative purposes. In the discussion that follows, a unidirectional laminate loaded parallel to the fibers is identified as a [0] laminate. A unidirectional laminate loaded transferse to the fibers is identified as a [90] laminate.

STRESS-STRAIN RELATIONSHIPS

Figure 2-1 is a plot of the tensile and compressive stress-strain curves for a [0] laminate. Both the tension and compression curves are linear to the "B" allowable stresses and exhibit the same modulus of elasticity. The allowable tensile fiber strain from the load-free state is 0.01475 in./in. while that in compression is 0.0145 in./in. These critical data are as taken from table 1-8.

Figure 2-2 is a plot of the tensile stress-strain curve for a [90] laminate. The basic data is from a current-technology, matrix-critical system. As noted previously, development of the polyimide matrix system anticipates vast improvement in the matrix strain capability. Since no major reduction in the modulus can be sustained without loss of fiber compressive strength, it has been assumed that the matrix improvement would be realized as plastic strain beyond the current matrix allowable tensile strain. This plastic strain terminates at the critical tensile fiber strain (fig. 2-1).

Figure 2-3 is a plot of the compressive stress-strain curve for a [90] laminate. Since the allowable fiber compressive strain is less than the allowable matrix compressive strain, the fiber strain will be critical in a $[0_i/\pm45_i/90_k]$ laminate.

The secant moduli at the critical fiber strains are shown on figures 2-2 and 2-3. The tensile and compressive moduli are unequal. These moduli are averaged to get a single value to use for either tensile or compressive loads. This average modulus is plotted in figure 2-4 along with replots of figures 2-2 and 2-3 to illustrate the effect of the foregoing procedure. While the changes in allowable stresses, strains and moduli illustrated in figure 2-4 appear quite large, it should be emphasized that the contributions of the fibers to the strength and stiffness of a fiber critical laminate is much greater than that of the matrix, and therefore, these altered matrix properties are inconsequential in predicting the strength and stiffness of a $[0_i/\pm45_j/90_k]$ laminate.

Figures 2-5 and 2-6 are plots of the tensile and compressive stress-strain curves, respectively, for a $[\pm 45]_S$ laminate loaded along the 0° axis. In each case, the allowable strain of the $[\pm 45]_S$ laminate exceeds the allowable fiber strain (fig. 2-1). The secant moduli were calculated at the critical fiber strain as shown. The average of these secant moduli is plotted on figure 2-7 along with the original curves from figures 2-5 and 2-6. The deviation from the original curves is slight and is acceptable for evaluating any laminate which incorporates this $[\pm 45]_S$ laminate as a subset. These data will be used later to establish the inplane shear modulus of a unidirectional laminate.

Section 1 identified values for Poisson's ratios for a [0] laminate and a [±45]_S laminate. The Poisson's ratio for a [90] laminate (which as noted above is the Poisson's ratio for a unidirectional laminate loaded transversely) may be calculated from classical lamination theory (CLT), (ref. 2-2) as

$$\mu_{\rm T} = \frac{E_{\rm T}}{E_{\rm L}} \,\mu_{\rm L} \tag{2-1}$$

where the T denotes [90] - and L denotes [0] - values.

The data presented in section 1 did not identify shear properties of the various laminates because of the difficulties typically encountered in both rail shear and picture-frame shear testing. Properly tested, buckle-free torque tube test data was not apparently available. Thus, the shear properties were calculated using CLT as discussed below. The technique parallels that employed in reduction of sandwich cross-beam test data.

From figure 2-7

$$E_x = E_v = 2.58 \text{ Msi}$$

From table 1-8

$$\mu_{XV} = \mu_{VX} = 0.80$$

Since the [±45] laminate is orthotropic with respect to the X-Y axes, the reduced stiffnesses are given in terms of the engineering constants as (ref. 2-2).

$$Q_{11} = \frac{E_x}{1 - \mu_{xy} \mu_{yx}} = \frac{2.58 \times 10^6}{1 - (.8)^2} = 7.1667 \times 10^6 \text{ psi}$$

$$Q_{22} = \frac{E_y}{1 - \mu_{xy} \mu_{yx}} = \frac{2.58 \times 10^6}{1 - (.8)^2} = 7.1667 \times 10^6 \text{ psi}$$

$$Q_{12} = \mu_{VX} Q_{11} = 0.8 (7.1667 \times 10^6) = 5.7333 \times 10^6 \text{ psi}$$

$$Q_{66} = G_{xy}$$

$$Q_{16} = Q_{26} = 0$$
, as a consequence of orthotropy

The reduced stiffnesses relate the strains to the stresses as

$$\begin{cases}
\sigma_{X} \\
\sigma_{y} \\
\tau_{xy}
\end{cases} = \begin{bmatrix}
Q_{11} Q_{12} Q_{16} \\
Q_{22} Q_{26} \\
(Sym) Q_{66}
\end{bmatrix} \begin{cases}
\epsilon_{X} \\
\epsilon_{y} \\
\gamma_{xy}
\end{cases} = 10^{6} \begin{bmatrix}
7.1667 & 5.7333 & 0 \\
& 7.1667 & 0 \\
(Sym) & Q_{66}
\end{bmatrix} \begin{cases}
\epsilon_{X} \\
\epsilon_{y} \\
\gamma_{xy}
\end{cases} \tag{2-2}$$

The strain-stress relations are derived from [Q]⁻¹ as

$$\begin{cases}
\epsilon_{X} \\
\epsilon_{y} \\
\gamma_{XY}
\end{cases} = 10^{6} \begin{bmatrix}
0.38758 & -0.31006 & 0 \\
0.38758 & 0 \\
(Sym) & Q_{66}
\end{bmatrix} \begin{bmatrix}
\sigma_{X} \\
\sigma_{y} \\
\tau_{XY}
\end{cases} \tag{2-3}$$

For the specified loading

$$\begin{cases}
\sigma_{X} \\
\sigma_{X}
\end{cases} = \begin{cases}
N/t \\
-N/t
\end{cases}$$
(2-4)

The strains for the specified loadings are

$$\begin{cases}
\epsilon_{\mathbf{x}} \\
\epsilon_{\mathbf{y}} \\
\gamma_{\mathbf{x}\mathbf{y}}
\end{cases} = 1\overline{0}^{6} \begin{bmatrix}
0.38758 & -0.31006 & 0 \\
0.38758 & 0 \\
Q_{66}^{-1} \end{bmatrix} \begin{bmatrix}
N/t \\
-N/t \\
0
\end{bmatrix} = \begin{cases}
0.69764 \times 1\overline{0}^{6} & N/t \\
-0.69764 \times 1\overline{0}^{6} & N/t \\
0
\end{cases} \tag{2-5}$$

The strains are now transformed to the 1-2 axis system which is coincident with the fibers in the $[\pm 45]_S$ laminate.

$$\begin{cases}
\epsilon_{1} \\
\epsilon_{2} \\
\frac{1}{2}\gamma_{12}
\end{cases} = \begin{bmatrix}
\cos^{2}45^{\circ} & \sin^{2}45^{\circ} & 2\sin45^{\circ}\cos45^{\circ} \\
\sin^{2}45^{\circ} & \cos^{2}45^{\circ} & -2\sin45^{\circ}\cos45^{\circ} \\
-\sin45^{\circ}\cos45^{\circ} & \sin45^{\circ}\cos45^{\circ} & \cos^{2}45^{\circ}-\sin^{2}45^{\circ}
\end{bmatrix} \begin{cases}
\epsilon_{X} \\
\epsilon_{y} \\
\frac{1}{2}\gamma_{XY}
\end{cases} \tag{2-6}$$

The stresses (loading) may be similarly transformed

$$\begin{cases}
\sigma_1 \\
\sigma_2 \\
\tau_{12}
\end{cases} = \begin{bmatrix}
\frac{1}{2} & \frac{1}{2} & 1 \\
\frac{1}{2} & \frac{1}{2} & -1 \\
-\frac{1}{2} & \frac{1}{2} & 0
\end{bmatrix} \begin{pmatrix}
N/t \\
-N/t \\
0
\end{pmatrix} = \begin{cases}
0 \\
0 \\
N/t
\end{cases}$$
(2-8)

It may be seen from the transformed stress that the specified loading is applied shear only in the 1-2 axis system. This is a loading wherein the matrix only carries the shear load and is considered equivalent to a shear loading on a unidirectional laminate. The shear modulus is given by

$$G_{12} = \frac{\tau_{12}}{\gamma_{12}} = \frac{-N/t}{2(-0.69764 \times 10^{-6} \text{ N/t})} = 0.717 \text{ Msi}$$
 (2-9)

As a check, CLT was used to obtain the strain-stress relations for a $[\pm 45]_S$ laminate using the following properties for an unidirectional laminate

$$E_1 = 20. \text{ Msi}$$
 $E_2 = 1.13 \text{ Msi}$
 $G_{12} = 0.717 \text{ Msi}$
 $\mu_{12} = 0.31$

The apparent elastic properties of the [±45]_S laminate in the X-Y (0°-90°) axis system are

$$E_X$$
 = E_y = 2.54 Msi (vs. 2.58 Msi from figure 2-7)
 μ_{XY} = μ_{YX} = 0.77 (vs 0.80 from section 1)
 G_{XY} = 5.14 Msi (not reported in section 1)

These values are in excellent agreement with the reported values of section 1. The basic laminate elastic properties noted above will be used in conjunction with CLT to determine the elastic characteristics of the $[0_i/\pm 45_i/90_k]_S$ laminates evaluated.

The procedure to determine the inplane shear strength of a unidirectional laminate is shown below. It is assumed that the inplane shear strength of a unidirectional laminate equals that of a $[0/90]_S$ laminate. The stress-strain relations for a $[0/90]_S$ laminate are

$$\begin{cases}
\sigma_{X} \\
\sigma_{y} \\
\tau_{xy}
\end{cases} = 10^{6} \begin{bmatrix}
10.6226 & 0.35191 & 0 \\
& 10.6226 & 0 \\
& (Sym) & 0.717
\end{bmatrix} \begin{cases}
\epsilon_{X} \\
\epsilon_{y} \\
\gamma_{xy}
\end{cases} (2-10)$$

The strain-stress relations are

$$\begin{cases}
\epsilon_{x} \\
\epsilon_{y} \\
\gamma_{xy}
\end{cases} = 10^{6} \begin{bmatrix}
0.094242 & -0.0031221 & 0 \\
0.094242 & 0 \\
(Sym) & 1.3947
\end{bmatrix} \begin{cases}
\sigma_{x} \\
\sigma_{y} \\
\tau_{xy}
\end{cases} (2-11)$$

For a shear stress only the strains are

$$\begin{cases}
\epsilon_{\mathbf{x}} \\
\epsilon_{\mathbf{y}} \\
\gamma_{\mathbf{x}\mathbf{y}}
\end{cases} = \begin{cases}
0 \\
0 \\
1.3947 \times 10^{-6} \tau_{\mathbf{x}\mathbf{y}}
\end{cases}$$
(2-12)

Transforming these strains to a 1-2 axis system at ±45° from the X-Y axis gives

$$\begin{cases}
\epsilon_{1} \\
\epsilon_{2} \\
\frac{1}{2}\gamma_{12}
\end{cases} = \begin{bmatrix}
\frac{1}{2} & \frac{1}{2} & 1 \\
\frac{1}{2} & \frac{1}{2} & 1 \\
-\frac{1}{2} & \frac{1}{2} & 0
\end{bmatrix}
\begin{cases}
0 \\
0 \\
1.3947 \times 10^{-6} \tau_{xy/2}
\end{cases} = \begin{cases}
1.3947 \times 10^{-6} \tau_{xy/2} \\
1.3947 \times 10^{-6} \tau_{xy/2}
\end{cases}$$
(2-13)

In a $[0_i/\pm 45_j/90_k]_S$ fiber critical laminate, the critical compressive fiber strain is 0.0145 in./in. Thus, the matrix shear strength may be defined by substituting this value for ϵ_2 . The shear strength is then given by

$$\tau_{\text{xy}}$$
 allow. = $\frac{-14500 \times 10^{-6}}{(-1.3947 \times 10^{-6})/2}$ = 20800 psi (2-14)

Interlaminar shear strengths are assumed equal to the shear strength of a unidirectional laminate.

THERMAL EFFECTS

Coefficients of thermal expansion were given for [0] and [90] laminates at room temperature. In checking the data source, it was discovered that the given values were an average over a temperature range greater than room temperature to $450^{\circ}F$. Therefore, the same values are used at room temperature and $450^{\circ}F$.

Thermal conductivities are shown in section 1 for [0] and [90] laminates. These values were obtained from tests on graphite/epoxy at 450°F. Since the fibers are the main contributors to the conductivity, the values for the [0] laminates should be quite close. The [90] laminate conductivities will be dependent upon the assumption that the conductivity of epoxy is approximately that of polyimide.

While some tentative values for other thermophysical properties are tabulated in section 1 and the section 2 tables, these values are subject to revision by our thermal analyst (see section 10).

MATERIAL ALLOWABLES

Tables 2-1 through 2-4 list the unidirectional laminate properties for the candidate advanced composite material systems. As noted above, all $[0_i/\pm45_j/90_k]_S$ laminates evaluated will have properties based on the unidirectional laminate properties with the specific properties based on classical lamination theory.

REFERENCES

- 2-1 Mazzio, V. F.; Mehan, R. L.; and Mullin, J. V.: Basic Failure Mechanics in Advanced Composites. NASA CR-134525, 1973.
- Jones, R. M.: Mechanics of Composite Materials. McGraw-Hill, 1975.

Table 2-1. - Estimated Mechanical Properties of High Strength Graphite/Polyimide Available in 1986.

	Available in 1986. V _f = 0.60		Room temperature	450 °F
Design	Longitudinal tensile ultimate, ksi	F _L tu	295	265
strengths "B" values	Transverse tensile ultimate, ksi	16.7	13.7	
	Longitudinal compression ultimate, ksi	FL ^{cu}	290	260
	Transverse compression ultimate, ksi	F _T cu	16.4	13.4
	Inplane shear ultimate, ksi	F _{LT} su	20.8	12.0
	Interlaminar shear ultimate, ksi	F ^{isu}	20.8	12.0
	Ultimate longitudinal tensile strain, μ in./in.	ϵ_{L}^{tu}	14 750	13 250
	Ultimate longitudinal compressive strain, μ in./in.	ϵ_{L}^{cu}	14 500	13 000
Elastic	Longitudinal tension modulus, 10 ⁶ lb/in ²	ΕĽ	20.0	
properties (typ)	Transverse tension modulus, 10 ⁶ lb/in ²	E_T^t	1.13	1.03
	Longitudinal compression modulus, 10 ⁶ lb/in ²	ELc	20.0	20.0
	Transverse compression modulus, 10 ⁶ lb/in ²	E _T c	1.13	1.03
	Inplane shear modulus, 10 ⁶ lb/in ²	G_LT	0.717	0.462
	Longitudinal Poisson's ratio	μ_{LT}	0.31	0.31
	Transverse Poisson's ratio	μ_{TL}	0.018	0.016
Physical	Density, lb/in ³	ρ	0.056	0.056
(typ)	Longitudinal coefficient of thermal expansion, μ in./in./ $^{ m o}$ F	$lpha_{L}$	-0.17	-0.17
	Transverse coefficient of thermal expansion, μ in./in./ $^{ m o}$ F	α_{T}	17.0	17.0
	Longitudinal thermal conductivity, Btu in. hr ft ² °F	K _T	160	_
	Transverse thermal conductivity, Btu in. hr ft ² °F	κ_{T}	16	-
	Absorptivity	α	0.85	_
	Emissivity	ϵ		•

Table 2-2. - Estimated Mechanical Properties of High Modulus Graphite/Polyimide

	Available in 1986. V _f = 0.60		Room temperature	450 °F
Design	Longitudinal tensile ultimate, ksi	F _L tu	148	133
strengths "B" values	Transverse tensile ultimate, ksi	F_T^tu	6.7.	5.3
	Longitudinal compression ultimate, ksi	F _L cu	126	113
	Transverse compression ultimate, ksi	FT ^{cu}	5.7	4.5
	Inplane shear ultimate, ksi	F _{LT} su	6.2	4.6
	Interlaminar shear ultimate, ksi	F ^{isu}	6.2	4.6
	Ultimate longitudinal tensile strain, μ in./in.	ϵ_{L}^{tu}	3700	3325
	Ultimate longitudinal compressive strain, μ in./in.	ϵ_{L}^{cu}	3150	2825
Elastic	Longitudinal tension modulus, 10 ⁶ lb/in ²	ELt	40.0	40.0
properties (typ)	Transverse tension modulus, 10 ⁶ lb/in ²	E_T^t	1.8	1.6
	Longitudinal compression modulus, 10 ⁶ lb/in ²	E ^L c	40.0	40.0
	Transverse compression modulus, 10 ⁶ lb/in ²	ETC	1.8	1.6
	Inplane shear modulus, 10 ⁶ lb/in ²	G _{LT}	0.98	0.82
	Longitudinal Poisson's ratio	μ_{LT}	0.29	0.29
	Transverse Poisson's ratio	μ_{TL}	0.013	0.012
Physical	Density, lb/in ³	ρ	0.058	0.058
constants (typ)	Longitudinal coefficient of thermal expansion, μ in./in./ $^{\circ}$ F	α_{L}	-0.4	-0.4
	Transverse coefficient of thermal expansion, μ in./in./°F	α_{T}	17.0	17.0
	Longitudinal thermal conductivity, Btu in.	κ _L	370	-
	Transverse thermal conductivity, Btu in. hr ft ² °F	κ _T	20	-
	Absorptivity	α	0.85	-
	Emissivity	ϵ		

Table 2-3. - Estimated Mechanical Properties of Boron/Polyimide Available in 1986.

	$V_{f} = 0.50$		Room temperature	450 °F
Design	Longitudinal tensile ultimate, ksi	FL ^{tu}	195	175
strengths "B" values	Transverse tensile ultimate, ksi	F_T^tu	14.6	13.0
	Longitudinal compression ultimate, ksi	FL ^{cu}	350	315
	Transverse compression ultimate, ksi	F _T cu	26.4	23.1
	Inplane shear ultimate, ksi	F _{LT} su	8.3	7.1
	Interlaminar shear ultimate, ksi	F ^{isu}	8.3	7.1
	Ultimate longitudinal tensile strain, μ in./in.	ϵ_{L}^{tu}	6 100	5,900
	Ultimate longitudinal compressive strain, μ in./in.	ϵ_{L}^{cu}	11 000	10 500
Elastic	Longitudinal tension modulus, 10 ⁶ lb/in ²	E _L ^t	32.0	30.0
properties (typ)	Transverse tension modulus, 10 ⁶ lb/in ²	E_T^t	2.4	2.2
	Longitudinal compression modulus, 10 ⁶ lb/in ²	ELc	32.0	30.0
	Transverse compression modulus, 10 ⁶ lb/in ²	E^T^c	2.4	2.2
	Inplane shear modulus, 10 ⁶ lb/in ²	G_LT	0.68	0.60
	Longitudinal Poisson's ratio	μ_{LT}	0.21	0.21
	Transverse Poisson's ratio	μ_{TL}	0.016	0.015
Physical	Density, lb/in ³	ρ	0.0725	0.0725
constants (typ)	Longitudinal coefficient of thermal expansion, μ in./in./°F	$\alpha_{ extsf{L}}$	2.6	2.6
	Transverse coefficient of thermal expansion, μ in./in./ $^{ m o}$ F	α_{T}	15.1	15.1
	Longitudinal thermal conductivity, Btu in. hr ft ² °F	κ_{L}	16	_
	Transverse thermal conductivity, Btu in. hr ft ² °F	κ _T	8	_
	Absorptivity	α	0.85	_
	Emissivity	ϵ		

Table 2-4. - Estimated Mechanical Properties of 5.7 Mil Borsic/Aluminum

	Available in 1986. V _f = 0.50		Room temperature	450°F
Design	Longitudinal tensile ultimate, ksi	F _L tu	195	180
strengths "B" values	Transverse tensile ultimate, ksi	F _T tu	17.3	15.0
	Longitudinal compression ultimate, ksi	F _L cu	352	320
	Transverse compression ultimate, ksi	F _T cu	31.1	26.8
	Inplane shear ultimate, ksi	F _{LT} su	8.1	6.8
	Interlaminar shear ultimate, ksi	F ^{isu}	8.1	6.8
	Ultimate longitudinal tensile strain, μ in./in.	ϵ_{L}^{tu}	6 100	5 900
	Ultimate longitudinal compressive strain, μ in./in.	ϵ_{L}^{cu}	11 000	10 500
Elastic	Longitudinal tension modulus, 10 ⁶ lb/in ²	E _L ^t	32.0	30.5
properties (typ)	Transverse tension modulus, 10 ⁶ lb/in ²	E _T ^t	2.83	2.55
	Longitudinal compression modulus, 10 ⁶ lb/in ²	ELc	32.0	30.5
	Transverse compression modulus, 10 ⁶ lb/in ²	ETC	2.83	2.55
	Inplane shear modulus, 10 ⁶ lb/in ²	G_LT	0.67	0.58
	Longitudinal Poisson's ratio	μ_{LT}	0.30	0.30
	Transverse Poisson's ratio	μ_{TL}	0.027	0.025
Physical	Density, lb/in ³	ρ	0.098	0.098
constants (typ)	Longitudinal coefficient of thermal expansion, μ in./in./ $^{\circ}$ F	$lpha_{L}$	3.2	3.2
	Transverse coefficient of thermal expansion, μ in./in./ $^{ m o}$ F	$lpha_{T}$	10.6	10.6
	Longitudinal thermal conductivity, Btu in. hr ft ² °F	κ _L	600	-
	Transverse thermal conductivity, Btu in. hr ft ² °F	κ _T	440	_
	Absorptivity	α		-
	Emissivity	ϵ	_	_

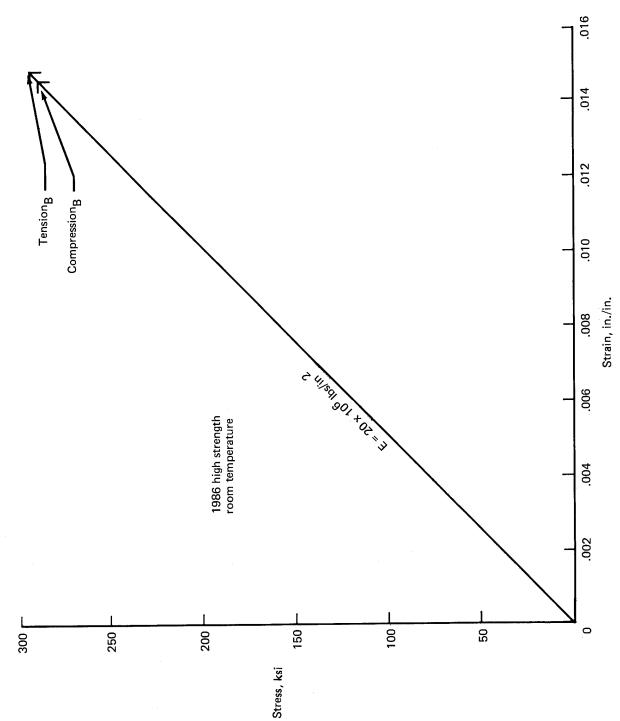


Figure 2-1.— Graphite/Polyimide Stress-Strain, Tension and Compression, [0] Orientation

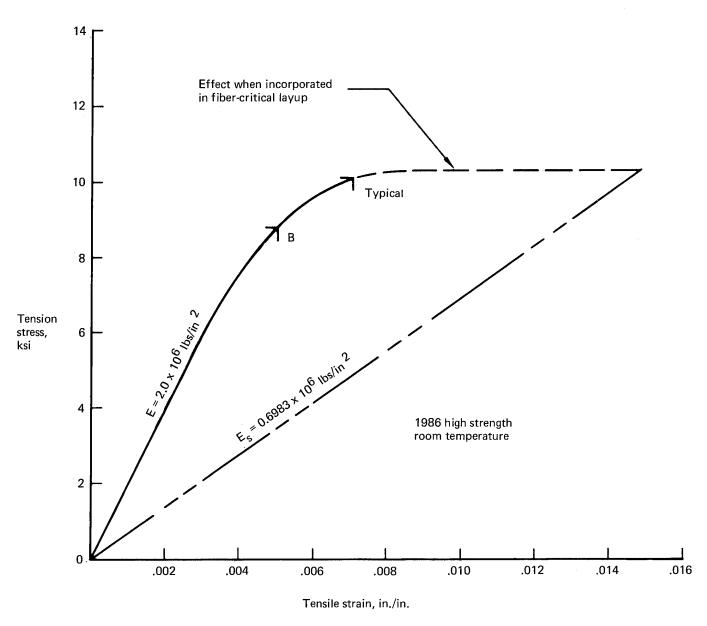


Figure 2-2.—Graphite/Polyimide Stress-Strain, Tension, [90] Orientation

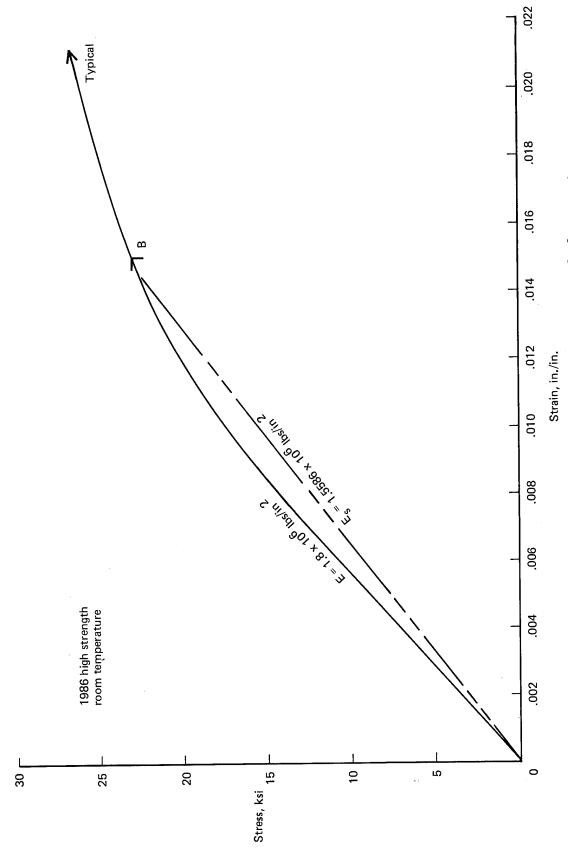


Figure 2-3.—Graphite/Polyimide Stress-Strain, Compression, [90] Orientation

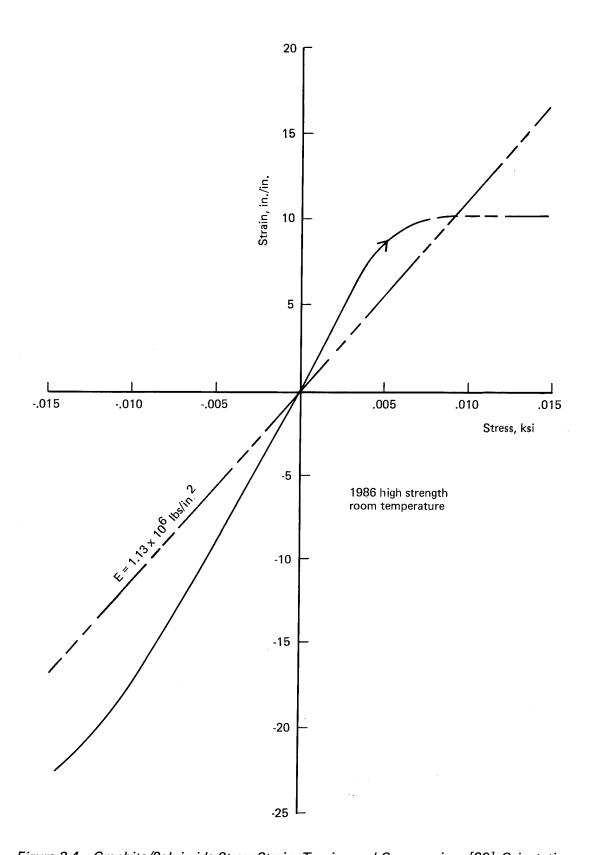


Figure 2-4.—Graphite/Polyimide Stress-Strain, Tension and Compression, [90] Orientation

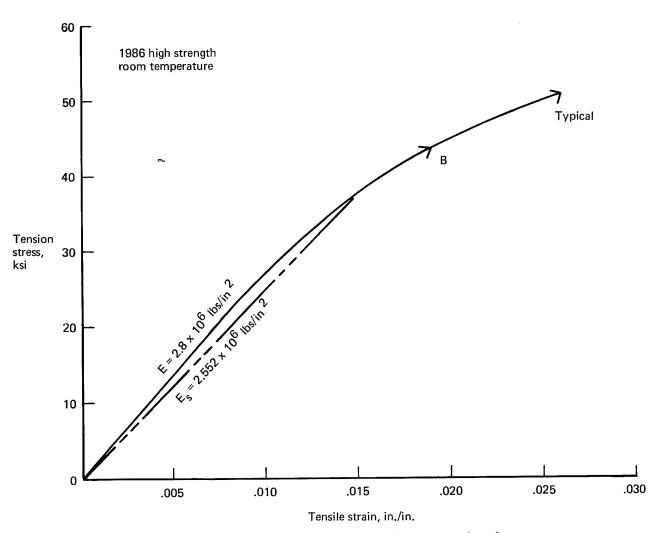


Figure 2.5.—Graphite/Polyimide Stress-Strain, Tension [± 45] $_{S}$ Orientation

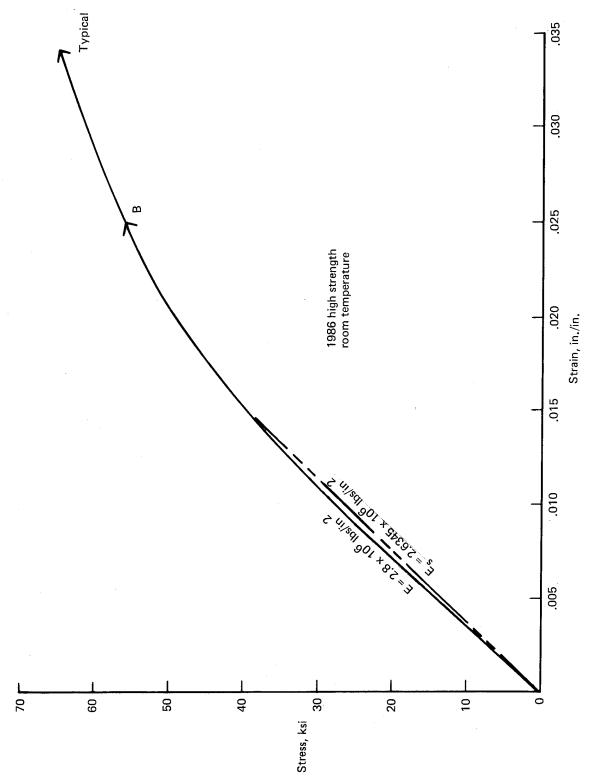


Figure 2-6.—Graphite/Polyimide Stress-Strain, Compression, $[\pm 45]_S$ Orientation

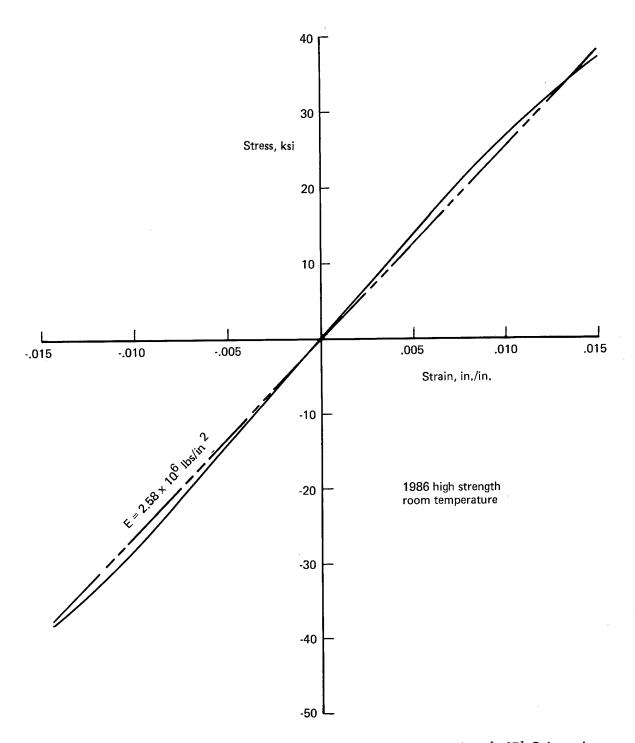


Figure 2-7.—Graphite/Polyimide Stress-Strain, Tension and Compression, $[\pm 45]$ Orientation

Blank Pages

SECTION 3

CONCEPT DESIGN AND MATERIAL SELECTION

by

V. D. BESS

CONTENTS

																	Page
INTRODUCTION	•		•	•					•					•			54
CONCEPT SELECTION																	
MATERIAL SELECTION	•								•	•	•	•	.•	•	•	•	55
REFERENCES																	59

TABLES

No.				-	Page
3-1	Control Point Loads				60
3-2	Specific Mechanical Properties, [0]				
3-3	Specific Mechanical Properties, [±45] S Layups				62
3-4	Mechanical Properties and Specific Mechanical Properties, Room Temperature				63
3-5	Mechanical Properties and Specific Mechanical Properties, 450°F · · · · ·	•	•	•	64

FIGURES

No.		Page
3-1	Wing and Body Control Points	65
3-2	Borsic/Aluminum Concept Comparison	66
3-3	Borsic/Aluminum Skin Reinforced Titanium Stiffeners	67
3-4	Borsic/Aluminum Skin, Thin Titanium Core, Reinforced Titanium Stiffeners	69
3-5	Borsic/Aluminum Skin, Titanium Core	71
3-6	Graphite/PPQ Skin, Titanium Core	73
3-7	Baseline, Integrally Machined and Welded Titanium Skin and Stiffeners	75
3-8	Weight Comparison, Advanced Structural Concepts, Wing Lower Surface	77
3-9	Wing Skin Panel, Al Brazed Titanium Honeycomb	78
3-10	Weight Comparison, Advanced Structural Concepts, Wing Upper Surface	79
3-11	Borsic/Aluminum Skin, Reinforced Titanium Stiffeners, 17.75 Inch Frame Spacing	81
3-12	Borsic/Aluminum Skin, Titanium Core, Reinforced Titanium Stiffeners, 17.75 Inch	
	Frame Spacing	83
3-13	Borsic/Aluminum Skin, Titanium Core, 35.5 Inch Frame Spacing	85
3-14	Graphite/PPQ Skin, Titanium Core, 35.5 Inch Frame Spacing	87
3-15	Baseline, Titanium Skin and Stiffeners, 17.25 Inch Frame Spacing	89
3-16	Weight Comparison, Advanced Structural Concepts, Body	91
3-17	Minimum Gage Considerations	
3-18	Panel Weights for Spanwise Compression Loading	
3-19	Panel Weights for Chordwise Loading	
3-20	Panel Weights for Shear Loading	95

SYMBOLS

Ł:	Modulus of elasticity
E_c	Modulus of elasticity in compression
E _t	Modulus of elasticity in tension
Fcu	Ultimate compressive stress
F_{su}	Ultimate stress in pure shear
F _{tu}	Ultimate tensile stress
G	Modulus of rigidity (shear)
N	Load per inch of edge length, applied at the neutral axis of sandwich
t	Skin thickness or face thickness
ρ	Weight density
L	Longitudinal
T	Transverse

INTRODUCTION

The titanium arrow-wing structure that was developed during the Task II effort, reference 3-1, was redesigned to utilize composite material in the wing surfaces to assess the potential impact of advanced composites on the strength and flutter characteristics. Because of limited budget, it was decided to retain the titanium substructure as designed in Task II, initially, and to develop a new design for the external wing shell utilizing advanced composite materials. After resizing the surfaces, internal members would be appropriately resized in subsequent cycles of analysis of a more detailed study.

Composite concepts were studied at two different times during the arrow wing contract. During Task II three concepts (sheet-stiffener, stiffened thin honeycomb sandwich, and conventional sandwich panels) were used in exploratory design studies in fuselage and skin panels. The material combinations considered in these studies were: titanium stiffeners reinforced with borsic/aluminum, borsic/aluminum composite skins, sandwich panels composed of borsic/aluminum surfaces and titanium honeycomb core, and sandwich panels with graphite/PPQ surfaces and titanium honeycomb core. These concepts were used in the design of wing and fuselage panels for comparison with baseline titanium designs, and the most efficient concepts were identified.

Early in Task III, the material selection task was reopened and expanded to include consideration of polyimide resin, since significant progress had been made in solving the manufacturing problems associated with this organic matrix material. Only the conventional sandwich concept was considered at this stage, since that concept had been shown to be most efficient for all of the materials considered. The following sections describe these activities in greater detail.

CONCEPT SELECTION

Three advanced composite concepts were studied in Section 14 of reference 3-1. These consisted of skin stiffener, stiffened thin sandwich, and conventional sandwich designs. Initially, each concept was studied for application to a body panel at point 5, and upper and lower wing panels at point 269, as shown in figure 3-1. The study was limited to these two locations so that each concept could be developed in sufficient detail to establish feasibility for practical component design. This initial comparison was based on the design of full panels for each application. Each concept was designed using borsic/aluminum, and the conventional sandwich was also designed using the graphite/PPQ material for the face sheets. A unit weight comparison of the three concepts using borsic/aluminum is presented in figure 3-2. This shows that the conventional sandwich panel is lightest in weight. It should be noted that three of the wing surface panels have been evaluated with two different shear allowables since the preliminary published data contained inconsistent low values. Following consultation with NASA personnel, unpublished test data, providing justification for the higher theoretical allowables, were obtained, as explained in Section 2. These panels were designed for the loads presented in table 3-1.

The three types of skin panels designed for the wing lower surface are shown in figures 3-3, 3-4, 3-5 and 3-6. The baseline concept is the integrally machined and welded titanium skin and stiffener design shown in figure 3-7. Comparative weights of these designs are presented in figure 3-8, showing that

the graphite/PPQ conventional sandwich is lightest and the borsic/aluminum conventional sandwich is next lightest of the three designs.

Skin panel designs for the wing upper surface are also shown in figures 3-3, 3-4, 3-5 and 3-6. The baseline concept for comparison is the conventional aluminum brazed titanium honeycomb sandwich design presented in figure 3-9. The weight comparison of these designs is presented in figure 3-10, showing that graphite/PPQ conventional sandwich has a significant weight advantage over the others.

Fuselage skin panel designs are presented in figures 3-11, 3-12, 3-13, and 3-14. The baseline panel design is the titanium skin and stiffener panel with 17.25 in. frame spacing, shown in figure 3-15. Comparative weights of these designs are presented in figure 3-16, showing that the conventional graphite/PPQ sandwich is lightest with the conventional borsic/aluminum sandwich second. Based on these comparisons, it is clear that the graphite/PPQ conventional sandwich is the lightest design concept for all locations considered. This concept was recommended for further consideration.

MATERIAL SELECTION

Initially, interest centered on borsic-aluminum since this material showed great promise of maintaining significant strength at the temperatures at which the arrow wing supersonic cruise aircraft operates. Consequently, borsic/aluminum was selected for evaluation on the first set of three concepts: skinstringer, stiffened thin sandwich, and conventional sandwich.

Subsequently, however, interest in the organic matrix increased because of the much greater ease of fabrication, and the lower thermal conductivity. Fuel heating is a critical design consideration for supersonic cruise since the fuel is used as a heat sink for the environmental control system and other heat sources within the airplane. Because of this requirement, and the high conductance of aluminum brazed material, insulation is required for aluminum brazed titanium honeycomb sandwich panels. The use of aluminum matrix material for wing panel face sheets would provide a further increase in thermal conductance of the panels. The organic materials have lower conductivity and, therefore, will alleviate the thermal problem. There has been only limited development work on high temperature polymers, with the polyimide resins getting the greatest emphasis currently, and there is considerable promise that polyimide development problems will be overcome. The development risk is offset by the attractive characteristics of relatively low cost, low density, high shear strength, and moderate manufacturing complexity, compared to the metal matrix composites.

The four materials selected for evaluation were:

- High strength graphite/polyimide
- High modulus graphite/polyimide
- Boron/polyimide, and
- Borsic/aluminum

Design allowable strength, and typical elastic and physical properties, shown in Section 1, were projected through ten years of additional development. The material properties resulting from this projection were submitted to and approved by NASA Langley Research Center. Based on these

data, specific strengths and stiffnesses were compared, as shown in tables 3-2 and 3-3. The high strength graphite/polyimide and the boron/polyimide were selected for further study on this basis.

Tables 3-4 and 3-5 show the comparison of the specific properties for the selected candidates at room temperature and at 450°F, indicating generally that graphite has higher specific strength while boron has higher specific stiffnesses. These materials were next used in the design of skins for honeycomb panels to provide a broader basis for engineering evaluation.

The following ground rules were adopted for this study:

- (1) Layups were designed to be fiber-critical
- (2) All laminates were designed as balanced, symmetrical layups.

Ground rule (1) is consistent with expected improvements in properties of matrix materials to be achieved prior to 1986. Ground rule (2) was adopted to avoid unsymmetrical deformations due to curing and to the application of external loads. Minimum gage criteria were established to provide acceptable practical durability from operational considerations.

The minimum gages selected for the Task II titanium honeycomb skins were as follows:

	Wing Upper Surface	Wing Lower Surface
Inner Skin	.010	.010
Outer Skin	-015	.020

These values were based upon experience and stemmed from consideration of:

Walking loads, material handling, hail damage, runway debris, practical fabrication limits, and lightning strike.

It was recognized that the advanced composites are more susceptible to damage from impact and in general less forgiving than the conventional metals. Because of this, a somewhat arbitrary decision was made to use minimum gages such that the local moment of inertia of each skin would be four times that of the titanium equivalent. Since

$$I = \frac{b t^3}{12}$$

it follows that

$$4 (t_{\text{titanium}})^3 = (t_{\text{adv. composite}})^3$$

$$\frac{t_{adv. composite}}{t_{titanium}} = \sqrt[3]{4} = 1.5874 \approx 1.6$$

The resulting minimum gages for the advanced composites were:

	Wing Upper Surface	Wing Lower Surface
Inner Skin	.016	.016
Outer Skin	.024	.032

A second procedure for estimating minimum gages is as follows: The ply thicknesses expected to be available by 1986 for these materials are:

Boron/Polyimide

5.2 mil, 7.0 mil and thicker

H.S. graphite/polyimide

2 mil, 3 mil, 4 mil and thicker

In order to comply with the indicated ground rules, the following layups were established for minimum gage areas:

$$\frac{\text{Boron/Polyimide}}{[0/\pm 45/90]_{\text{S}}}$$
7 plies x .0052 = .0364

This resulted in the following:

	Wing Upper Surface	Wing Lower Surface
Inner Skin	.0364	.0364
Outer Skin	.0364	.0364
Graphite/Polyimide [0/±45/90] _S		
8 plies x .002, .003 ar	nd .004 = .016, .024 and .032	

This resulted in the following:

	Wing Upper Surface	Wing Lower Surface
Inner Skin	.016	.016
Outer Skin	.024	.032

A comparison was then made of the skin weights per square foot for the titanium, boron/polyimide and H.S. graphite/polyimide. Weight densities of 0.16 lb/in³, .0725 lb/in³ and .056 lb/in³, respectively, were used.

The resulting weights are presented in figure 3-17 and show the H.S. graphite/polyimide to be significantly lighter.

A review of the wing structure that was resized during Task II using titanium showed that approximately 50% of the area was minimum gage. The resized area lies generally between the rear spar and the leading edge spar and between the side of body and the wing mounted fin. The control surfaces and the fixed leading edge structure were minimum gage.

Using H.S. graphite, and with the anticipated change in loads, it is estimated that 30-35% of the resize portion will be minimum gage. Using boron/polyimide it is estimated that 70% of this area would be minimum gage.

For structure designed by tension loads it is obvious, from a comparison of specific tensile strengths, that the H.S. graphite will be the lightest. This is true even after restricting the allowable strain to that of titanium.

In areas where loads require less than minimum gage it is again apparent that H.S. graphite will be the lightest.

A final parametric comparison was made to establish which of the materials would result in the lightest cover panels to resist spanwise compression, chordwise compression and shear loads considering typical layups and ply orientations. Figure 3-18 compares the weight of boron and graphite layups designed to carry the indicated spanwise compression loads. From this figure, it can be seen that the high strength graphite results in lighter panels across the complete loads range. Figure 3-19 presents similar data for the range of chordwise compression loads, with a similar conclusion. Figure 3-20 is a similar presentation for shear loads. The graphite layups again are significantly lighter than the boron layups.

Based on these data and analyses, the high strength graphite fibers are selected for use in the conventional sandwich structural panels.

REFERENCES

3-1 Boeing Staff: Study of Structural Design Concepts for an Arrow Wing Supersonic Transport Configuration. NASA Langley Research Center, CR 132576-1 and -2, 1976.

Table 3-1.— Control Point Loads

Body: control point 5 (lower body skin panel)

Design condition					
N _X	(11.92 kips/in.)				
Pressure	(10.78 lb/in ²)				
Temperature	(450° F)				

Wing: control point 269

Component	Design condition					
Upper panel	N _x N _y N _{xy} Temperature	-10.9 kips/in. - 1.48 kips/in. 6.32 kips/in. 250° F				
Lower panel	N _X N _y N _{XY} Temperature	11.82 kips/in. 2.04 kips/in. 6.89 kips/in. Room temperature				

Table 3-2.—Specific Mechanical Properties

	F _{tt}	$F_{tu/ ho}$ in x 10^3	F _c	$F_{cu/\rho}$ in $\times 10^3$	$F_{\text{Su}/\rho}$ in $\times 10^3$	$E_{t/ ho}$ in x 10	$E_{t/ ho}$ in x 10^6	$E_{\rm C}/ ho$ in $ imes$ 10	$E_{c/ ho}$ in $ imes 10^6$	G/ ho in $ imes 10^6$
		F		L	LT		F	1	F	LT
High strength graphite, $\rho = 0.056$ lbs/in ³	5268	298	5179	293	371	357	20	357	20	13
High modulus graphite, $\rho = 0.058$ lbs/in ³	2552	116	2172	86	107	069	31	069	31	17.0
Boron/polyimide, $\rho = 0.0725 \text{ lbs/in}^3$	2690	201	4828	364	114	441	33	441	33	9.0
Borsic/aluminum, $\rho = 0.098 \text{ lbs/in}^3$	1990	177	3592	317	83	327	29	327	29	7.0

Table 3-3.—Specific Mechanical Properties [± 45] $_{S}$ Layups

Material	F _{tu/p} in. x 10 ³	F _{cu/p} in. x 10 ³	F _{su/p} in. x 10 ³	Ε/ρ in. x 10 ⁶	G/ρ in. x 10 ⁶
High strength graphite, $\rho = 0.056$ lbs/in 3	679	670	2643	46	91
High modulus graphite, ρ = 0.058lbs/in 3	222	190	1109	60	176
Boron/polyimide, $\rho = 0.0725$ lbs/in ³	210	379	1407	34	116
Borsic aluminum, ρ = 0.098 lbs/in. ³	149	269	1031	24	85

Table 3-4.—Mechanical Properties and Specific Mechanical Properties, Room Temperature

[0]

	F _{tu}	$F_{tu/\rho}$	F _{cu}	F _{cu/p}	F _{su/p}	E	Ε/ρ	G G/ρ
	L	Т	L	Т	LT	L	Т	LT
Material	ksi in, x 10 ³	ksi in. x 10 ³	10 ⁶ psi in. x 10 ⁶	10 ⁶ psi in. x 10 ⁶	10 ⁶ psi in. x 10 ⁶			
High strength graphite	295.0	16.7	290.0	16.4	20.8	20.0	1.1	0.72
Boron/polyimide	195.0	14.6	350.0 4828	26.4	8.3	32.0 441	2.4	0.68

[±45]

Material	F _{tu} F _{tu/p} ksi in. x 10 ³	ksi	ksi	10 ⁶ psi	G G/p 10 ⁶ psi in. x 10 ⁶
High strength graphite	38.0	37.4	148.0	2.6	5.1
Boron/polyimide	15.2	27.5	102.0	2.5	116

Table 3-5.—Mechanical Properties and Specific Mechanical Properties, 450 $^\circ$ F

[0]

·	F _{tu}	$F_{tu/\rho}$	F _{cu}	F _{cu/p}	F _{su} F _{su/p}	E	Ε/ρ	G G/ρ
Material	L	Т	L	Т	LT	L	Т	G
	ksi in. x 10 ³	10 ⁶ psi in. x 10 ⁶	10 ⁶ psi in. x 10 ⁶	10 ⁶ psi in. x 10 ⁶				
High strength graphite	265.0 4732	13.7	260.0 4643	13.4	12.0	20.0	1.0	0.46 8.25
Boron/polyimide	175.0	13.0	315.0 4345	23.1	7.1	30.0	2.2	0.6 8.28

[±45]

	F _{tu}	F _{cu}	F _{su}	E	G
Matarial	F _{tu/ρ}	/C) /r	Ε/ρ	G/ρ
Material	in, x 10 ³	in. x 10 ³	in. x 10 ³		10 ⁶ psi in. x 10 ⁶
High strength graphite	22.5	22.1	132.6	1.7	5.1 91
Boron/polyimide	13.6	332	92.0	2.3	7.8

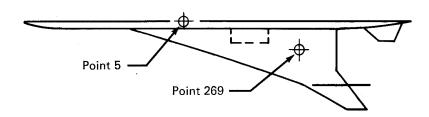


Figure 3-1.—Wing and Body Control Points

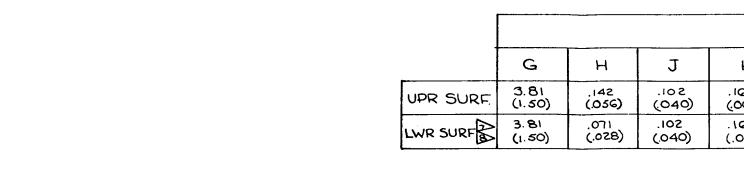
		C	
		Unit weight, lb/ft ²	
Structural concept	Body	Wing upper surface	Wing lower surface
Titanium Borsic/aluminum	4.34 (Includes 0.0 36 braze)	4.29 (Includes 0.020 braze)	4.24 3.46 ^a (Includes 0.017 braze)
Titanium Borsic/aluminum	4.29 (Includes 0.104 core 0.219 braze)	3.95 3.37 ^a (Includes 0.143 core 0.176 braze)	4.40 (Includes 0.056 core 0.124 braze)
Titanium Borsic/aluminum	3.61 (Includes 0.681 core 0.348 braze)	3.61 (Includes 0.519 core 0.248 braze)	4.01 3.42 ^a (Includes 0.384 core 0.202 braze)

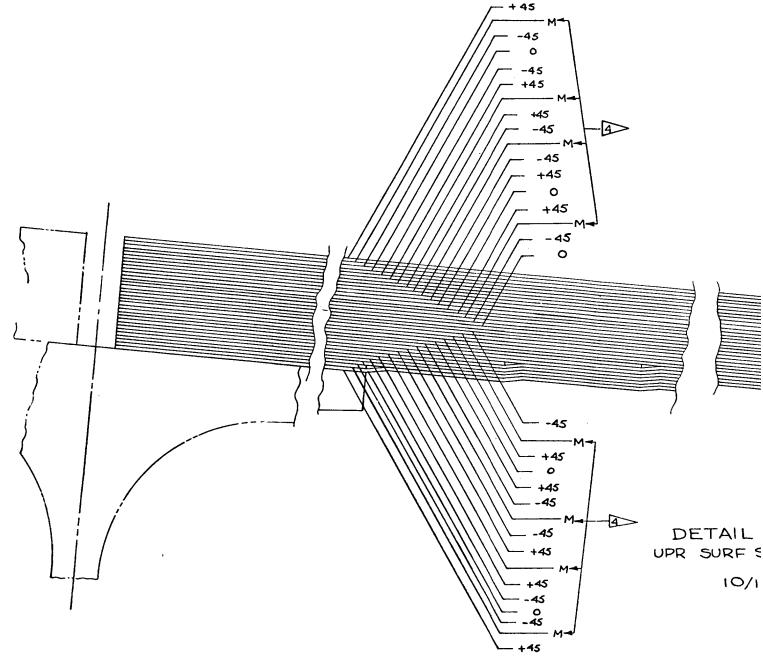
Note: Indicated weights do not include thermal insulation,

Figure 3-2.—Borsic/Aluminum Concept Comparison

^aHigh shear allowable derived from NASA-LRC tests.

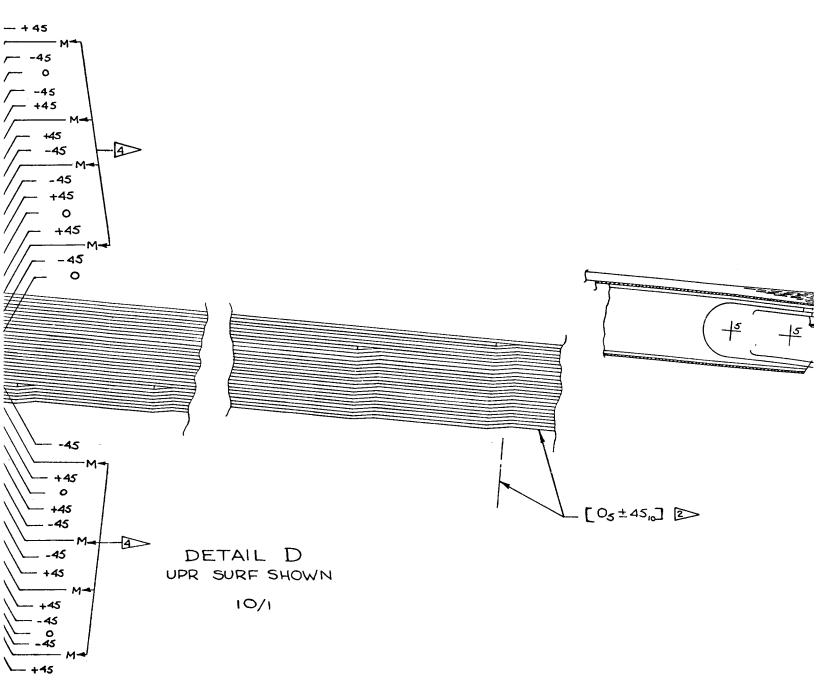


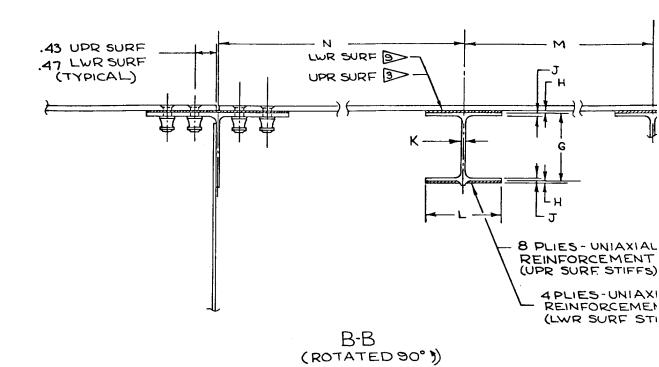




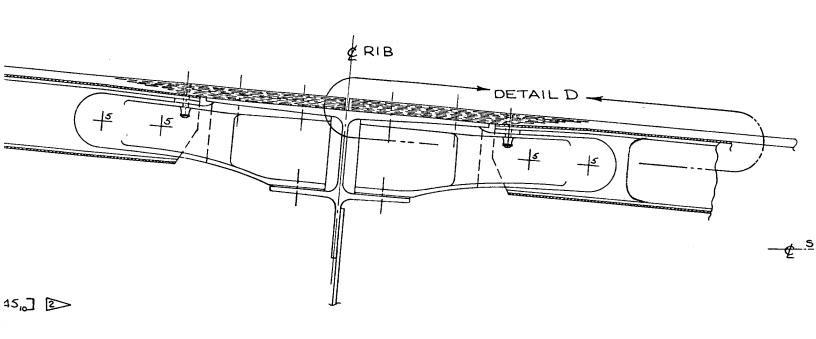


	DIMENSION									
Ī	G	Н	J	К	L	М	N			
۲F.	3.81 (1.50)	.142 (.056)	.10 2 (040)	.1GO (.0G3)	4.06 (1.60)	12.19 (4.80)	13.97 (5.50)			
200	3. <i>81</i> (1.50)	,071 (850.)	.102 (.040)	.160 (.063)	4.06 (1.60)	17.02 (6.70)	18.92 (7.45)			

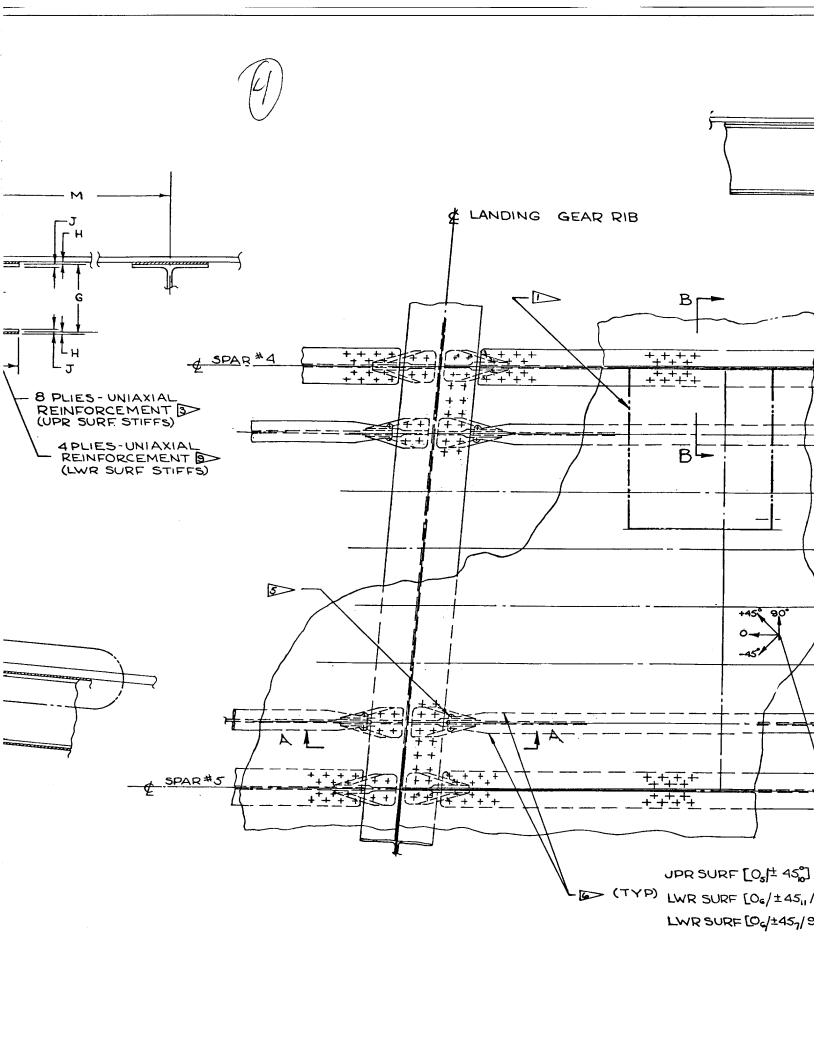


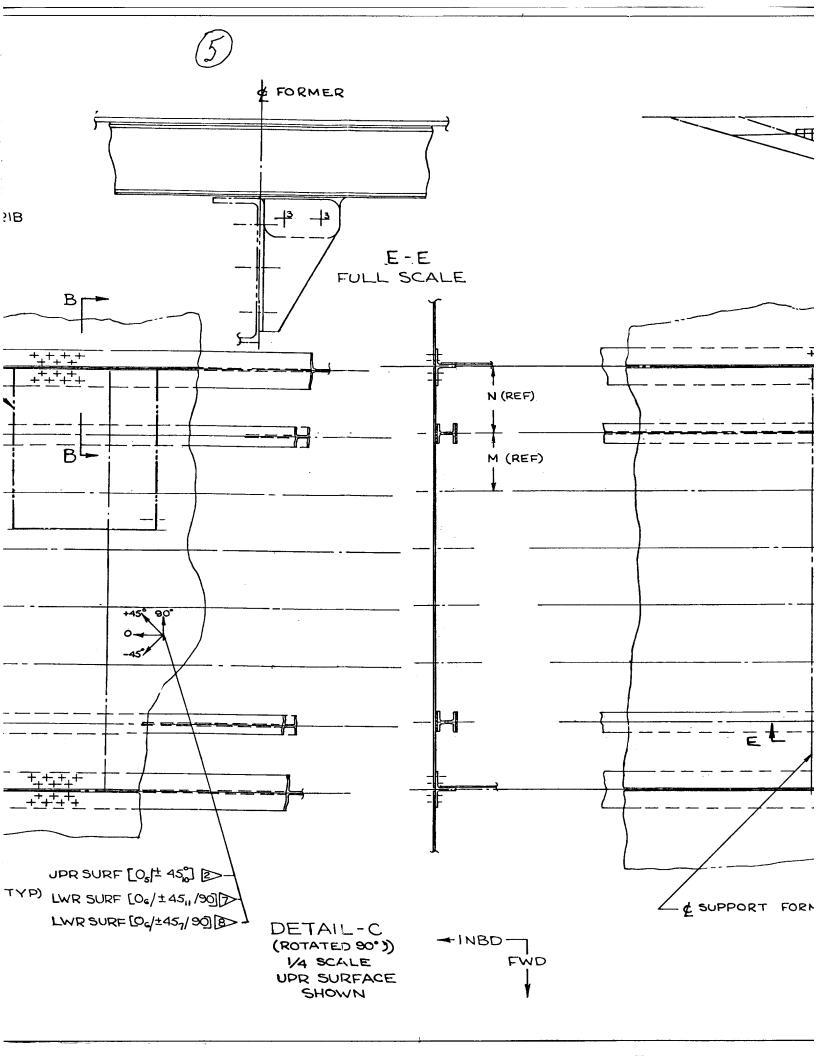


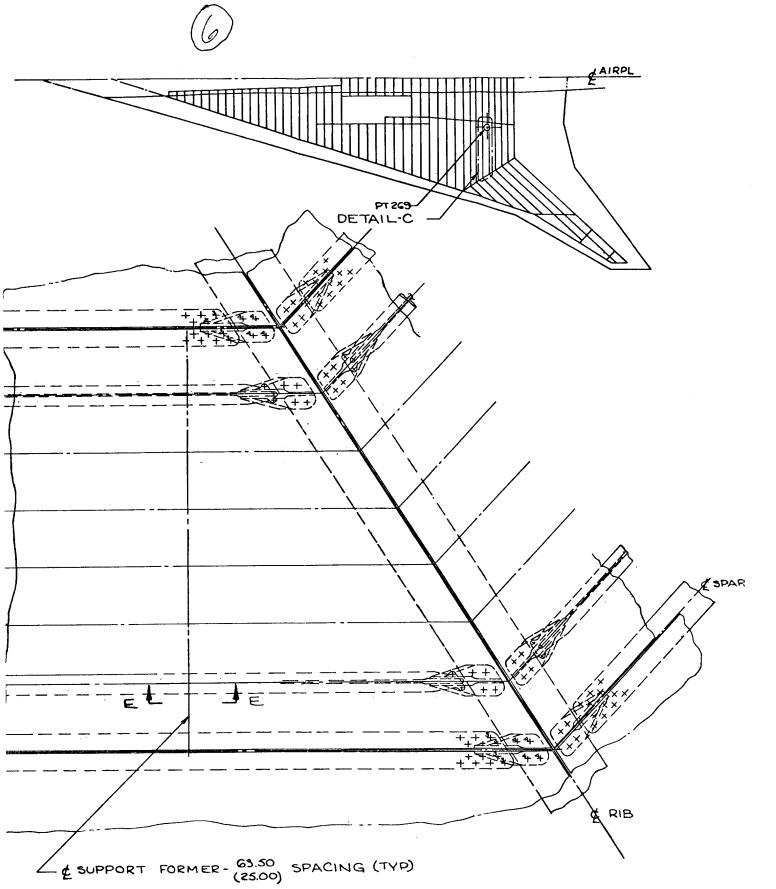
FULL SCALE



A-A FULL SCALE







Figur

	CHG	DESCRIPTION:	DATE	Vobo
7	Δ.	REVISED DUG TO ADD LUR WING SURFACE REQUIRMENTS ADDELD BY THEIJ BY	6/6/74	DESIGN N H.T. STNESS.

- BS/AL UNIAXIAL REINFORCEMENT
 (4)- O'PLIES PER LOCATION, .007 IN /PLY
 MATL LWR SURFACE STIFFS (TYP)
- PER A.F. DELSIGN GUIDEL DATA EXCLEPT FOR SHEAR PROJECTED FROM NASA-LANGLEY DATA WING UPR SURFACEL BS./AL SKIN ASSY (DASOLIDATED OF 21 PLIES OF .007 IN/PLY MATL. (G)-C'PLIES, (7)+ 45°PLIES, (7)-45°PLIES, (1) 90°PLY. SEE DETAIL D FOR REINFORCEMENT DETAIL.
- PER A.F. DESIGN GUIDE DATA. WING LOWER SURFACE BS/AL SKIN ASSEMBLY CONSOLIDATED OF 29 PLIES OF .007 INL/PLY MATERIAL.

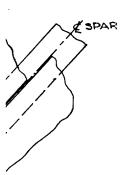
 (G)-0° PLIES, (II)+45° PLIES (II)-45° PLIES, (I)-50° PLY SEE DETAIL D FOR REINFORCEMENT DETAIL.
- SPOTBRAZE STIFFENERS TO FACE SHEET (SPOTWELD SPEC AND BRAZE TIME. & CYCLE UNDETERMINED)
- 5/32 IN DIA. HI LOC FASTENERS TO PREVENT BRAZE PEELING
- 007 IN THICK TITANIUM SHIM-GAL-4V. 8 REQD UPR & LWR SURF (TYPICAL)
- BORSIC ALUMINUM-UNIAXIAL REINFORCEMENT (8)- O' PLIES PER LOCATION .007 IN / PLY MATERIAL - UPR SURFACE STIFFS (TYP)
- WING UPPER SURFACE
 BORSIC ALUMINUM SKIN ASSY CONSOLIDATED
 OF 25 PLIES OF .007 IN./PLY MATERIAL
 (5)-0°PLIES, (10) + 45°PLIES, (10) 45°PLIES
 SEE DETAIL D FOR END REINFORCEMENT
 DETAILS
- PT 269 CONTROL POINT COUPON SIZE AND LOCATION SAME AS FOR TASK I

BASIC DIMENSIONS - CENTIMETERS

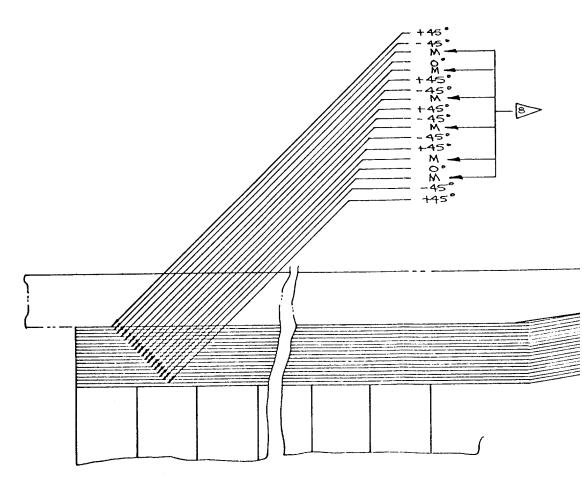
() DIMENSIONS - INCHES

Ref. WING DRAWING AWS-143

Figure 3-3.—Borsic/Aluminum Skin, Reinforced
Titanium Stiffeners

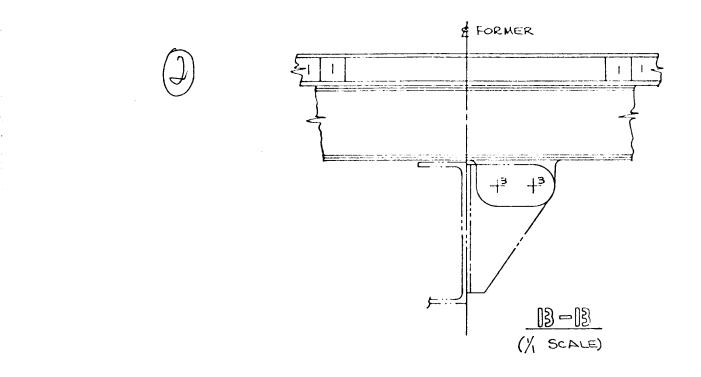


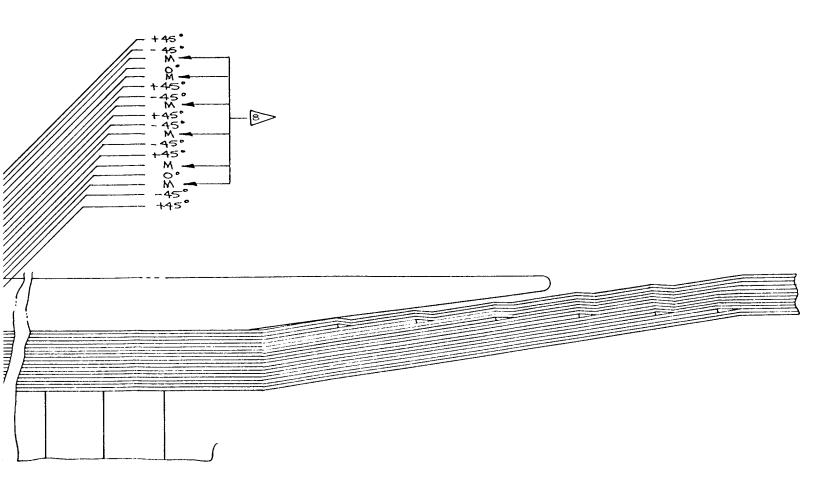




DETAIL -E

(b/1 SCALE)
(UPPER SURFACE SHOWN ONLY)

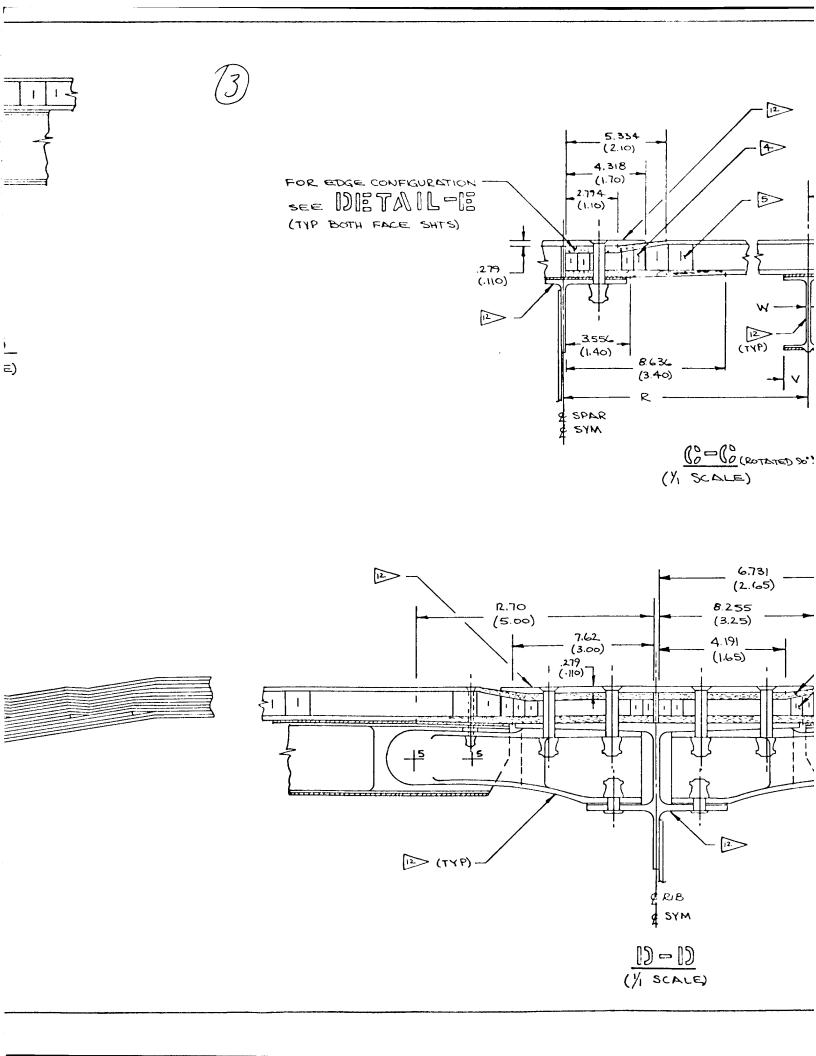


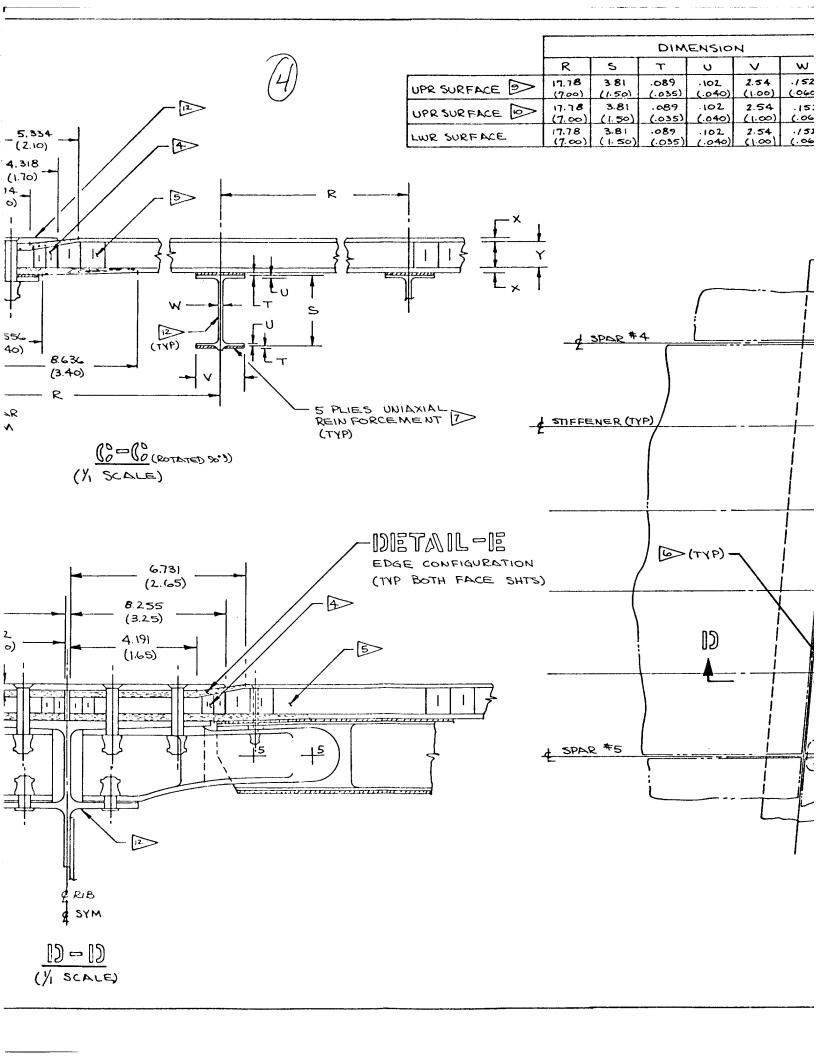


erall - E

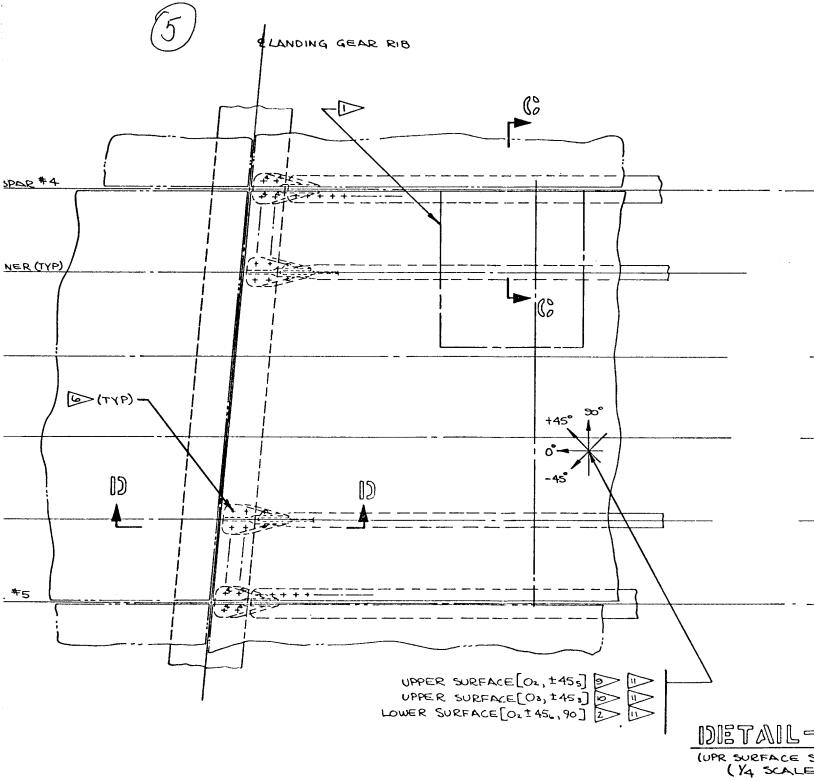
1/1 SCALE)

SURFACE SHOWN ONLY)



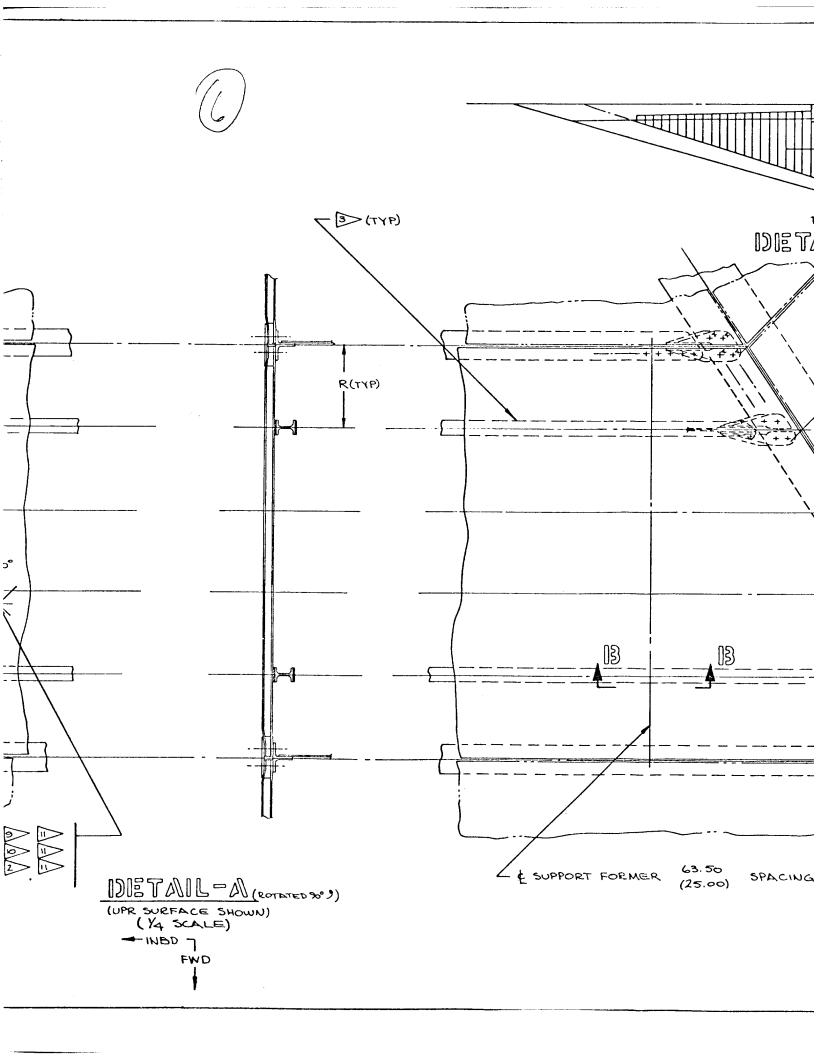


	DIM	ENSIO	7		_	
5	т	v	>	W	×	Υ
3.81	.089 (.035)	·102 (.040)	2.54 (1.00)	.152	, 213 (084)	.762 (·30)
3.81	.089 (.035)	.102 (.040)	2.54 (1.∞)	(.060)	.160	.762.
3.81	.089 (.035)	.102	2.54	·/52 (.060)	.267	.386



- INBD 7

FWD



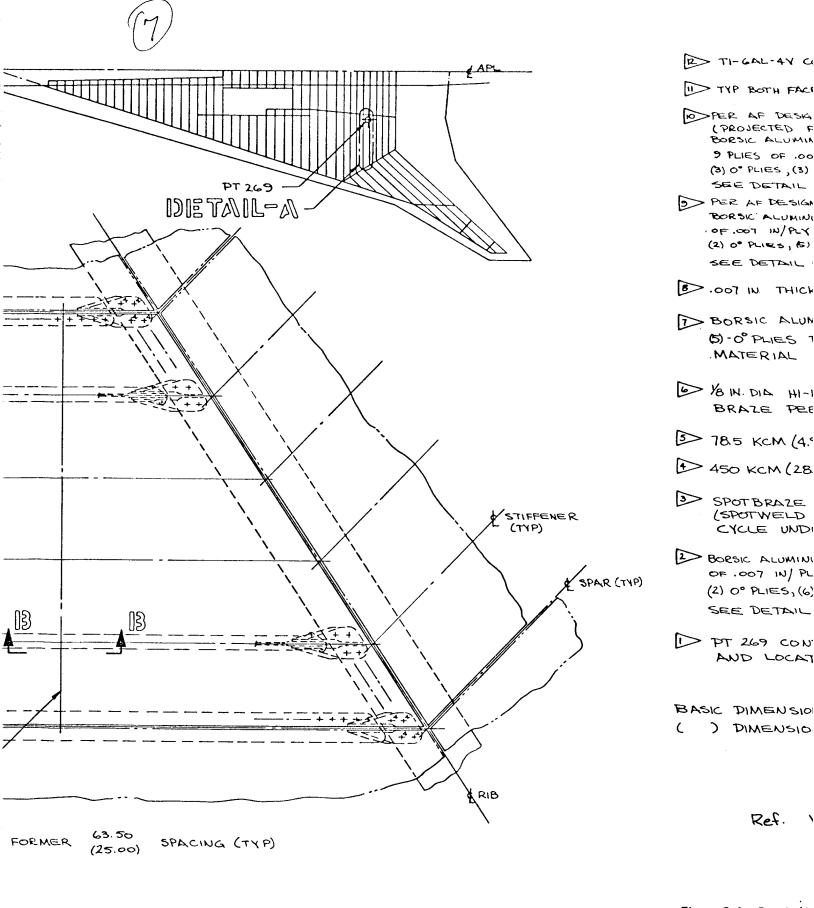


Figure 3-4.—Borsic/Al Core, Rei



- R TI-GAL-4Y COND I
- TYP BOTH FACE SHTS FACE SHTS SYM ABOUT & OF CORE
- PER AF DESKN GUIDE DATA EXCEPT FOR SHEAR DATA
 (PROJECTED FROM NASA-LANGLEY DATA). UPR SURFACE
 BORSIC ALUMINUM SKIN ASSY CONSOLIDATED OF

 9 PLIES OF .OOT IN/PLY MATERIAL
 (3) O' PLIES, (3) + 45° PLIES, (3)-45° PLIES
 SEE DETAIL E FOR END REINFORCEMENT
- PER AF DESIGN GUIDE DATA. UPPER SURFACE

 BORSIC ALUMINUM SKIN ASSY CONSOLIDATED OF 12 PLIES

 OF .007 IN/PLY MATERIAL

 (2) 0° PLIES, E)+45° PLIES, E)-45° PLIES

 SEE DETAIL E FOR END REINFORCEMENT
- 8 .007 IN THICK TITANIUM SHIM TI-GAL-4V
- BORSIC ALUMINUM UNIAXIAL REINFORCEMENT

 (5)-0° PLIES PER LOCATION .007 IN/PLY

 MATERIAL
- BRAZE PEELING
- > 785 KCM (4.9 RF) SC4-20 CORE TI-3AL-2.5V
- \$ 450 KCM (281 PCF) \$\$2-60 CORE TI-GAL-4V
- SPOTBRAZE STIFFENERS TO FACE SHEET (SPOTWELD SPEC & BRAZE TIME & CYCLE UNDETERMINED)
- BORSIC ALUMINUM SKIN ASSY CONSOLIDATED OF 15 PLIES OF .007 IN/PLY MATERIAL

 (2) 0° PLIES, (6)+45° PLIES, (6)-45° PLIES, (1) 90° PLY

 SEE DETAIL E FOR END REINFORCEMENT
- PT 269 CONTROL POINT COUPON SIZE AND LOCATION SAME AS FOR TASK I

BASIC DIMENSIONS - CENTIMETERS

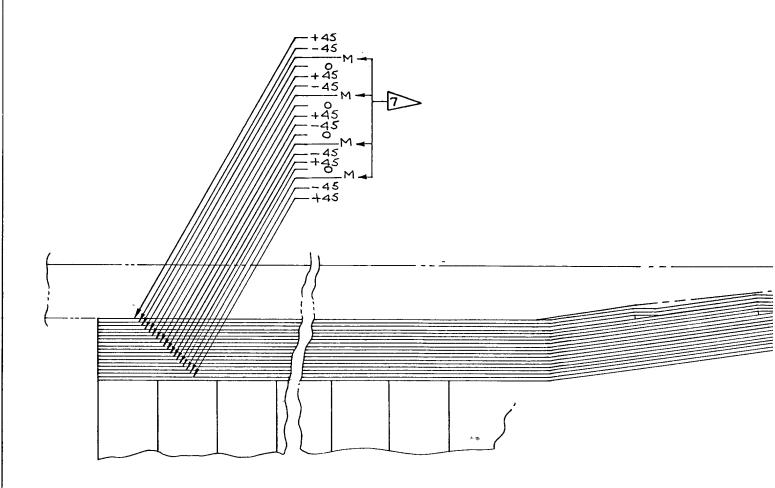
() DIMENSIONS - INCHES

AR (TYP)

Ref. WING DRAWING AWS-149

Figure 3-4.—Borsic/Aluminum Skin, Thin Titanium Core, Reinforced Titanium Stiffeners



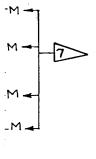


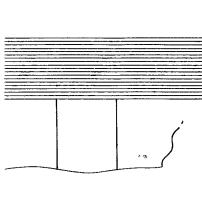
(UPPER SURFACE SHOWN ONLY)

DETAIL D

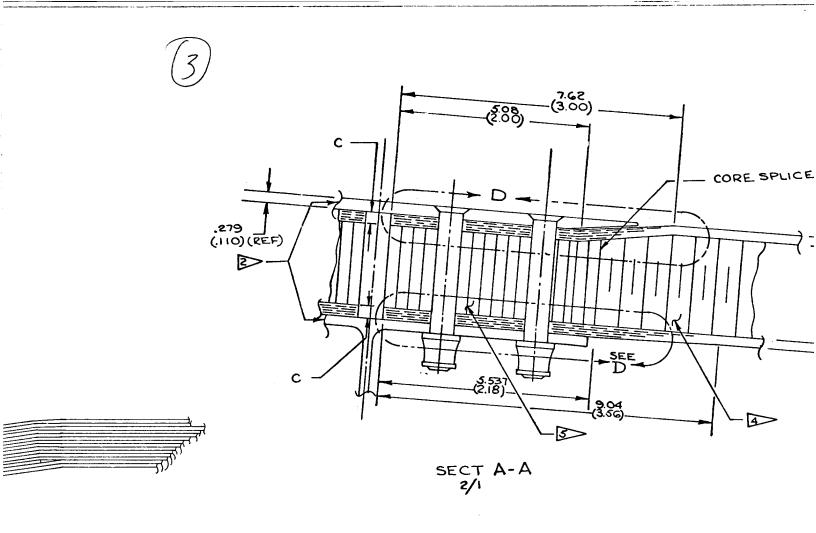
10/1



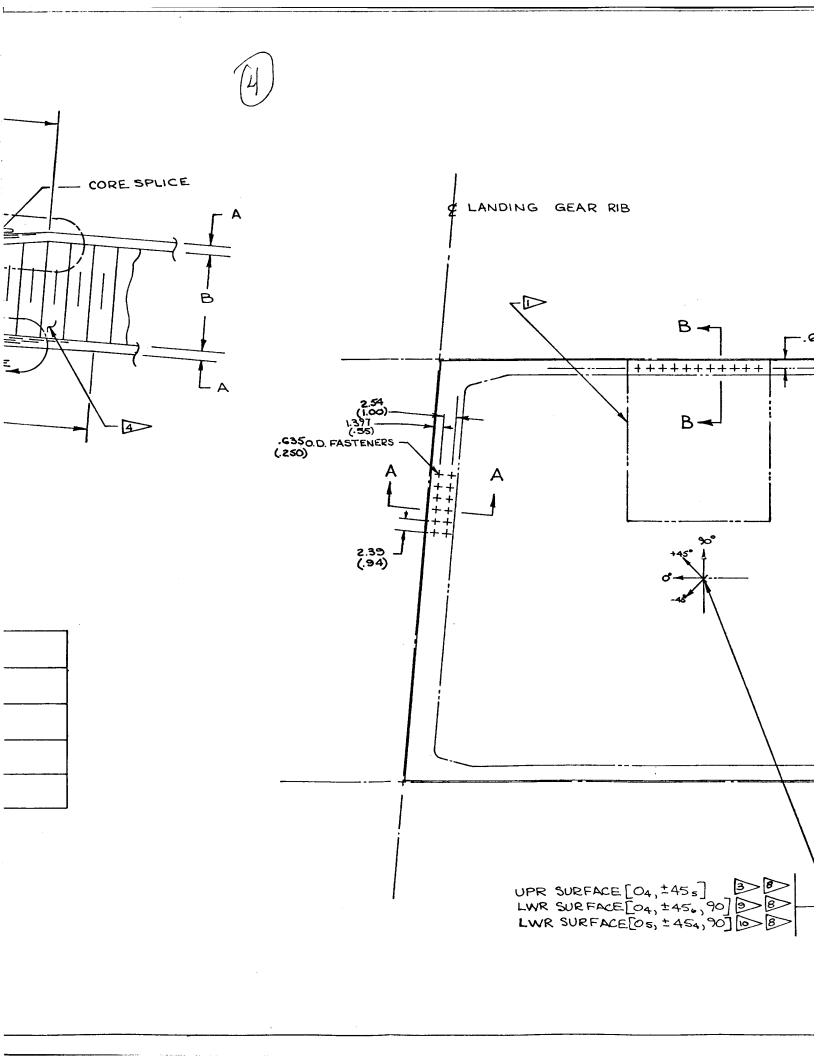


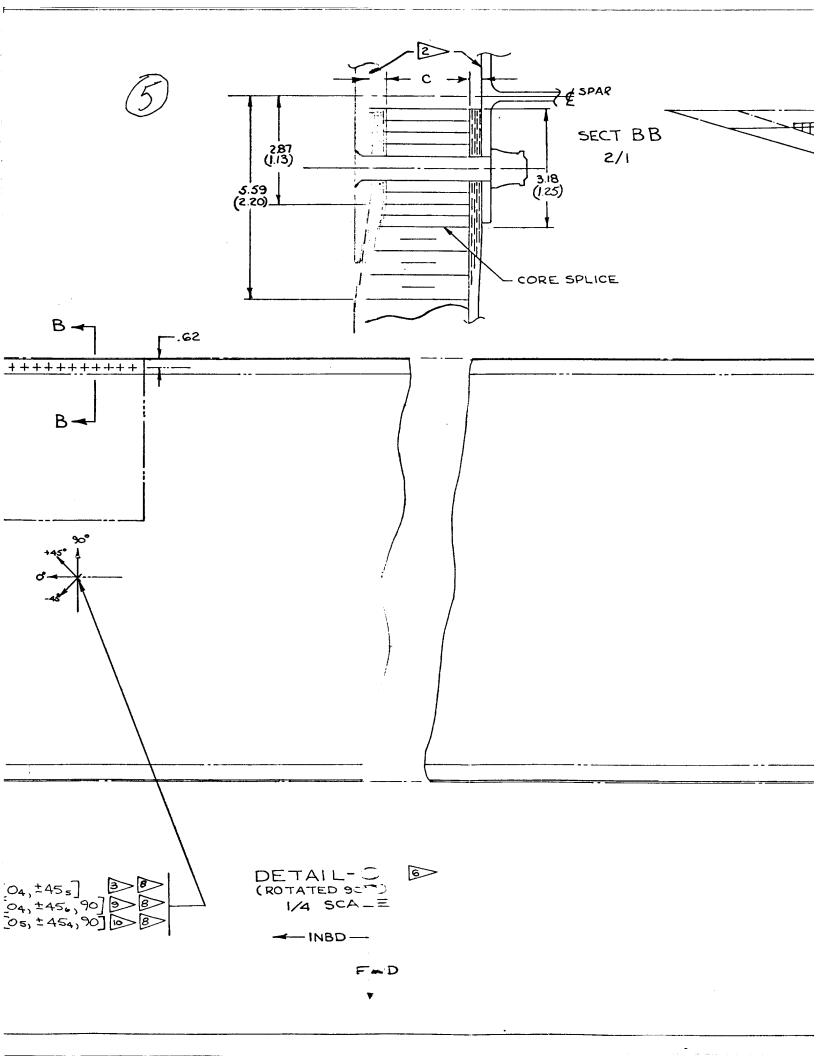


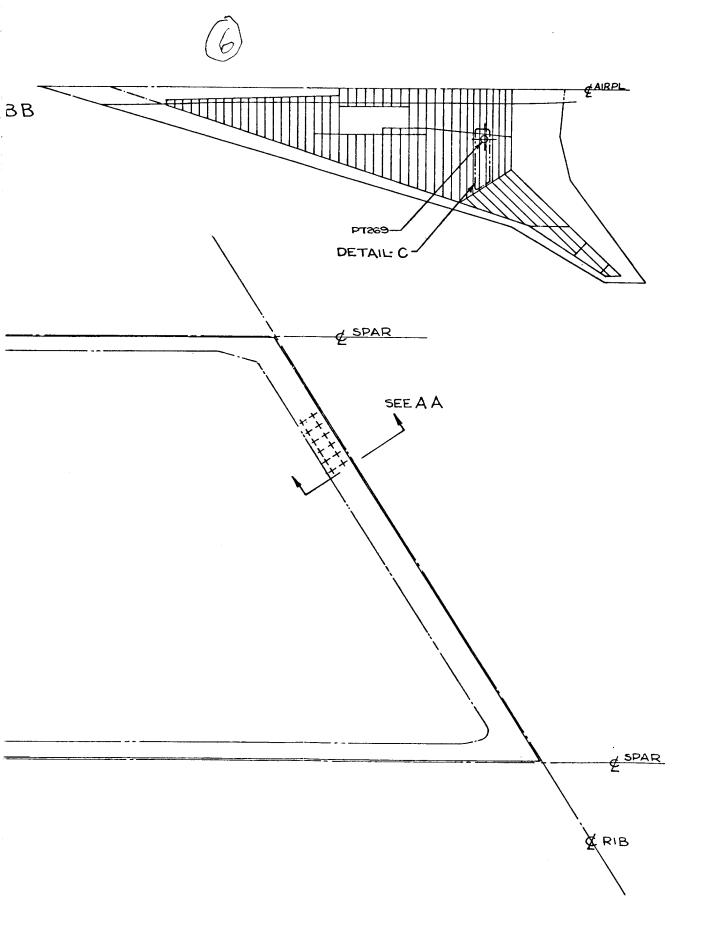
N ONLY)



	<u>.</u>	DIMENSION								
LOCATION	А	В	С							
UPR SURFACE	.248 (098)	2.54 (1.00)	.320 (.126)							
LWR SURFACE	.302 (211.)	1.91 (75)	. 373 (.147)							
LWR SURFACE	.249 (.098)	1.91 (25.)	.32 <i>0</i> (.126)							







PER PER SKIN 8> TYP : 700. BRAZ TEM **5**> 450 78.5 BORS 14PLI (4) (3> TITA PT 26 USEE SEE AV BASIC D) DI

(PRC BOR OF. (5) c

TAM (4) c

4 ME UPPE

Figure 3-5.—Bors

REF.

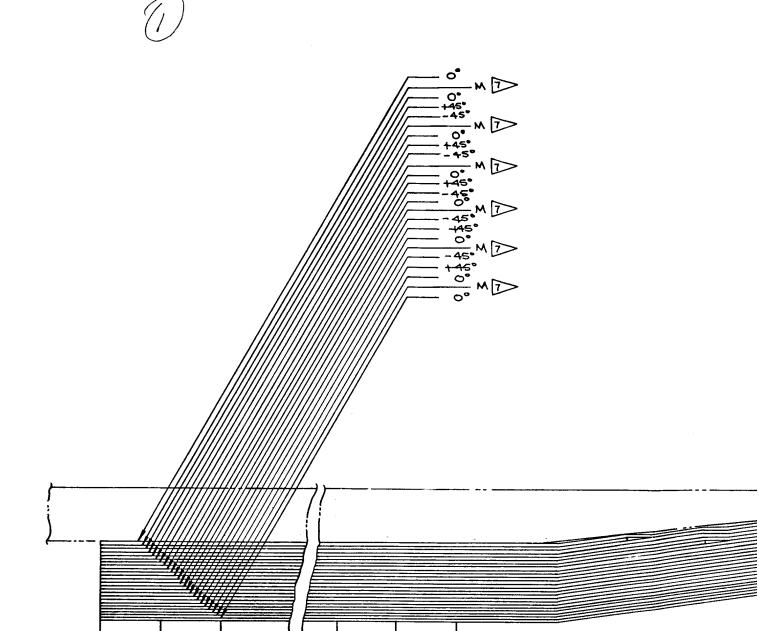
Mantelland : 41 cm				
	CHG.	DESCRIPTION	DATE	APPO.
	A	REVISED DWG TO REFLECT ONE UPR & TWO LWR SURFACE DESKUE REVISED B> D>B> ADDED B>D>> CHANGED TO SHT 1 OF 2	5-30-74	PERMAN PSQ STRESS;
(PROBORING SEIN) PER SKIN MAT (4) C TYP 4 ME	SIC ALI SIC ALI PLIE: AF DE LASSY C ETEIAL PLIES THICK- TAL PI	SIGN GUIDE DATA EXCEPT FOR SHIP FROM NASA-LAXALEY DATA) LOWE UM SKIN ASSY CONSOLIDATED OF PLY MATERIAL S, (4)-45° PLIES, (4)-45° PLIES, SIGN GUIDE DATA. LWR SURFACE DINSOLIDATED OF 17 PLIES OF . (6)+45° PLIES, (6)-45° PLIES, (1) KINS. SKINS SYM ABOUT & OF CATTANIUM SHIM GAL-4Y COUD I LES PER SKIN REQUIRED FOR B. LOWER PANEL ASSEMBLIES	14 PL (1) 90° 1 : BORS 007 IN) 90° PI DRE	I=ACE LIES FLY IIC/ALUM PLY
		NEL ASSEMBLY - (BRAZE CYCL TURE UNDETERMINED)	E TIMI	EI 4
№ 450	KCM	(28.IPCF) 552-60 CORE THEAL-	4٧	
_		4.9 PCF) - SC4-20 CORE TI-3AL		
(4)	D. Bries	MINUM SKIN ASSEMBLY CONSOLI .007 IN/PLY MATERIAL 5, (5)+45° PLIES, (5)-45° PLIES GAL-4V COND. I	DATED	OF
PT 20 USED	9 CON	TROL POINT COUPON SIZE AND LOCATI	TION SA	ME AS
SEE AI	JS-10	O FOR LOADS & ENVIRONMENTA	L CONI	DITIONS

BASIC DIMENSIONS - CENTIMETERS () DIMENSIONS - INCHES

PAR

REF. WING DRAWING AWS 145

Figure 3-5.—Borsic/Aluminum Skin, Titanium Core



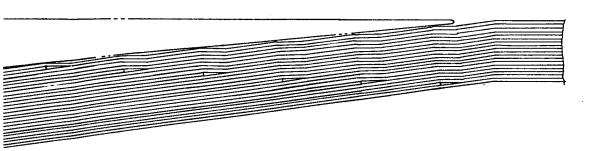
(TYP BOTH FACE SHTS)

DITTALL - D

10/1 SCALE

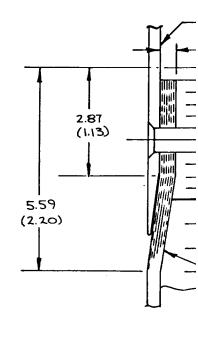
(URR SURFACE PANEL SHOWN, LWR SURFACE TYP)



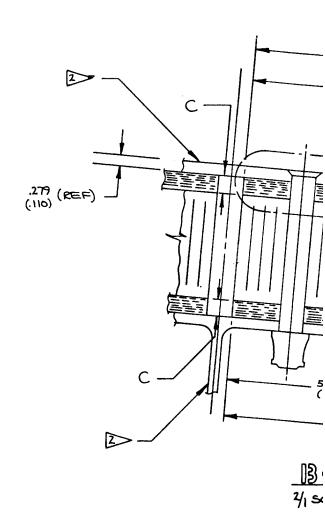


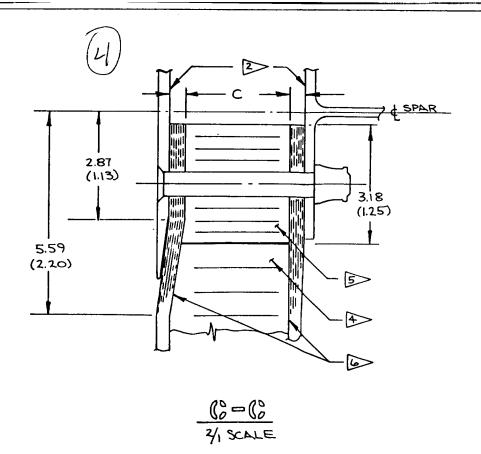
LOCATION	A	
UPR SURFACE	.2377 (.0936)	
LWR SURFACE	.2509 (.0988)	



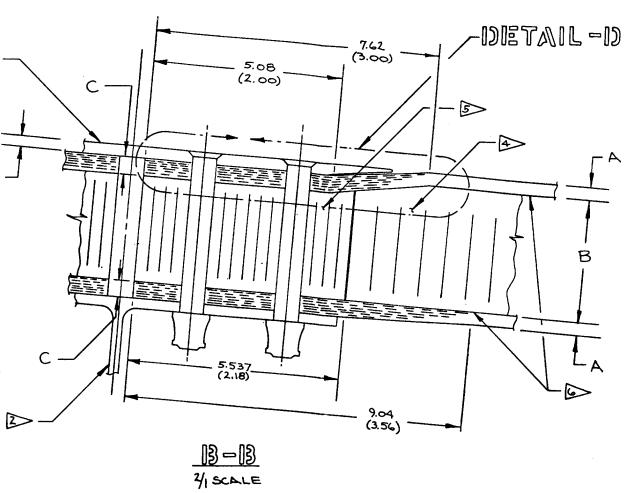


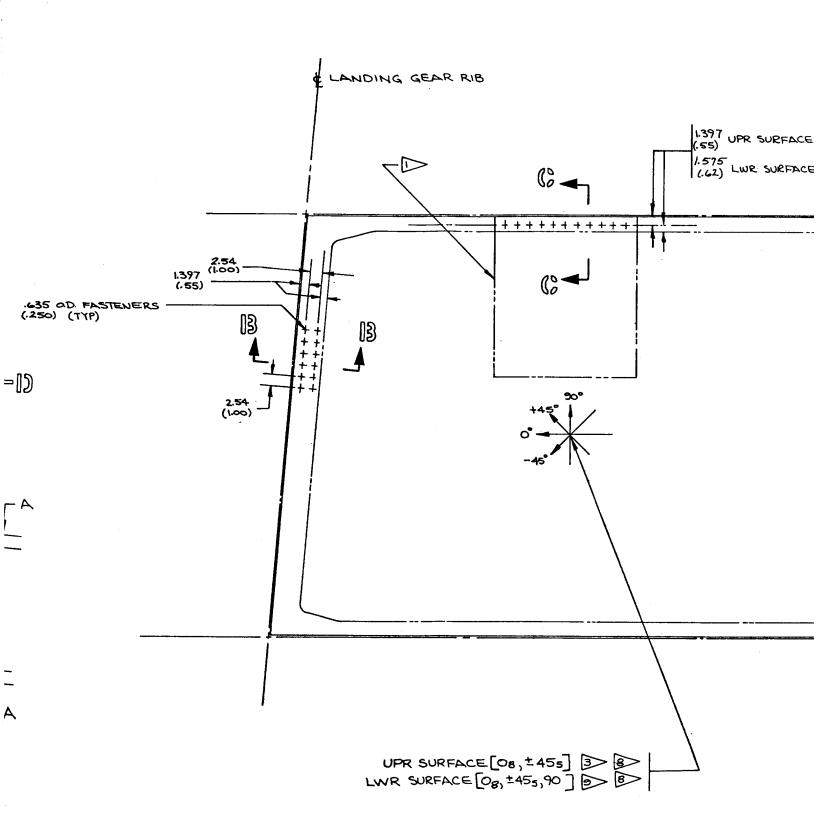
		DIMENSION							
LOCATION	A	В	С						
UPR SURFACE	.2377 (.0936)	3.175 (1.25)	(.1356)						
LWR SURFACE	.2509 (.0988)	1.905 (.75)	.3576 (.1408)						

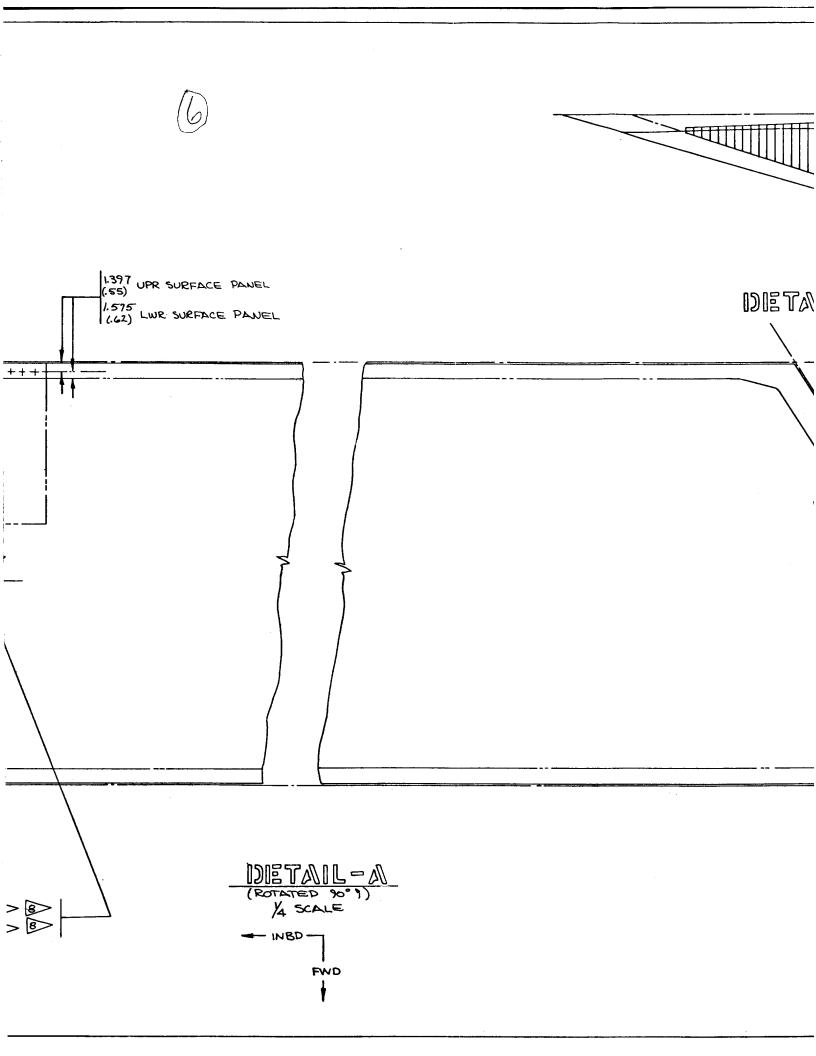




.635 OD FASTENERS (.250) (TYP)







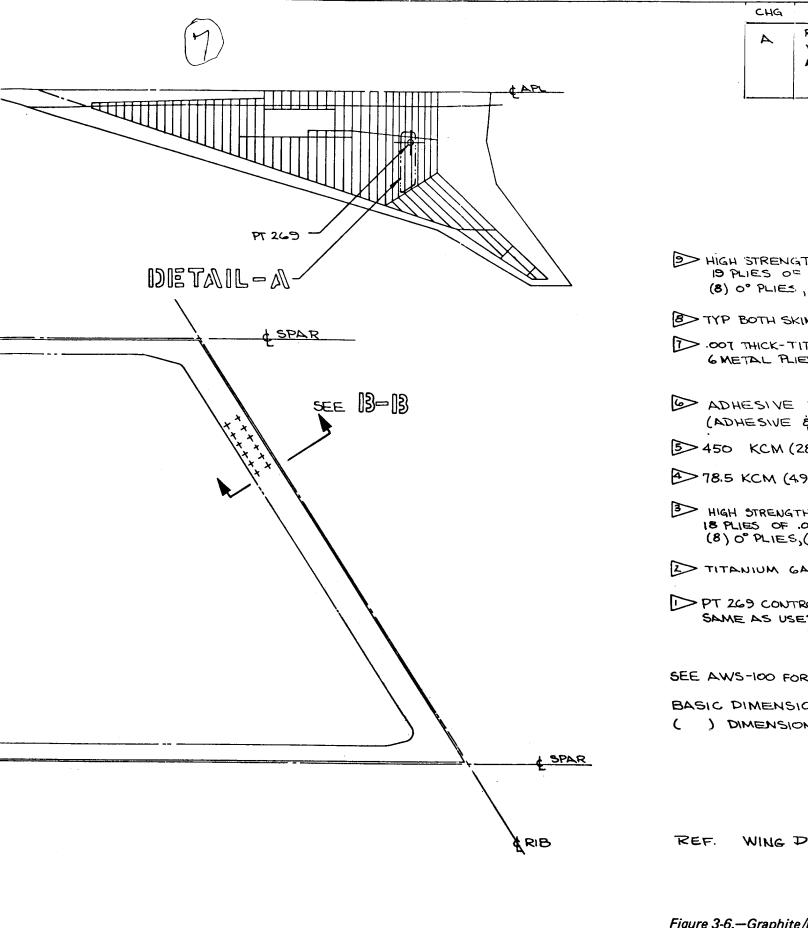


Figure 3-6.—Graphite/

CHG	DESCRIPTION	DATE	APPD.
4	REVISED DWG TO ADD LWR WING SURFACE DESIGN ADDED	6/19/74	DESIGN: PSS. STERESS: ~BAND



- HIGH STRENGTH GRAPHITE / PPQ SKIN ASSEMBLY
 19 PLIES OF .0052 IN/PLY MATERIAL
 (8) 0° PLIES, (5) + 45° PLIES, (5)-45° PLIES, (1) 90° PLIES
- BYP BOTH SKINS. SKINS SYM ABOUT & OF CORE
- D .007 THICK-TITANIUM SHIM GAL- 4Y COND I GMETAL PLIES PER SKIN REQUIRED
- ADHESIVE BOND

 (ADHESIVE & CURE CYCLE UNDEFINED)
- 5>450 KCM (281PCF) SS2-60 CORE TI-GAL-4V
- 78.5 KCM (4.9 PCF) SC4-20 CORE TI-3AL-2.5V
- HIGH STRENGTH GRAPHITE /PPQ SKIN ASSEMBLY
 18 PLIES OF .0052 IN/PLY MATERIAL
 (8) O" PLIES, (5) +45° PLIES, (5)-45° PLIES
- Z TITANIUM GAL-44 COND I
- PT 269 CONTROL POINT COUPON SIZE & LOCATION SAME AS USED FOR TASK I

SEE AWS-100 FOR LOADS & ENVIRONMENTAL CONDITIONS

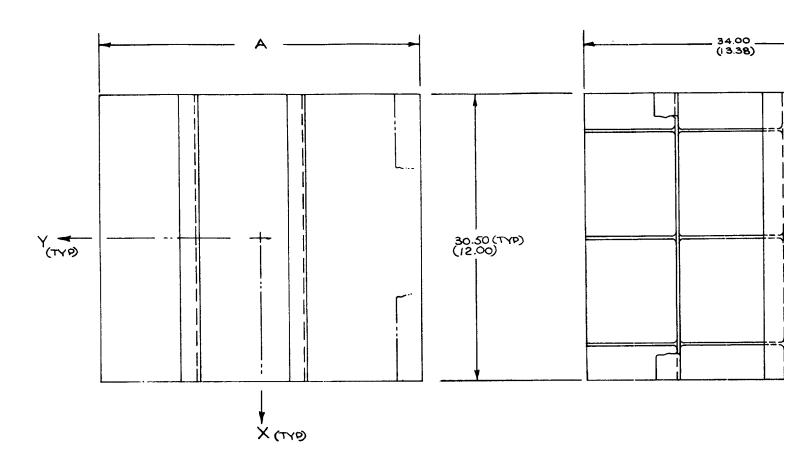
BASIC DIMENSIONS - CENTIMETERS

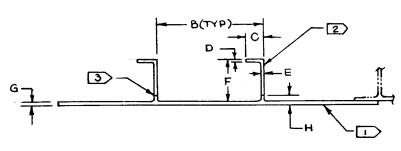
() DIMENSIONS - INCHES

REF. WING DRAWING AWS-146

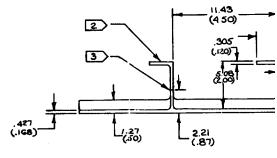
Figure 3-6.—Graphite/PPQ Skin, Titanium Core







PT 269 LWR SURF PT 431 UPR & LWR SURF



PT. 269 U

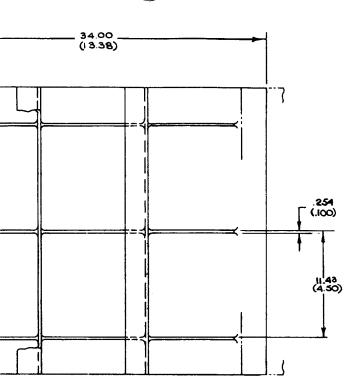
POINT	Α	В	С	D	Ε	F	G.	Н	
249									UPPER PANEL LOWER PANEL
269	34.00 (13.38	11.43	1.91		.178	4.45 (1.75)	317		UPPER PANEL LOWER PANEL
431	39.03 ((5.37)	(4.80) (4.35 (5.65) 44.35 (5.65)	2.54 (1.00) 2.54 (1.00)	(356 (49)	305 (120) .203 (.080)	\$ 000 (200) 4.45 (1.75)	(.125) .546 (.215) .394 (.155)	1.422 (560) 1.283 (505)	UPPER PANEL LOWER PANEL

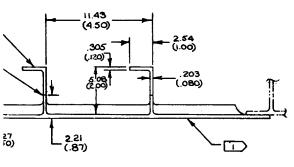
(3) (2)

SEE AW Basic I

()01







PT. 269 UPR SURF

REF. WING DRAWING AWS 108

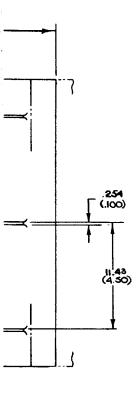
- 3 WELD PER BAC 5947 CLASS A
- MACHINED FROM GAL-4V EXTR PER BMS 7-44 CLASS B
- AL-4V COND I

SEE ALIS-100 FOR PANEL POINT LOCATIONS BASIC DIMENSIONS - CM

() DIMENSIONS - IN.

Figure 3-7.—Baseline, Integrally Machined and Welded Titanium Skin and Stiffeners







- 🗀

REF. WING DRAWING AWS 108

SAC 5947 CLASS A FROM GAL-4V EXTR 7-44 CLASS B ND I

POINT LOCATIONS

M

IN.

Figure 3-7.—Baseline, Integrally Machined and Welded
Titanium Skin and Stiffeners

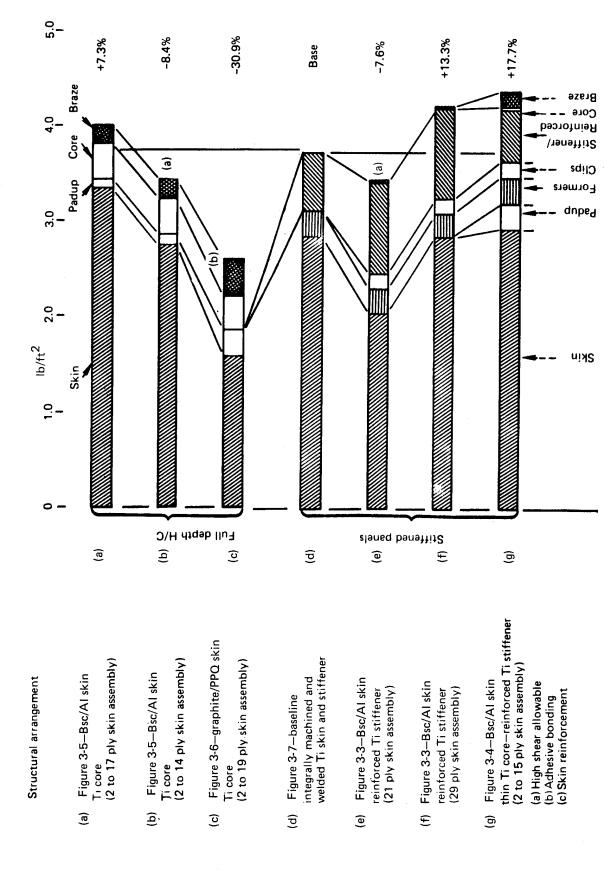


Figure 3-5. —Weight Comparison, Advanced Structural Concepts, Wing Lower Surface

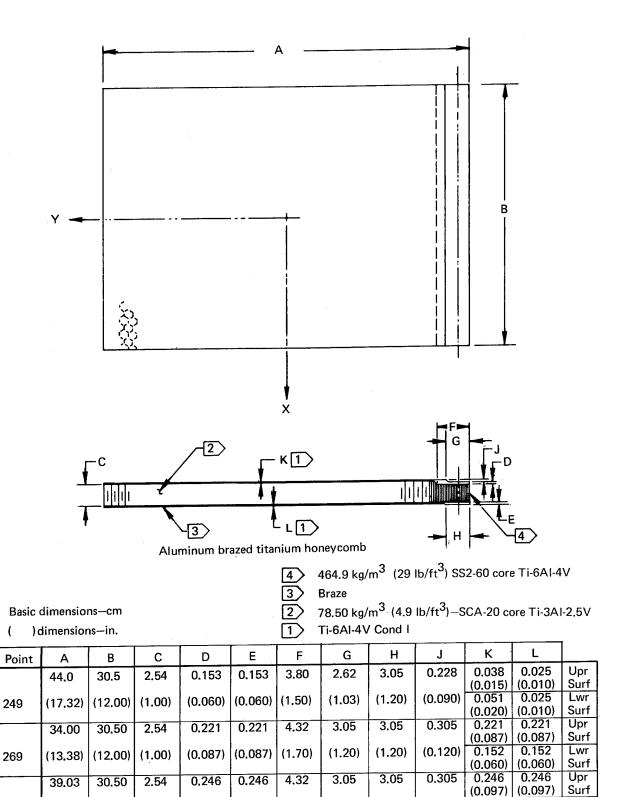


Figure 3-9.—Wing Skin Panel, Al Brazed Titanium Honeycomb

(0.097) (1.70)

(0.097)

(15.37) (12.00) (1.00)

(1.20)

(1.20)

(0.120)

0.224

(0.088)

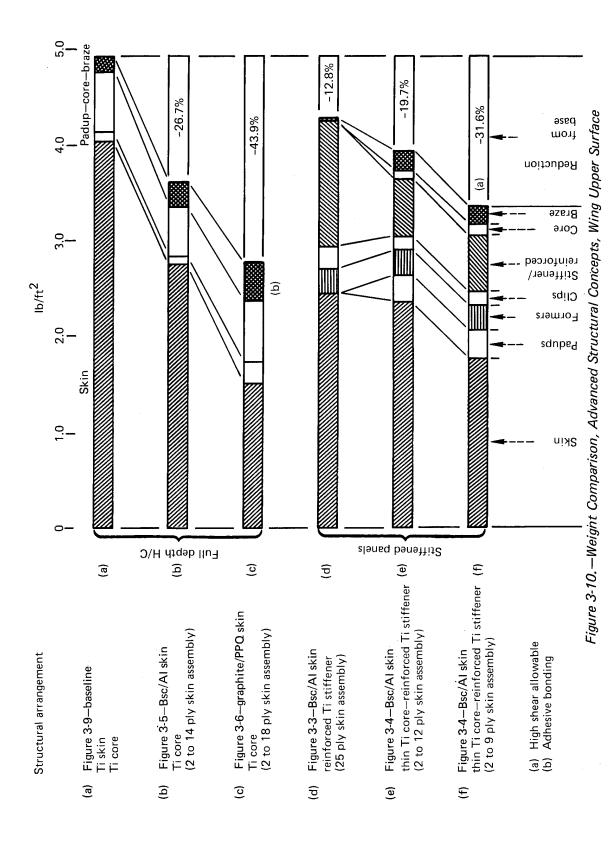
0.224

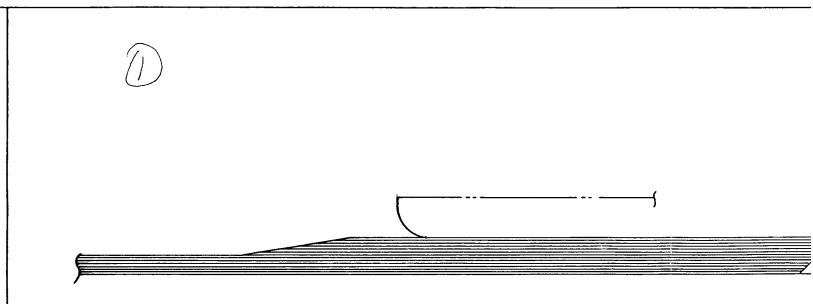
(0.088)

Lwr

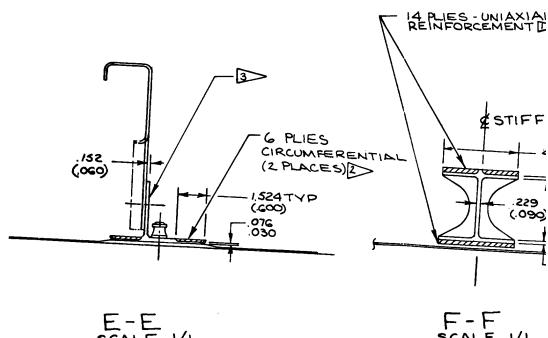
Surf

431

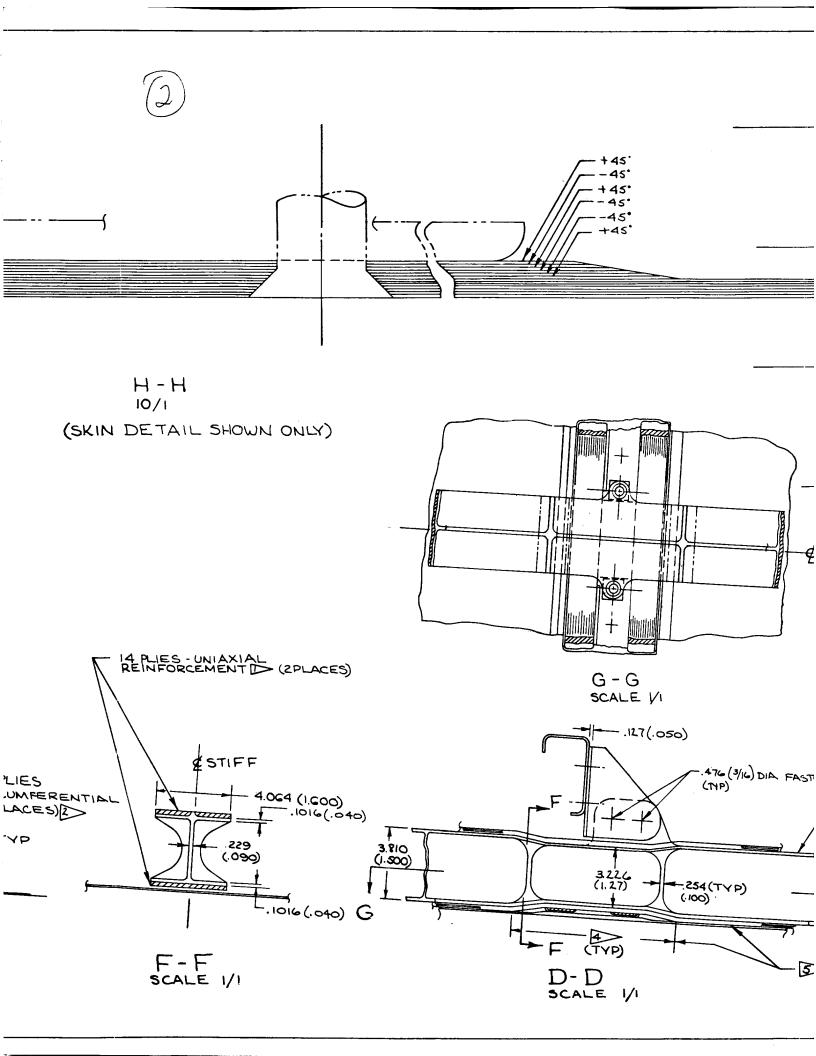


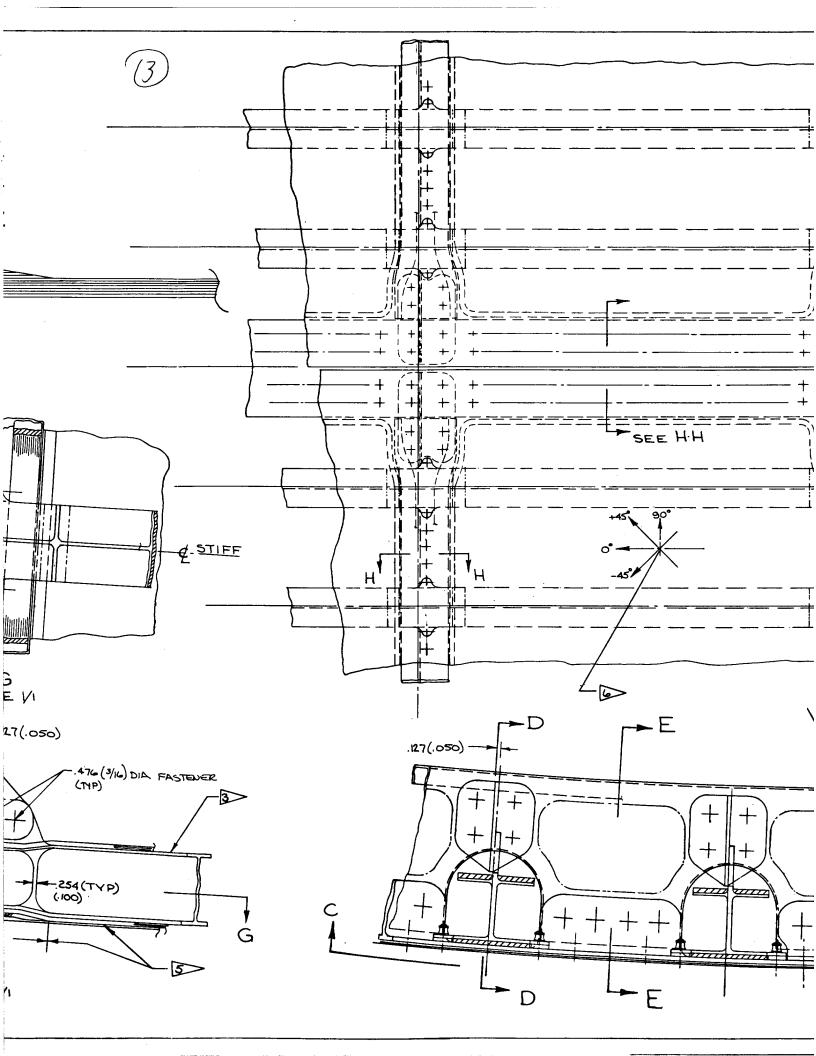


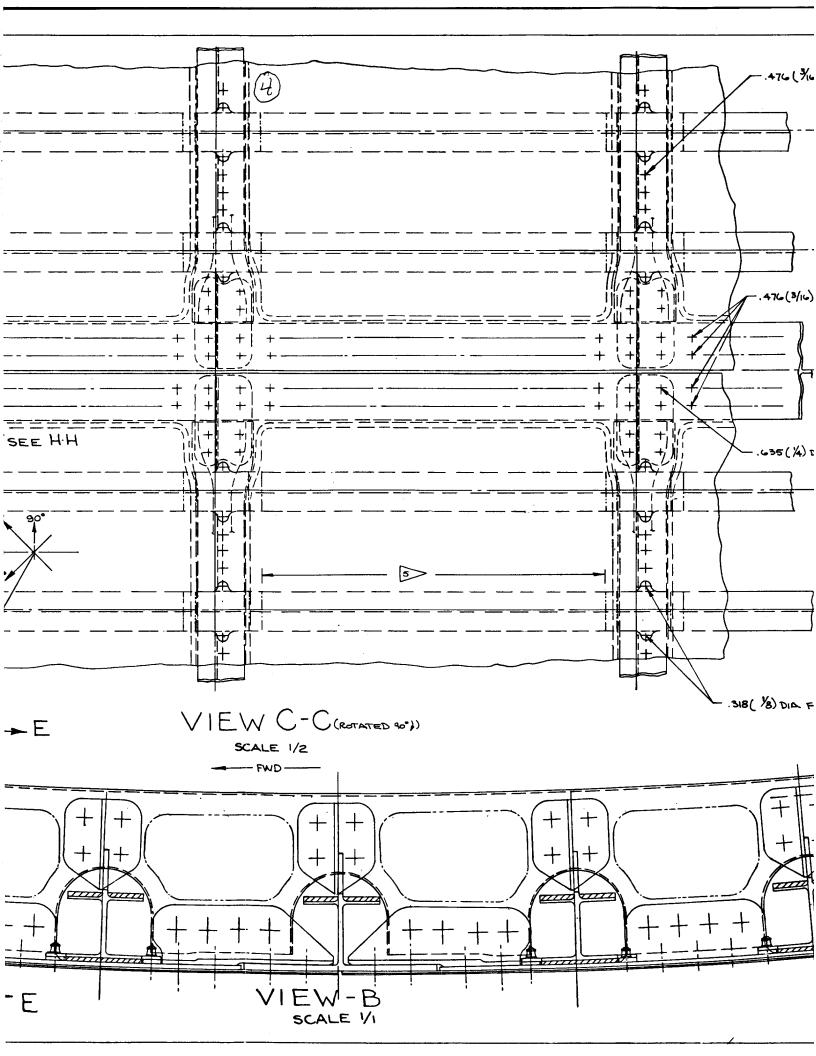
H - H 10/1 (SKIN DETAIL SHOW

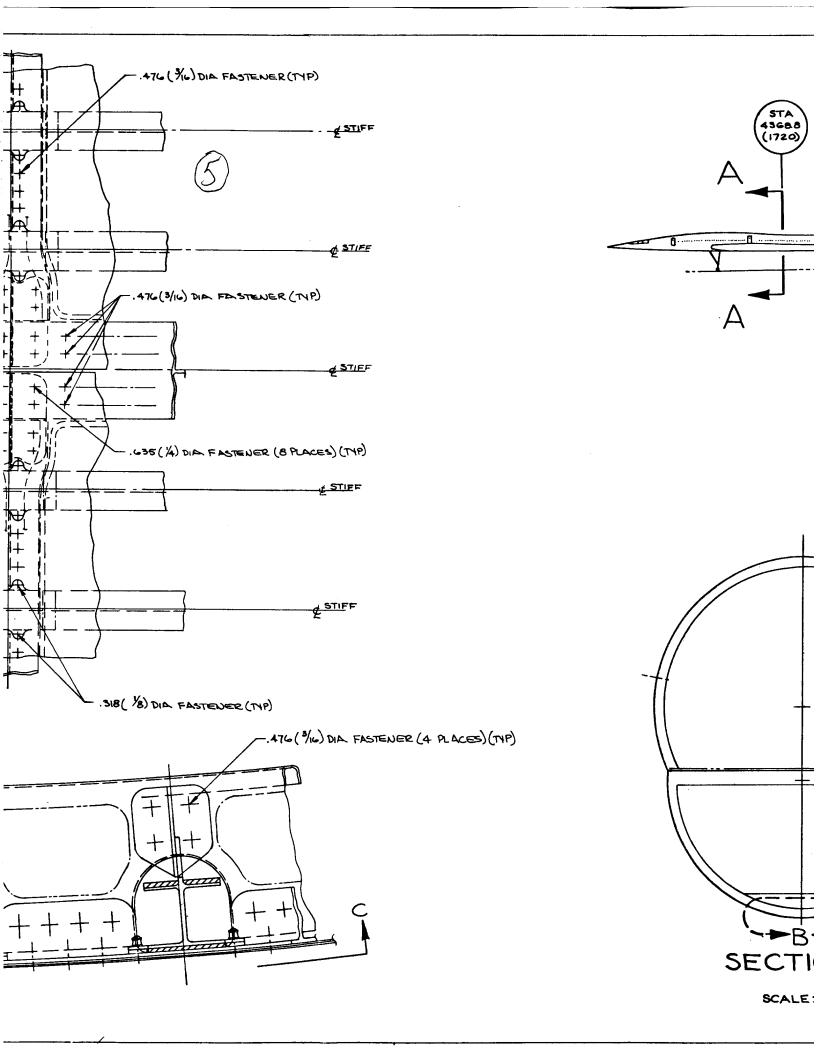


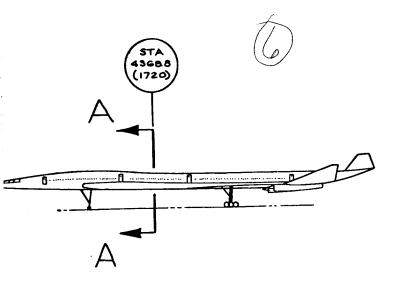
F-F SCALE 1/1

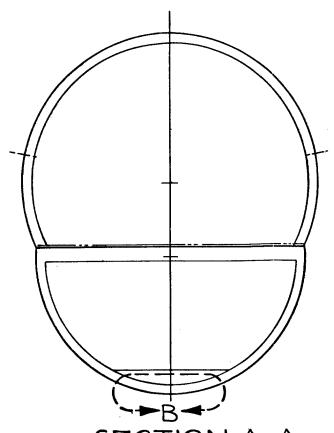












SECTION A-A

SCALE: 150

BORSIC ALUMINU

7 PLIE SKIN: (1) + 45

6 PLI

(3)+4

: aag

S SPOTBRAZE

(SPOTWELD ST

BO DO NOT SPOT IN THIS AREA

MACHINED TI GAL-4V PER

BORSIC ALUMIN GPLIES -. 007 IN

BORSIC ALUM 14 PLIES PER

BASIC DIMENSION () DIMENSIONS

Figure 3



- BORSIC ALUMINUM SKIN ASSY CONSOLIDATION
 - SKIN: 7 PLIES .007 IN /PLY MATERIAL (2) 0° PLIES,
 - (1)+45° PLY , (1)-45° PLY , (3) 90° PLIES
 - PAD: 6 PLIES . 007 IN/PLY MATERIAL
 - (3)+45° PLIES, (3)-45° PLIES
- SPOTBRAZE STIFFENERS TO FACE SHEET.

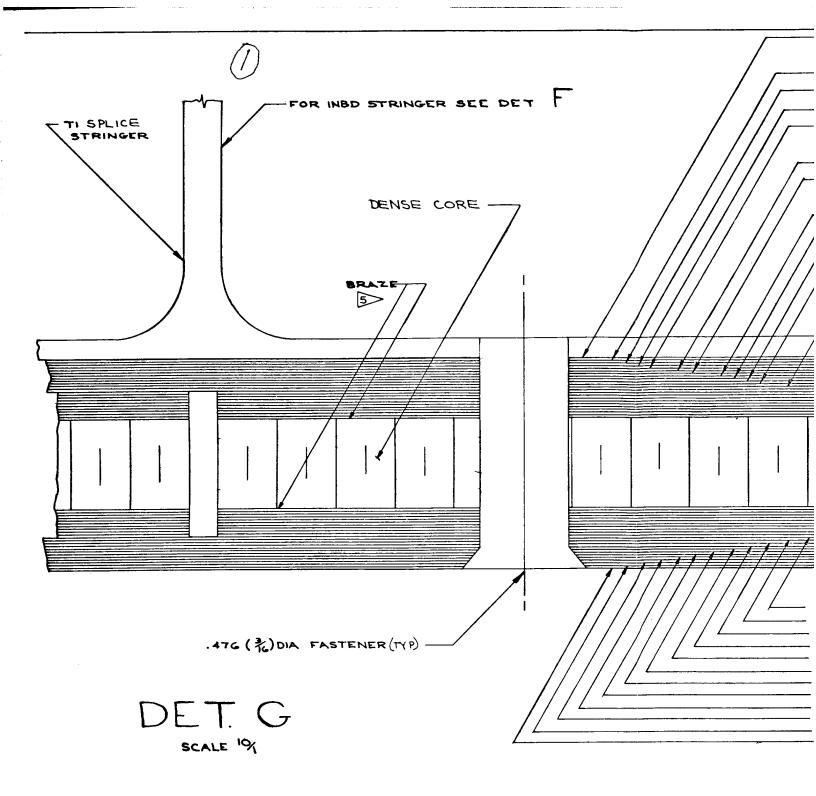
 (SPOTWELD SPEC AND BRAZE TIME & TEMP CYCLE UNDEFINED)
- DO NOT SPOT BRAZE STIFFENER TO SKIN ASSY IN THIS AREA.
- MACHINED TITANIUM EXTRUSION

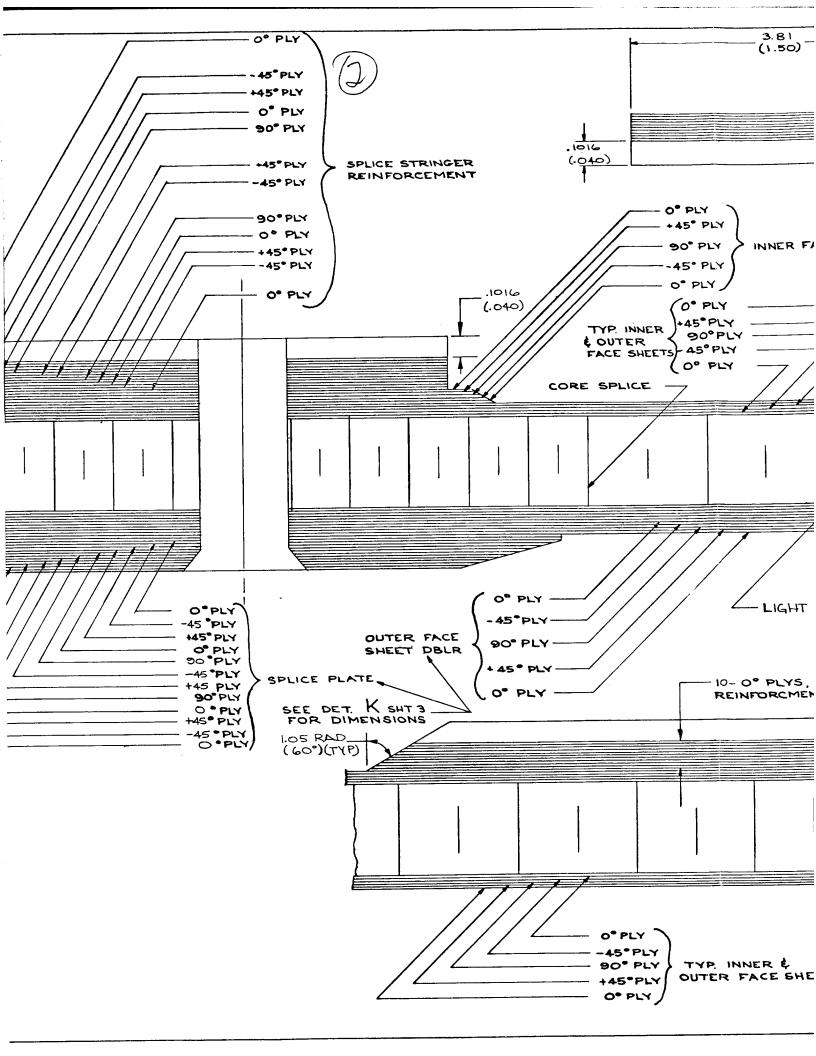
 GAL-4V PER BMS 7-44 CLASS B
- BORSIC ALUMINUM REINFORCEMENT CIRCUMFERENTIAL
 G PLIES -.007 IN/PLY MATL PER LOCATION
- BORSIC ALUMINUM UNIAXIAL REINFORCEMENT [0]
 14 PLIES PER LOCATION .007 IN./PLY MATERIAL

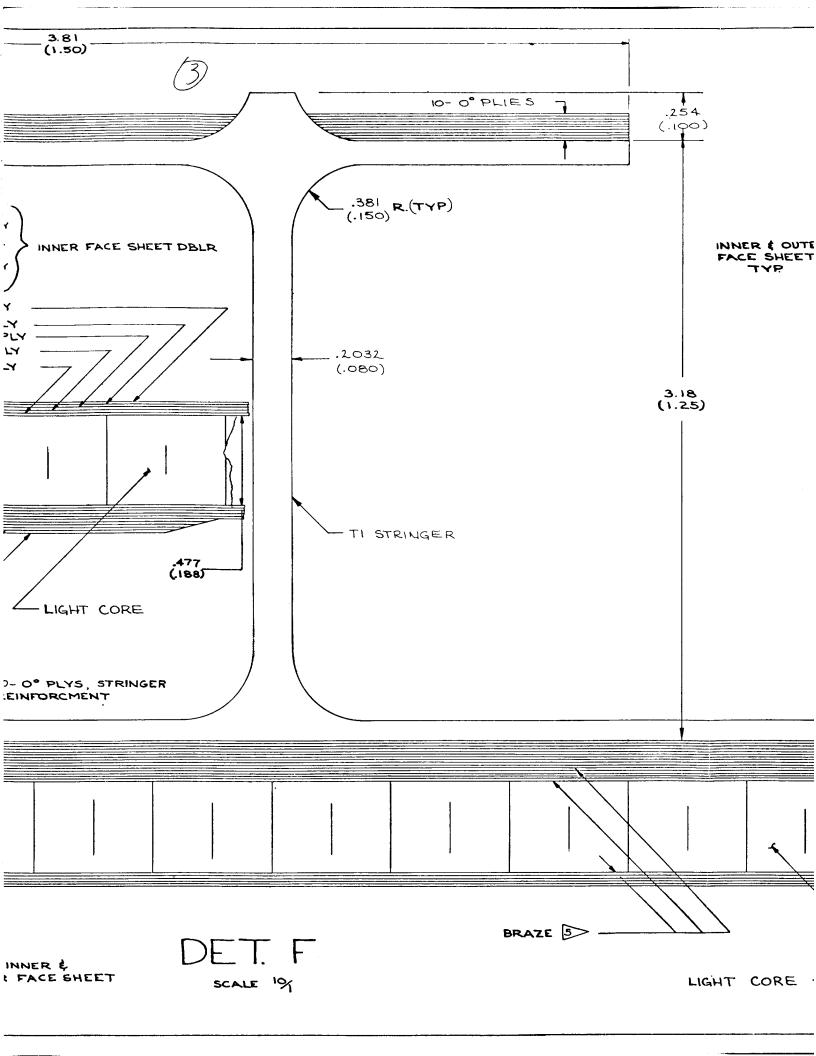
BASIC DIMENSIONS - CENTIMETERS
() DIMENSIONS - INCHES

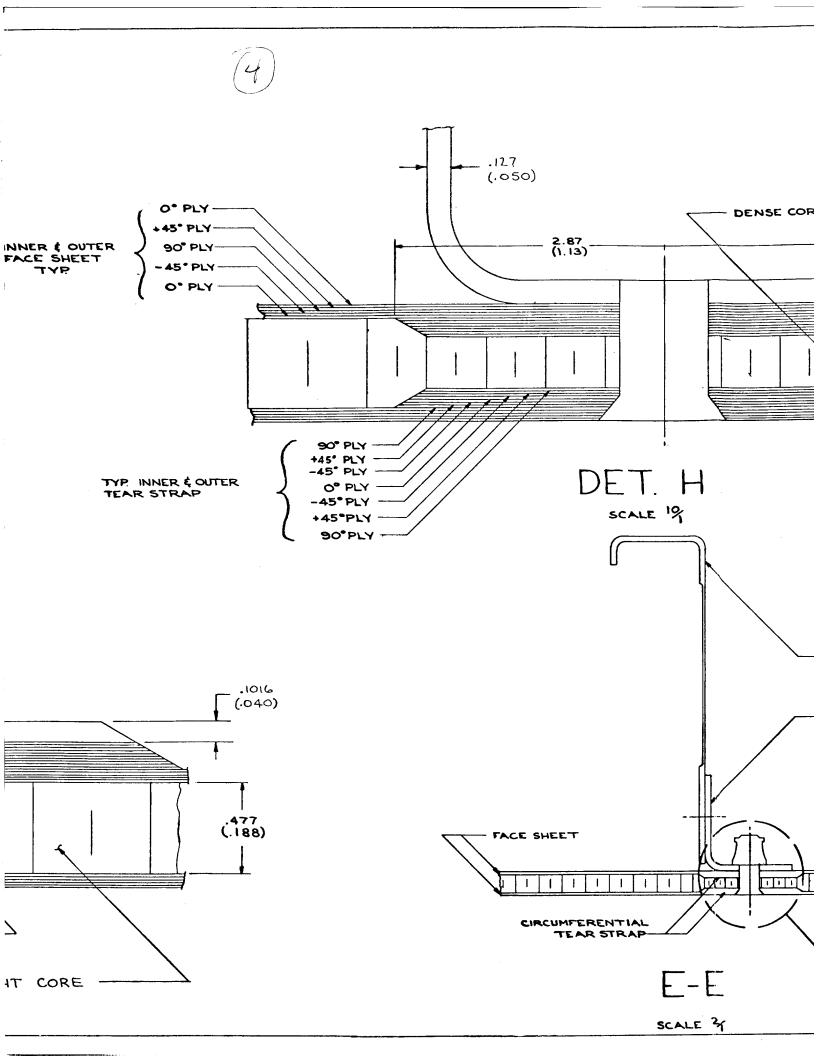
REF. FUSELAGE DRAWING AWS-140

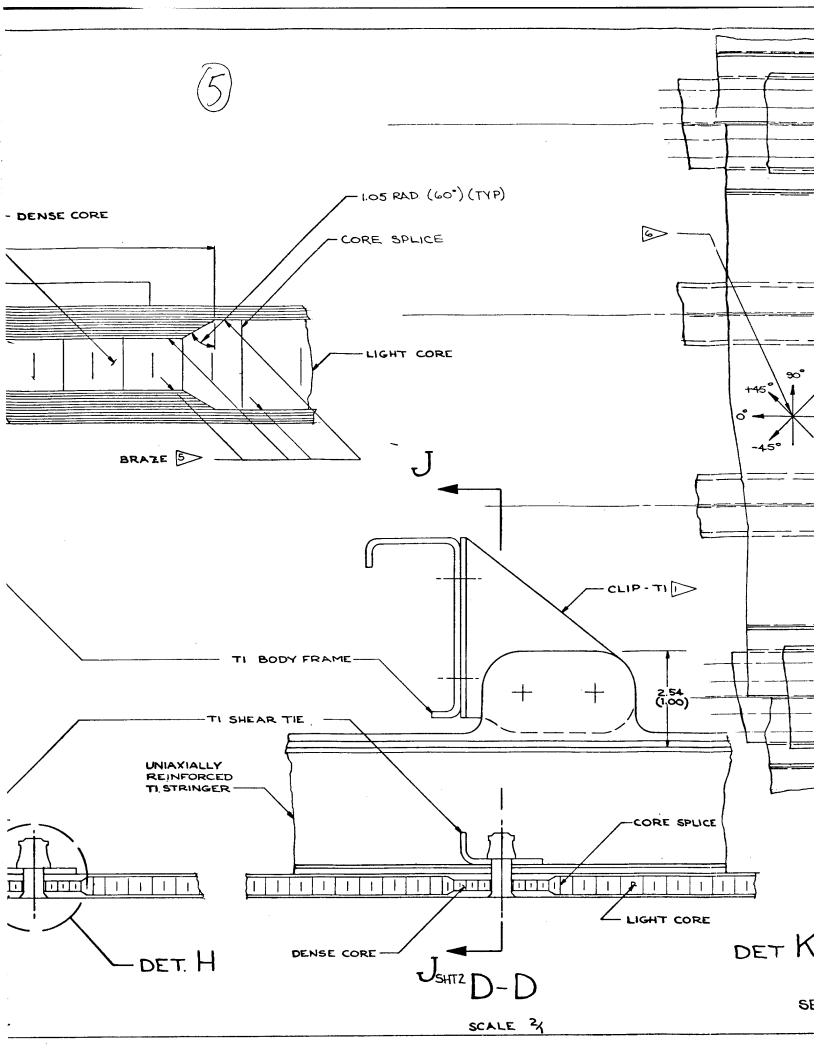
Figure 3-11.—Borsic/Aluminum Skin, Reinforced Titanium Stiffeners, 17.75-in. Frame Spacing

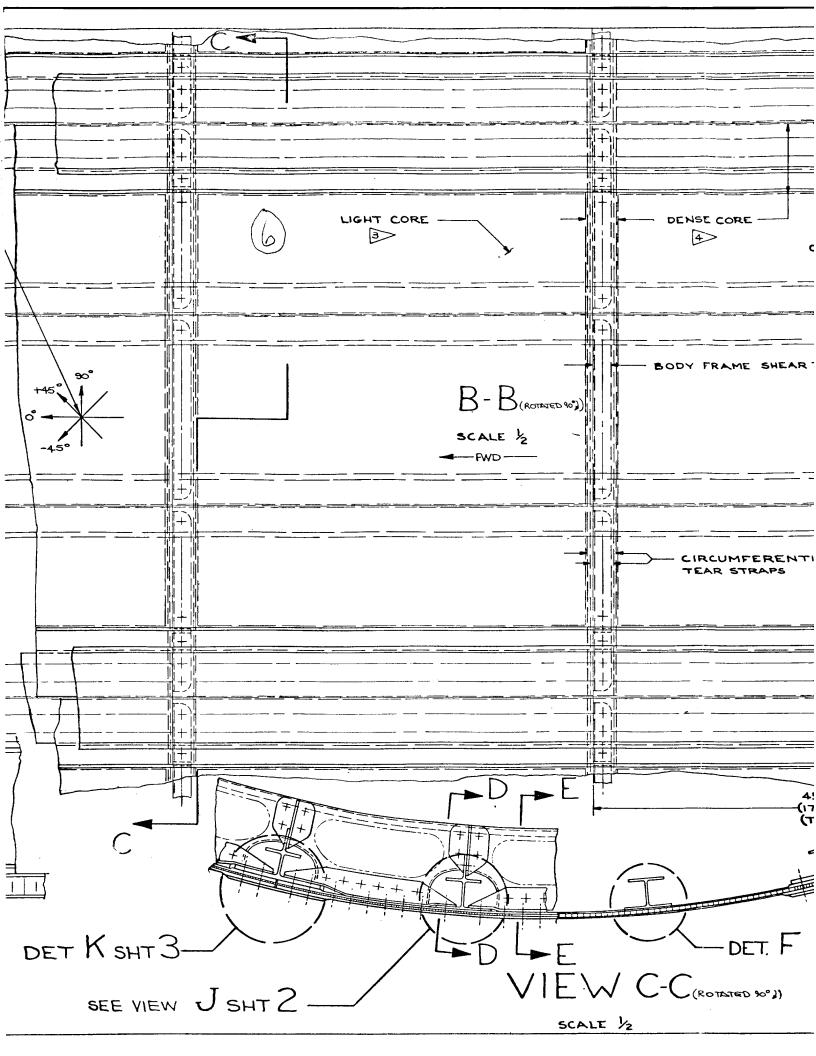


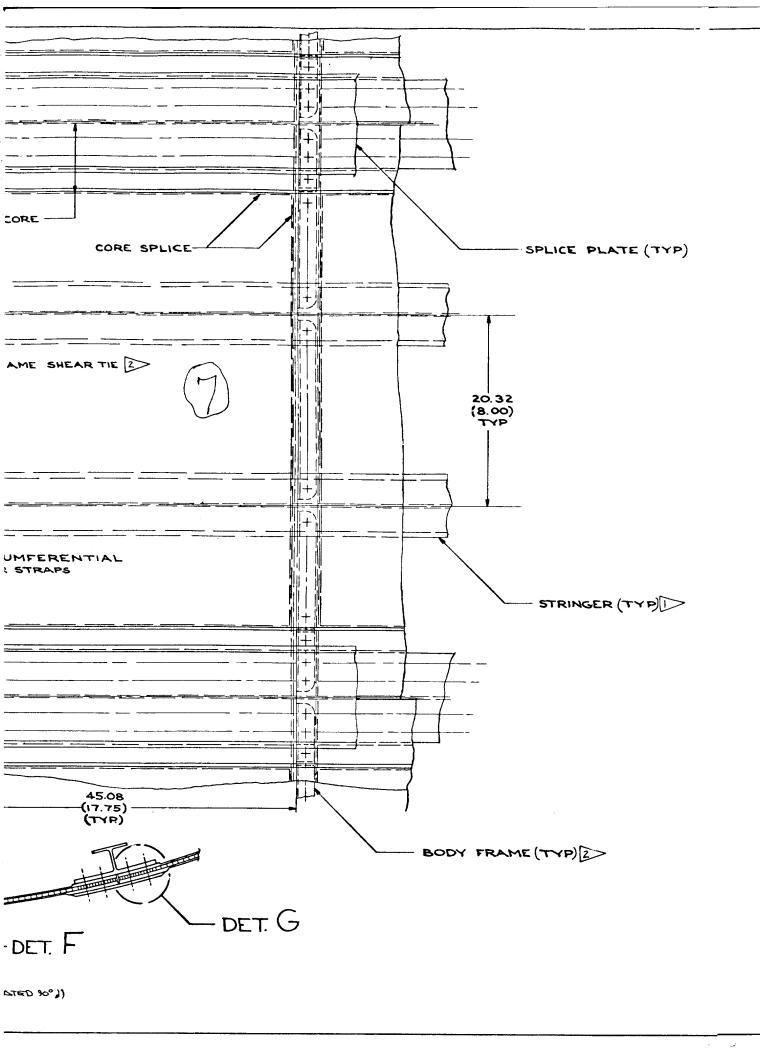


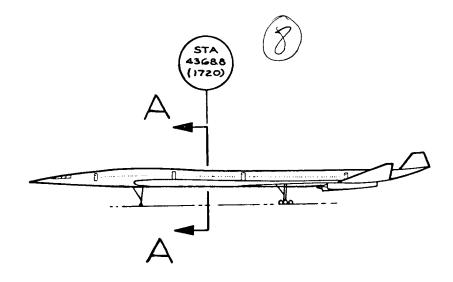


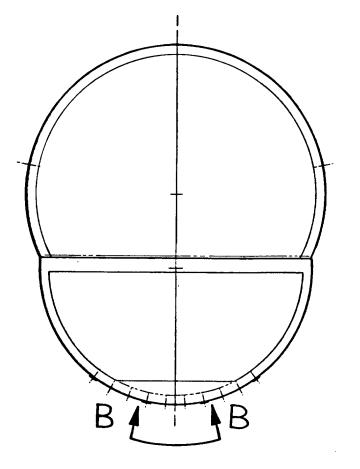












VIEW A-A

SCALE 1/20



- BASIC PLY ORIENTATION FOR ALL ASSY CONSOLIDATIONS . DOT IN PLY MATERIAL
 - A) STIFFENER ASSY CONSOLIDATION: TITANIUM STRINGER AND FLANGE REINFORCE MENT
 - 8) INNER FACE SHT ASSY CONSOLIDATION: FACE SHEET, TEAR STRAP AND DOUBLER
 - c) OUTER FACE SHT ASSY CONSOLIDATION: FACE SHEET, TEAR STRAP AND DOUBLER
 - 0) OUTER SPLICE PLATE CONSOLIDATION

ALUMINUM BRAZE
(BRAZE TIME & TEMP. CYCLE UNDEFINED)

226 Kg/M3(14.1 Lb/FT3) H/C CORE SS 2-30 TI-GAL-4V

3> 78 Kg/M3 (4.9 Lb/FT3) H/C CORE SC4-20 TI-3AL-2.5V

TI-GAL-4V COND I

TI-GAL-4V EXTRUSION PER BMS 7-44 COND I

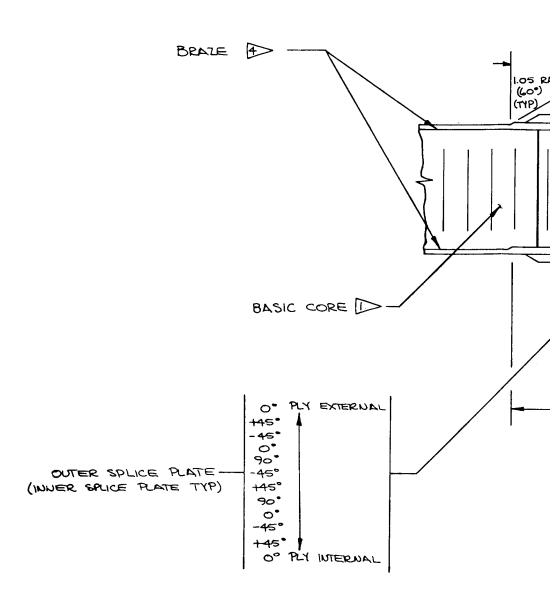
BASIC DIMENSIONS - CENTIMETERS

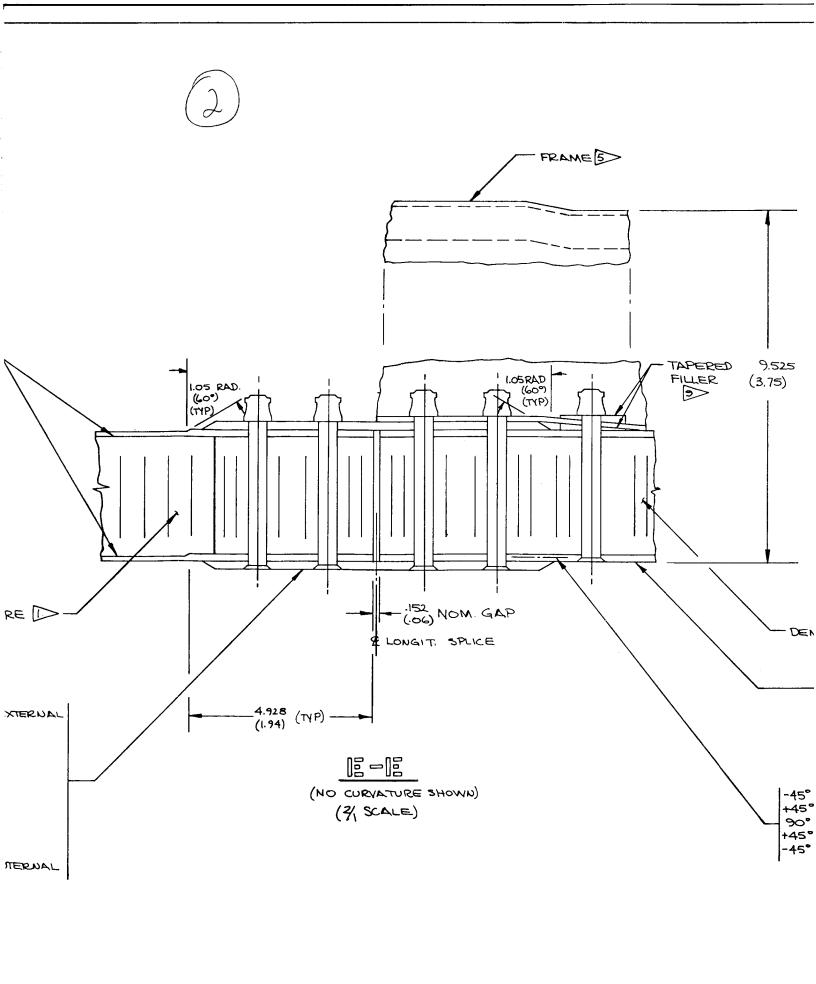
() DIMENSIONS - INCHES

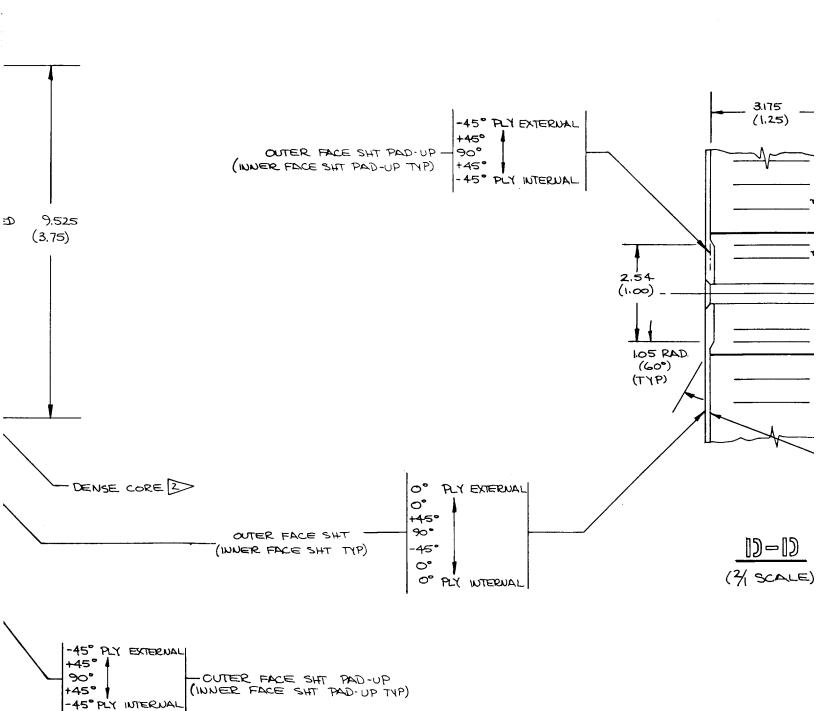
REF. FUSELAGE DRAWING AWS-139

Figure 3-12.—Borsic/Aluminum Skin, Titanium Core, Reinforced Titanium Stiffeners, 17,75-in. Frame Spacing

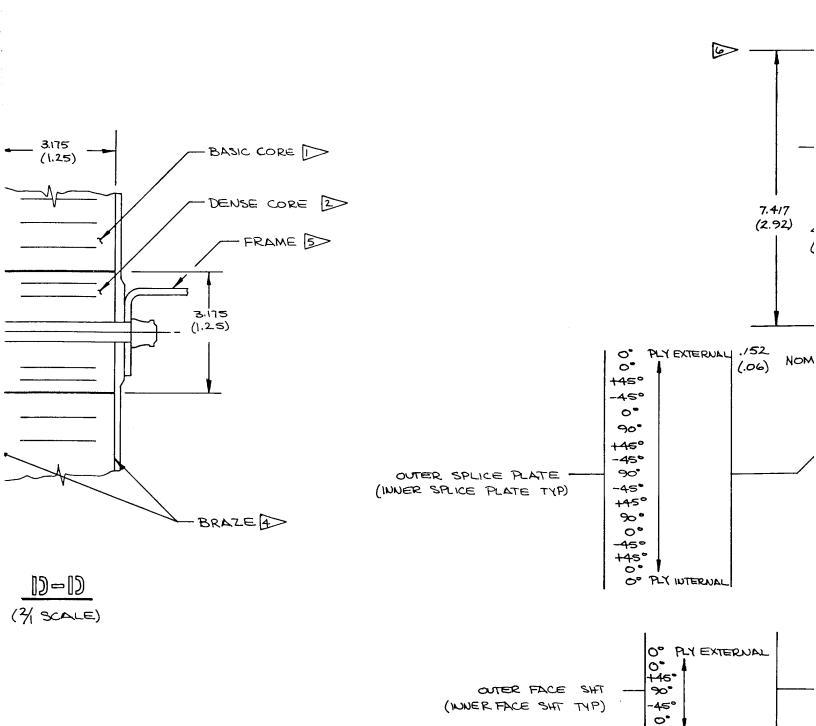




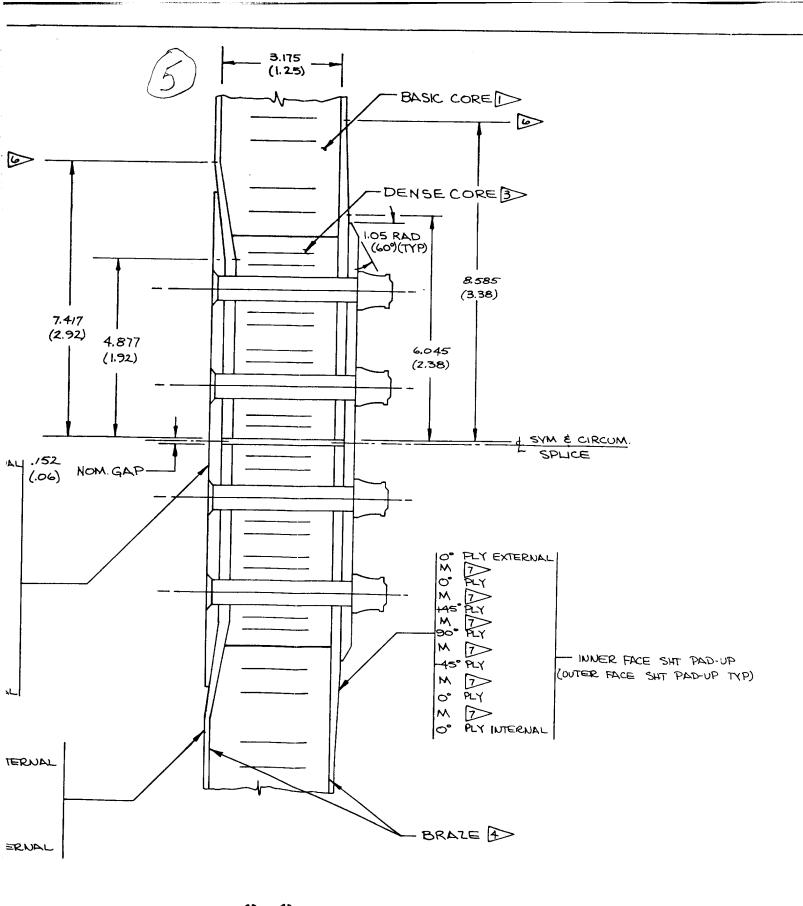




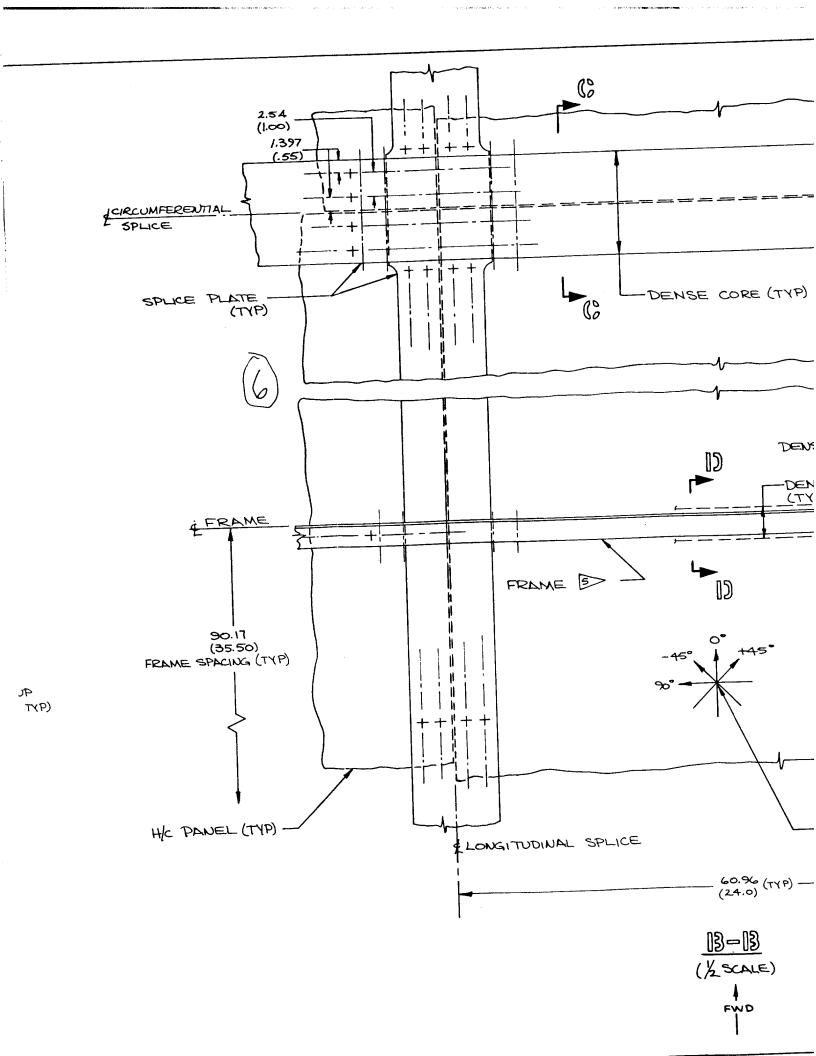


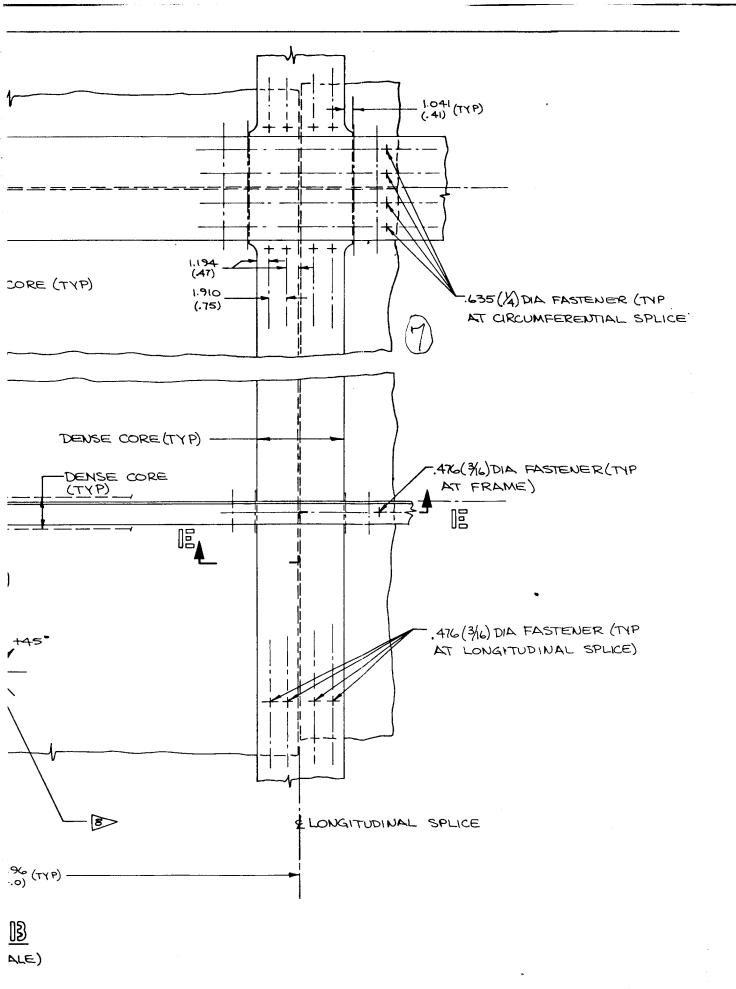


O" PLY INTERNAL

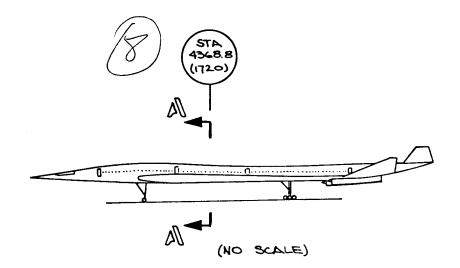


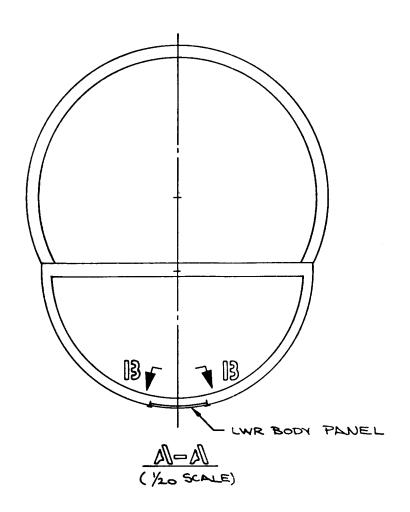
(3/ SCALE)





D







- 9> 2024-T3 ALUMINUM
- BASIC PLY ORIENTATION FOR ALL ASSY CONSOLIDATIONS .007 IN/PLY MATERIAL
 - A) INNER AND OUTER FACE SHT ASSY CONSOLIDATIONS:
 FACE SHT AND PAD-UP
 - B) INNER AND OUTER SPLICE PLATE CONSOLIDATIONS
- 1.009 THICK SHIM TI-GAL-4V CONDI
- DEDGE TITANIUM SHIM
- 5> TI- GAL-4Y COND I
- ALUMINUM BRAZE
 (BRAZE TIME & TEMP CYCLE UNDEFINED)
- 3> 450 Kg/M3 (281 Lb/FT3) H/C CORE S\$2-60
- 226 Kg/M3 (14.1 Lb/FT3) H/C CORE SS 2-30 TI-6AL-4V
- 1 78 Kg | M3 (4.9 Lb / FT3) HC CORE SC4-20

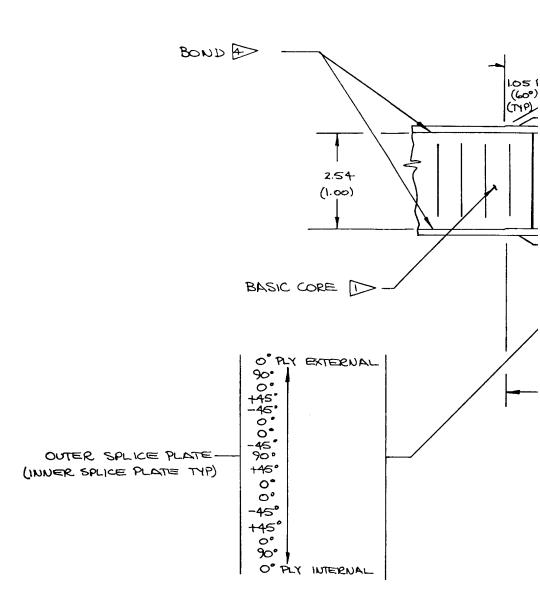
BASIC DIMENSIONS-CENTIMETERS

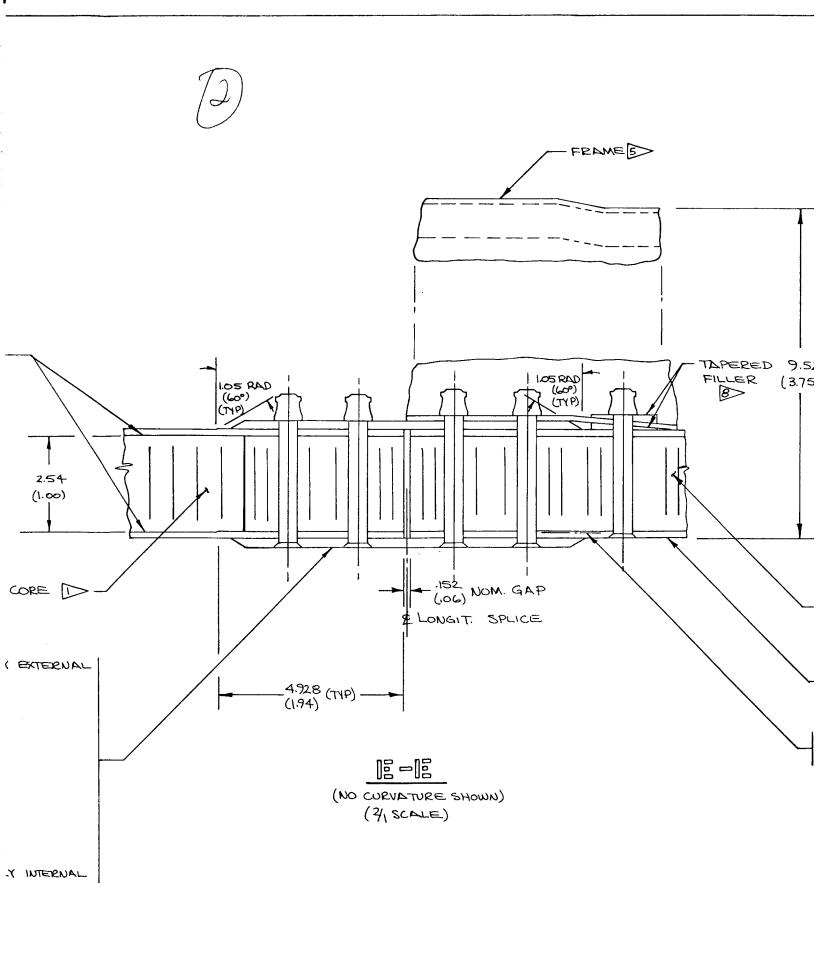
() DIMENSIONS-INCHES

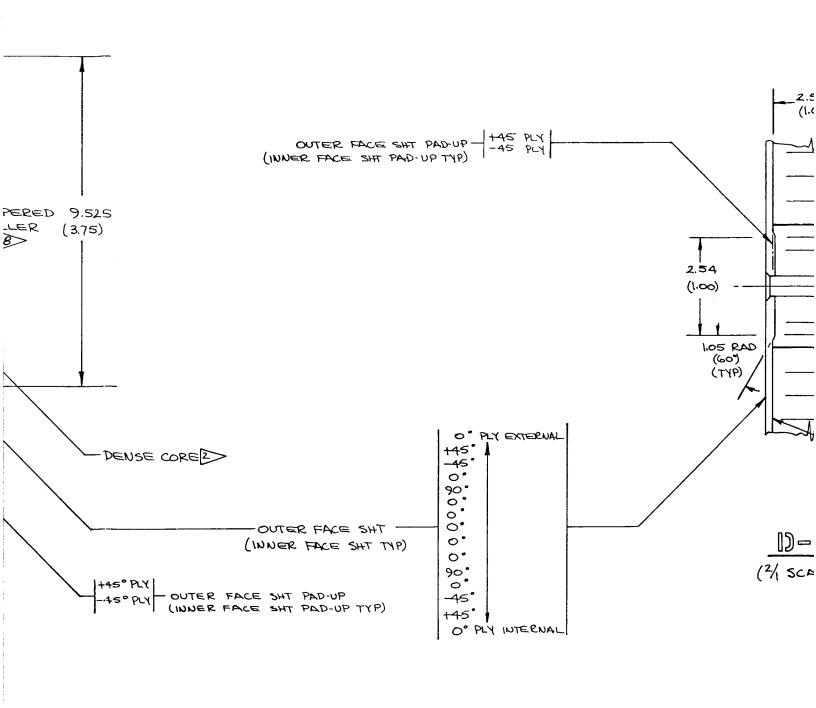
REF. FUSEAGE DRAWING AWS-142

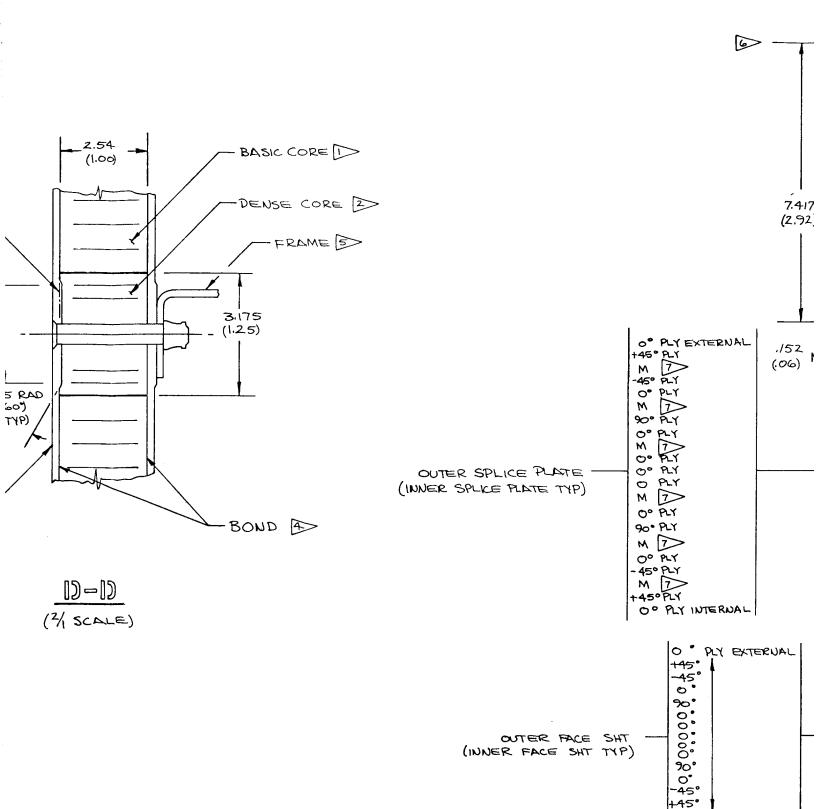
Figure 3-13.—Borsic/Aluminum Skin, Titanium Core, 35.5-in. Frame Spacing



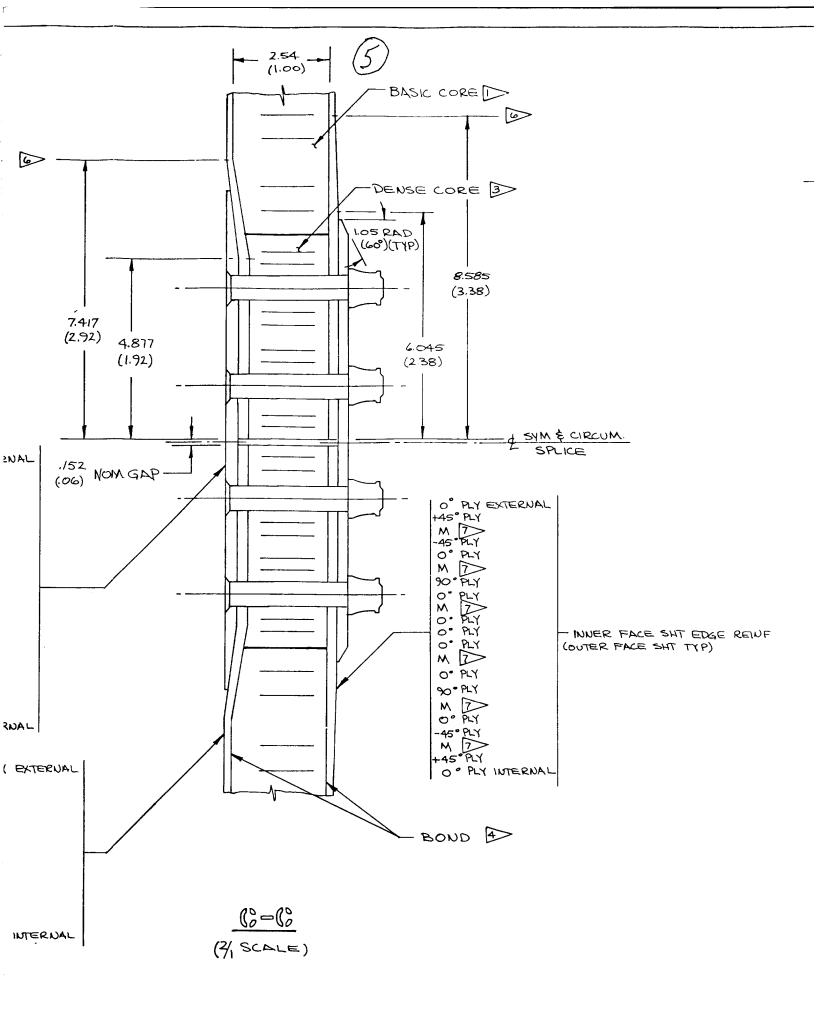


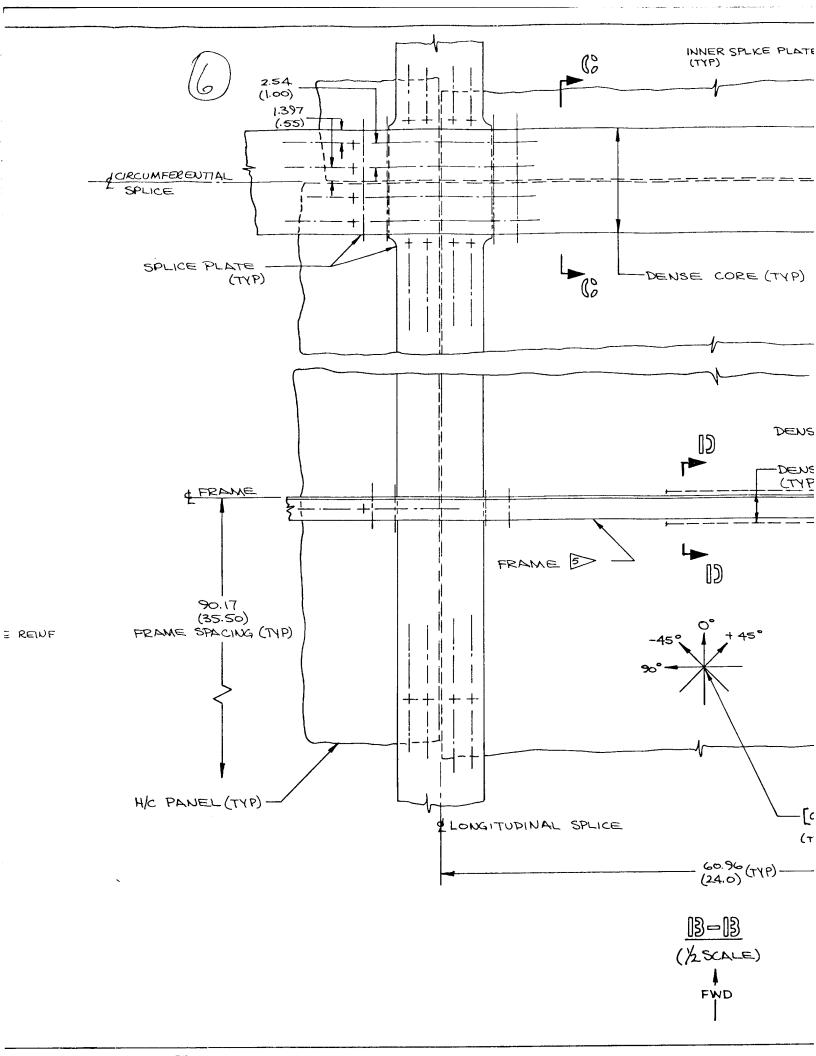


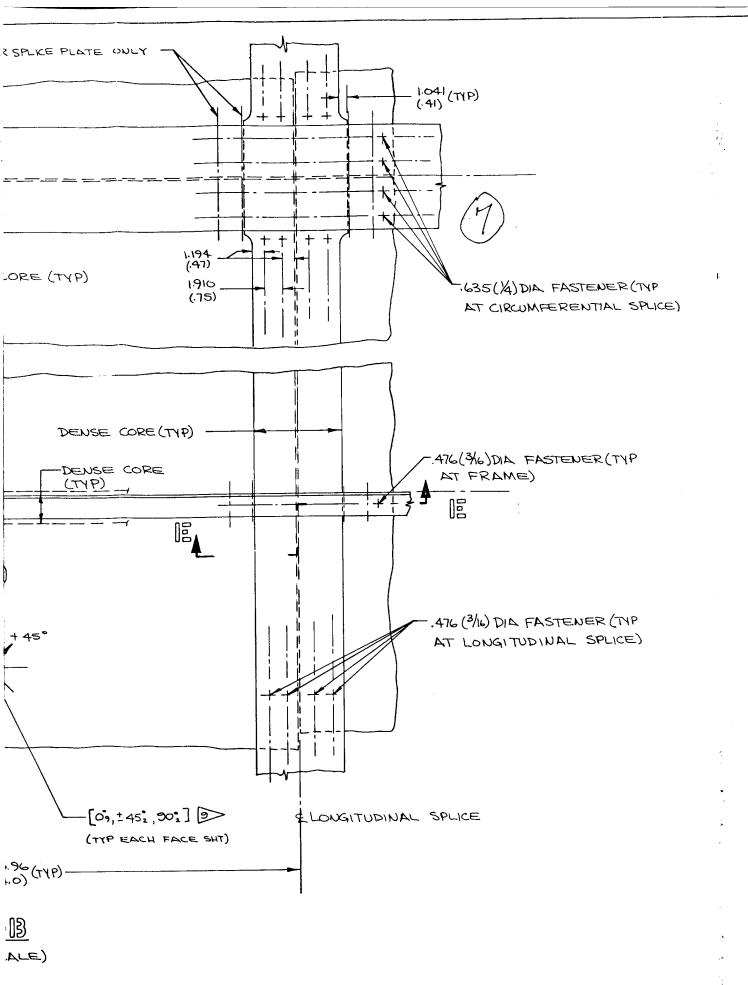




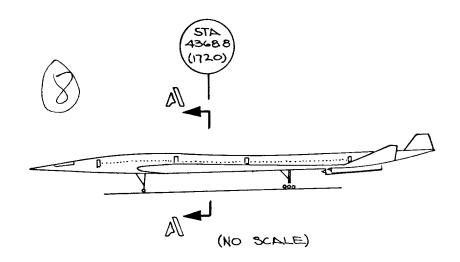
O' PLY INTERNAL

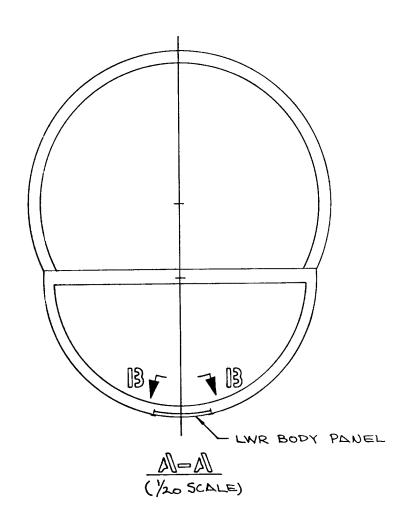






ID







- DESIG PLY ORIENTATION FOR ALL ASSYS
 .0052 IN/PLY HIGH STRENGTH GRAPHITE/PPQ MATERIAL
 - A) INNER & OUTER FACE SHT ASSYS: FACE SHT & PAD-UP B) INNER & OUTER SPLICE PLATE ASSYS
- 8> 2024-T3 ALUMINUM
- 7.007 THICK SHIM TI-GAL-4Y COND I
- SEDGE TITANIUM SHIM
- 5> TI-GAL-4Y COND I
- ADHESIVE BOND

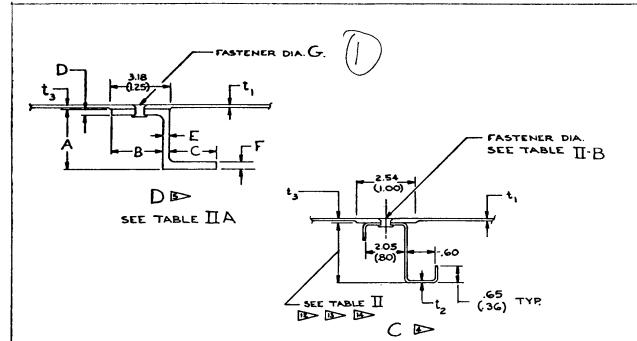
 (ADHESIVE & CURE CYCLE UNDEFINED)
- 3> 450 Kg/M3 (281 Lb/FT3) H/C CORE SC2-60 TI-6AL-4V
- 2> 226 Kg/M3 (14.1 Lb/FT3) H/C CORE SC2-30 TI-6AL-4V
- 78Kg/M3(4.9Lb/FT3) H/C CORE SC4-20 T1-3AL-2.5V

BASK DIMENSIONS-CENTIMETERS

() DIMENSIONS-INCHES

REF. FUSELAGE DRAWING AWS-141

Figure 3-14.—Graphite/PPQ Skin, Titanium Core, 35.5-in. Frame Spacing



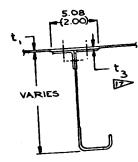
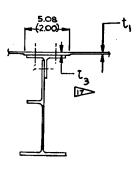


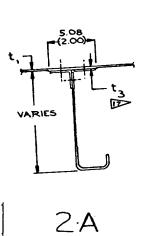
TABLE II A										
				DIME	VSIONS	رس (۱۸)				
PT.		Α	В	С	D	E	F	G	t ₃	AREA cm² (in²)
3	SPLICE STRINGER	3.18 (1.25)	2.03 (-80)).52 (.60)	.305 (.12)	.203 (.08)	.254 (.10)	.397 (.156)	.137 (.054)	1.652 (,256)
5	STRINGER	3.18 (1.25)	2.74 (1.08)	2.54 (1.00)	.381 (.15)	.152	.635 (.25)	.476 (.188)	.183 (.072)	3.142 (.487)
J	SPLICE STRINGER	3.18 (1,25)	2.74 (1.08)	(i'ia) 3'05	.381 (.15)	.305 (.12)	.762 (.30)	.476 (.188)	.183 (.072)	4.316 (.669)
	STRINGER	3.18 (1.25)	2.74 (1.08)	2.54 (1.00)	.305 (-12)	.305 (.12)	.508 (20)	.635 (.25)	.254 (.100)	3.097 (.480)
6	SPLICE STRINGER	3.18 (1.25)	2.74 (1.08)	2.54 (1.00)	.305 (.12)	.305	.508 (.20)	.635 (.25)	.254 (.100)	3.097 (.480)
7	STRINGER	2.54 (1.00)	2.74 (1.08)	1.90 (.75)	.229 (.09)	.152 (.06)	.228 (.09)	.635 (.25)	.228 (.090)	1. 4 52 (. 2 25)
8	STRINGER	3.18 (j.25)	2.74 (1.08)	2.54 (1.00)	.305 (.12)	.152 (.06)	.305 (-12)	.476 (.188)	.183 (.072)	2.097 (;325)
)	SPLICE STRINGER	3.18 (1.25)	2.74 (1.08)	2.54 (1.00)	.279 (۱۱,)	.254 (.10)	.635 (.25)	.476 (-188)	.183 (.072)	3.187 (.494)
10	STRINGER	3.18 (1,25)	2.74 (1.08)	2.54 (1,00)	.381 (.15)	.152 (.06)	.381 (.15)	.635 (.25)	.24 4 (.096)	2.4 9 7 (.387)
	SPLICE STRINGER	3.18 (1.25)	2.74 (1.08)	2.54 (1.00)	.381 (.15)	.152 (.06)	.635 (, 25)	.635 (.25)	.244 (.096)	3.142 (.487)

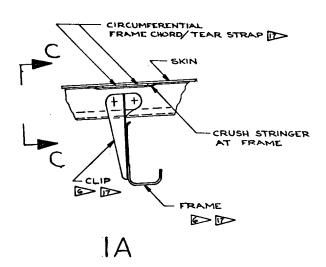


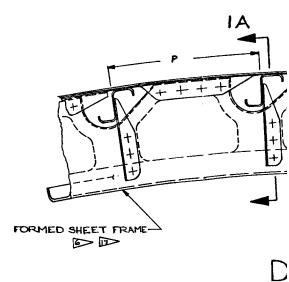


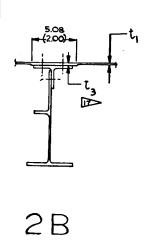
2B

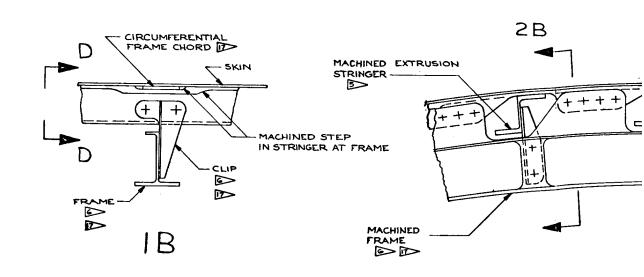




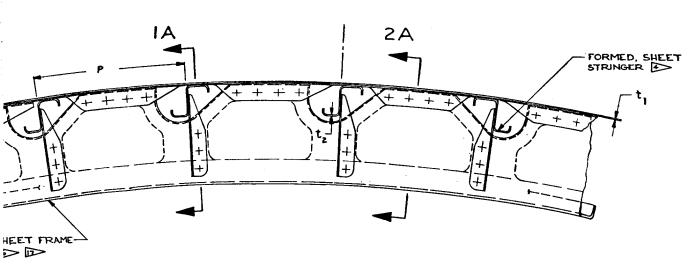






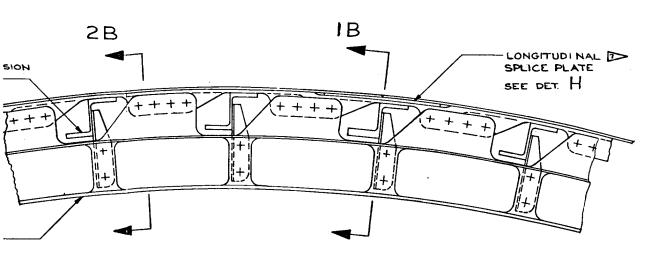






DETAIL A

(SEE TABLE II)



DETAIL B

(4

(H)

TABLE II

•				•						
PT. NO.	BODY STA. CM (IN) CIRCUME	DETAIL	SKIN t, ts	STRINGER t ₂	AREA Cm²	STRINGER SPACING CM	EFFECTIVE AREA PAD UP & SPLICE MTL Cm ²	EFFECTIVE T	103 NM	DESIG LOAT CONDITI
	LOCATION STA (2552.70) 1005.00	STRINGER	(IN)	(IN)	(1N ²)	(IN)	(IN ²)	2 A A	(LB/IN)	
l	UPR CROWN	A C	.076 (030) .137 (.054)	.076 (.030)	.761 (.118) Is>	13.97 (5.50)	2.41 (.374)	. 142 (.056)	435 TEN (2,485) 348 COMP (1,988)	LOW AND OF ATTA MAX CANAS
2	SIDE PANEL	A C	.076 (030) .137 (.054)	.076 (.030)	.761 (.118)	12.70 (5.00)		.136 (.054)	106 SHEAR (605) 23 SHEAR	DYNAI LANDII IG CRUISI PANEL S
	STA 4368.80 (1720.00)								(103)	
3	UPR CROWN	A C	.1016 (040) .137 (054)	.152 (.060)	1.393 (.2.16)	12.70 (5.00)	2.99 (464)	.224 (.088)	957 (5,570)COMP	END O CRUISI MAX CANAR
4	SIDE PANEL	A	.076 (.030) .137 (.054)	.076 (.030)	.761 (:118)	12.70 (5.00)		.136 (.054)	155 SHEAR (888) 46 (261) SHEAR	END OF CRUISE IG CRUI PANEL ST
5	LWR	A	.127	SEE TABLE	3.32	11.18	6.58	.456	2087 (11,921)	
	.CROWN	D	.183	II-A	(515)	(4.40)	(1.010)	(.178)	613 (3,500)	IG CRUI PANEL S
	STA G283.90 (2474.00)					,				
6	UPR CROWN	BD	.203 (080) .254 (.100)	SEE TABLE II-A	3,258 (.505)	11.43 (4.50)	6.76 (1.048)		4827 (27,564) TEN 1532 (8,750) COMP	3G TA
7	SIDE PANEL	ВО	855. (080) 855. (0e0.)	SEE TABLE II-A	1.529	12.70 (5.00)		(.127)	697 (3,980) ^{SHEAR} 256 SHEAR (1460)	IG CRUI
	STA 7874.00 (3100.00)		(050)						(1460)	PANEL ST
8	UPR CROWN	A D	.152 (.060) .183 (.072)	SEE TABLE II-A	2.19 (.340)	11.18 (4.40)	5.13 (.795)		2376 TEN. (13,570) TEN. 1954 (1,160)	TRANSC CLIMB NEGATIVI MANUEV
9	SIDE PANEL B>	A	.132 (052) .183 (.072)	.127 (.050)	1.09 (.169) (2	12.70 (5.00)		.554 (.086)	343 (1960) ^{SHEAR} 101 (575) ^{SHEAR}	TRANSO CLIMB IG CRUI PANEL ST
10	LWR	A	.2438 (.096)	SEE TABLE	.983	11.68	6.051	.495	2737 (15,627) ^{COMP}	TRANSON CLIMB
10	CROWN	D	.2438 (.096)	II-A	(.387) S	(4.60)		(.195)	802 (4,580) ^{COMP}	IG CRUIS PANEL ST

TORMED, SHEET

	П				
7	EFFECTIVE AREA PAD UP \$ SPLICEMTE CM ² (1N ²)	ELLECTIVE	PANEL LOAD #103 MM	DESIGN LOAD CONDITION	PANEL
		AA			
	2.41 (.374)	.142 (.056)	435 (2,485) TEN 348 (1,988)	LOW ANGLE OF ATTACK MAX CANARD	
		.136 (054) (2>	106 (605) 23 (133)	DYNAMIC LANDING IGCRUISE PANEL STAB	•
	,				
	2.99 (.464)	.224 (.088)	1164 TEN. (6,646) TEN. 957 COMP. (5,570)	ايجمعا	
		.136 (.054)	155 (888) SHEAR 46 (261) SHEAR	END OF CRUISE IG CRUISE PANEL STAB.	
	6.58 (1.010)		2087 (11,921)	END OF CRUISE IG CRUISE PANEL STAB	
			(3,500)	PANEL STAB	
	6.76 (1.048)	1.432 (222)	1532 COMP	3G TAXI NEGATIVE MANUEVER	
)		(.323) (.127)	697 (3,980) ^{SHEAR} 256 SHEAR (1460)	3G TAXI	
				·	
	5.13 (.795)		2376 TEN. (13,570) TEN. 1954 (1,160)	TRANSONIC CLIMB NEGATIVE MANUEVER	
			343 SHEAR (1960) SHEAR 101 (575) SHEAR	TRANSONK CLIMB IG CRUISE PANEL STAB	,
	6.051	.495	2737 (15,627) ^{COMP}	TRANSONIC CLIMB	
	(.938)	(.195)	802 (4,580)	IG CRUISE PANEL STAB	

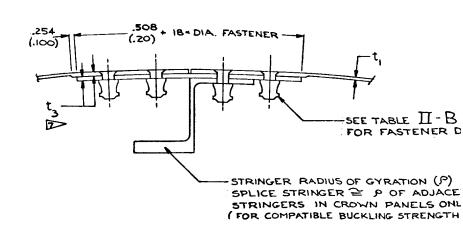




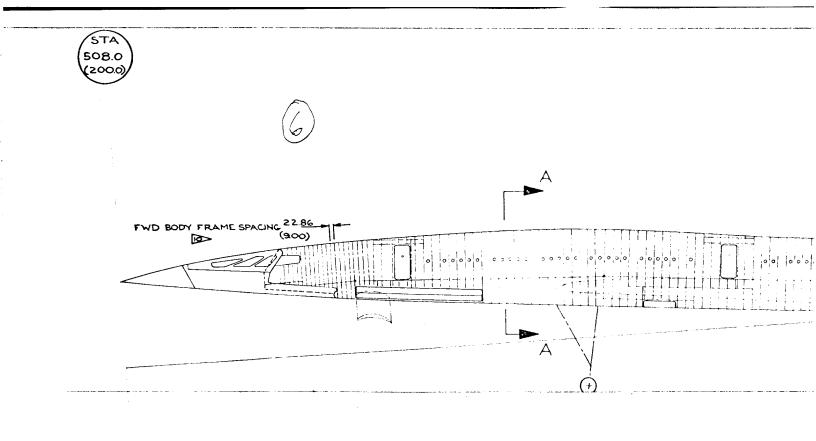
FWD BODY FRAM

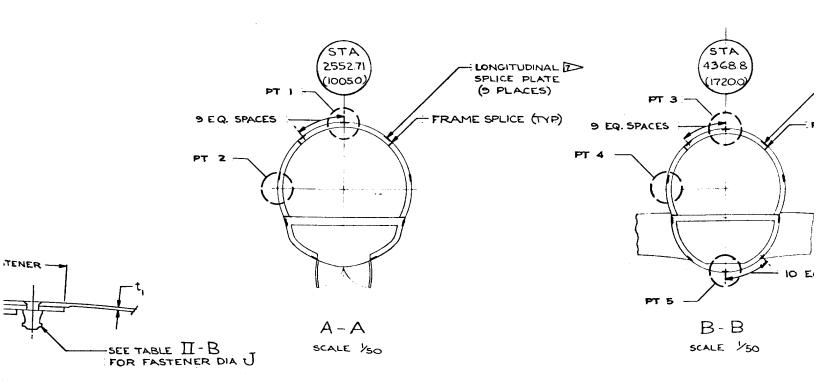
TABLE II-B FASTENER DIA PT. CM) NO. .397 (156) :397 2 (156) .39.7 3 (.156).397 (.156) 4 .476 (.188) 5 .635 (.250).635 (.250)476 8 (1881) 476 9 (188)

10> .635 (.250) 10

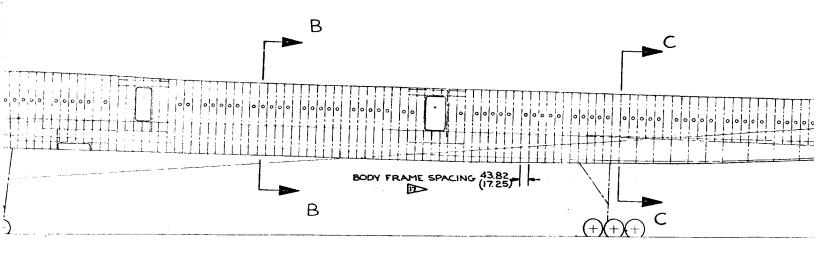


DET. H

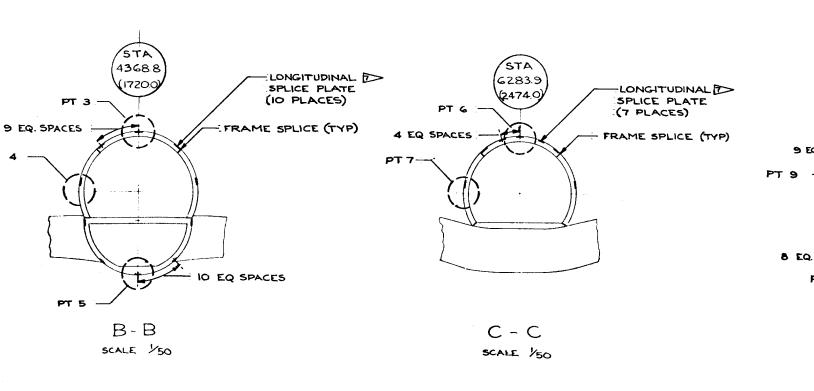


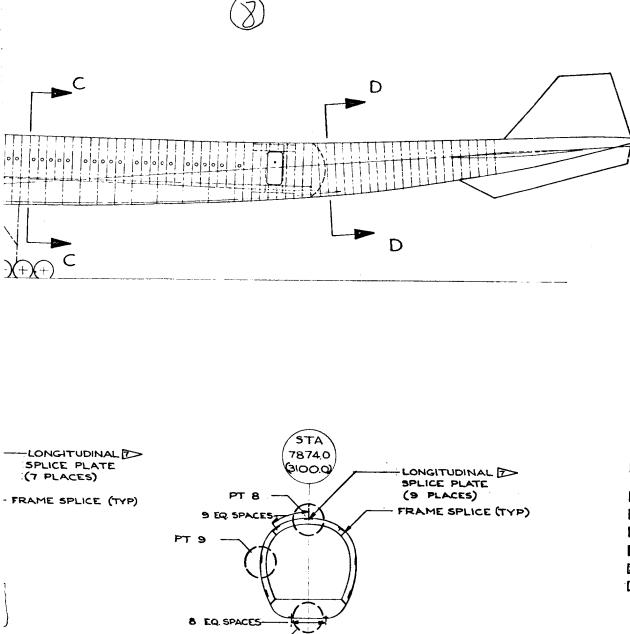






LEFT SIDE VIEW





PT 10 :

D-D

SCALE 150

D LOCAL SKIN PADUP IS

STRINGERS NOT REQD

PADUP & SPLICE MATL
INCLUDED IN TOTAL E

EFFECTIVE AREA SHO
SKIN PADUP, SPLICE PL

LONGITUDINAL SPLICE IS INCLUDED IN TOTAL

D CIRCUMFERENTIAL BOD JOINTS NOT INCLUDE SEE TABLE II-A FOR SEE THIS STRINGER IS ALSO DEPTH STRINGER DEPTH IS 3.18

STRINGER DEPTH IS 2.

FRAME & CLIP MATE IS

EXTRUDED STRINGER MA

FORMED STRINGER MATE

SKIN MATE IS TI GAL-4V

SKIN MATL IS TI GAL-4V
PANEL T SHOWN IS IN TI

NOTE : BASIC UNIT SYSTEM IS ENGLISH UNIT SYSTEM

REF. FUSEI

Figure 3-15.—Base 17.2:



- ► CIRCUMFERENTIAL BODY FRAME & SKIN PAD UP AND BODY SECTION JOINTS NOT INCLUDED IN EFFECTIVE ₹.
- SEE TABLE II-A FOR SPLICE STRINGER AREA & GEOMETRY.
- THIS STRINGER IS ALSO USED AT THE PANEL SPLICE
- \blacktriangleright SPLICE STRINGER DEPTH IS 3.18 (1.25) AND t_{g} IS .1016 (.04)
- STRINGER DEPTH 15 3.18 (1.25)
- STRINGER DEPTH IS 2.54 (100)
- D LOCAL SKIN PAD UP IS INCLUDED IN STRINGER AREA
- STRINGERS NOT REOD
- PAD UP & SPLICE MATE ON SIDE PANELS IS NOT INCLUDED IN TOTAL EFFECTIVE \$
- ES EFFECTIVE AREA SHOWN IS FOR ONE COMPLETE SPICE, INCLUDES SKIN PAD UP, SPLICE PLATE & STRINGER.
- D LONGITUDINAL SPLICE (PADUP MATL IN CROWN PANELS IS INCLUDED IN TOTAL EFFECTIVE \$
- FRAME & CLIP MATE IS TI GAL-4V COND I
- EXTRUDED STRINGER MATL IS TI GAL 4V COND III
- FORMED STRINGER MATL IS TI GAL-4V COND I
- 5KIN MATL IS TI GAL-4V COND I
- SKIN MATL IS TI GAL-4V COND I EL!
- PANEL E SHOWN IS IN TITANIUM [

NOTE : BASIC UNIT SYSTEM IS THE INTERNATIONAL SI SYSTEM ENGLISH UNIT SYSTEM EQUIVALENT VALUES ARE SHOWN IN (

REF. FUSELAGE DRAWING AWS-126

Figure 3-15.—Baseline, Titanium Skin and Stiffeners, 17.25-in. Frame Spacing

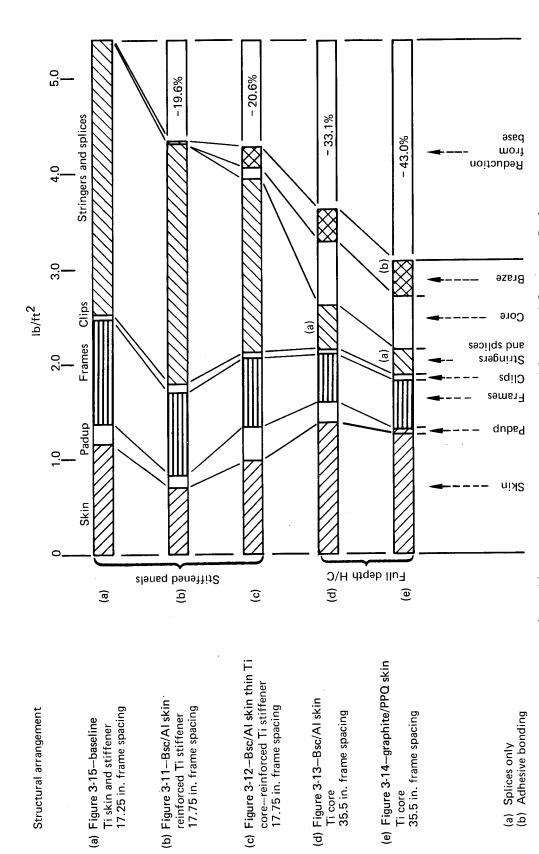


Figure 3-16.—Weight Comparison, Advanced Structural Concepts, Body

		Upper surfa	ce		Lower surfa	face			
	Skin	gage	Weight,	Skin	gage	Weight,			
Material	Inner	Outer	Ib/ft ²	Inner	Outer	Ib/ft ²			
Titanium H/S graphite/polyimide, (0/±45/90) _S	0.010 0.016	0.015 0.024	0.576 0.323	0.010 0.016	0.020 0.032	0.691 0.387			
Boron/polyimide, (0/±45/90) _S	0.0364	0.0364	0.76	0.0364	0.0364	0.76			

Based on:

Minimum gage of tapes available by 1986

Graphite/polyimide

2 mil/ply

Boron/polyimide

5.2 mil/ply

Minimum gage for practical considerations Graphite/polyimide

3 mil/ply upper-surface outer skins

4 mil/ply lower surface outer skins

Figure 3-17.—Minimum Gage Considerations

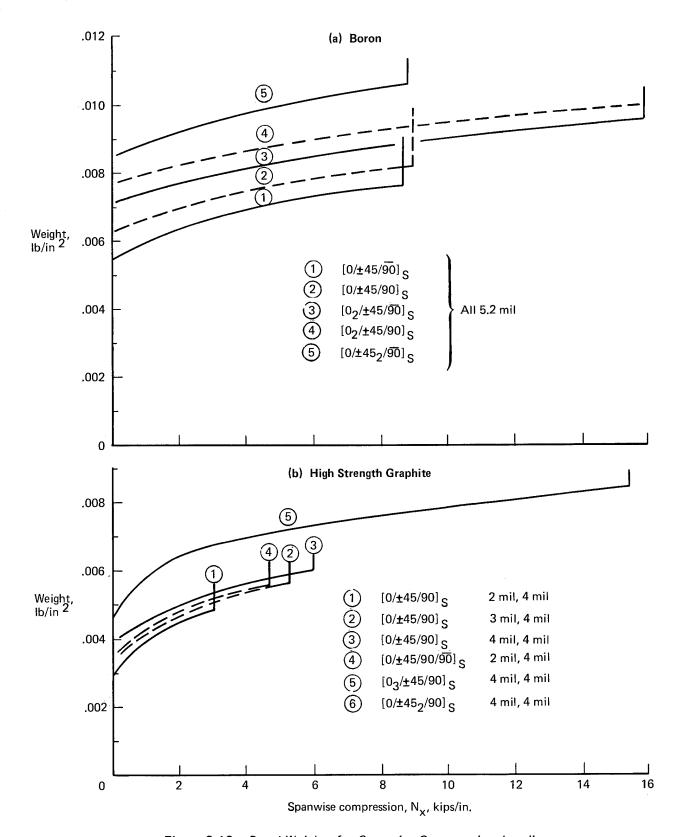


Figure 3-18.—Panel Weights for Spanwise Compression Loading

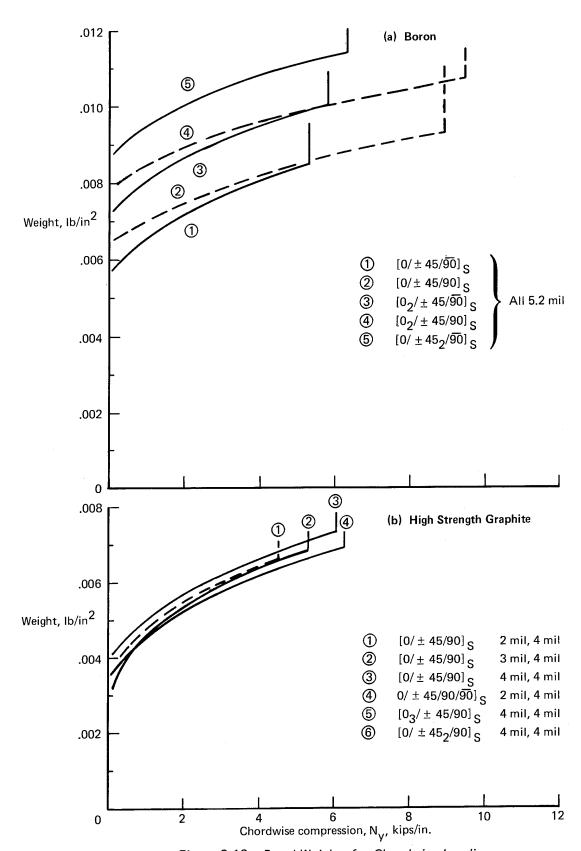


Figure 3-19.—Panel Weights for Chordwise Loading

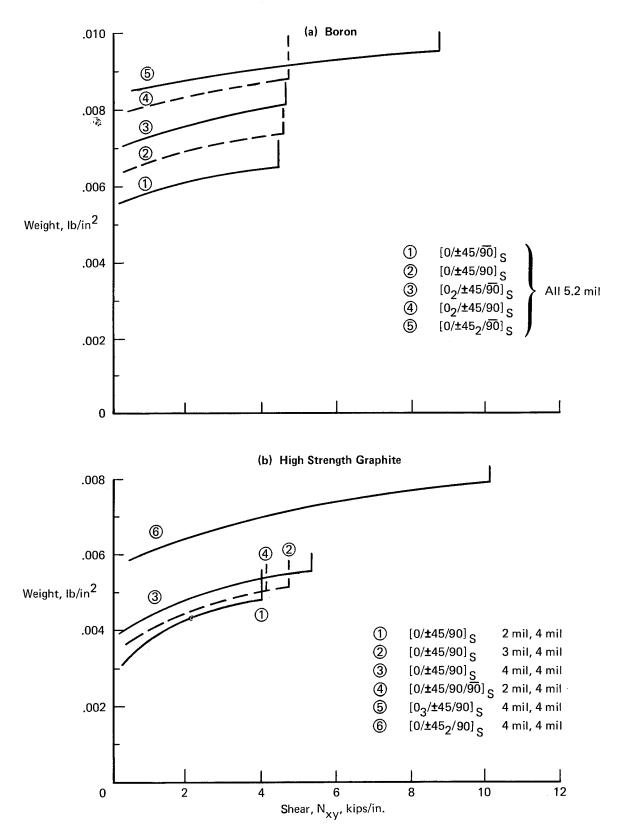


Figure 3-20.—Panel Weights for Shear Loading

SECTION 4

PANEL DESIGN

by

C. L. ABELL

CONTENTS

	Page
WING PANEL DESIGN OBJECTIVES	101
PANEL SELECTION	101
PANEL LOADS	101
COMPOSITE WING PANEL DESIGN	102
ALUMINUM BRAZED TITANIUM WING PANEL DESIGN	105
REFERENCES	

FIGURES

No.		Page
4-1	Design for Nonoptimum Factors, Panel Locations	108
4-2	Lower Wing Panel, Light Gage Bonded Graphite/Polyimide Sandwich,	
	Model 969-512B	109
4-3	Lower Wing Panel, Medium Gage Bonded Graphite/Polyimide Sandwich,	
	Model 969-512B	111
4-4	Lower Wing Panel, Heavy Gage Bonded Graphite/Polyimide Sandwich,	
	Model 969-512B	113
4-5	Upper Wing Panel, Medium Gage Bonded Graphite/Polyimide Sandwich,	
	Model 969-512B	115
4-6	Upper Wing Panel, Heavy Gage Bonded Graphite/Polyimide Sandwich,	
	Model 969-512B	117
4-7	Composite Skin Layup Diagram, Minimum Gage, Lower Wing Panel	
4-8	Composite Skin Layup Diagram, Medium Gage, Lower Wing Panel	120
4- 9	Composite Skin Layup Diagram, Heavy Gage, Lower Wing Panel	
4-10	Composite Skin Layup Diagram, Medium Gage, Upper Wing Panel	
4-11	Composite Skin Layup Diagram, Heavy Gage, Upper Wing Panel	
4-12	Lower Wing Panel, Light Gage Brazed-Titanium Sandwich, Model 969-512B	125
4-13	Lower Wing Panel, Medium Gage Brazed-Titanium Sandwich, Model 969-512B	127
4-14	Lower Wing Panel, Heavy Gage Brazed-Titanium Sandwich, Model 969-512B	129
4-15	Upper Wing Panel, Medium Gage Brazed-Titanium Sandwich, Model 969-512B	131
4-16	Upper Wing Panel, Heavy Gage Brazed-Titanium Sandwich, Model 969-512B	133

SYMBOLS

 $\begin{array}{ll} N_{X} & \text{Stress resultant in the x direction} \\ N_{y} & \text{Stress resultant in the y direction} \end{array}$

N_{xy} Shear Stress resultant

WING PANEL DESIGN OBJECTIVES

There were two primary objectives to be achieved in the panel design effort: to evaluate and identify problem areas; and to design in detail the panel edges and joint. To evaluate and identify problem areas, it was necessary to develop and display a rational detail design approach using the selected 1986 high strength graphite/polyimide composite in the bonded honeycomb sandwich wing panels. Detail designs relating the panel edge and joint features to the basic panel requirements were necessary to support the development of theoretical-to-actual factors for weight calculations.

It was also necessary to develop and display aluminum brazed titanium honeycomb sandwich panel designs, equivalent in their response to strength and environmental requirements, to relate the composite design to the titanium data base. A more detailed discussion of the development of theoretical-to-actual factors may be found in Section 5.

PANEL SELECTION

Five specific primary wing panels were selected on model 969-512B for the presentation of the detail designs. The 969-512B configuration was developed in the preceding study, as described in reference 4-1. Panel locations were selected to cover a representative load range. They include a lower surface minimum gage panel, upper and lower surface intermediate gage panels and upper and lower surface heavy gage panels. Figure 4-1 shows the locations of the representative panels.

It should be noted that the structural arrangement for Model 969-512B was developed with titanium as the baseline structural material. It does not necessarily follow that it is as near to optimum if composite materials were used. Additional improvement in the areas of weight and producibility should be attainable. However, reconfiguration of the structural arrangement to further exploit the composite materials is considered beyond the scope of this study and should be the subject of future work.

PANEL LOADS

The loads for the wing panel design effort were taken directly from the final Task II analysis in reference 4-1 with no adjustment for differences in static aeroelastic deformation between the Task II titanium aircraft and the Task III composite aircraft. In Task II there were specified spar loads and panel loads. This effort used the panel loads with the assumption that a difference in spar area to panel area ratio would not cause a significant change in the panel loads or effect the theoretical-to-actual factor.

Each wing panel covered an area represented by four to seven "cover plates" in the math model. Twenty-five load cases were evaluated for their criticality with regard to combined stresses, buckling interaction, and critical joint stress resultants. Critical N_x , N_y , and N_{xy} loads were identified for each "cover plate." Both sets of panels were designed to these loads.

COMPOSITE WING PANEL DESIGN

Figures 4-2, 4-3, 4-4, 4-5, and 4-6 show the detail design for the five representative composite panels. The detail shown is limited to the basic panels and their interfaces at joints and supports. Details are omitted with regard to corners, concentrated load points and access provisions because they depend on the detail design of the inner structure and systems which is a subject outside the scope of this effort. However, the aluminum-brazed titanium panels were given the same treatment in this respect and can be related to the titanium data base which does include all the nonoptimum features.

The graphite/polyimide honeycomb panels were analyzed according to procedures outlined in Section 6 of this report.

COMPOSITE SKINS

The basic inner and outer skins are fiber critical laminates, made of 1986 high strength graphite/polyimide unidirectional tapes having orientations of [0], [±45] and [90]. These tapes have a volume fraction of .6 and are laid up in an order that is symmetrical about the centerline of each skin thickness. The tapes are .004 in. thick in most areas, however, .002 in. thick tapes are used in the upper and lower panel inner skins in the minimum gage and low load areas. Also, .003 in. thick tapes are used in the upper panel outer skins in minimum gage and low load areas.

The skins are bonded to the core using a polyimide adhesive. The adhesive formulation is based upon improved addition reaction polyimide resins which have thermal and processing characteristics superior to present systems. The weight of the adhesive is assumed to be $.085 \text{ lb/ft}^2$ per bond line in the skin to core application.

The load in each "cover plate" was considered in arriving at layups that were practical for each wing panel. Skins were tapered to meet changing load requirements by adding or terminating lamina symmetrically in each skin. Terminations were staggered to minimize step heights.

Figures 4-7, 4-8, 4-9, 4-10 and 4-11 show the layup order of the five representative panels in more detail. No reflection of contour, pad up or thickness relationships is intended. The titanium interleaves exist only at joints and supports and are indicated to show only relative location with respect to the basic composite laminae. For panel edge design details see figures 4-2, 4-3, 4-4, 4-5 and 4-6.

The external lamina for each skin was consistently oriented in the spanwise direction [0]. The orientations of the remaining laminae were alternated as far as possible to reduce the chances of suffering damage to all the laminae of a given orientation in the event of a surface scratch.

COMPOSITE CORE

The honeycomb core used consists of 1986 high strength graphite fiber reinforcement in a polyimide matrix. The fiber orientation is tailored for different applications of shear and tension-compression to optimize design. Shear applications will rely on [±45] fiber orientation. Tension-compression applications will utilize [0] and [90] oriented fiber. A density of 3.5 lb/ft³ was selected for the basic center core for all panels. For a discussion of core allowables see Section 2. A discussion of panel thickness follows.

During the process of selecting the structural concept and the material to be used (discussed in more detail in Section 3) an evaluation of buckling strength versus core thickness was made. Although each specific layup was different, the general conclusions reached were: (1) 1 in. core was required to prevent shear buckling at ultimate allowable shear stress. (2) 1.5 in. core was required to prevent spanwise buckling at ultimate allowable spanwise compression stress. (3) 2.0 in. core was required to prevent chordwise buckling at ultimate allowable chordwise compression stress.

The majority of the wing upper surface is designed by high spanwise compression, medium shear and low chordwise compression loading.

Significant chordwise compression strains exist near the body on the wing lower surface and on both wing surfaces near the wing ribs. Large portions of the wing lower surface skins are established by combined tension and shear stresses but the core thickness is still established by the wing down bending conditions which are basically comp-comp-shear. A cursory examination of the wing upper surface was made utilizing the internal load distributions resulting from Task II. Core thicknesses over 1.5 in. would add more core weight than it would save skin weight. Core thickness less than 1.5 in. would add more skin weight than it would save core weight. The complications involved in changing core thicknesses are many and varied and result in weight penalties.

The allowable chordwise (and spanwise) strain in the covers was reduced to be compatible with the titanium ribs and spars. A 1.5 in. core was required to prevent buckling at this chordwise strain.

For these reasons, 1.5 in. core was selected for the entire wing primary structure. It is possible, though only at the expense of very many manhours, to save a small percentage of the core weight by further optimizing, but it would not be a significant amount.

JOINTS AND SUPPORTS

All load conditions were reviewed in consideration of the joint design requirements. Critical joint loads were not necessarily found to be the same as the critical panel loads. Fastener sizes and spacing were picked to meet the criteria for loads, fail safety and fuel containment. In the minimum gage area, 3/16 in. diameter fasteners were adequate. In the remaining areas, one and sometimes two rows of 1/4 in. diameter fasteners were required.

In the region of the fasteners, titanium interleaves were used to increase the bearing strength and to bridge the load between fasteners. The widths of these interleaves are varied in increments to achieve the effect of a taper. The joints were analyzed for ultimate load utilizing only the titanium interleaves for bearing. Fail safety analysis considered the interleaves plus the composite for bearing.

Also in the region of the fasteners in the spanwise joints, the unidirectional laminae having [0] orientation were replaced with [±45] woven graphite/polyimide fabric to reduce the stress concentration at fastener holes.

The skin thicknesses at the panel edges are made up of the basic panel laminae plus the sum of the titanium interleaves plus the polyimide adhesive required to bond the interleaves to the composite laminae. The relative location of the interleaves to the specific laminae is shown in figures 4-7, 4-8, 4-9, 4-10, and 4-11. The locations were specifically picked to provide more uniform load distribution to the interleaves with a minimum of interlaminar shear. The adhesive in this application is .0035 in.

thick and weighs $.03 \text{ lb/ft}^2$ per bond line. In addition to the above, the inner skin pad up includes an integral shim made of [± 45] woven graphite/polyimide fabric to account for panel thickness tolerance. The shim includes a machining allowance of 0.03 in. over and above the nominal height. The shim is ground down to achieve a constant panel thickness which will facilitate matching the panel to the inner structure and adjacent panels at installation.

The panel edge core is similar to the center core, but is more dense in order to react the bolt clamp up forces. Core having a density of 7 lb/ft^3 is used with 3/16 in. diameter bolts and core having a density of 14 lb/ft^3 is used with 1/4 in. diameter bolts.

The core splice locations are such that all the skin eccentricities occur in the dense core region. The polyimide core splice adhesive is a formulation very similar to the structural adhesive used in the laminated and sandwich areas. Handling and processing is comparable to present systems. The average core splice bond line thickness is assumed to be .10 in. with a density of 30 lb/ft³. High temperature stable potting material used to seal the edges of the honeycomb sandwich core is a polyimide based structural foam with a formulation very similar to the bonding and core splice adhesive. For weight estimating purposes, an average thickness of .1 in. and a density of 44 lb/ft³ was assumed.

OTHER DESIGN CONSIDERATIONS

Lightning

No attempt was made to solve the problems of lightning protection, but an attempt was made to include a weight penalty representative of a realistic solution.

The joint concept selected for this program employs titanium splice plates which will act as a grid work of bus bars on both wing surfaces running spanwise at 35 in. spacing and connected together at the leading edge spar, the wing ribs and the body.

Lightning strikes and discharges on metal airplanes generally occur at the airplane extremities and utilize the structure in between as a conductive path.

Similar behavior would be expected for an "all composite" airplane but unique problems should be anticipated for structure utilizing various mixtures of metal and nonmetal materials.

Weights needed for adequate protection of this airplane will probably range from nearly zero to .1 lb/ft^2 depending on location. The lightning strike protection system is designed to conduct a 200 000 amp discharge. It is assumed to weigh .05 lb/ft^2 and is incorporated as an integral part of the structure or applied to the exterior surface in operations subsequent to fabrication.

Exterior Finish

The high temperature stable conductive and/or decorative paint used on the exterior of the composite structure is assumed to be formulated from a polyimide or other stable resin base and conductive graphite powder. The estimated weight is $0.027 \, lb/ft^2$.

Producibility

Consideration was given to producibility in arriving at the designs shown in figures 4-2 through 4-6. The skins are each balanced symmetrical laminates. This should reduce the tendency for warpage. An integral shim with excess machining allowance is included on the inner skin at joints and supports to account for panel thickness tolerances. The drawings were reviewed by manufacturing with the conclusion that the panels could be produced using current manufacturing technology.

ALUMINUM-BRAZED TITANIUM WING PANEL DESIGN

Figures 4-12 to 4-16 show the detail design for the five representative aluminum-brazed titanium panels. The scope of the detail shown is the same as that shown for the equivalent composite panels. In general, the design technology is like the 2707-300 SST because that detail design effort is the source of the data base for aluminum-brazed titanium wing panel theoretical-to-actual factors.

The titanium honeycomb panels were analyzed according to procedures outlined in Section 4 of reference 4-1.

TITANIUM SKINS

The titanium inner and outer skins are chem-milled Ti-6Al-4V sheet. As discussed under panel loads, the loads in each "cover plate" were considered in arriving at the basic skin thicknesses. The skins are tapered where the loads vary within a panel.

The skins are aluminum brazed to the core. The total braze alloy thickness per panel as .016 in.

TITANIUM CORE

The basic core used in the panel center consists of composition 2, SC4-20NM honeycomb core with a density of 4.9 lb/ft³. The core depth is 1.00 in. These values are the same as for the 2707-300 SST data base design.

JOINTS AND SUPPORTS

The same design conditions were applied to the titanium panel joint and support features as were used for the composite panels resulting in the same fastener sizes and spacing. The thickness of the external splice straps is the same also, since it is a function of the countersunk bolt heads. The skins are chem-milled leaving a padded up strip at all joints and supports to account for the flush external splice strap recess and to achieve adequate bearing strength and to distribute the bolt crushing forces to the core.

The core in the region of the fasteners is more dense in order to withstand the crushing loads due to bolt clamp up forces. Composition 3 SS2-30NM honeycomb core with a density of 14.1 lb/ft^3 , is used with 3/16 in. diameter fasteners in minimum gage panels. Composition 3, SS2-60NM honeycomb core with a density of 28.1 lb/ft^3 is used with 1/4 in. diameter fasteners in medium and heavy gage panels.

The joints between the center and edge core are spotwelded and are located so that all of the local eccentricities are in the region of the dense core.

The exposed edges of the panels at joints are given two coats of primer to inhibit corrosion.

OTHER DESIGN CONSIDERATIONS

Lightning

Again no attempt was made to solve the various problems of lightning protection. However, because the aluminum brazed wing panels are all metal and are supported on titanium inner structure, no weight penalty for lightning protection has been included.

Exterior Finish

No provision for an exterior finish has been made.

Producibility

The detail design shown is consistent with the technology developed on the 2707-300 SST program during which hardware was produced. Fit up tolerances to achieve a good braze are very exacting. To facilitate fit up, only one step height was allowed on the inner surface of the outer skin within any one panel. This is a compromise with optimum pad up requirements for the sake of producibility.

REFERENCE

4-1 Boeing Staff: Study of Structural Design Concepts for an Arrow Wing Supersonic Transport Configuration. NASA Langley Research Center, CR 132576-1 and -2, 1976.

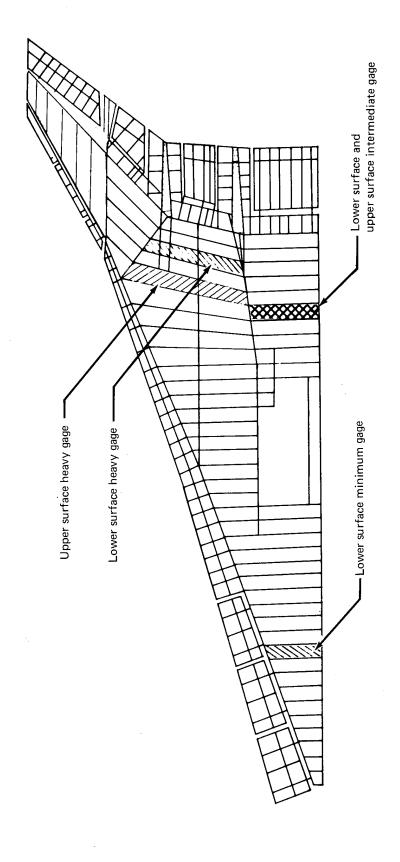
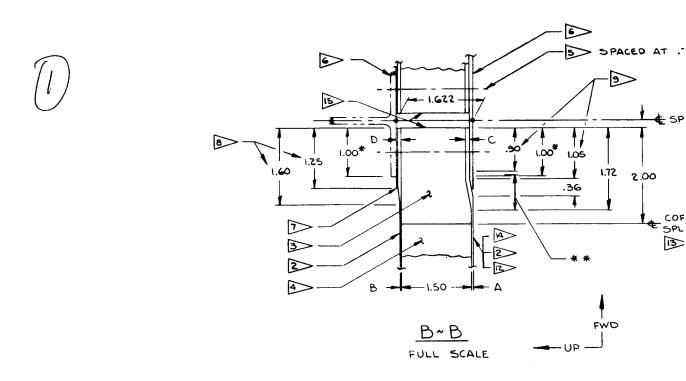
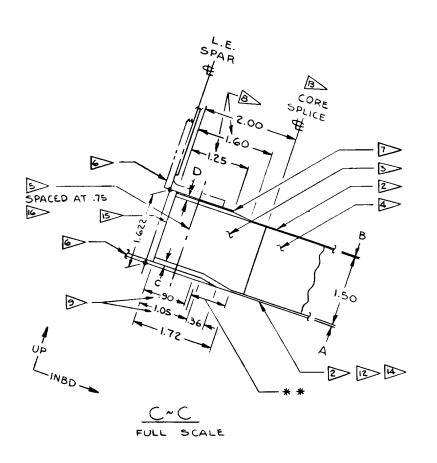
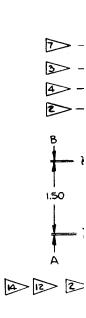
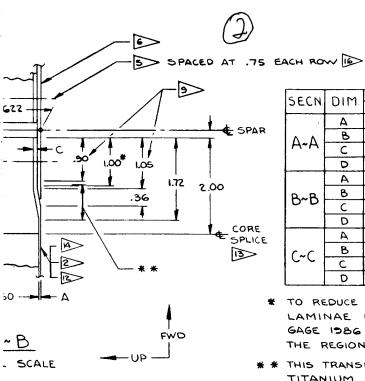


Figure 4-1.—Design for Nonoptimum Factors, Panel Locations



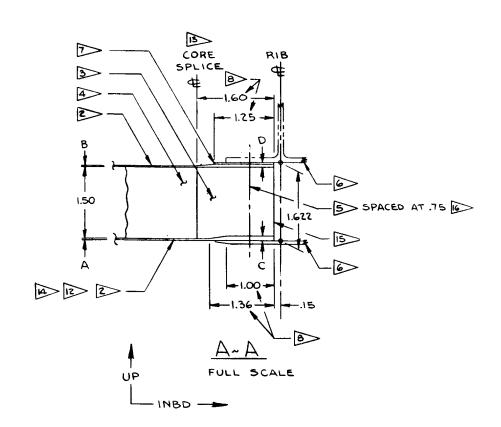






SECN	DIM	IM GAGE		LAYUP D D			
0 - 0	011 1.	TOTAL	ΣTI	LATOI			
	Α	.032		[0/+45/90/-45]s			
A~A	В	.016		SAME AS 'A'			
H~A	C	.092	.032	[0/T1/+45/90/T1/-45]s			
<u> </u>	٥	oeo.	.016	SAME AS C PLUS .030 THICK SHIM 7>			
	Α						
B~B	В						
וטייטן	С			GAGES & LAYUP			
	D			SAME AS SECN. A-A			
	Α						
C~C	В						
	С						
L	D						

- * TO REDUCE THE STRESS CONCENTRATION FACTOR, UNI-DIRECTIONAL LAMINAE HAVING O° ORIENTATION ARE REPLACED WITH EQUIVALENT GAGE 1386 HIGH STRENGTH GRAPHITE/POLYIMIDE WOVEN FABRIC (±45°) IN THE REGION OF THE BOLT HOLES AS INDICATED BY * IN SECH. B~B.
- * * THIS TRANSITION REGION IS LIKE C' (SEE TABLE) EXCEPT THE
 TITANIUM BEARING LAMINAE & ASSOCIATED ADHESIVE ARE REPLACED
 BY EQUIVALENT GAGE LAMINAE OF 1986 HIGH STRENGTH GRAPHITE/
 POLYIMIDE WOVEN FABRIC (± 45°) OF VARYING WIDTH TO ACHIEVE
 THE ENVELOPE SHOWN.

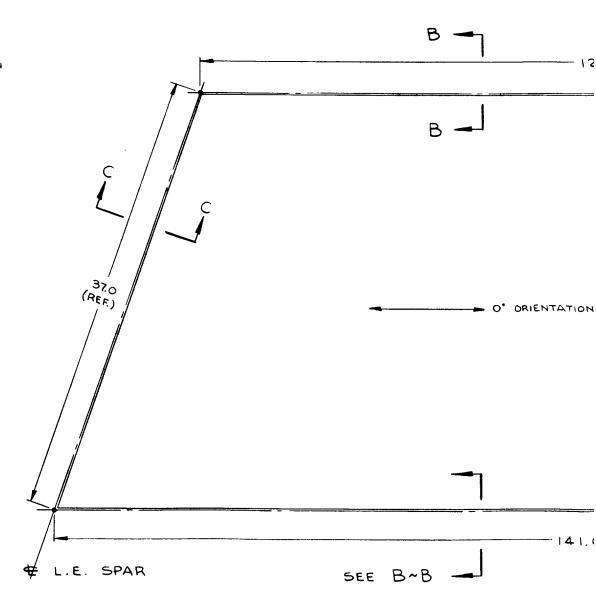


3

۶
rv-45]s
LUS .030 THICK SHIM 7>
ES & LAYUP E AS SECN. A-A

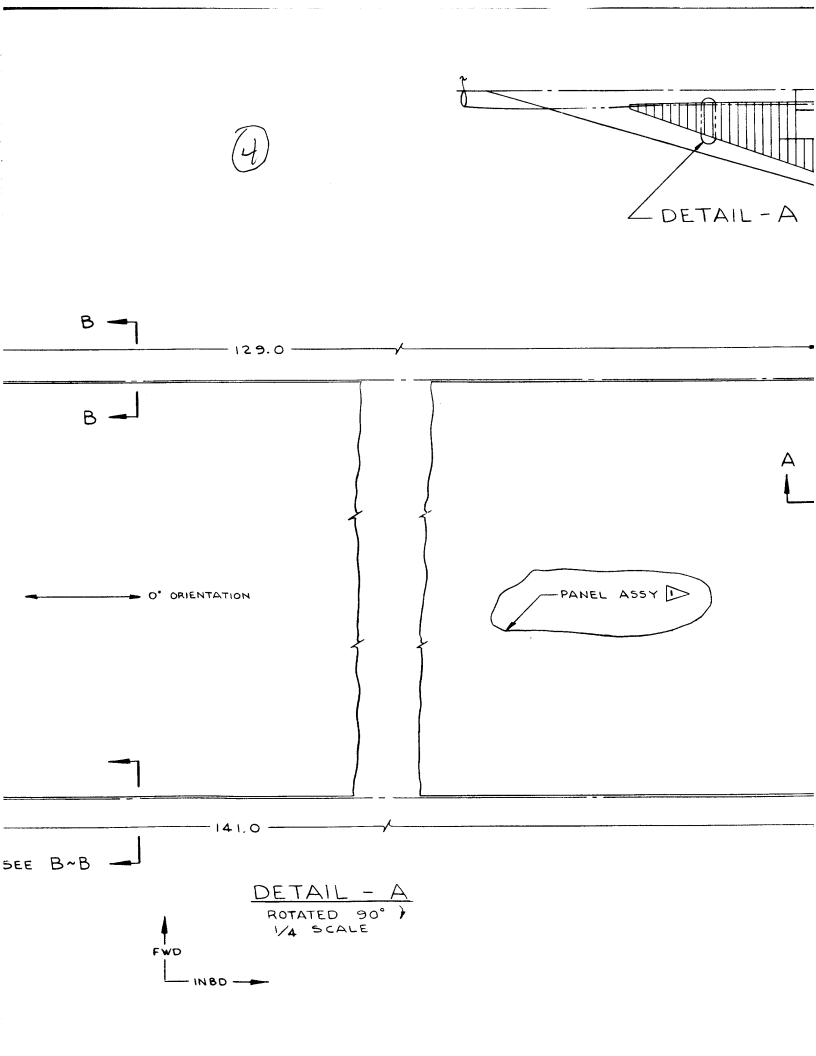
FACTOR, UNI-DIRECTIONAL
REPLACED WITH EQUIVALENT
OLYIMIDE WOVEN FABRIC (±45°) IN
INDICATED BY * IN SECH. B~B.

SEE TABLE) EXCEPT THE
ATED ADHESIVE ARE REPLACED
36 HIGH STRENGTH GRAPHITE/
ARYING WIDTH TO ACHIEVE



- INBO -

75 6



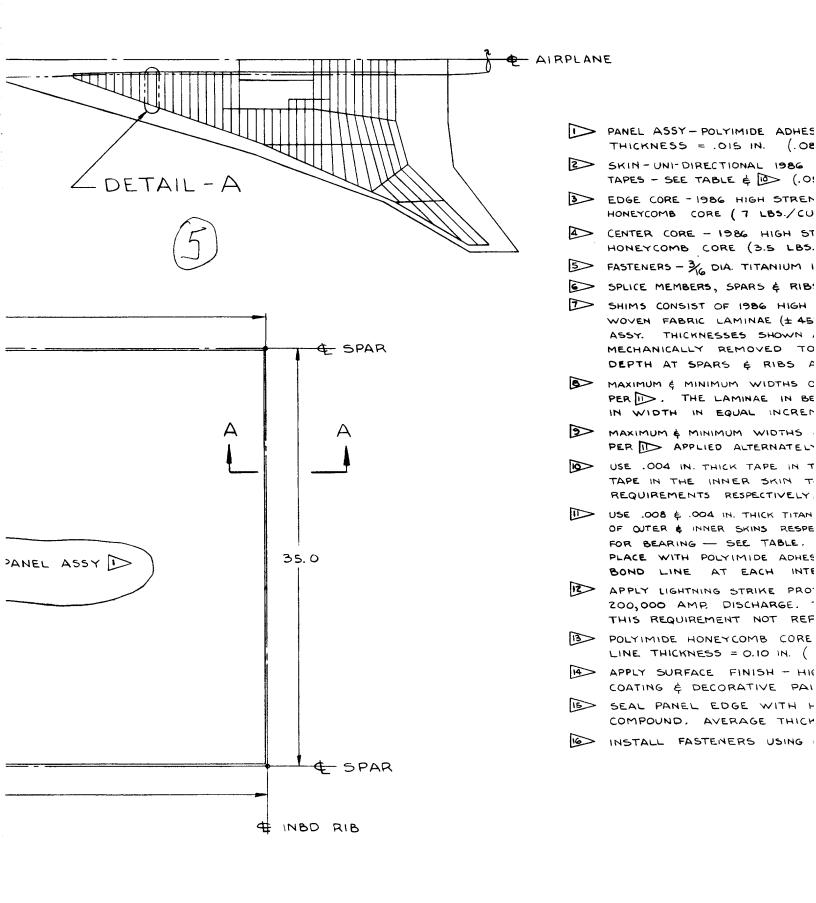


Figure 4-2.—Lo GI



- PANEL ASSY POLYIMIDE ADHESIVE BONDED SANDWICH. ADHESIVE THICKNESS = .015 IN. (.085 LBS./SQ. FT./BOND LINE.).
- SKIN-UNI-DIRECTIONAL 1986 HIGH STRENGTH GRAPHITE/POLYIMIDE TAPES SEE TABLE & (.056 LBS./CUBIC IN.) .
- EDGE CORE 1986 HIGH STRENGTH GRAPHITE / POLYIMIDE HONEYCOMB CORE (7 LBS./ CUBIC FT.) .
- CENTER CORE 1986 HIGH STRENGTH GRAPHITE/POLYIMIDE HONEYCOMB CORE (3.5 LBS./CUBIC FT.) .
- FASTENERS 3/6 DIA. TITANIUM 100° CSK. SHEAR HEAD BOLTS.
- SPLICE MEMBERS, SPARS & RIBS ARE TI-GAL-4V.
- SHIMS CONSIST OF 1986 HIGH STRENGTH GRAPHITE/POLYIMIDE WOVEN FABRIC LAMINAE (± 45°) INTEGRAL WITH THE PANEL ASSY. THICKNESSES SHOWN ARE NOMINAL. EXCESS IS MECHANICALLY REMOVED TO ACHIEVE CONSTANT PANEL DEPTH AT SPARS & RIBS AS SHOWN.
- MAXIMUM & MINIMUM WIDTHS OF TI-GAL-4V BEARING LAMINAE
 PER . THE LAMINAE IN BETWEEN VARY PROGRESSIVELY
 IN WIDTH IN EQUAL INCREMENTS.
 - MAXIMUM & MINIMUM WIDTHS OF TI-GAL-4V BEARING LAMINAE PER IN APPLIED ALTERNATELY.
- USE .004 IN. THICK TAPE IN THE OUTER SKIN & .002 IN. THICK TAPE IN THE INNER SKIN TO MEET DIM. 'A' & 'B'
 REQUIREMENTS RESPECTIVELY.
- USE .008 \$.004 IN. THICK TITANIUM INTER LEAVES IN PAO UP AREAS

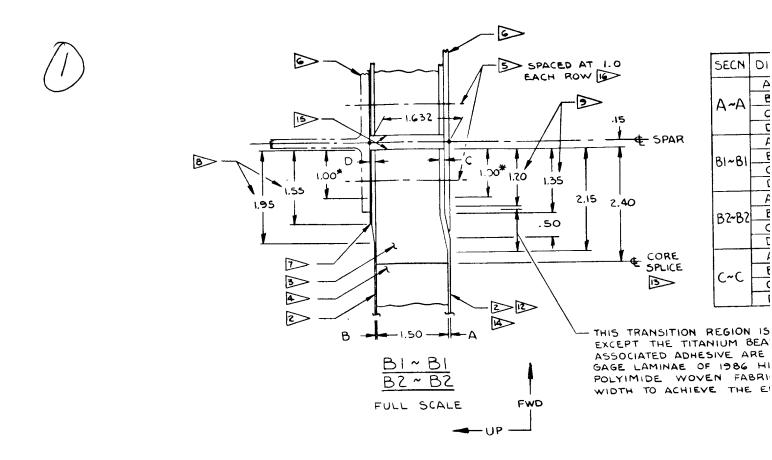
 OF OUTER \$ INNER SKINS RESPECTIVELY TO MEET Σ TI REQUIREMENTS

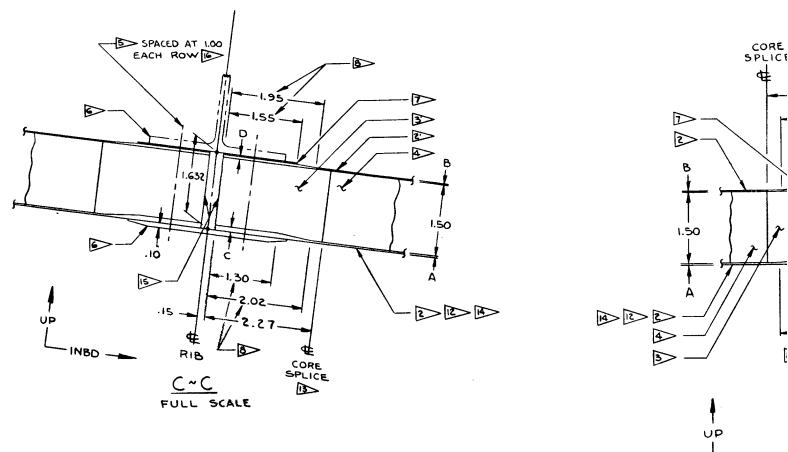
 FOR BEARING SEE TABLE. INTER LEAVES ARE BONDED IN

 PLACE WITH POLYIMIDE ADHESIVE HAVING A .0035 IN. THICK

 BOND LINE AT EACH INTERFACE. (.03 LBS./SQ.FT/BONDLINE).
- APPLY LIGHTNING STRIKE PROTECTIVE SURFACE COATING TO CARRY 200,000 AMP. DISCHARGE. THICKNESS = .002 IN. (.05 LB5/5Q. FT.)
 THIS REQUIREMENT NOT REFLECTED IN THE TABLE.
- POLYIMIDE HONEYCOMB CORE SPLICE ADHESIVE AVERAGE BOND LINE THICKNESS = 0.10 IN. (30 LBS/CUBIC FT.).
- APPLY SURFACE FINISH HIGH TEMPERATURE STABLE CONDUCTIVE COATING & DECORATIVE PAINT. (.027 LBS./SQ. FT.) .
- SEAL PANEL EDGE WITH HIGH TEMPERATURE STABLE POTTING COMPOUND. AVERAGE THICKNESS = 0.10 (44 LBS./CUBIC FT.).
- INSTALL FASTENERS USING UNCURED FLUOROSILICONE COATING.

Figure 4-2.—Lower Wing Panel, Light Gage Bonded GR/PI Sandwich Extruded 969–512B





INBO -



> SPACE			
EACH	R	wc	16>

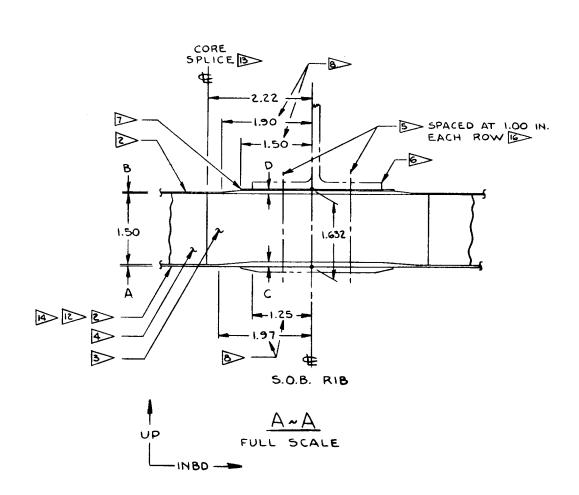
FWD

	-[2>>	15	
20 1.35		SPAR	
.50	2,15	2.40	
		CORE SPLICE	

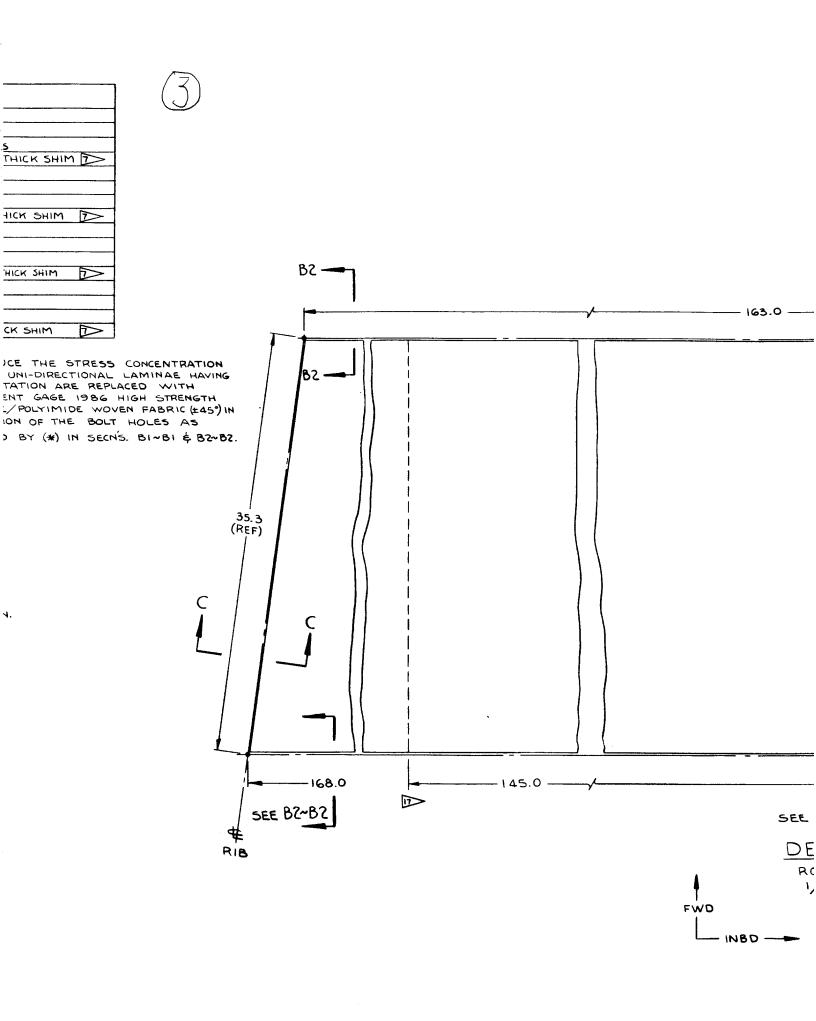
6550	0.114	GA	GE	
SECN	DIM	TOTAL		LAYUP D D
	Α	.036	_	[0/90/+45/-45/50]s
A~A	В	·018		SAME AS A'
	C	.104	.040	[0/T1/90/+45/T1/-45/90]s
	0	-096	.020	SAME AS C' PLUS .030 THICK SHIM T
	Α	.036	_	[0*/90/45/-45/90]5
BI~BI	В	.018		SAME AS 'A'
	C	.104	.040	[0*/T1/90/+45/T1/-45/50]s
	O	.096	.020	SAME AS C PLUS .030 THICK SHIM
	Α	.032		[0*/+45/90/-45]5
B2~B2	В	.016	_	SAME AS A'
	С	.10	.040	[O*/TI/+45/90/TI/-45]5
	D	.100	.020	SAME AS C PLUS .036 THICK SHIM
	Α	.032 .		[0/+45/90/-45]5
C~C	В	.016		SAME AS A
	С	.100	.040	[0/T1/+45/90/T1/-45]5
	D	.100	.020	SAME AS C' PLUS .036 THICK SHIM

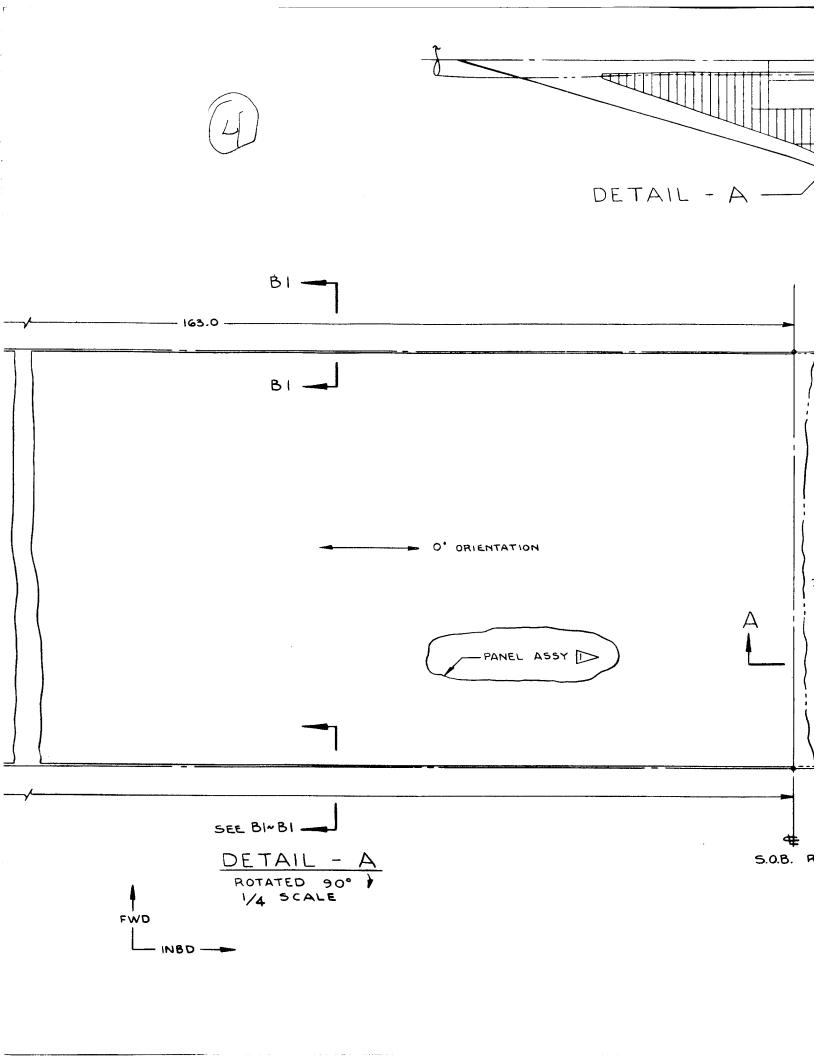
-THIS TRANSITION REGION IS LIKE C'(SEE TABLE)
EXCEPT THE TITANIUM BEARING LAMINAE &
ASSOCIATED ADHESIVE ARE REPLACED BY EQUIVALENT
GAGE LAMINAE OF 1986 HIGH STRENGTH GRAPHITE/
POLYIMIDE WOVEN FABRIC (± 45°) OF VARYING
WIDTH TO ACHIEVE THE ENVELOPE SHOWN.

* TO REDUCE THE STRESS CONCENTRATION FACTOR, UNI-DIRECTIONAL LAMINAE HAVING O' ORIENTATION ARE REPLACED WITH EQUIVALENT GAGE 1986 HIGH STRENGTH GRAPHITE/POLYIMIDE WOVEN FABRIC (±45°) IN THE REGION OF THE BOLT HOLES AS INDICATED BY (*) IN SECNS. BI~BI & B2~B2.



35. (RE





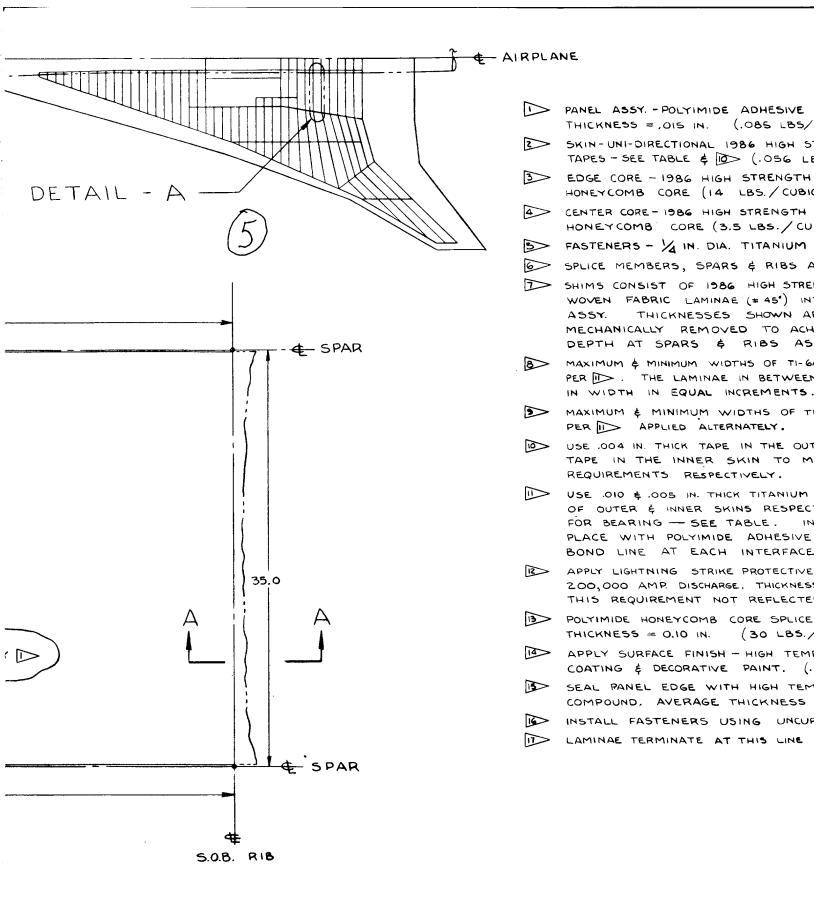


Figure 4-3.—Low



PANEL ASSY. - POLYIMIDE ADHESIVE BONDED SANDWICH, ADHESIVE THICKNESS = .015 IN. (.085 LBS/SQ. FT/BOND LINE).

SKIN-UNI-DIRECTIONAL 1986 HIGH STRENGTH GRAPHITE/POLYIMIDE.TAPES - SEE TABLE & DO (.056 LBS./CUBIC IN.).

EDGE CORE - 1986 HIGH STRENGTH GRAPHITE / POLYIMIDE HONEY COMB CORE (14 LBS. / CUBIC FT.) .

CENTER CORE - 1986 HIGH STRENGTH GRAPHITE / POLYIMIDE HONEY COMB CORE (3.5 LBS. / CUBIC FT.).

FASTENERS - 1/2 IN. DIA. TITANIUM 100° CSK. SHEAR HEAD BOLTS.

SPLICE MEMBERS, SPARS & RIBS ARE TI-GAL-4V.

SHIMS CONSIST OF 1986 HIGH STRENGTH GRAPHITE/POLYIMIDE WOVEN FABRIC LAMINAE (± 45°) INTEGRAL WITH THE PANEL ASSY. THICKNESSES SHOWN ARE NOMINAL. EXCESS IS MECHANICALLY REMOVED TO ACHIEVE CONSTANT PANEL DEPTH AT SPARS & RIBS AS SHOWN.

MAXIMUM & MINIMUM WIDTHS OF TI-GAL-4V BEARING LAMINAE PER . THE LAMINAE IN BETWEEN VARY PROGRESSIVELY IN WIDTH IN EQUAL INCREMENTS.

MAXIMUM & MINIMUM WIDTHS OF TI-GAL-4V BEARING LAMINAE PER I APPLIED ALTERNATELY.

USE .004 IN THICK TAPE IN THE OUTER SKIN \$.002 IN THICK TAPE IN THE INNER SKIN TO MEET DIM A' & B' REQUIREMENTS RESPECTIVELY.

USE .010 \$.005 IN. THICK TITANIUM INTER LEAVES IN PAD UP AREAS

OF OUTER \$ INNER SKINS RESPECTIVELY TO MEET & TI REQUIREMENTS

FOR BEARING — SEE TABLE. INTER LEAVES ARE BONDED IN

PLACE WITH POLYIMIDE ADHESIVE HAVING A .0035 IN. THICK

BOND LINE AT EACH INTERFACE. (.03 LBS./SQ.FT/BOND LINE).

APPLY LIGHTNING STRIKE PROTECTIVE SURFACE COATING TO CARRY 200,000 AMP. DISCHARGE. THICKNESS = .002 IN. (.05 LB5/SQ. FT.) THIS REQUIREMENT NOT REFLECTED IN THE TABLE.

POLYIMIDE HONEYCOMB CORE SPLICE ADHESIVE AVERAGE BOND LINE THICKNESS = 0.10 IN. (30 LBS./CUBIC FT.).

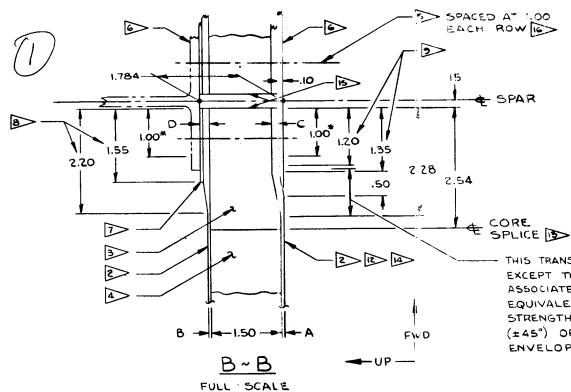
APPLY SURFACE FINISH - HIGH TEMPERATURE STABLE CONDUCTIVE COATING & DECORATIVE PAINT, (.027 LBS./ 59. FT.) .

SEAL PANEL EDGE WITH HIGH TEMPERATURE STABLE POTTING COMPOUND. AVERAGE THICKNESS = 0.10 (44 LB5./ CUBIC FT.)

INSTALL FASTENERS USING UNCURED FLUOROSILICONE COATING.

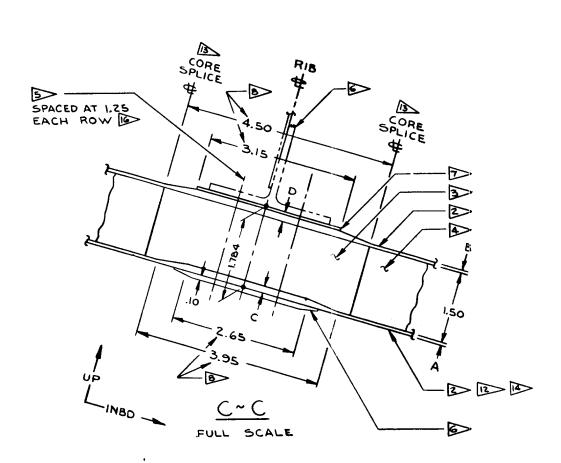
LAMINAE TERMINATE AT THIS LINE IN EACH SKIN.

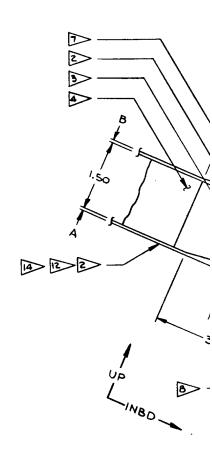
Figure 4-3.— Lower Wing Panel, Medium Gage Bonded GR/PI Sandwich, Model 969–512B



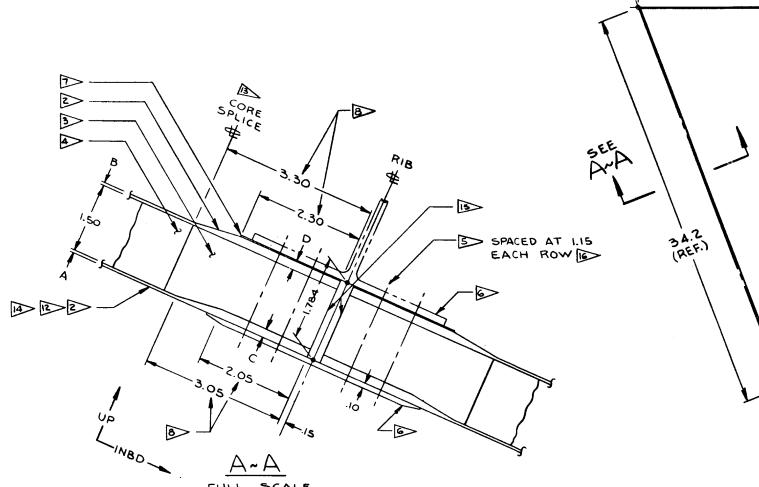
SECN	DIM	GAGE		
SECIT	017	TOTAL	ZT	
	4	.064		
۸.۸	В	.064		
A~A	C	.190	.06:	
	D	.220	.061	
	Α	.064		
	В	.064		
В~В	С	.148	.04	
	D	.220	.04	
	Α	.064		
	В	.064	_	
C~C	. C	.148	.04	
	D	.220	.04	

THIS TRANSITION REGION IS LIKE IN EXCEPT THE TITANIUM BEARING LE ASSOCIATED ADHESIVES ARE REPLEQUIVALENT GAGE LAMINAE OF STRENGTH GRAPHITE POLYIMIDE (±45°) OF VARYING WIDTH TO ENVELOPE SHOWN.



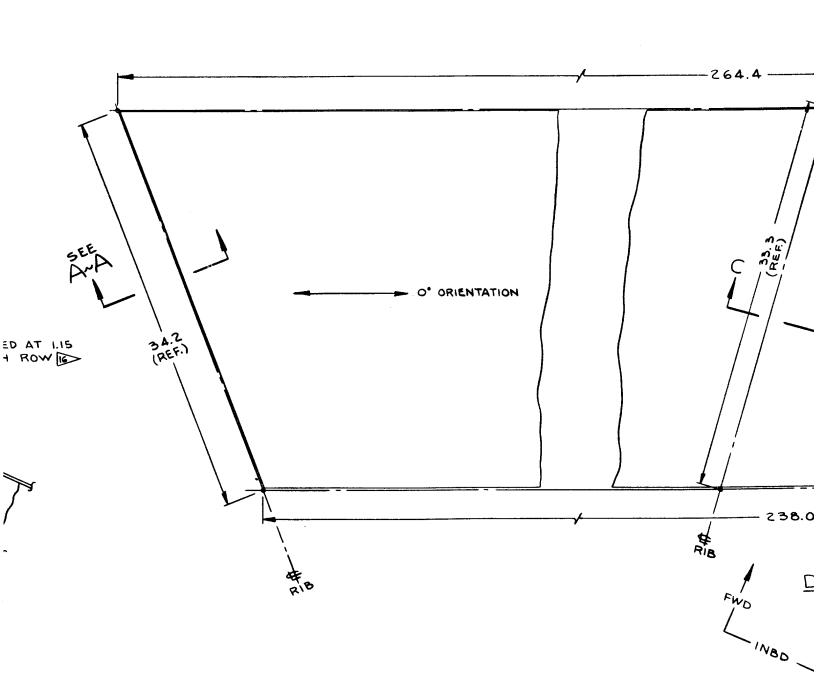


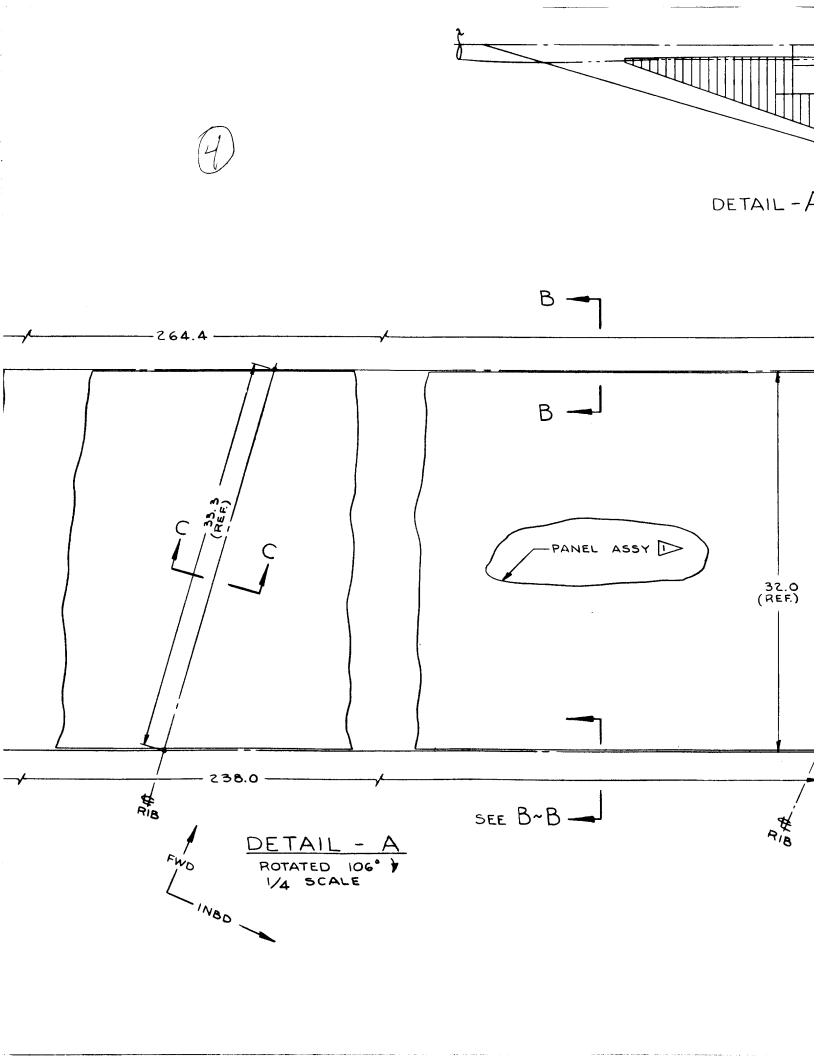
CONTRA CE						
ROW [i]>>	SECN	DIM	GA(LAYUP D ID	# TO REDUCE THE ST
		A	.064		[0/+45/0/-45/0/90/0z]s	UNI- DIRECTIONAL LA
	1, ,	В	.064		SAME AS A	ARE REPLACED WITH
	A~A	C	.190	.063	[9/11/45/9/11/-45/0/11/90/0/11/0/71]5	STRENGTH GRAPHITE
E SPAR		D	.220	.063	SAME AS 'C' PLUS .030 THICK SHIM	
E OFAN		Α	.064	_	[0*/+45/0*/-45/0*/90/0*z]s	BY (* IN SECN. B
	B~B	В	.064		SAME AS A'	
	D~D	С	.148	.042	[O*/TV+45/O*/TV-45/O*/TV99/O*]3	
	1	D	.220	.042	SAME AS C'PLUS .072 THICK SHIM	
		Α	.064		[0/+45/0/-45/0/90/0z]s	
		В	.064		SAME AS A'	
	C~C	. C	.148	.042	[0/TI/+45/0/TI/-45/0/TI/90/0z]5	
		D	.220	.042	SAME AS'C' PLUS .072 THICK SHIM	•
	E TITA D ADHE IT GAG GRAPH	NIUM SIVES E LAI	BEARING ARE F MINAE POLYIMI	G LAM REPLAC OF 191 DE WO	INAE \$ ED BY 3G HIGH DVEN FABRIC	
ENVELOPE			NIDIA	10 A	CHIEVE THE	
				\ \	CORE DE	CEE



* TO REDUCE THE STRESS CONCENTRATION FACTOR, UNI-DIRECTIONAL LAMINAE HAVING O' ORIENTATION ARE REPLACED WITH EQUIVALENT GAGE 1986 HIGH STRENGTH GRAPHITE/POLYIMIDE WOVEN FABRIC (±45°) IN THE REGION OF THE BOLT HOLES AS INDICATED BY (* IN SECN. B~B.

(3)





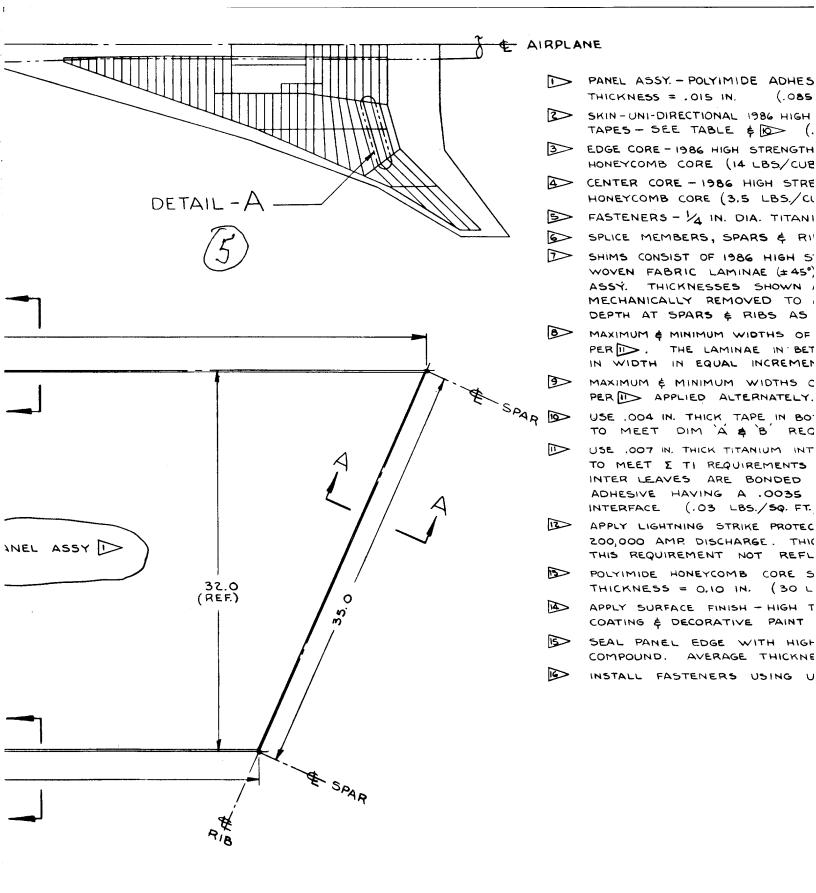


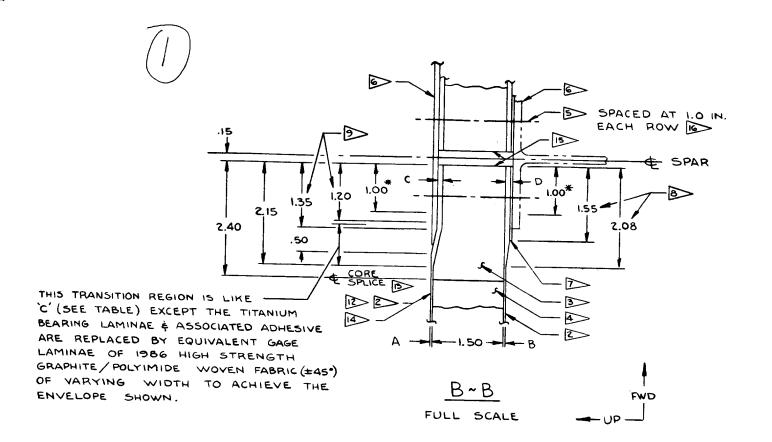
Figure 4-4.—

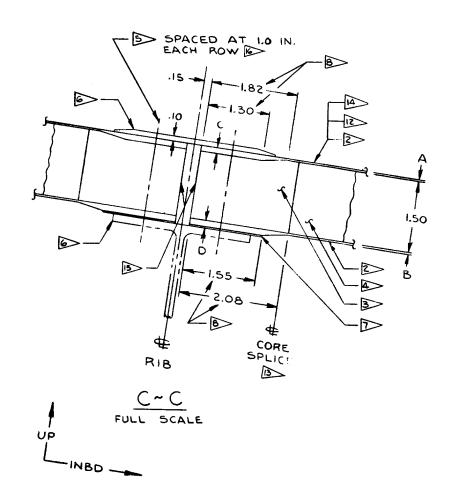
-ANE



- > PANEL ASSY. POLYIMIDE ADHESIVE BONDED SANDWICH. ADHESIVE THICKNESS = .015 IN. (.085 LBS./SQ. FT./ BOND LINE).
- > SKIN-UNI-DIRECTIONAL 1986 HIGH STRENGTH GRAPHITE/POLYIMIDE TAPES SEE TABLE \$ 100 (.056 LBS. / CUBIC IN.) .
- > EDGE CORE 1986 HIGH STRENGTH GRAPHITE/FOLYIMIDE HONEYCOMB CORE (14 LBS/CUBIC FT.) .
- > CENTER CORE 1986 HIGH STRENGTH GRAPHITE / POLYIMIDE HONEYCOMB CORE (3.5 LBS./CUBIC FT.) .
- > FASTENERS 1/4 IN. DIA. TITANIUM 100° CSK. SHEAR HEAD BOLTS.
- SPLICE MEMBERS, SPARS & RIBS ARE TI-GAL-4V.
- SHIMS CONSIST OF 1986 HIGH STRENGTH GRAPHITE/POLYIMIDE WOVEN FABRIC LAMINAE (±45°) INTEGRAL WITH THE PANEL ASSY. THICKNESSES SHOWN ARE NOMINAL. EXCESS IS MECHANICALLY REMOVED TO ACHIEVE CONSTANT PANEL DEPTH AT SPARS & RIBS AS SHOWN.
- MAXIMUM & MINIMUM WIDTHS OF TI-GAL-4V BEARING LAMINAE PER . THE LAMINAE IN BETWEEN VARY PROGRESSIVELY IN WIDTH IN EQUAL INCREMENTS.
 - MAXIMUM & MINIMUM WIDTHS OF TI-GAL-4V BEARING LAMINAE PER ID APPLIED ALTERNATELY.
 - USE .004 IN. THICK TAPE IN BOTH INNER & OUTER SKINS
 TO MEET DIM 'Á & 'B' REQUIREMENTS.
 - USE .007 IN. THICK TITANIUM INTER LEAVES IN PAD UP AREAS
 TO MEET IT REQUIREMENTS FOR BEARING SEE TABLE.
 INTER LEAVES ARE BONDED IN PLACE WITH POLYIMIDE
 ADHESIVE HAVING A .0035 IN. THICK BOND LINE AT EACH
 INTERFACE (.03 LBS./50. FT./BOND LINE).
- > APPLY LIGHTNING STRIKE PROTECTIVE SURFACE COATING TO CARRY 200,000 AMP. DISCHARGE. THICKNESS = .002 IN. (.05 LBS:/Sq. FT.)
 THIS REQUIREMENT NOT REFLECTED IN THE TABLE.
- POLYIMIDE HONEYCOMB CORE SPLICE ADHESIVE AVERAGE BOND LINE
 THICKNESS = 0.10 IN. (30 LBS./CUBIC FT.).
- APPLY SURFACE FINISH HIGH TEMPERATURE STABLE CONDUCTIVE COATING & DECORATIVE PAINT (.027 LBS. / 50. FT.)
- > SEAL PANEL EDGE WITH HIGH TEMPERATURE STABLE POTTING COMPOUND. AVERAGE THICKNESS = 0.10 (44 LBS./CUBIC FT.).
- INSTALL FASTENERS USING UNCURED FLUOROSILICONE COATING.

Figure 4-4.—Lower Wing Panel, Heavy Gage Bonded GR/PI Sandwich, Model 969-512B





1 1 N

1.50

(2)

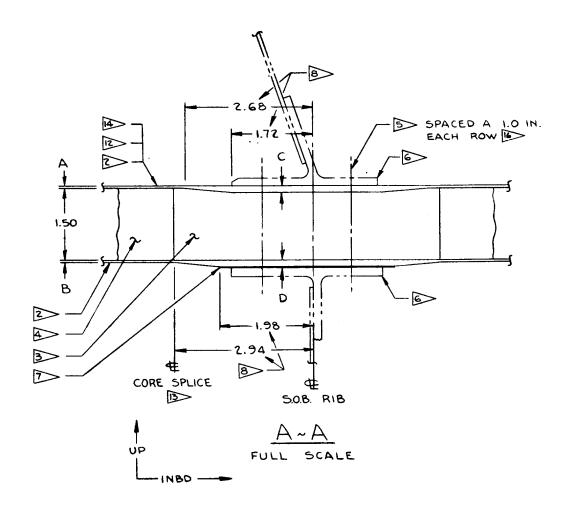
D AT 1.0 IN. ROW IS

+ SPAR

/─®

SECN.	DIM	GAGE		LAYUP DE	
OLC:		TOTAL	ΣTI		
A~A	Α	.040		[0/90/+45/0/-45]s	
	В	.040	_	SAME AS 'A'	
	U	.130	.055	[0/TI/30/+45/TI/0/-45/TI]5	
	٥	160	.055	SAME AS C'+ .030 THICK SHIM	
B~B	Α	.040	_	[07/90/+45/07/-45]5	
	В	.040	_	SAME AS A	
	С	1100	.025	[0*/TI/90/+45/TI/0*/-45/TI]s	
	D	.160	.025	SAME AS 'C' + .060 THICK SHIM D	
C~C	Α	.040		[0/90/+45/0/-45]5	
	В	.040	_	SAME AS 'A'	
	С	.130	.055	[0/T1/90/+45/T1/0/-45/T1]5	
	D	.160	.055	SAME AS 'C' + .030 THICK SHIM D	

* TO REDUCE THE STRESS CONCENTRATION FACTOR, UNI-DIRECTIONAL LAMINAE HAVING O' ORIENTATION ARE REPLACED WITH EQUIVALENT GAGE 1986 HIGH STRENGTH GRAPHITE/POLYIMIDE WOVEN FABRIC (±45°) IN THE REGION OF THE BOLT HOLES AS INDICATED BY (*) IN SECN. B~B.

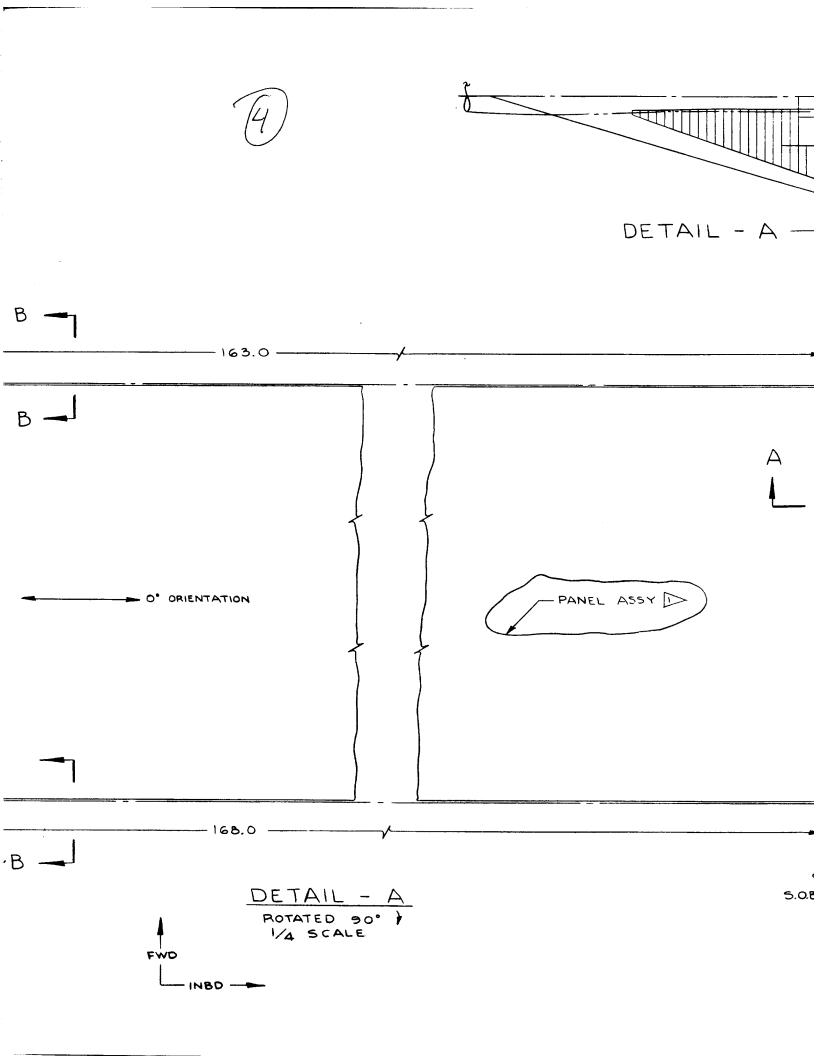


٦

<u>}</u>

(

TI)5 CK SHIM → TI]s T)s В 3, UNI-DIRECTIONAL -163 ACED WITH TE / POLYIMIDE WOVEN LES AS INDICATED - O' ORIENTATION 1.0 IN. 35.3 (REF) **与** - 168.C SEE B~B RIB - INBD -



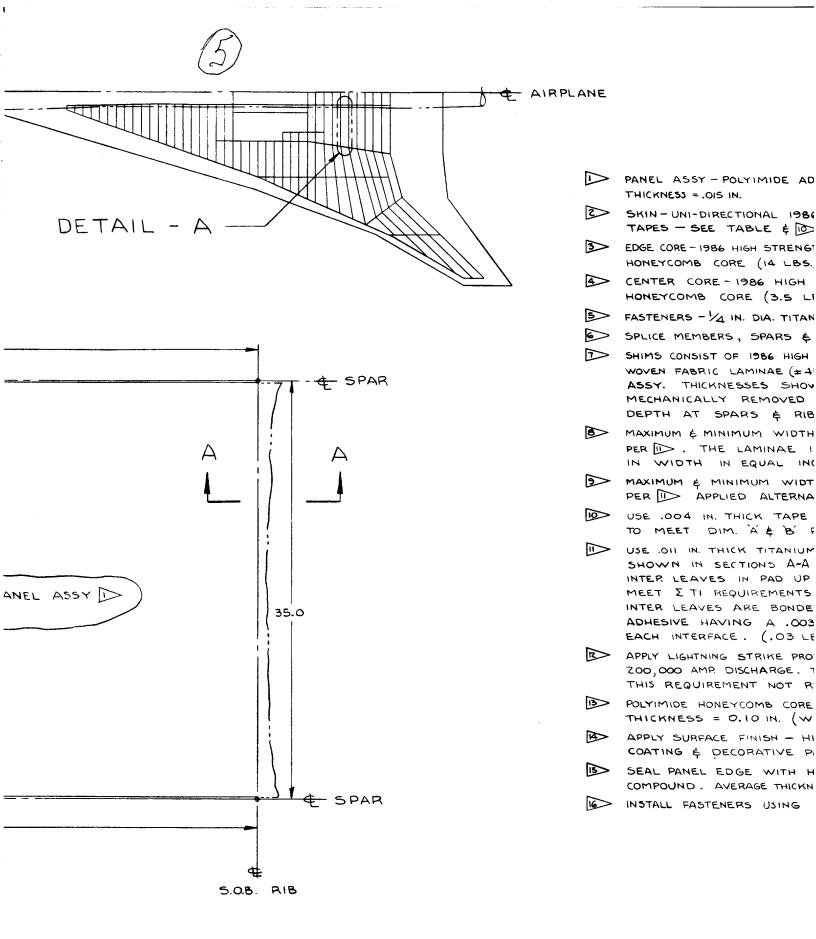
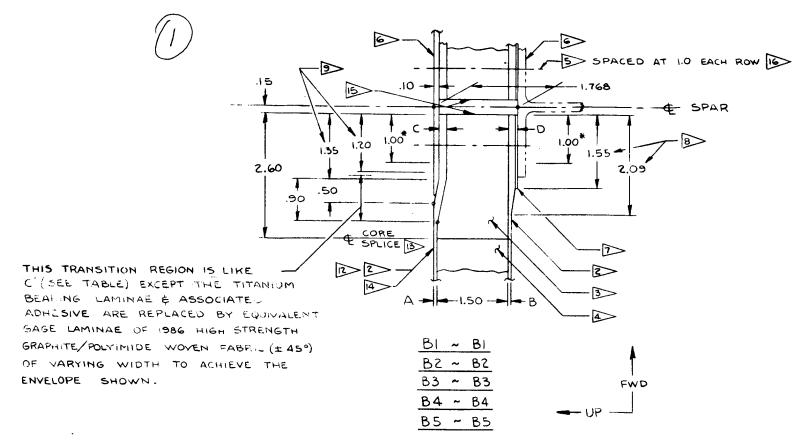


Figure 4-5.—

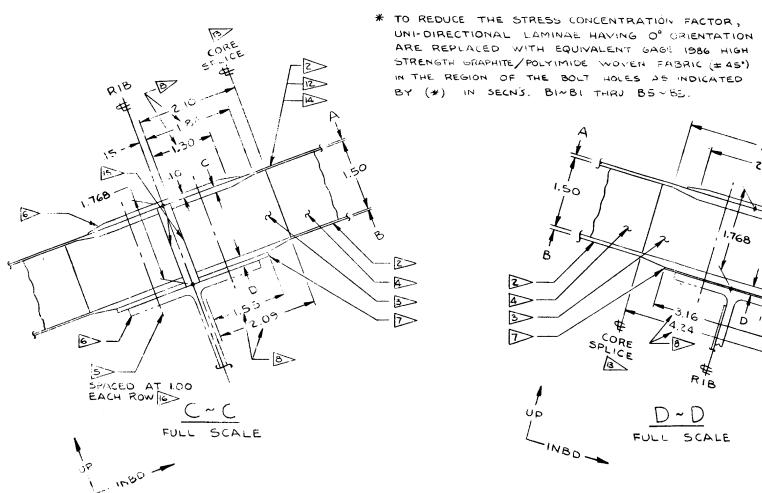


- PANEL ASSY POLYIMIDE ADHESIVE BONDED SANDWICH. ADHESIVE THICKNESS = .OIS IN. (.OBS LBS./SQ. FT./BOND LINE).
- SKIN-UNI-DIRECTIONAL 1986 HIGH STRENGTH GRAPHITE/POLYIMIDE TAPES SEE TABLE \$ 10 (.056 LBS./CUBIC IN.).
- EDGE CORE-1986 HIGH STRENGTH GRAPHITE/POLYIMIDE HONEYCOMB CORE (14 LBS./CUBIC FT.).
- CENTER CORE 1986 HIGH STRENGTH GRAPHITE/POLYIMIDE HONEYCOMB CORE (3.5 LBS./CUBIC FT.).
- FASTENERS 1/4 IN. DIA. TITANIUM 100° CSK. SHEAR HEAD BOLTS.
- SPLICE MEMBERS, SPARS & RIBS ARE TI-GAL-4V.
- SHIMS CONSIST OF 1986 HIGH STRENGTH GRAPHITE/POLYIMIDE
 WOVEN FABRIC LAMINAE (±45°) INTEGRAL WITH THE PANEL
 ASSY. THICKNESSES SHOWN ARE NOMINAL. EXCESS IS
 MECHANICALLY REMOVED TO ACHIEVE CONSTANT PANEL
 DEPTH AT SPARS & RIBS AS SHOWN.
- MAXIMUM & MINIMUM WIDTHS OF TI-GAL-4V BEARING LAMINAE PER . THE LAMINAE IN BETWEEN VARY PROGRESSIVELY IN WIDTH IN EQUAL INCREMENTS.
- MAXIMUM & MINIMUM WIDTHS OF TI-GAL-4V BEARING LAMINAE PER () APPLIED ALTERNATELY.
- USE .004 IN. THICK TAPE IN THE OUTER & INNER SKINS
 TO MEET DIM. A & B REQUIREMENTS RESPECTIVELY.
- USE .OII IN. THICK TITANIUM INTER LEAVES IN PAD UP AREAS SHOWN IN SECTIONS A-A & C-C & USE .OOS IN. THICK TITANIUM INTER LEAVES IN PAD UP AREAS SHOWN IN SECN. B-B TO MEET & TI REQUIREMENTS FOR BEARING SEE TABLE. INTER LEAVES ARE BONDED IN PLACE WITH POLYIMIDE ADHESIVE HAVING A .OOSS IN. THICK BOND LINE AT EACH INTERFACE. (.O3 LBS./SQ. FT/BOND LINE).
- APPLY LIGHTNING STRIKE PROTECTIVE SURFACE COATING TO CARPY ZOO, OOO AMP. DISCHARGE. THICKNESS = .OOZ IN. (.OS LBS/SQ. FT.)
 THIS REQUIREMENT NOT REFLECTED IN THE TABLE.
- POLYIMIDE HONEYCOMB CORE SPLICE ADHESIVE AVERAGE BOND LINE THICKNESS = 0.10 IN. (WEIGHT = 30 LBS/CUBIC FT.).
- APPLY SURFACE FINISH HIGH TEMPERATURE STABLE CONDUCTIVE COATING & DECORATIVE PAINT (.027 LBS./SQ. FT.).
- SEAL PANEL EDGE WITH HIGH TEMPERATURE STABLE POTTING COMPOUND. AVERAGE THICKNESS = 0.10 (44 LB5/CUBIC FT.).
- INSTALL FASTENERS USING UNCURED FLUOROSILICONE COATING.

Figure 4-5.—Upper Wing Panel, Medium Gage Bonded GR/PI Sandwich, Model 969-512B



FULL SCALE





SPACED AT 1.0 EACH ROW

768		
	- +	SPAR
1.55 - 2.	09	8

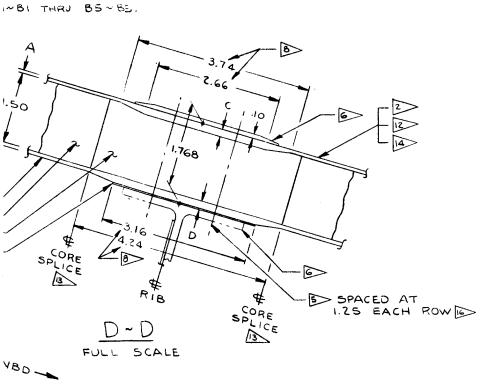
-[]> -[]>

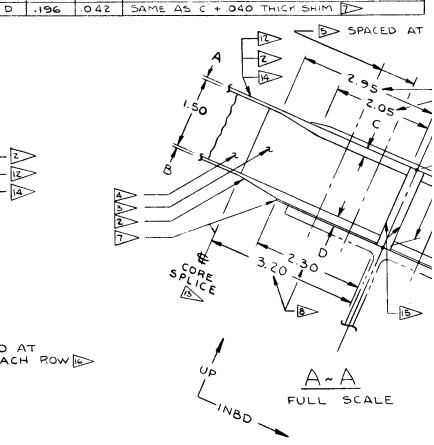
-[4>

FWD

S CONCENTRATIÓN FACTOR,
NAE HAVING O° ORIENTATION
EQUIVALENT GAGE 1986 HIGH
MIDE WOVEN FABRIC (±45°)
BOLT HOLES AS INDICATED

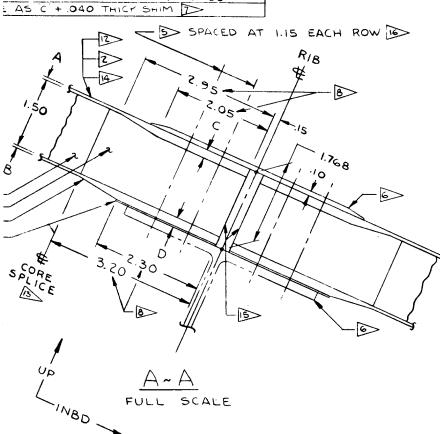
SECN	DIM	GAGE		LAYUP ID ID		
		TOTAL	ΣΤΙ			
	Α	.056	_	[0/+45/9/-45/99/0]5		
A~A	В	.056		SAME AS A'		
	С	.182	.063	[0/TI/+45/0/TI/-45/90/TI/0/TI/0/TI]5		
·	0	.212	.063	SAME AS C' +.030 THICK SHIM D		
	Α	.056		[0]/+45/0]/-45/90/0]/5		
BI-BI	В	.056		SAME AS 'A'		
	С	.140	.042	[♂\T1/+45/ ♂ \T1/-45/ 9 0/♂\T1/♂\S		
	D	. 212	.042	SAME AS C'+.072 THICK SHIM 7>		
	Α	-072		[0]+45/0]-45/90/0]±45/0]s		
BZ~BZ	В	.072	_	SAME AS 'A'		
	С	.156	.042	[0"/TV/+45/0"/Ti/-45/90/0"/+45/TV/-45/0"]5		
	D	.196	.042	SAME AS C' + .040 THICK SHIM		
ſ	А	.064		[0/+45/0*/-45/90/0*/±45]5		
B3~B3	В	.064	T —	SAME AS A'		
	С	.148	.042	[O*/TV+45/0*/TV-45/90/0*/+45/TV-45]5		
L	D	.204	.042	SAME AS C' +.056 THICK SHIM 7		
	Α	.048	_	[0*/+45/0*/-45/90/0*]s		
B4~B4	В	-048	_	SAME AS A		
	С	.132	.042	[J/T1/+45/0*/T1/-45/90/J/T1]s		
	D	.220	-042	SAME AS C'+.088 THICK SHIM T>		
	Α	.040		[0/+45/0/-45/90]5		
B5~B5	В	.040		SAME AS A'		
	С	.124	.042	[O)/TI/+45/0)/TI/-45/90/TI]S		
	D	.228	.042	SAME AS C'+.104 THICK SHIM		
	A	.040		[0/+45/0/-45/90]5		
C~C	В	.040	T	SAME AS A		
	С	.124	.042	[0/T1/+45/0/TV-45/90/T1]5		
	D	.228	.042	SAME AS C'+ . 104 THICK SHIM D		
	A	.072		[0/+45/0/-45/90/0/+45/-45/0]s		
D~D	В	.072		SAME AS A		
	С	. 156	.042	0/11/+45/0/T1/-45/90/0/+45/T1/-45/0]5		
•		196	0.42	SAME AS C + DAD THICK SHIM TO		

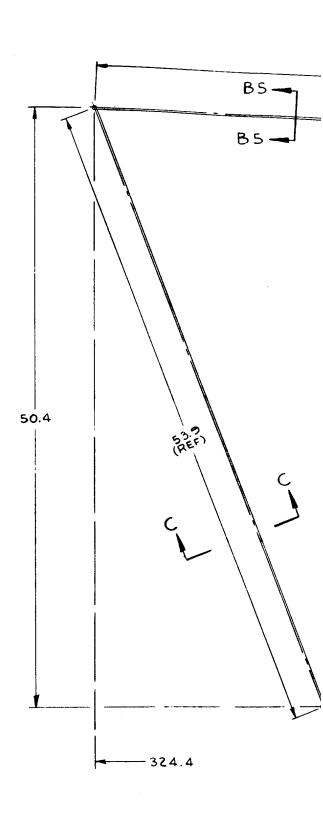


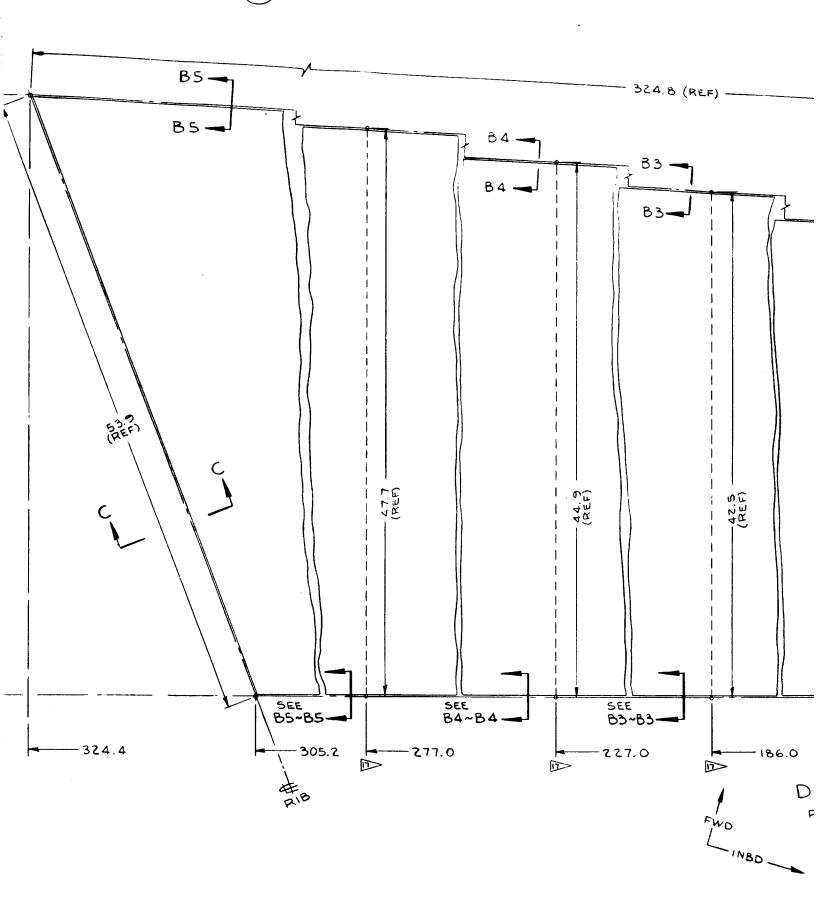


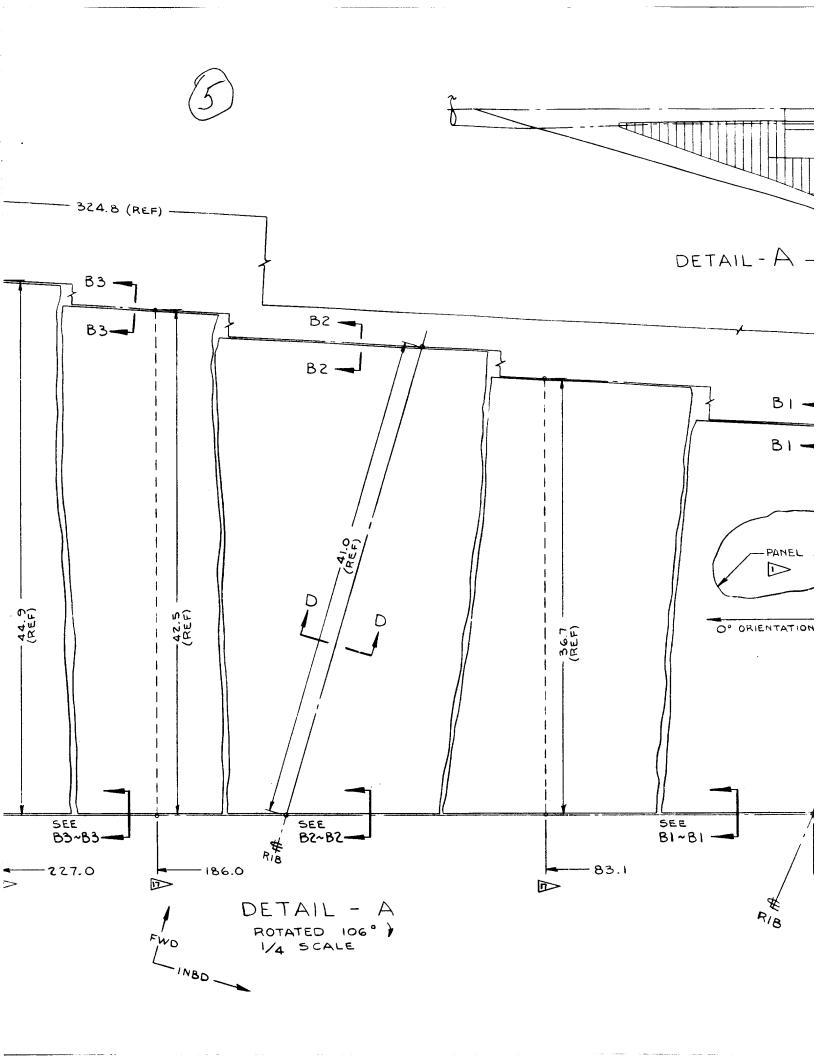


AYUP DO 100
√9-45/39/0z]s
E AS 'A'
1+45/0/TI/-45/90/TI/0/TI/0/TI]5
E 45 C' + .030 THICK SHIM D
·/o//-45/90/07{]5
E AS 'A'
+45/ 0 /T1/-45/90/07/T1/07]5
E AS C' + .072 THICK SHIM T
107-45/90/07/±45/05/5
E AS 'A'
+45/07/TI/-45/90/0*/+45/TI/-45/0*]s
AS C' + .040 THICK SHIM D
10*/-45/90/0*/±45]5
E AS A'
+45/0/TV-45/90/0*/+45/TV-45]5
. AS C' +.056 THICK SHIM T
3/0*/-45/90/0*]s
IE AS A
+45/0*/TI/-45/90/0*/TI]s
: A5 C + .088 THICK SHIM >>
5/ <i>0</i> /-45/90]5
IE AS A
+45/0*/TI/-45/90/TI]S
. AS C'+.104 THICK SHIM
5/0/-45/90]5
E AS A
·45/0/TV-45/90/TI]5
MS C'+.104 THICK SHIM
VO/-45/90/0/+45/-45/0]s
TE AS A'
+45/0/TI/-45/90/0/+45/TI/-45/0]s
AS C + .040 THICK SHIM
E SOUTED AT









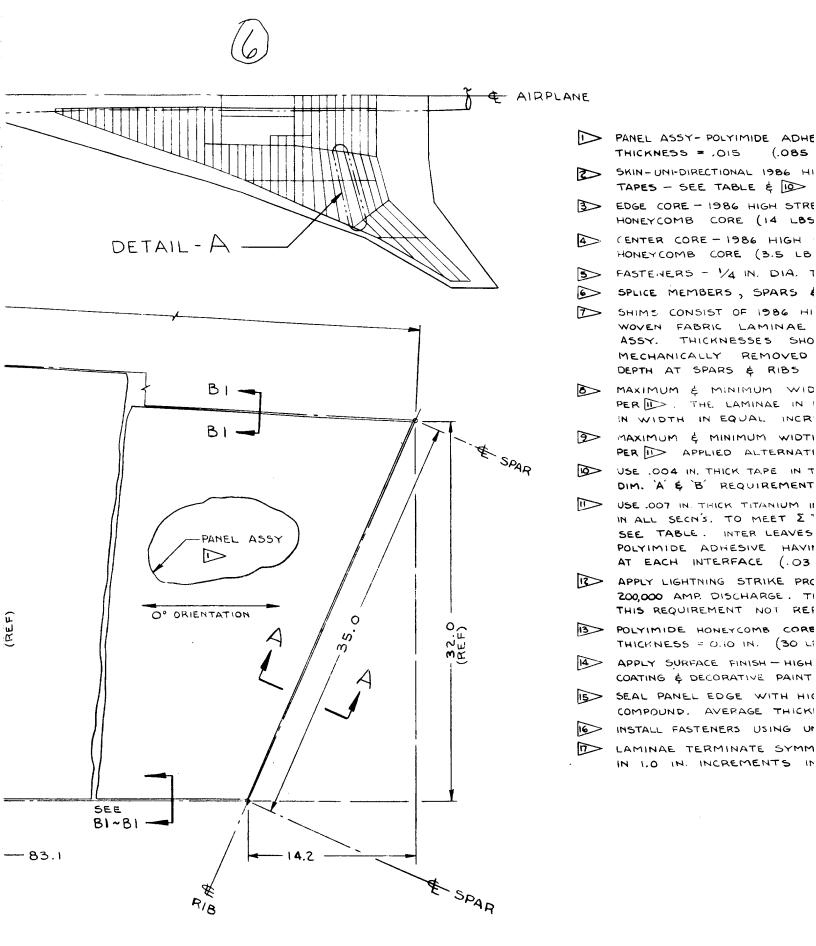
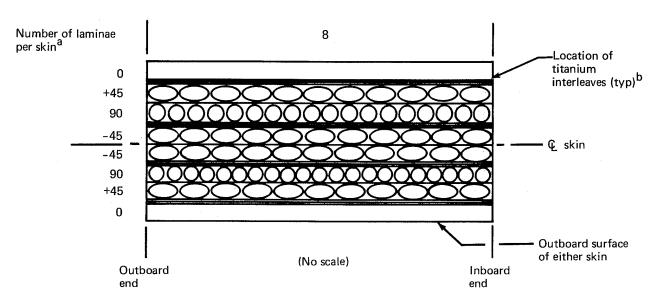


Figure 4-6.—L



NE

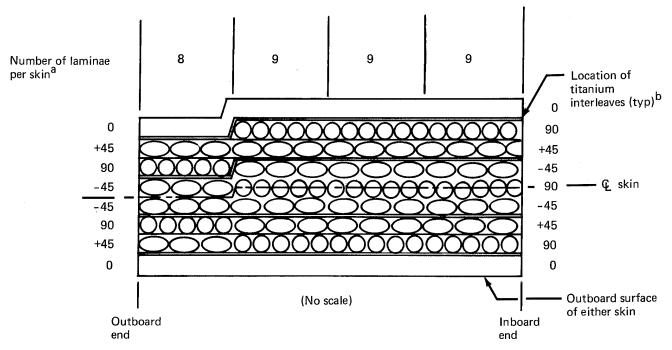
- PANEL ASSY- POLYIMIDE ADHESIVE BONDED SANDWICH, ADHESIVE THICKNESS = .015 (.085 LBS./SQ. FT. / BOND LINE).
- SKIN-UNI-DIRECTIONAL 1986 HIGH STRENGTH GRAPHITE / POLYIMIDE TAPES SEE TABLE & 100 (.056 LBS./CUBIC IN.).
- BY EDGE CORE 1986 HIGH STRENGTH GRAPHITE/POLYIMIDE HONEYCOMB CORE (14 LBS./CUBIC FT.).
- (ENTER CORE 1986 HIGH STRENGTH GRAPHITE/POLYIMIDE HONEYCOMB CORE (3.5 LBS./CUBIC FT.).
- FASTENERS 1/4 IN. DIA. TITANIUM 100° CSK. SHEAR HEAD BOLTS.
- SPLICE MEMBERS, SPARS & RIBS ARE TI-GAL-4V.
- SHIME CONSIST OF 1986 HIGH STRENGTH GRAPHITE POLYIMIDE WOVEN FABRIC LAMINAE (± 45°) INTEGRAL WITH THE PANEL ASSY. THICKNESSES SHOWN ARE NOMINAL. EXCESS IS MECHANICALLY REMOVED TO ACHIEVE CONSTANT PANEL DEPTH AT SPARS & RIBS AS SHOWN.
- MAXIMUM & MINIMUM WIDTHS OF TI-GAL-4V BEARING LAMINAE PER ID. THE LAMINAE IN BETWEEN VARY PROGRESSIVELY IN WIDTH IN EQUAL INCREMENTS.
- MAXIMUM & MINIMUM WIDTHS OF TI-GAL-4V BEARING LAMINAE
 PER ID APPLIED ALTERNATELY.
- USE .004 IN. THICK TAPE IN THE OUTER & INNER SKINS TO MEET DIM. A & B REQUIREMENTS RESPECTIVELY.
- USE .007 IN. THICK TITANIUM INTER LEAVES IN PAD UP AREAS SHOWN IN ALL SECH'S. TO MEET Σ TI REQUIREMENTS FOR BEARING ——SEE TABLE. INTER LEAVES ARE BONDED IN PLACE WITH POLYIMIDE ADHESIVE HAVING A .0035 IN. THICK BOND LINE AT EACH INTERFACE (.03 LBS/SQ.FT/BOND LINE).
- APPLY LIGHTNING STRIKE PROTECTIVE SURFACE COATING TO CARRY 200,000 AMP. DISCHARGE. THICKNESS = .002 IN. (.05 LBS/SQ.FT.).
 THIS REQUIREMENT NOT REFLECTED IN THE TABLE.
- POLYIMIDE HONEYCOMB CORE SPLICE ADHESIVE AVERAGE BOND LINE THICKNESS = 0.10 IN. (30 LOS./ CUBIC FT.)
- APPLY SURFACE FINISH HIGH TEMPERATURE STABLE CONDUCTIVE COATING & DECORATIVE PAINT (.027 LBS./5Q. FT.).
- SEAL PANEL EDGE WITH HIGH TEMPERATURE STABLE POTTING
 COMPOUND. AVERAGE THICKNESS = 0.10 (44 LBS./CUBIC FT.).
- IS INSTALL FASTENERS USING UNCURED FLUOROSILICONE COATING.
- IN 1.0 IN INCREMENTS IN EACH SKIN.



^aUnidirectional 1986 high strength graphite/polyimide tape (Outer skin: 4 mil; inner skin: 2 mil).

Figure 4-7.—Composite Skin Layup Diagram, Minimum Gage, Lower Wing Panel

 $[^]bOuter\ skin: \ \Sigma\ Ti$ = 4 x 0.008 = 0.032 all four edges Inner skin: $\Sigma\ Ti$ = 4 x 0.004 = 0.016 all four edges.



^aUnidirectional 1986 high strength graphite/polyimide tape (outer skin: 4 mil; inner skin: 2 mil).

Figure 4-8.—Composite Skin Layup Diagram, Medium Gage, Lower Wing Panel

bOuter skin: Σ Ti = 4 x 0.010 = 0.040 all four edges Inner skin: Σ Ti = 4 x 0.005 = 0.020 all four edges.

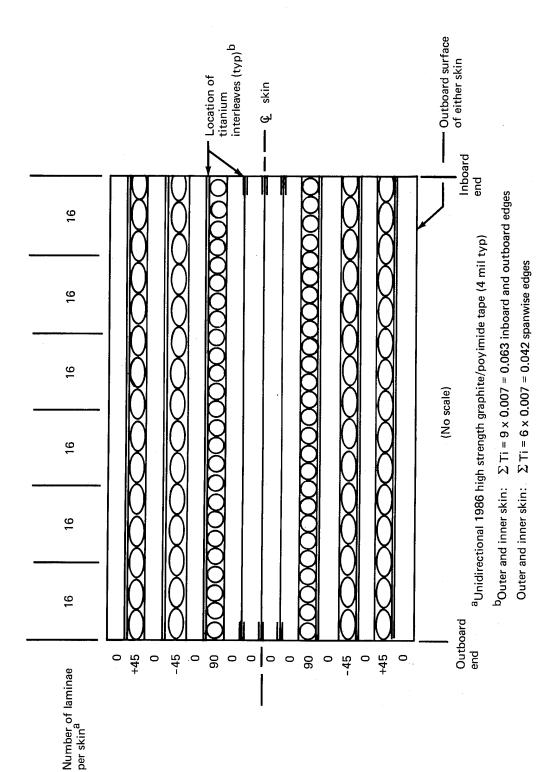
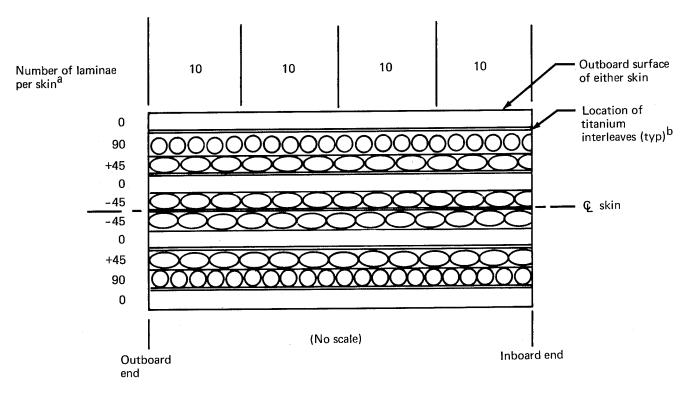


Figure 4-9.—Composite Skin Layup Diagram, Heavy Gage, Lower Wing Panel



^aUnidirectional 1986 high strength graphite/polyimide tape (4 mil typ).

bOuter skin: Σ Ti = 5 x 0.011 = 0.055 all four edges Inner skin: Σ Ti = 5 x 0.005 = 0.025 all four edges.

Figure 4-10.—Composite Skin Layup Diagram, Medium Gage, Upper Wing Panel

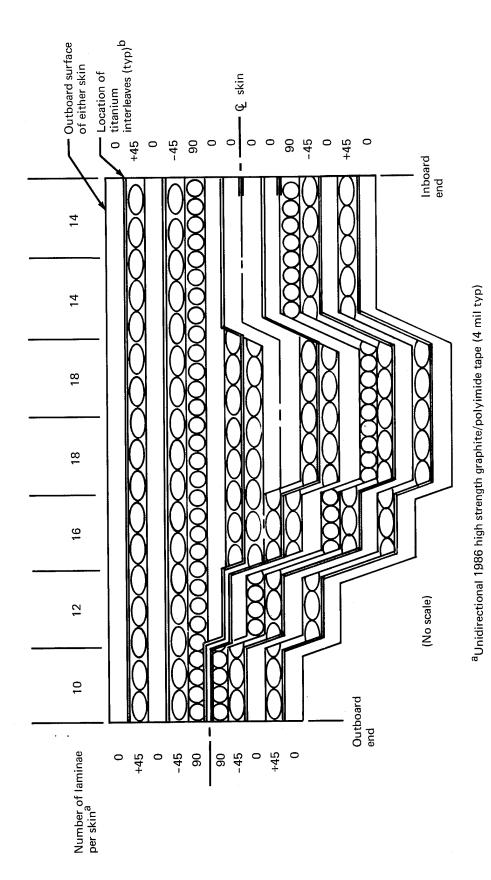
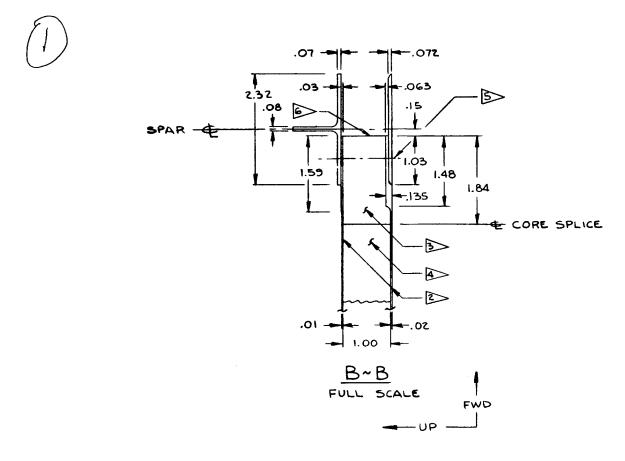
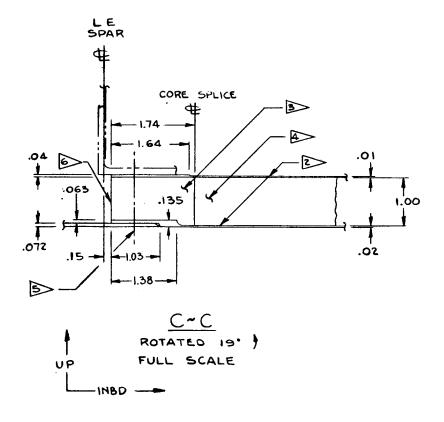
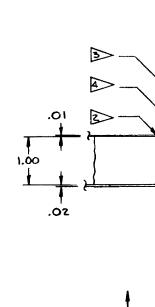


Figure 4-11.—Composite Skin Layup Diagram, Heavy Gage, Upper Wing Panel

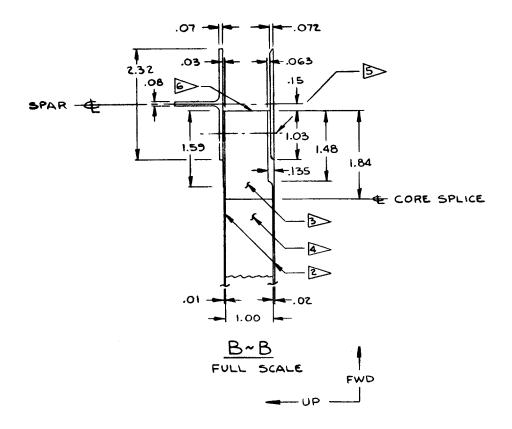
^bOuter and inner skin: Σ Ti = 9 x 0.007 = 0.063 inboard edge Outer and inner skin: Σ Ti = 6 x 0.007 = 0.042 outboard and spanwise edges

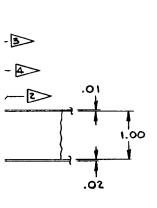


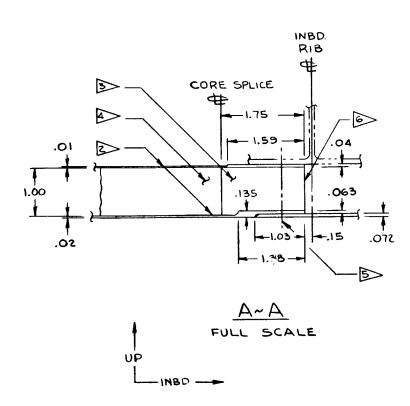


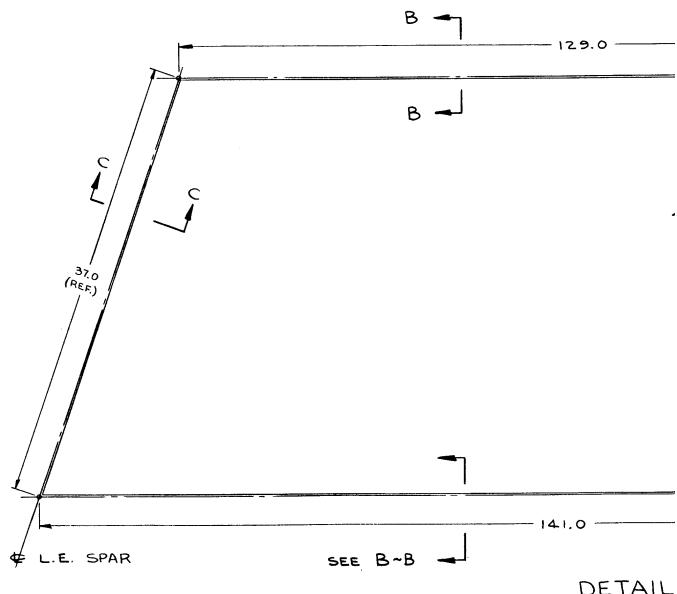






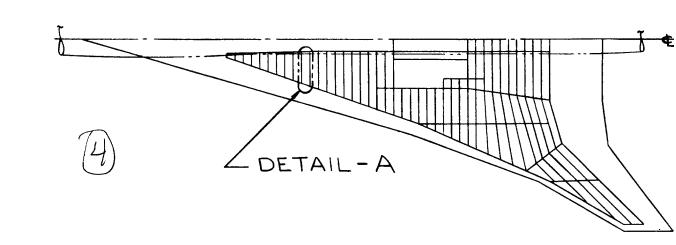


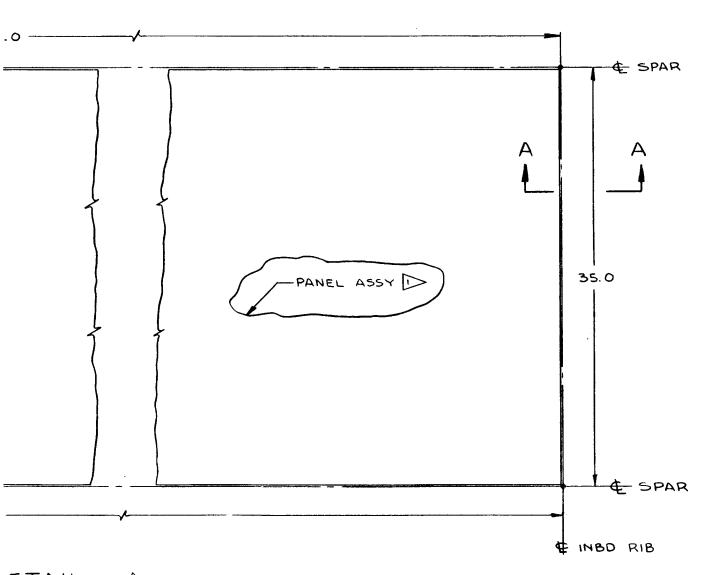




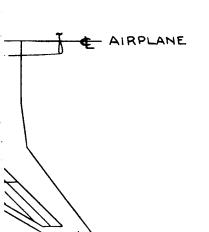
<u>L</u> 72

DETAIL
ROTATED
1/4 SCA
FWO





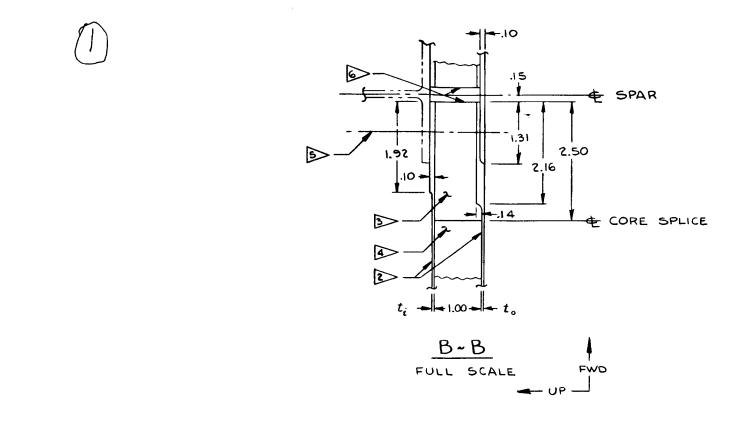
POTATED 90°)
1/4 SCALE

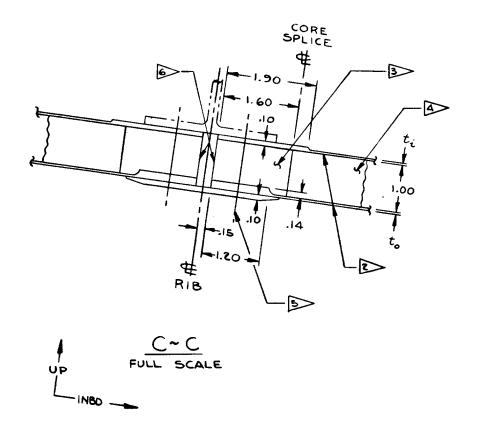


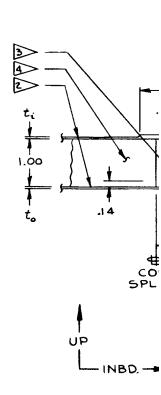


- FINISH HONEYCOMB PANEL EDGES ONLY: 2 COATS PRIMER PER BAC 5710 TYPE 45.
- FASTENERS 3 DIA. TITANIUM 100° CSK SHEAR HEAD BOLTS SPACED AT 4D (.75) TYP.
- CENTER CORE + COMPOSITION 2, SC 4 ZONM, HONEYCOMB CORE (4,9 LB5/CUBIC FT.). TOTAL BRAZE ALLOY/PANEL ASSY. = .016 IN.
- 3> EDGE CORE COMPOSITION 3, SS Z 30 NM, HONE: COMB CORE (14.1 LBS./CUBIC FT.). TOTAL BRAZE ALLOY/PANEL ASSY. = .044 IN.
- 3> SKIN (TI-GAL-4V SHEET)
- PANEL ASSY (ALUMINUM BRAZE)

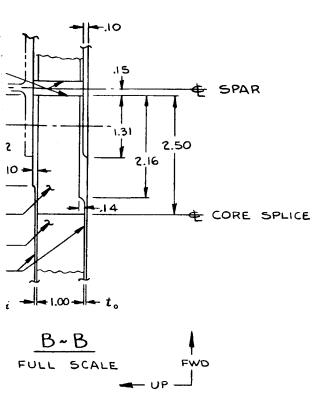
Figure 4-12.—Lower Wing Panel, Light Gage Brazed-Titanium Sandwich, Model 969-512B

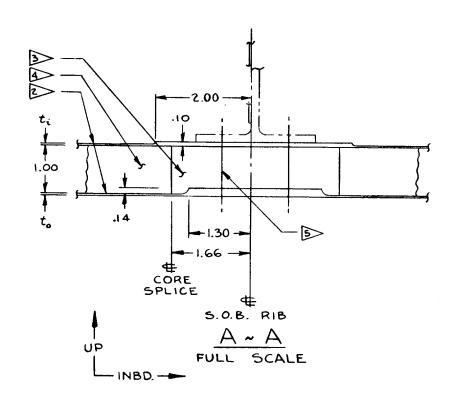


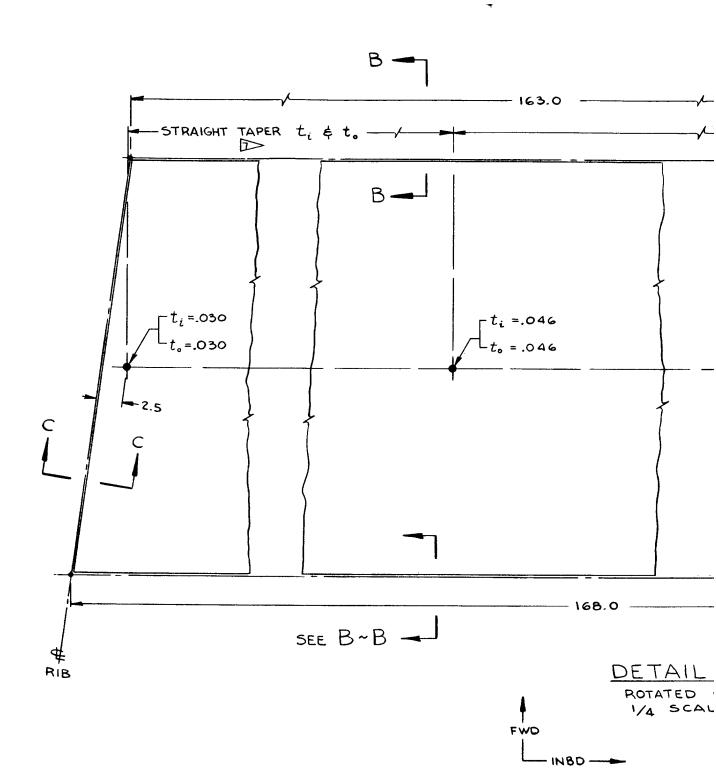


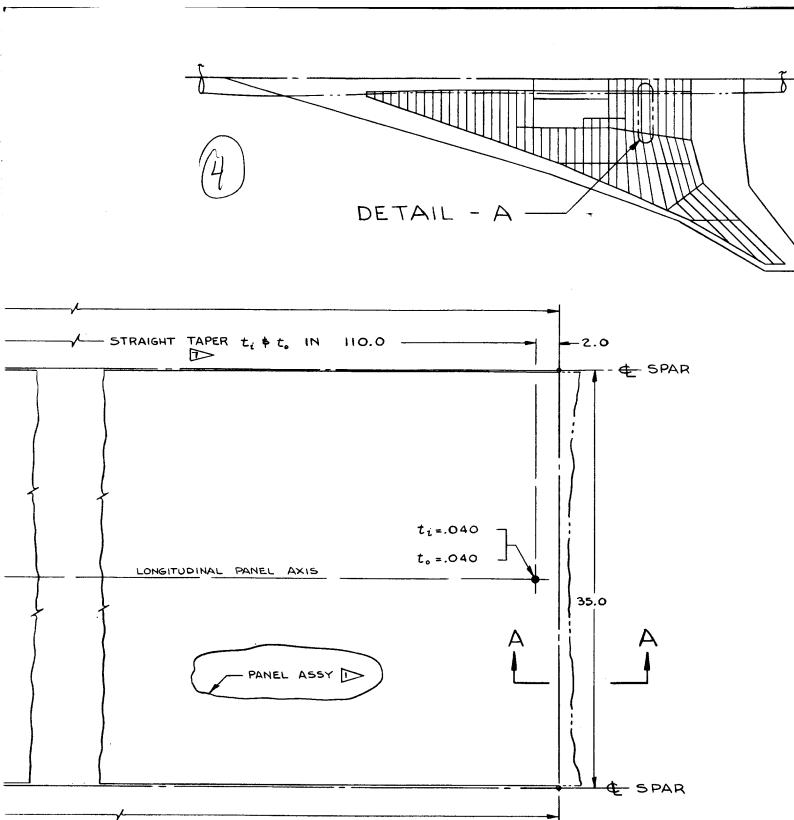






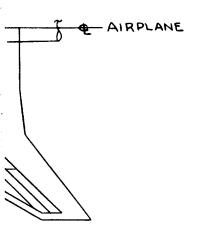






5.0.B. RIB

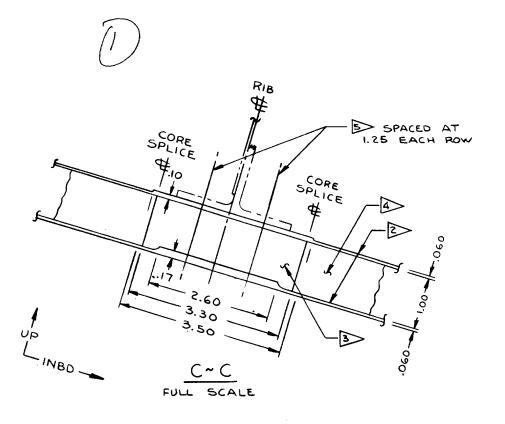
ETAIL - A
ROTATED 90°)
I/4 SCALE

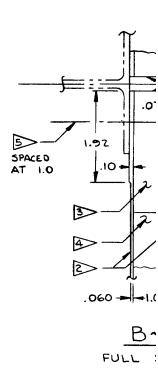


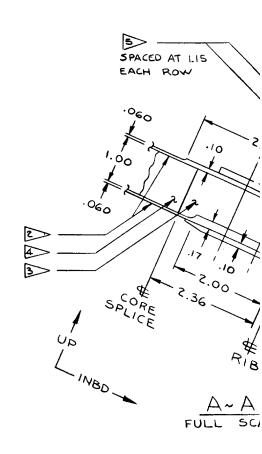


- TAPER RUNS PARALLEL TO THE LONGITUDINAL PANEL AXIS
 IN PLANES THROUGH CONTROL POINTS.
- FINISH HONEYCOMB PANEL EDGES ONLY: 2 COATS PRIMER PER BAC 5710 TYPE 45.
- FASTENERS 1 DIA. TITANIUM 100° CSK. SHEAR HEAD BOLTS SPACED AT 4D (1.00) TYP.
- CENTER CORE (COMPOSITION 2, SC4-20 NM, HONEYCOMB CORE (4.9 LBS/CUBIC FT.). TOTAL BRAZE ALLOY/PANEL ASSY. .016 IN.
- EDGE CORE (COMPOSITION 3, 552-60 NM, HONEYCOMB CORE(28.1 LBS/CUBIC FT.). TOTAL BRAZE ALLOY/PANEL ASSY. = .044 IN.
- 3> SKIN (TI-GAL-4V SHEET)
- PANEL ASSY (ALUMINUM BRAZE)

Figure 4-13.—Lower Wing Panel, Medium Gage Brazed-Titanium Sandwich, Model 969-512B



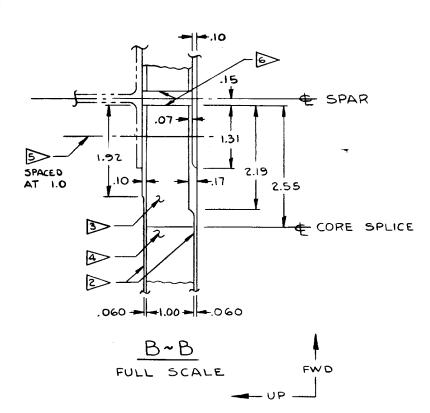


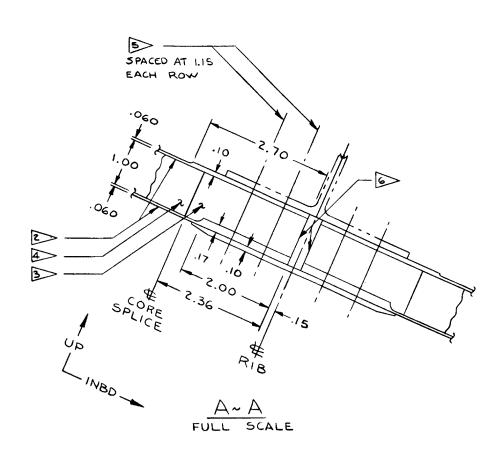


(1)

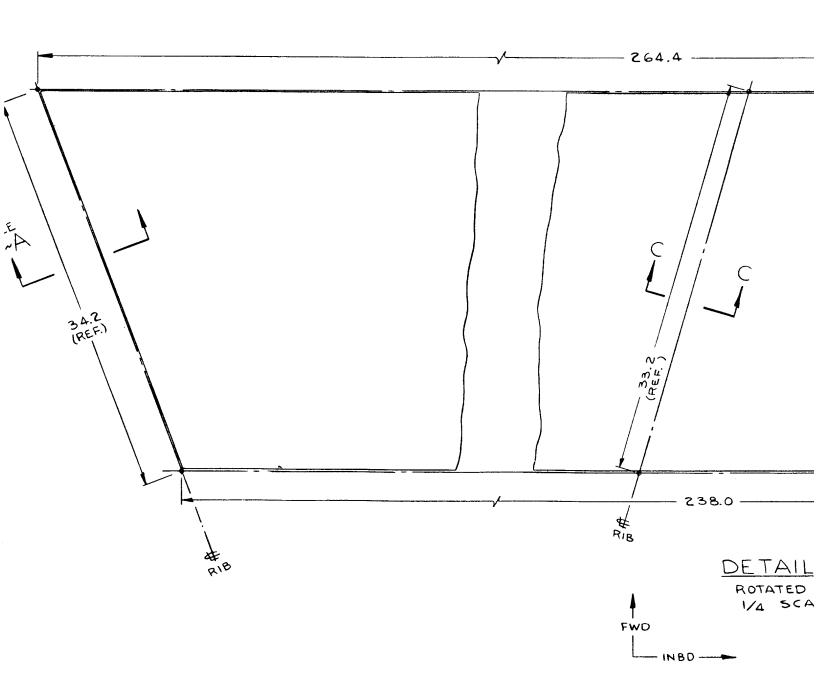
SPACED AT

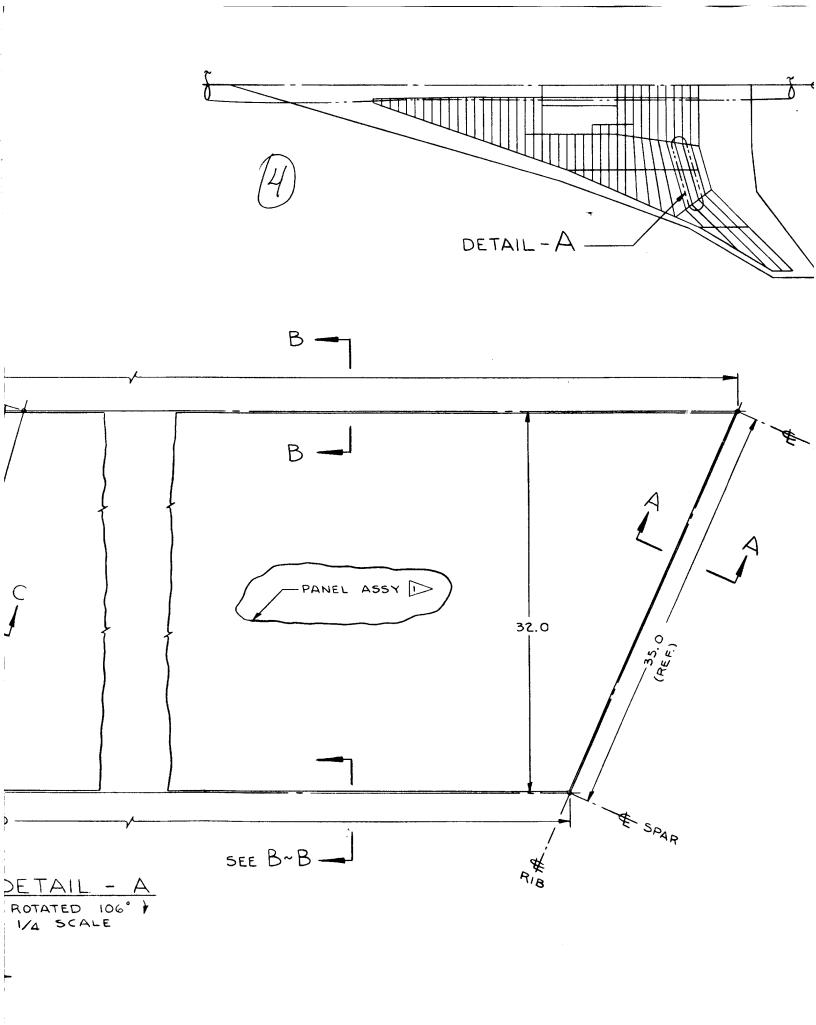
090. The oo.

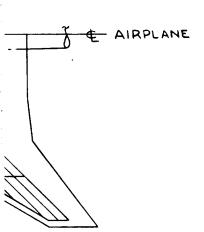




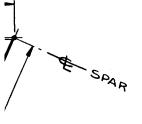






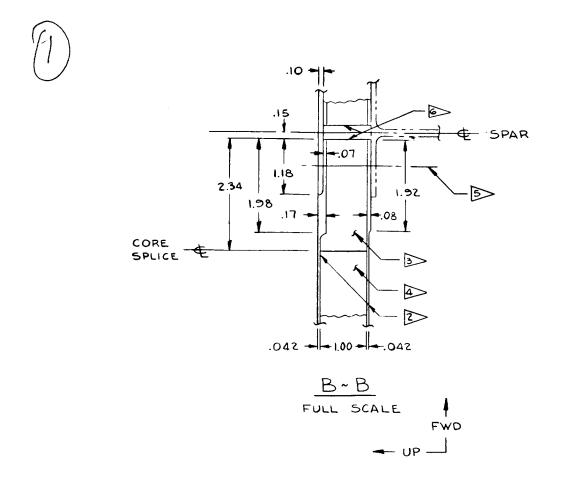


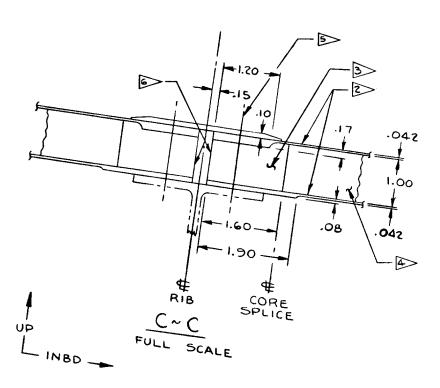


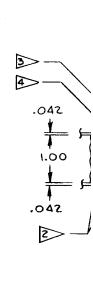


- FINISH HONEYCOMB PANEL EDGES ONLY: 2 COATES PRIMER PER BAC 5710 TYPE 45.
- 5 FASTENERS 1 DIA. TITANIUM 100° CSK SHEAR HEAD BOLTS.
- (ENTER CORE (COMPOSITION 2, SC 4-ZONM, HONEYCOMB CORE (4.9 LBS./CUBIC FT.). TOTAL BRAZE ALLOY/PANEL ASSY. = . OIG IN.
- EDGE CORE (COMPOSITION 3, 552-60 NM, HONEYCOMB CORE (28.1 LBS/CUBIC FT.). TOTAL BRAZE ALLOY/PANEL ASSY. = .044 IN.
- SKIN (TI-GAL-4V SHEET)
- PANEL ASSY (ALUMINUM BRAZE)

Figure 4-14.—Lower Wing Panel, Heavy Gage Brazed-Titanium Sandwich, Model 969-512B

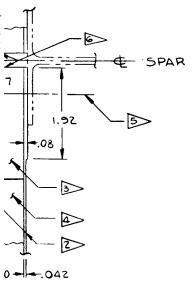


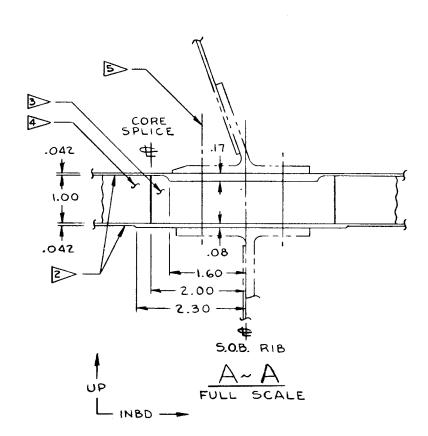


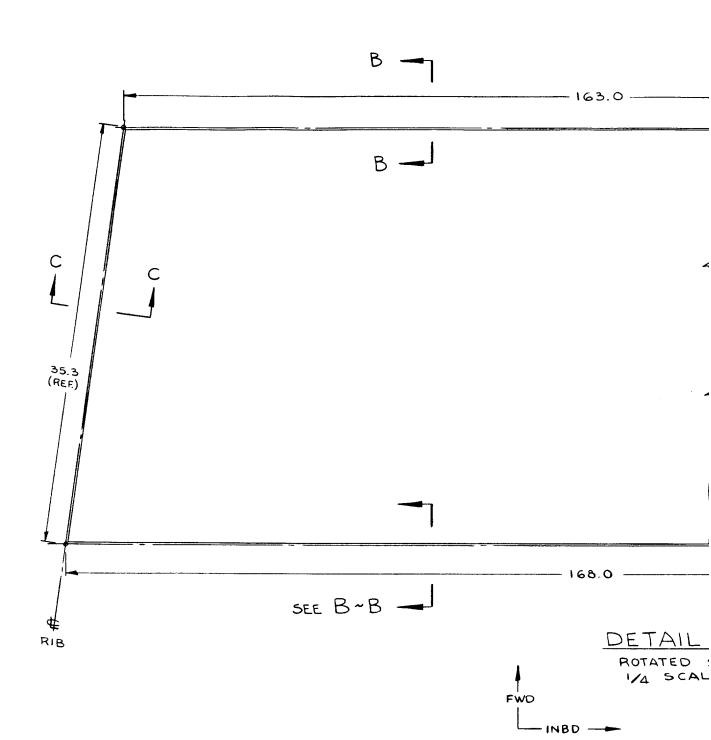


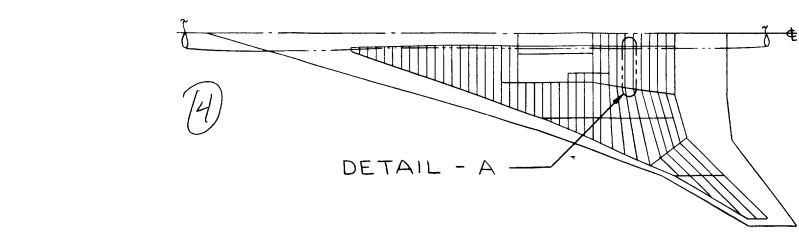
UF

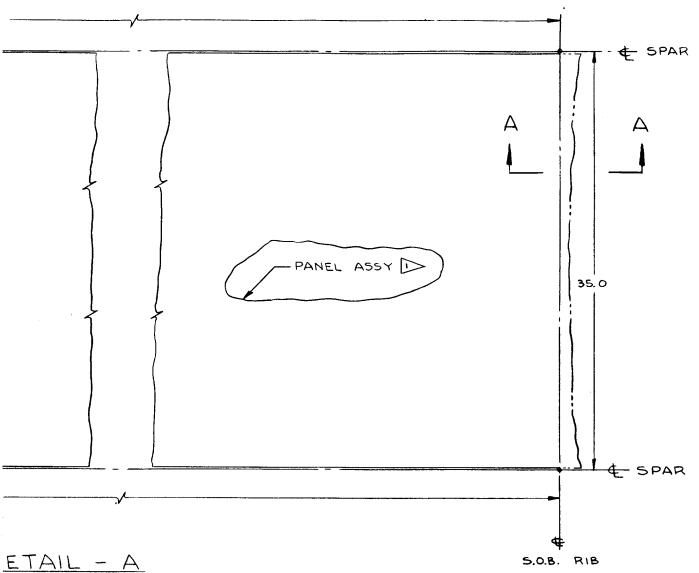




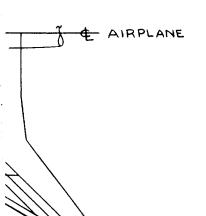








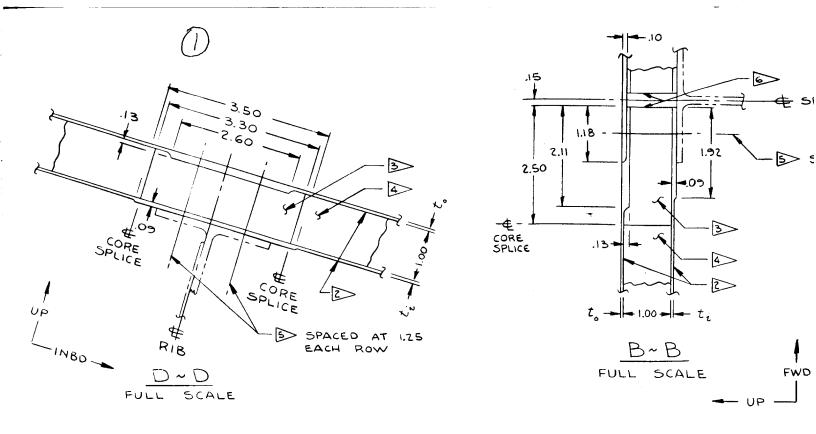
OC DETATOR

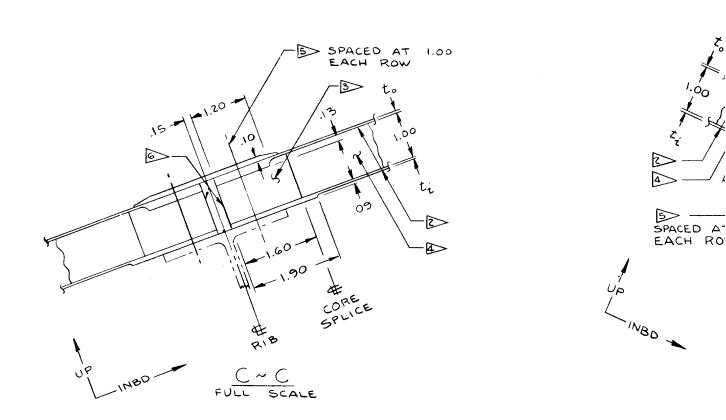


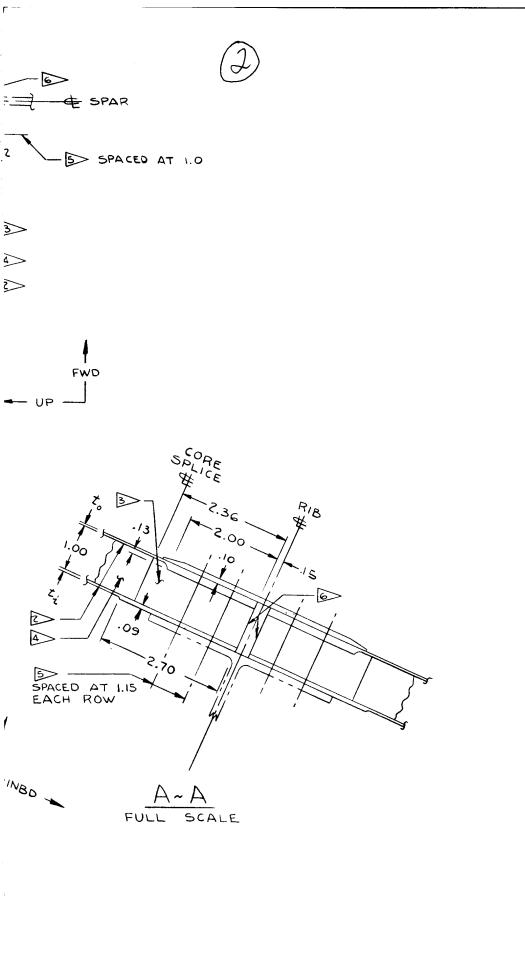


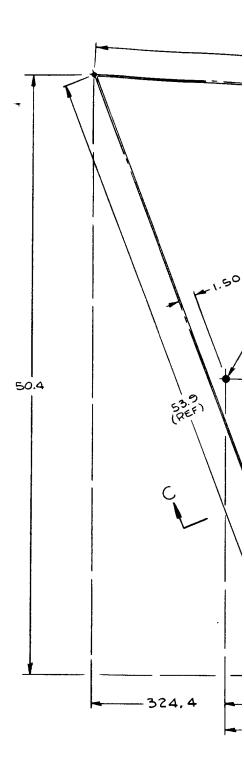
- FINISH HONEYCOMB PANEL EDGES ONLY: 2 COATES PRIMER PER BAC 5710 TYPE 45.
- FASTENERS 1 DIA. TITANIUM 100° CSK SHEAR HEAD BOLTS SPACED AT 40 (1.00) TYP.
- CENTER CORE (COMPOSITION 2, SC4-20 NM, HONEYCOMB CORE(4.9 LBS./CUBIC FT.). TOTAL BRAZE ALLOY/PANEL ASSY. = .016 IN.
- EDGE CORE (COMPOSITION 3, 552-60NM, HONEYCOMB CORE (28.1 LBS,/CUBIC FT.). TOTAL BRAZE ALLOY/PANEL ASSY. = .044 IN.
- 3> SKIN (TI-GAL-4V SHEET)
- PANEL ASSY (ALUMINUM BRAZE)

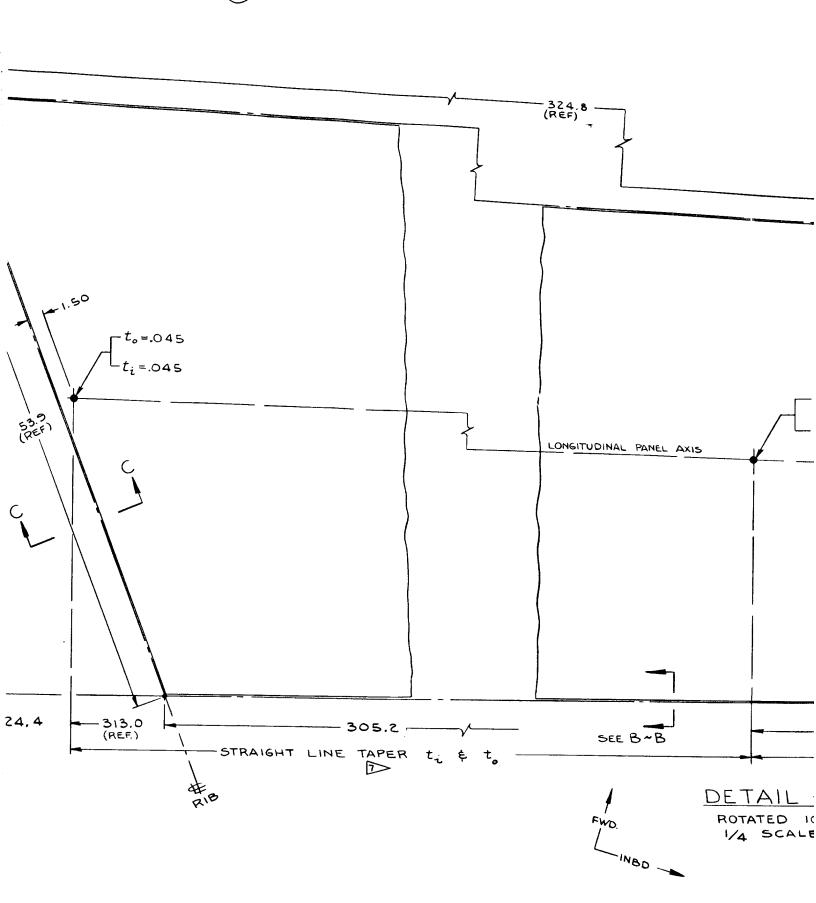
Figure 4-15.—Upper Wing Panel, Medium Gage Brazed-Titanium Sandwich, Model 969-512B

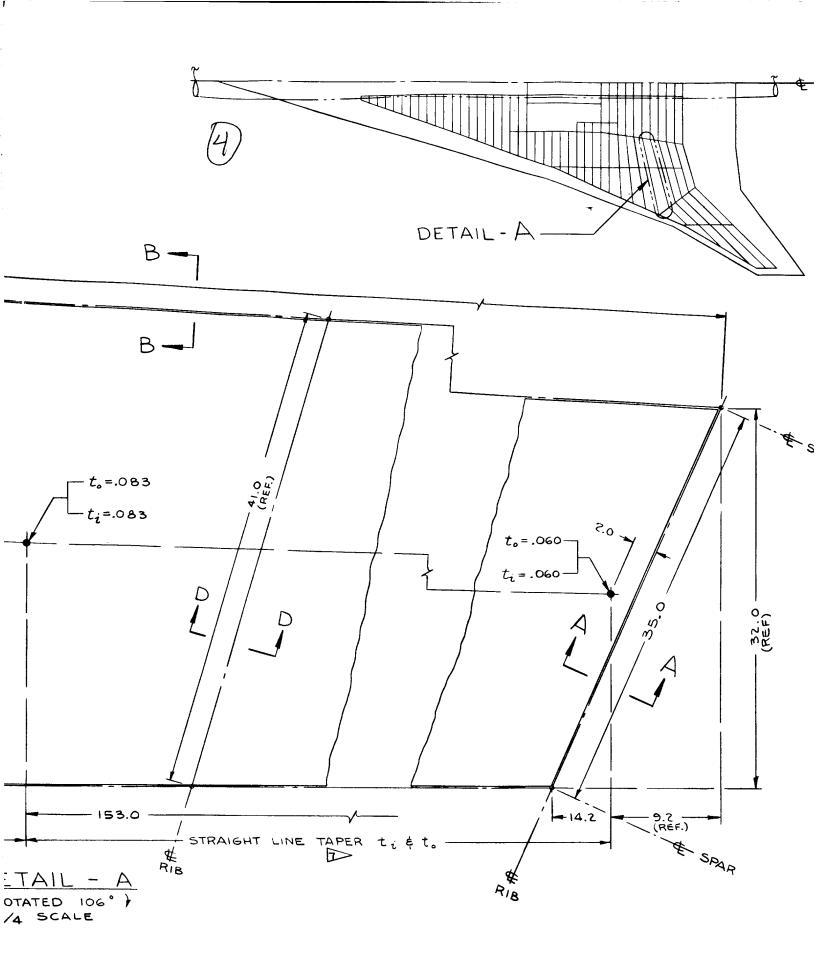


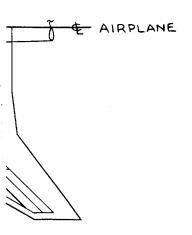














- TAPER RUNS PARALLEL TO THE LONGITUDINAL PANEL AXIS IN PLANES THROUGH CONTROL POINTS.
- FINISH HONEYCOMB PANEL EDGES ONLY: 2 COATES PRIMER PER BAC 5710 TYPE 45.
- 5 FASTENERS 1 DIA. TITANIUM 100° C5K SHEAR HEAD BOLTS.
- CENTER CORE (COMPOSITION 2, SC4-ZONM, HONEYCOMB CORE (4.9 LBS./CUBIC FT.). TOTAL BRAZE ALLOY/PANEL ASSY. = .016 IN.
- EDGE CORE (COMPOSITION 3, 552-60NM, HONEYCOMB CORE (28.1 LBS./CUBIC FT.) TOTAL BRAZE ALLOY/PANEL ASSY. = .044 IN.
- SKIN (TI-GAL-4V SHEET).
- PANEL ASSY. (ALUMINUM BRAZE).

Figure 4-16.—Upper Wing Panel, Heavy Gage Brazed-Titanium Sandwich, Model 969-512B

SECTION 5

THEORETICAL-TO-ACTUAL MASS FACTORS

by

M. D. HALVORSEN

CONTENTS

	Pa	ige
INTRODUCTION	. 13	39
SKIN THEORETICAL-TO-ACTUAL CONVERSION FACTORS	. 1	40
HONEYCOMB CORE	. 1	43
CORE TO SKIN ADHESIVE	. 1	43
CORÉ EDĞİNG (SPLİCE AND SEALING)	. 1	43
LIGHTNING PROTECTION AND SURFACE FINISH	. 1	43
SPAR AND RIB MASS INCREMENT		
PANEL MASS COMPARISON (TITANIUM VERSUS GRAPHITE/POLYIMIDE)		
DEEERENCES	. 1	45

TABLES

No.		Page
5-1	Titanium Honeycomb Panel Mass Summary	146
5-2	Graphite/Polyimide Honeycomb Panel Mass Summary	
5-3	Theoretical-To-Actual Mass Increment Derivation Honeycomb Panel Skin	
5-4	ATLAS Input Data to Support Mass Calculations	149
5-5	Mass Comparison, Titanium and Graphite/Polyimide Upper Surface Honeycomb Panels.	149
5-5	Mass Comparison, Titanium and Graphite/Polyimide Upper Surface Honeycomb Panels.	14

FIGURES

No.		Page
5-1	Theoretical-to-Actual Mass Increment, Titanium Honeycomb Panel Skin,	
<i>J</i> 1	National SST Data	150
	Skin Spanwise Edge Design	151
5-2	Skin Spanwise Edge Design	152
5-3	Skin Edge Padup Mass Increment, Titanium Honeycomb Panels	132
5-4	Skin Edge Padup Mass Increment, Graphite/Polyimide Honeycomb Panels	153
	Theoretical-to-Actual Mass Increment, Titanium Honeycomb Panel Skin	154
5-5	Theoretical-to-Actual Mass Increment, Ittalium Honeycomb Lanci Skin	155
5-6	Theoretical-to-Actual Mass Increment, Graphite/Polyimide Honeycomb Panel Skin	133

INTRODUCTION

The ATLAS finite element structural analysis provides the theoretical size and mass of modeled structural members. On the arrow wing, those members modeled in the wing box structure include the covers, spar and rib chords and spar and rib webs.

Calculation of total wing structural mass requires the inclusion of a number of additional features in the structural box and wing elements external to the box, e.g., leading edge, trailing edge, control surfaces, etc. This section discusses the development of the additional structural features in the wing box and related conversion factors. Total wing mass analysis is discussed in Section 9.

Items in the wing box for which additional mass must be calculated include the following:

- Skin padup, door reinforcement, skin tolerance etc.
- Honeycomb core
- Core to skin adhesive
- Core edging (splice and sealing)
- Lightning protection and surface finish
- Spar and rib web stiffeners
- Spar and rib padup, web tolerance, hole reinforcement, etc.

Structural sizing from the ATLAS analysis defines the theoretical structure required for the strength to carry design loads. The increments discussed above account for additional elements of the structure that are required to satisfy design criteria not covered by theoretical analysis.

Prior to the development of the theoretical-to-actual mass factor for the graphite/polyimide construction, it was found necessary to first revise the theoretical-to-actual conversion factors used for the titanium construction (ref. 5-1). These revised titanium factors were used to change the wing mass reported in reference 5-1 as noted in Section 9. Five titanium honeycomb panels and five graphite/polyimide honeycomb panels were designed as described in Section 4. Evaluation of the components of these panels provided the data to generate the graphite/polyimide theoretical-to-actual conversion factors and to revise the titanium factors (see tables 5-1 and 5-2).

SKIN THEORETICAL-TO-ACTUAL CONVERSION FACTORS

The five titanium and five graphite/polyimide panels discussed in Section 4 were all designed with production type edge attachments. None of the panels, however, included wing lower surface access doors or provisions for fitting attachments, nor were such items as corner construction fully developed for the ten panels. These additional features add mass and increase the theoretical-to-actual factors.

The skin spanwise edge padup for the titanium honeycomb panels can be accounted for in three different ways in finite element structural analysis. First, the spanwise edge padup can be included in the cover material, which then becomes a part of the effective skin thickness. The chordwise skin padup, corner treatment, door cutout reinforcement, fuel system provisions, material tolerance, etc., are accounted for in the theoretical-to-actual factor. This first case is shown by curves 1 in figure 5-1, where the theoretical-to-actual increment is plotted versus the effective theoretical skin thickness based on data from the National SST program. The second alternate is to consider the spanwise padup as a part of the spar chord area. The skin thickness in the structural model is then equal to the theoretical thickness, t. The third alternate is to include the spanwise skin padup as a part of the theoretical-to-actual mass increment. This alternate is applicable to lightly loaded areas of the wing, where the minimum spar chord areas are dictated by minimum gage design constraints.

Figure 5-2 identifies the components of a typical panel and splice. Tables 5-1 and 5-2 list the data used in developing the theoretical-to-actual mass increments. The following paragraphs describe the development of these data.

Table 5-1 gives a detailed mass buildup of each of the five titanium wing skin panels that were designed for the arrow wing study. Figure 5-3 shows the skin edge padup increment, ratioed to the skin mass, as a function of skin thickness. Separate sets of curves labeled $\boxed{2}$, $\boxed{3}$, and $\boxed{4}$ are shown for chordwise edge padup, spanwise edge padup and total edge padup, respectively.

Mass data for the five graphite/polyimide panels that were designed for the present study are presented in table 5-2 and figure 5-4. Curve 5 in figure 5-4 shows the mass increment for spanwise titanium interleaves along the graphite/polyimide panel edges, as a function of skin thickness, t. Curve 6 shows the remainder of the edge padup, which includes the spanwise graphite/polyimide padup, chordwise graphite/polyimide padup and chordwise titanium interleaves. Curve 7 represents the total edge padup increment.

Principal steps in the derivation of theoretical-to-actual mass increment for the titanium and graphite/polyimide skin panels are shown in table 5-3. Selected skin thicknesses for either titanium or graphite/polyimide, covering the range of interest, are listed at the top of the table. Corresponding values of \overline{t}/t , obtained from the five titanium panel designs discussed in Section 4, are listed in line (1) where t is the basic skin thickness and \overline{t} is the effective theoretical skin thickness including the spanwise edge padups. These \overline{t}/t values can be obtained by adding 1.000 to the values from curves $\overline{3}$ in figure 5-3. The corresponding \overline{t} 's for the t's listed at the top of table 5-3 are obtained by forming product (t) x (\overline{t}/t) as given in line (2).

The original theoretical-to-actual increment for the skin of titanium honeycomb panels was developed during the study reported in reference 5-1 by collecting data on calculated panel masses from the

National SST program. These data were used to prepare the graph shown in figure 5-1. In that presentation spanwise edge padup is included as a part of effective theoretical skin mass (thickness denoted by \overline{t}), and the remaining padup is represented as a function of t. If we define

 w_X = mass increment for spanwise padup

 w_v = total mass increment

 w_t = mass of basic skin (thickness t)

 $w_{\overline{t}} = w_t + w_x$

then the incremental mass plot \(\begin{aligned} 1 \\ 1 \end{aligned} \] in figure 5-1 shows the variable

$$P_1 = (w_v - w_x)/w_{\overline{t}} \tag{5-1}$$

versus T

Values for P_1 are listed on line (3) of table 5-3 for the \overline{t} values listed on line (2).

In the more highly loaded portion of the titanium arrow wing the spanwise skin edge padup was considered as effective structural material included as a part of the spar chord, while the National SST Program considered this material as part of the skin t. In this second case the variable

$$P_2 = (w_v - w_x)/w_t$$
 (5-2)

is treated as a function of t. Since

$$P_2 = \left(\frac{w_y - w_x}{w_t}\right) \left(\frac{w_t}{w_t}\right)$$

and

$$w_{\overline{t}}/w_{t} = \overline{t}/t$$

it follows that

$$P_2 = \left(\frac{w_y - w_x}{w_{\overline{t}}}\right) \left(\frac{\overline{t}}{t}\right)$$

or.

$$P_2 = P_1(\overline{t}/t) \tag{5-3}$$

In the third case which is applicable to the more lightly loaded forward portion of the titanium arrow wing the spanwise skin padup becomes a part of the theoretical-to-actual mass increment. Then the variable

$$P_3 = w_v/w_t \tag{5-4}$$

is also treated as a function of t.

Since

$$w_X/w_y = (\overline{t} - t)/t = \overline{t}/t - 1$$

then

$$P_3 = P_1 (\overline{t}/t) + \overline{t}/t - 1 \tag{5-5}$$

 P_2 and P_3 , based on data from the national SST program and the five titanium panel designs, are tabulated in lines (4) and (5) of table 5-3. P_2 and P_3 are also represented, as functions of t, by curves $\boxed{8}$ and $\boxed{9}$, respectively in figure 5-5. Thus far the development of the theoretical-to-actual mass increment for the skin of the titanium honeycomb panels has been presented. The remainder of the tabulation in table 5-3 gives the steps in the development of the theoretical-to-actual mass increment for the skin of the graphite/polyimide honeycomb panels.

Values of P_4 in line (6), representing total edge padup for titanium panels, are taken from curve $\boxed{4}$ in figure 5-3. Values in line (7) for the edge padup increment, P_4 , for graphite/polyimide panels were calculated from the five advanced composite panel designs discussed in Section 4 and plotted as curve $\boxed{7}$ of figure 5-4. In deriving values of the theoretical-to-actual increment, P_3 , listed in line (8), it has been assumed that the ratio P_3/P_4 for graphite panels is equal to the ratio P_3/P_4 for titanium panels. These values of P_3 , applicable to light gage regions of the wing, include spanwise titanium interleaves as incremental mass. Values of the mass increment for spanwise interleaves, P_5 , from curve $\boxed{5}$ in figure 5-4, are listed in line (9). Finally, values of the theoretical-to-actual increment P_2 , omitting the contribution of spanwise interleaves (considered as spar chord area), are listed in line (10). Data from lines (8) and (10) have been used in plotting curves $\boxed{10}$ and $\boxed{11}$, respectively, in figure 5-6

The computation of the actual honeycomb skin mass in ATLAS requires the input of a mass factor, rather than a mass increment. These theoretical-to-actual mass factors for the skin are obtained by adding unity to the incremental values from figures 5-5 and 5-6.

Table 5-4 gives a summary of additional data required for the complete wing structure. The chart also shows a comparison of the theoretical-to-actual factors for both the titanium and composite honeycomb wing panel construction. The following paragraphs discuss the basis for significant additional items that are included in the analysis.

HONEYCOMB CORE

Density of the basic 1.5 in. polyimide honeycomb core is 3.5 lbm/ft³, and the mass per unit area is .4375 lbm/ft². This basic core mass must be multiplied by a factor of 1.2 on the upper wing surface and 1.25 on the lower wing surface to account for the dense core required around panel edges and around access doors on the lower surface.

CORE TO SKIN ADHESIVE

The core to skin adhesive for the graphite/polyimide panels is .015 in. thick and its area density is .170 lbm/ft². The adhesive is uniform in thickness, regardless of the core density.

CORE EDGING (SPLICE AND SEALING)

The mass of splice adhesive between dense core and basic core and the mass of the panel edge seal are functions of the panel perimeter-to-area ratio as well as the thickness and density of the material. In this case, however, masses of both core splice adhesive and the panel edge seal are treated as functions of panel area. This is based on an average panel perimeter-to-area ratio, resulting in a core splice adhesive mass of .025 lbm/ft² on the upper surface and .030 lbm/ft² on the lower surface. The factor for the lower surface is greater, due to the dense core splice around access doors in the lower surface. The area density of panel edge seal is estimated to be .046 lbm/ft² for an average panel geometry.

LIGHTNING PROTECTION AND SURFACE FINISH

The average lightning strike protective coating is .002 in. thick and its area density is .050 lbm/ft². The surface finish is a high temperature stable conductive coating and decorative paint, with area density of .027 lbm/ft².

SPAR AND RIB MASS INCREMENT

The sizing and mass of the basic chords and webs for the spars and ribs are calculated by the ATLAS design module. Some of the webs are of sine wave construction while the remainder are flat with stiffeners. The developed lengths of the sine wave webs were accounted for by altering the material density. The stiffeners for the flat webs were not modeled or sized within the program but the mass was accounted for by introduction of a factor within the program. For flat webs the stiffener mass was accounted for by multiplying the web mass by a factor of 1.5. This factor was further increased to account for additional increments to spar and rib mass. The final theoretical-to-actual mass conversion factors for the flat webs were:

```
Mass Factor for Flat Spar Webs = (1.5) (1.15) = 1.725 Mass Factor for Flat Rib Webs = (1.5) (1.18) = 1.770
```

The sine wave webs and chords for the spars and ribs were also multiplied by the following theoretical-to-actual conversion factors:

Factor for Sine Wave Spar Webs = 1.15 Factor for Sine Wave Rib Webs = 1.18 Factor for Spar Chords = 1.15 Factor for Rib Chords = 1.18 These are the factors, derived for the National SST Program, that were used in reference 5-1 for the titanium wing substructure.

PANEL MASS COMPARISON (TITANIUM VERSUS GRAPHITE/POLYIMIDE)

An example of a detailed mass comparison of titanium and graphite/polyimide medium gage honeycomb panels, designed to the same criteria, is shown in table 5-5. The overall mass advantage for the composite panel is 30.7%; the basic skin shows a relative advantage of 60.7%. The theoretical-to-actual increment for the composite skin is 12.4% greater than the titanium increment, while the remainder of the incremental masses such as core, adhesive, finish, etc. show no relative advantage for either panel. The theoretical-to-actual conversion increment as a percent of the basic skin mass generated by ATLAS structural analysis is 86% (46% of panel mass) for the titanium panel, and 227% (69% of panel mass) for the composite panel.

REFERENCES

5-1 Boeing Staff: Study of Structural Design Concepts for an Arrow Wing Supersonic Transport Configuration. NASA CR 132576-1 and -2, 1976.

Table 5-1.—Titanium Honeycomb Panel Mass Summary

	1	L	ower surfa	ce	Upper s	urface
		Light gage	Medium gage	Heavy gage	Medium gage	Heavy gage
Average t (outer + inner skin) (in.)	.030	.083	.120	.084	.134
Basic skin mass	(lbm)	22.68	76.42	154.34	77,85	271.96
Chordwise skin edge padup	(lbm)	1.46	3.25	5.36	2.77	5,81
Chordwise skin edge padup/						
basic skin		.065	.042	.035	.035	.021
Spanwise skin edge padup	(lbm)	5.45	14.88	14.85	10.88	19.57
Spanwise skin edge padup/						
basic skin		.240	.195	.096	.140	.072
Total skin edge padup	(lbm)	6.91	18,13	20.21	13.65	25.38
Total skin edge padup/						
basic skin		.305	.237	.131	.175	.093
Basic core	(lbm)	13.40	16.43	22.79	16.43	35.87
Center core	(lbm)	11.66	13,80	18.51	13,89	30.72
Edge core	(lbm)	4.51	13,23	22,28	12,82	26.19
Center core + edge core/					_	
basic core		1.207	1.645	1.790	1.626	1,587
Basic braze	(lbm)	7.37	9.04	12,54	9.04	19.73
Center braze	(lbm)	6.42	7.59	10.18	7.64	16.90
Edge braze	(lbm)	2.52	3.77	6.26	3.67	7.46
Center braze + edge braze/						4.005
basic braze		1,213	1.257	1,311	1,251	1.235
Edge finish	(lbm)	.02	.03	.06	.03	.05
Edge finish mass/panel						004
area (lbm/ft ²)		.001	.001	.001	.001	.001
Total panel mass	(lbm)	54.72	132.97	231.84	129.55	378,66
Panel area (ft ²)		32.81	40,23	55.82	40.23	87.84
Panel mass/panel area (lbm/f	t ²)	1.67	3,31	4.15	3.22	4.31

Table 5-2.—Graphite/Polyimide Honeycomb Panel Mass Summary

		Lo	ower surfac	е	Uppers	surface
		Light gage	Medium gage	Heavy gage	Medium gage	Heavy gage
Average t (outer + inner ski	n) (in.)	.048	,053	.128	.080	.117
Basic skin mass	(lbm)	12.70	17.28	57.62	25.95	82.86
Spanwise Ti interleaves	(lbm)	2.31	3.97	10.56	4.05	12.74
Spanwise Ti interleaves/						
basic skin		.182	.230	.183	.156	.154
Spanwise skin edge padup le	ess					
spanwise Ti interleaves	(lbm)	3.30	5.56	14.14	7.70	17,74
Spanwise skin edge padup le	ess					
spanwise Ti interleaves/						
basic skin		.260	.322	.246	.297	.214
Total skin edge padup	(lbm)	5,61	9.53	24.70	11.75	30,48
Total skin edge padup/						
basic skin		.442	.552	.429	.453	.368
Basic core	(lbm)	14,36	17.60	24.42	17,60	38.43
Center core	(Ibm)	12.36	14.77	19.57	14.72	32,52
Edge core	(lbm)	8.78	10.47	17.95	10.67	22.84
Center core + edge core/						
basic core		1.124	1.434	1.536	1.443	1,441
Core to skin adhesive	(lbm)	5,58	6.84	9,49	6.84	14,93
Core splice adhesive	(lbm)	.84	1,00	1.50	.99	1,95
Splice adhesive mass/panel						
area (Ibm/ft ²)		.0256	.0249	.0269	.0246	.0222
Panel edge seal	(lbm)	1.67	1.84	2,56	1.84	3.40
Edge seal mass/panel						
area (lbm/ft ²)		.0509	.0457	.0459	.0457	.0387
Lightning strike protective						
coating	(lbm)	1.64	2.01	2.79	2.01	4.39
Surface finish	(lbm)	.89	1.09	1.51	1.09	2.37
Total panel mass	(lbm)	45.07	64.83	137.69	75.86	195.74
Panel area (ft ²)		32.81	40.23	55.82	40.23	87.84
Panel mass/panel area (lbm/	ft ²)	1.37	1.61	2.47	1.89	2.23

Table 5-3.—Theoretical-To-Actual Mass Increment Derivation Honeycomb Panel Skin

	t, skin thickness	LWR .030	UPR .030	<u>LWR</u> .060	<u>UPR</u> .060	<u>LWR</u> .090	090.	LWR .120	<u>UPR</u> .120	<u>LWR</u> .150	<u>UPR</u> .150	<u>LWR</u> .180	<u>UPR</u> .180
(1)	\overline{v} t, for Ti panel designs from ③ + 1 in figure 5-3	1.336	1.286	1.214	1.183	1.140	1.118	1.096	1,092	1.075	1.064	1.073	1.062
(2)	$t = (t) (\overline{t}/t)$	040	.039	.073	.071	.103	.101	.131	.130	.161	.160	.193	.191
(3)	P ₁ , defined by equation (5-1), from [I] in figure 5-1	.533	.418	.362	.282	.252	187	.187	.129	.154	.102	.150	.100
(4)	P ₂ , defined by equation (5-3)	.712	.538	.439	.334	.287	.209	.205	.140	.166	.109	.161	.106
(2)	P ₃ , defined by equation (5-5)	1.048	.824	.653	.517	.427	.327	.301	.222	.241	.173	.234	.168
(9)	P ₄ , Ti edge padup factor, from 4 in figure 5-3	.400	.341	.261	.220	.179	.147	.131	.105	.108	980.	.104	.085
3	P' ₄ , Gr/Pi total edge padup factor, from [7] in figure 5-4	.568	.568	.486	.486	.430	.430	.403	.403	.400	.400	.400	.400
(8)	$P'_{3,} = (P'_{4}) (P_{3}/P_{4}),$ GR/Pi theoreticalto-actual factor	1.488	1.375	1,210	1.113	1.023	.937	.923	.842	.892	.812	.882	.802
(6)	P ⁵ , mass factor for spanwise Ti interleaves from [5]			_,									
	in figure 5-4	.220	.220	.195	.195	.175	.175	.160	.160	.160	.160	.160	.160
(10)	(10) $P_2' = P_3' - P_5'$	1.268	1,155	1.015	.918	.848	.762	.763	.682	.732	.652	.722	.642
*	*These values have been adjusted to a smooth curve	sted to	a smooth	curve									

Table 5-4. ATLAS Input Data to Support Mass Calculations

	Titanium H/C panels from study reported in ref. 5-1	Composite H/C panels from present study
Basic skin t	Input t which is resized by ATLAS analysis	Input t which is resized by ATLAS analysis
Factor for skin	Values from fig. 5-5 plus 1.0	Values from fig. 5-6 plus 1.0
Basic H/C core	1 in. thick, 5,0 lbm/ft ³ .4167 lbm/ft ²	1.5 in. thick, 3.5 lbm/ft ³ .4375 lbm/ft ²
Factor for edge core	Upper surface 1.25 Lower surface 1.30	Upper surface 1.20 Lower surface 1.25
Basic core to skin braze or adhesive	Alum, braze/surface ,2246 lbm/ft ²	Polyimide adhesive/surface .170 lbm/ft ²
Factor for edge core braze or adhesive	Upper surface 1.25 Lower surface 1.30	Upper surface 1.00 Lower surface 1.00
Core splice adhesive		Upper surface .0 25 lbm/ft ² Lower surface .0 30 lbm/ft ²
Panel edge seal		.046 lbm/ft ²
Lightning strike protective coating		.050 lbm/ft ²
Surface finish		.027 lbm/ft ²
Basic spar structure	Input structure which is resized by ATLAS analysis	Input structure which is resized by ATLAS analysis
Factor for spar (incl. stiff.)	Flat spar webs 1.725 Sine wave spar webs and chords 1.15	Flat spar webs 1.725 Sine wave spar webs and chords 1.15
Basic rib structure	Input structure which is resized by ATLAS analysis	Input structure which is resized by ATLAS analysis
Factor for rib (incl. stiff.)	Flat rib webs 1.77 Sine wave rib webs and chords 1.18	Flat rib webs 1.77 Sine wave rib webs and chords 1.18

Table 5-5.—Mass Comparison, Titanium and Graphite/Polyimide Upper Surface Honeycomb Panels

	Titanium panel	Mass reduction	Graphite/polyimide panel
Basic skin gage	.0713 in.		.080 in.
Skin mass	66.1 lbm	-60.7%	26.0 lbm
Incremental skin mass	18.6 lbm	+12.4%	20.9 lbm
Core, adhesive finish, etc.	38.1 lbm		38.2 lbm
Total panel mass	122,8 lbm	-30.7%	85,1 lbm
Mass increment as % of basic skin	85.8%		227.3%

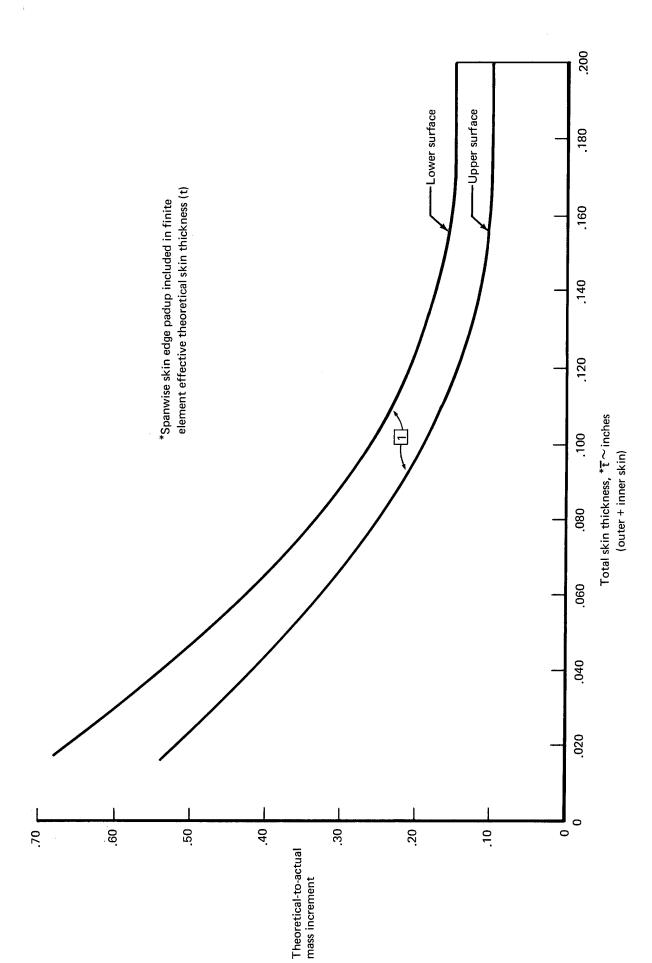


Figure 5-1.—Theoretical-To-Actual Mass Increment, Titanium Honeycomb Panel Skin, National SST Data

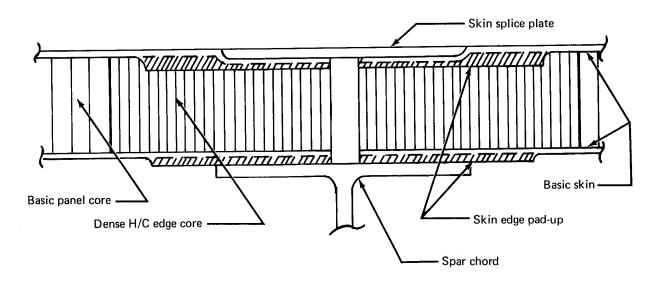


Figure 5-2.—Skin Spanwise Edge Design

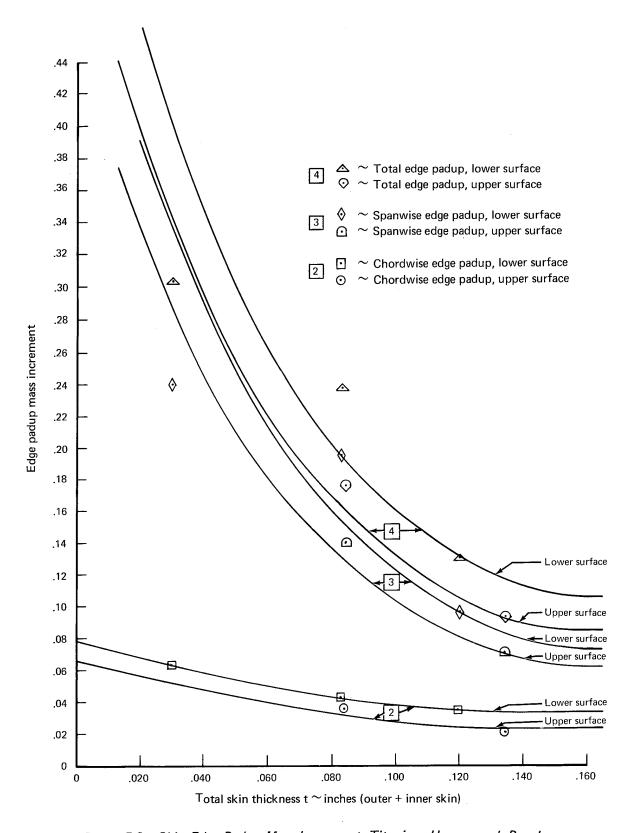


Figure 5-3.—Skin Edge Padup Mass Increment, Titanium Honeycomb Panels

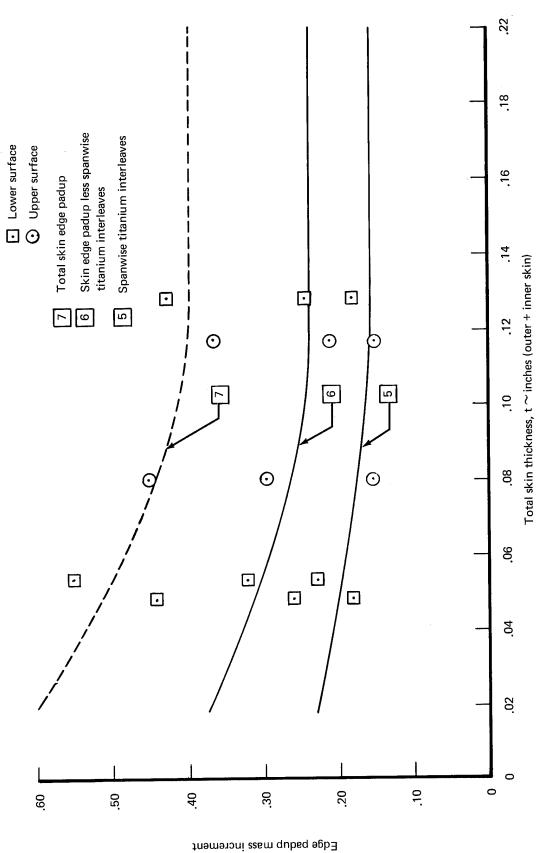


Figure 5-4.—Skin Edge Padup Mass Increment, Graphite/Polyimide Honeycomb Panels

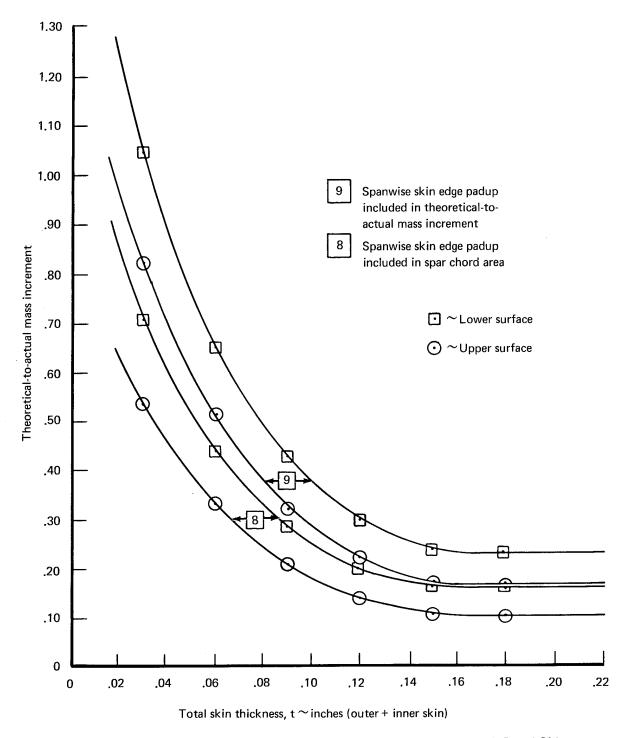


Figure 5-5.—Theoretical-To-Actual Mass Increment, Titanium Honeycomb Panel Skin

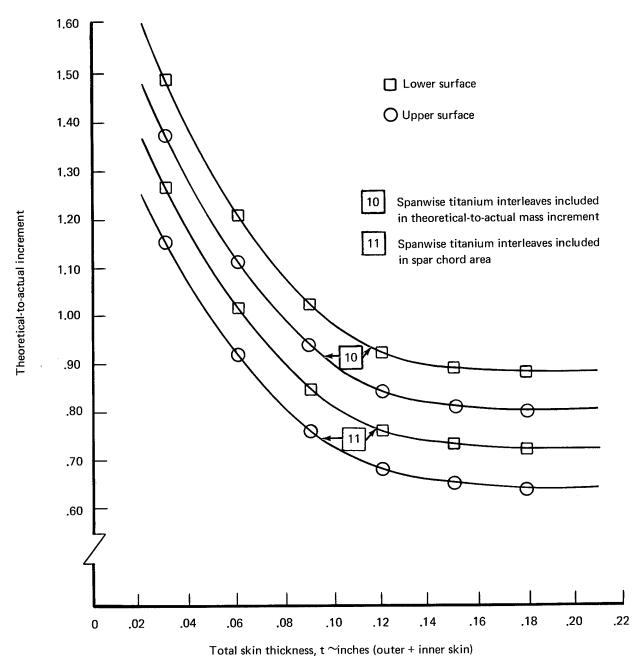


Figure 5-6.—Theoretical-To-Actual Mass Increment, Graphite/Polyimide Honeycomb Panel Skin

SECTION 6

COMPOSITE ANALYSIS AND DESIGN

by

F. D. Flood

CONTENTS

	Page
INTRODUCTION	162
COMPOSITE ANALYSIS IN ATLAS	162
STRENGTH OPTIMIZATION IN ATLAS	163
INITIAL SIZING PROCEDURES	165
ALLOWABLES FOR STRUCTURAL RESIZING	171
REFERENCE	176

TABLES

No.		Page
6-1	Allowable Buckling Stress Versus Core Thickness, Graphite/Polyimide, [0/±45/90] S	177
6-2	$[0/\pm45/90]_{S}$	
6-3	Allowable Buckling Stress Versus Core Thickness, Graphite/Polyimide, [0 ₃ /±45/90] _S	
6-4	Allowable Buckling Stress Versus Core Thickness, Graphite/Polyimide, $[0_4/\pm45/90]_S$	
6-5	Allowable Buckling Stress Versus Core Thickness, Graphite/Polyimide, $[0_2/\pm45/90]_S$	
6-6	Allowable Buckling Stress Versus Core Thickness, Graphite/Polyimide, $[0_2/\pm45_2/90]_S$	
6-7	Allowable Buckling Stress Versus Core Thickness, Graphite/Polyimide, [0/±45 ₂ /90] _S	
6-8	Allowable Buckling Stress Versus Core Thickness, Graphite/Polyimide, [0 ₃ /±45 ₂ /90] _S	
6-9	Allowable Buckling Stress Versus Core Thickness, Graphite/Polyimide, [0 ₄ /±45 ₂ /90] _S	
6-10	Allowable Buckling Stress Versus Core Thickness, Graphite/Polyimide, $[0_5/\pm 45/90]_S \cdot \cdot \cdot \cdot \cdot \cdot \cdot \cdot \cdot \cdot \cdot \cdot \cdot \cdot \cdot \cdot \cdot \cdot \cdot$	
6-11	Core Thickness Required to Develop Buckling Allowables Equal to Material Strength .	

FIGURES

No.		Page
6-1	Stiffness CPLATE Element	183
6-2	Stiffness CCOVER Element	184
6-3	ATLAS Composite Design Subsets (Illustrative Only)	185
6-4	Initial Buckling of Flat Rectangular Panels	186

SYMBOLS

E_c	Young's Modulus in compression
E_k	Subset of elements (region)
F	Allowable axial stress
F_c	Allowable compressive stress
F_{s}	Allowable inplane shear stress
G	Modulus of rigidity (shear)
R	Maximum stress ratio
T_{ik}	Allowable matrix
a	Spanwise dimension of a panel
b	Chordwise dimension of a panel
d	Distance between centroids of sandwich panel face sheets
t	Face sheet thickness
σ	Vector of stresses
μ	Poisson's ratio

Subscripts

x spanwisey chordwisexy diagonal

INTRODUCTION

This section discusses the advanced composite analysis and design capability within the ATLAS system. This capability was used to resize the honeycomb sandwich panels constructed of high strength graphite/polyimide. This section defines the procedures used for initial sizing prior to the automated resize activity described in Section 7. The choice of the maximum-strain failure criterion for the automated strength resize is discussed. The method of reducing the allowable strains such that the panels will be stable under combined biaxial compression and shear load for the strength-only resize is outlined. The subsequent panel stability evaluation indicated that buckling of the strength-sized panels was of very limited extent and required a negligible weight increase to preclude buckling altogether.

The design guidelines that were used in the automated strength sizing are discussed at length. The results of each of the automated resize cycles are shown in detail in Section 7.

COMPOSITE ANALYSIS IN ATLAS

To perform the advanced composite analysis and automated design, two special-purpose elements were added to the ATLAS system (ref. 6-1). The CPLATE element shown in figure 6-1 is used to model advanced composite laminates. The CCOVER element shown in figure 6-2 is a macro-element derived from the CPLATE element. The CCOVER element models the advanced composite laminates of the wing upper and lower surface panels simultaneously within a single element.

Each composite material (identified by a reference code) is defined by:

- 1) ply (layer) thickness
- 2) material area density defining the mass of a unit area of the ply (layer)
- 3) the following material properties for each applicable temperature
 - a) Young's moduli associated with the two orthogonal principal directions of the material
 - b) major Poisson's ratio in the plane determined by the above principal directions
 - c) shear modulus in the plane determined by the above principal directions
 - d) thermal strain for above temperature relative to 70°F for each of the two principal directions
 - e) allowable ultimate and yield (limit) tensile stresses for the two principal directions

- f) allowable ultimate and yield (limit) compressive stresses for the two principal directions
- g) allowable ultimate and yield (limit) shear stress in the plane determined by the principal directions

STRENGTH OPTIMIZATION IN ATLAS

The advanced composite optimization in ATLAS is of the "math programming" type. It operates solely on the CPLATE and CCOVER elements. The lamina thicknesses are minimized on the basis of user-defined specifications. The structure is considered to be divided into a number of regions. Each region constitutes an optimization problem which is considered independently of the others. A region may be defined as anything from a single element to all the elements composing the entire structure. The optimization of structure thus involves the solution of the problems (regions) that represent the entire structure. The remainder of this discussion of strength optimization in ATLAS will address only a single optimization problem (region).

A single optimization problem may be defined in the following manner (see figure 6-3). Given a subset of elements E_K (region) and an associated subset E_{KS} (design set), laminate strains for the design load cases and an initial set of lamina thicknesses upon which the strains are based; determine the set of lamina thicknesses having least weight for all composite elements in E_K based on the results of optimization of all elements in E_{KS} assuming regionally constant results.

The optimization procedure requires the repeated evaluation of stresses or strains as the design variables (lamina thicknesses) change. The lamina stresses or strains are based on the assumption that total laminate load remains constant and strain compatibility exists for all laminae. It is further assumed that all elements in \mathbf{E}_K have the same number of laminae, identical lamina orientations and that the lamina thicknesses can be regarded as real variables.

This composite optimization satisfies strength constraints for which two optional failure criteria are considered. The maximum strain failure criterion involves the comparison of applied strain components to allowable strain components. This criteria is performed for each lamina for each design load case. The most critical margin of safety is used to update the sizing. The alternative to the maximum strain criterion is the Tsai-Hill failure criterion. This may be defined as

$$\vec{\sigma}_{ik} T_{ik} \vec{\sigma}_{ik} \le 1.0 \tag{6-1}$$

where σ_{ik} is the vector of stresses for lamina i of the laminate k. The allowables matrix T_{ik} is defined as

$$T_{ik} = \begin{bmatrix} \frac{1}{F_{x_{ik}}^{2}} & \frac{-1}{2F_{x_{ik}}^{2}} & 0\\ \frac{-1}{2F_{x_{ik}}^{2}} & \frac{1}{F_{y_{ik}}^{2}} & 0\\ 0 & 0 & \frac{1}{F_{xy_{ik}}^{2}} \end{bmatrix}$$
(6-2)

where

 $F_{x_{ik}}$ = allowable axial stress in the x-direction $F_{y_{ik}}$ = allowable axial stress in the y-direction $F_{xy_{ik}}$ = allowable shear stress

The x- and y-directions are the two orthogonal principal directions of the orthotropic lamina i in the laminate k. Tensile or compressive allowable stress is selected to agree with the sign of the corresponding applied stress. To use the Tsai-Hill criterion as the basis for resizing, certain requirements must be satisfied regarding the allowable stresses. The allowables matrix cited above must be positive definite. If it were not, it would be possible to have stress fields for which the expression would remain negative for any lamina thickness. The determinant of the matrix T_{ik} is given by

$$\det T_{ik} = \frac{1}{F_{xy_{ik}}^2} \left[\frac{1}{F_{x}} \left(\frac{1}{F_{y_{ik}}^2} - \frac{1}{4F_{x_{ik}}^2} \right) \right]$$
 (6-3)

It may be seen that T_{ik} is not positive definite when $F_{yik} > 2F_{xxik}$. Thus it is required that the layer allowable axial stress always is associated with the x-direction within the lamina.

Each optimization problem is solved iteratively. Each cycle in this iteration involves a screening or definition phase and a solution phase. The screening phase searches subset E_{ks} to establish the critical element and load case for each lamina of the laminate. This screening is performed with the objective of establishing the strength constraints to be used during the optimization or solution phase. This procedure consequently requires all elements in subset E_k to have the same number of laminae in corresponding laminates. Subsets containing CCOVER elements are treated as two independent problems (i.e., upper and lower CPLATES). The solution phase involves the optimization for minimum weight with constraints as defined above. In a given cycle after the optimization is completed the screening is repeated. If the same element and load case is critical for each lamina, the solution is complete. Otherwise, another optimization is performed subject to the newly defined constraints. This iteration is continued until the constraint definitions have stabilized or for a maximum of ten times for each problem.

The optimization is based on the method of feasible directions. Weight is the merit function which is to be minimized subject to the defined constraints. The method of feasible directions (Zoutendyk's method) establishes a direction along which a small step can be taken without violating the constraints. In this method, this direction is defined by solving a linear programming problem in which the decrease in the merit function (weight) is maximized subject to the constraints which insure that the direction is feasible.

Prior to initiating optimization the design variables (lamina thicknesses) are scaled so that the largest constraint value is equal to zero. This same normalization is performed after the optimization is complete.

The optimization is considered to have converged if in three consecutive iterations the relative and absolute change in the value of the merit function is less than 0.001. As noted above, the maximum number of iterations is ten.

The user may define constraints that equate the thicknesses for different laminae. This results in an optimization problem with fewer design variables but the same number of constraints.

After the optimization problem has been solved for the values of the design variables, when the latter are regarded as real variables, each value is then transformed to an integer number of layers (plies) to describe the corresponding actual laminate. Since the primary purpose of the ATLAS Composite Design module in this application is to establish theoretical structural weight, the real-to-integer transformation is based on an arithmetic averaging concept. For example 6.3 layers would be rounded to six layers. This obviously does not insure positive margins throughout the structure, but is expected to yield a more realistic theoretical weight estimate for the total structure considered.

INITIAL SIZING PROCEDURES

The initial sizing of most of the elements of the advanced composite model for analysis and design via ATLAS is described in detail in Section 7. Not described in Section 7, however, is the core thickness of the honeycomb sandwich wing panels. These paragraphs will outline the manual analysis procedures used to evaluate core thickness requirements to develop the laminate strengths in spanwise or chordwise compression or shear. Similar results are shown for a number of laminates from which a core thickness was selected.

Abbreviated analysis procedures were established for general instability analyses of the advanced composite honeycomb sandwich panels by assuming the core was rigid. Panels sized by these abbreviated procedures were "spot-checked" with analyses using the more complex formulae that account for the core properties. Spanwise (0°) and chordwise compression allowables checked out within two percent (unconservative), while the shear allowables differed by about eight percent (conservative). Shear and compression intracell buckling were checked for 1/4 in. cell size with minimum skin gage. All local instability allowables exceeded the material strength for the $[0+45/90/-45]_S$ laminate with 2 mil ply thicknesses. The $[0/\pm45/90]_S$ laminate was shown to be appreciably weaker in chordwise compressive intracell buckling for which the laminate material strength was not developed.

The abbreviated formulae for panel general instability are given below. The allowable spanwise compressive stress (F_{C_X}) is given by

$$F_{c_X} = K E_X \left(\frac{t_e}{b\alpha^{1/4}}\right)^2$$
 (6-4)

where

$$K = a \text{ function of } \frac{a}{b\alpha^{1/4}}$$

a = spanwise dimension of panel

b = chordwise dimension of panel

$$\alpha = \frac{Ex}{Ey}$$

$$t_e = \frac{2\sqrt{t_1 t_2}}{t_1 + t_2}$$
 d $\sqrt{3}$ for unequal face sheet thicknesses

$$t_e = d\sqrt{3}$$
 for equal face sheet thicknesses

For unequal face gages the allowable spanwise compressive stress is given by

$$F_{c_X} = K E_X \frac{12 t_1 t_2}{(t_1 + t_2)} \left(\frac{d}{b\alpha^{1/4}}\right)^2$$
 (6-5)

For equal face gages the allowable spanwise compressive stress is given by

$$F_{c_X} = 3KE_X \left(\frac{d}{b\alpha^{1/4}}\right)^2 \tag{6-6}$$

The abbreviated formula for the chordwise compressive allowable stress, F_{cy}, is

$$F_{cy} = \frac{\pi^2}{12\lambda} E_y \left(\frac{t_e}{b}\right)^2 c_f$$
 (6-7)

where

$$\lambda = 1 - \mu_X \mu_V$$

c_f = end fixity factor provided the panel by the spars

For unequal face sheet thicknesses, the allowable chordwise compressive stress is given by

$$F_{cy} = \pi^2 \frac{E_y}{\lambda} \frac{t_1 t_2}{(t_1 + t_2)^2} \left(\frac{d}{b}\right)^2 c_f$$
 (6-8)

For equal face sheet thicknesses, the allowable chordwise compressive stress is given by

$$F_{cy} = \frac{\pi^2}{4} \frac{E_y}{\lambda} \left(\frac{d}{b}\right)^2 c_f$$
 (6-9)

The abbreviated formula for the allowable inplane shear stress F_{xy} , is given by

$$F_{xy} = K_s \frac{\pi^2}{12\lambda} E\left(\frac{t_e}{b}\right)^2 \tag{6-10}$$

where

E =
$$2(1 + \mu_e) G$$

 $\mu_e = (\mu_X \mu_Y)^{1/2}$
 $\lambda = 1 - \mu_X \mu_Y$
 $K_S = a \text{ function of a/b}$

For unequal face sheet thicknesses, the allowable shear stress is given by

$$F_{xy} = 2K_S \pi^2 \frac{G}{1-\mu_e} \frac{t_1 t_2}{\left(t_1 + t_2\right)} 2\left(\frac{d}{b}\right)^2$$
 (6-11)

For equal face sheet thicknesses, the allowable shear stress is given by

$$F_{xy} = \frac{K_S \pi^2}{2} \frac{G}{1 - \mu_e} \left(\frac{d}{b}\right)^2$$
 (6-12)

The more complex formulae for panel general instability which account for the core properties are given below. The allowable spanwise compressive stress is given by

$$F_{cx} = \frac{3 E_{x} \left(\frac{2h K_{c}}{t_{1} + t_{2}}\right)}{\left[\frac{b\alpha^{\frac{1}{4}}}{d k^{\frac{1}{2}}} \frac{t_{1} + t_{2}}{2\sqrt{t_{1} t_{2}}}\right]^{2} \left(\frac{2h K_{c}}{t_{1} + t_{2}}\right) + E_{x}}$$
(6-13)

where

h = c + t₁ + t₂ = d +
$$\frac{1}{2}$$
 (t₁ + t₂)
K_c = $\frac{1}{6}$ (G_{yz} + G_{xz})
k = K $\frac{\pi^2}{12(1 - \mu_x \mu_y)}$

The formula for the chordwise compressive allowable stress which accounts for the core properties is

$$F_{cy} = \frac{3 E_y \left(\frac{2h K_c}{t_1 + t_2}\right)}{\left[\frac{b}{d\sqrt{k}} \frac{t_1 + t_2}{2\sqrt{t_1 t_2}}\right]^2 \left(\frac{2h K_c}{t_1 + t_2}\right) + E_y}$$
(6-14)

where

h = c + t₁ + t₂ = d + ½ (t₁ + t₂)

$$K_c = \frac{1}{6} (G_{yz})$$

k = $\frac{\pi^2 c_f}{12 (1 - \mu_x \mu_y)} (\frac{b}{a})^2$
 $c_f = \text{the end fixity factor provided the panels by the spars}$

The formula for the allowable inplane shear stress accounting for the core properties is

$$F_{S} = \frac{G/2}{\frac{b}{d\sqrt{k_{s}}} \frac{t_{1} + t_{2}}{2\sqrt{t_{1} t_{2}}}^{2} + \left(\frac{G}{\frac{2h K_{c_{s}}}{t_{1} + t_{2}}}\right)^{2}}$$
(6-15)

where

$$K_{CS} = \frac{1}{2} (G_{yz} + G_{xz})$$

$$k_S = K_S \frac{\pi^2}{12(1 - \mu_X \mu_y)}$$
 $K_S = a \text{ function of } a/b$

It should be noted from Section 3 that the 1986 high-strength graphite/polyimide will be available in 2-, 3- and 4-mil thickness tapes. Also that 0.016 in. and 0.032 in. (0.024 in.) were selected as minimum gage for the inner and outer face sheet gages, respectively, for the lower (upper) surface. The inner and outer face sheets will be further constrained to exhibit the same stress-strain relations. For the subsequent calculations, the component laminates are assumed to have the properties shown below:

Property		Laminate	ıte	
Hoporty	0°	90°	±45°	
Compressive Strength, F _c (ksi)	290	16.4	37.4	
Poisson's Radio, μ	0.31	0.018	0.80	
Young's Modulus, E _c (msi)	20.0	1.13	2.58	
Shear Strength, F_S (ksi)	20.8	20.8	148.0	
Modulus of Rigidity, G (msi)	0.717	0.717	5.1	

In addition, the laminate density is taken as $0.056 \, \mathrm{lb/in^3}$ and that of the core as $0.00203 \, \mathrm{lb/in^3}$

Considering first the spanwise compressive allowable, consider equation 6-5 and 6-6. Since the value of the corrected aspect ratio is much larger than unity, the value of K is taken as the asymptotic value 3.62. Additionally, the loaded width b is the spar spacing, 35 in. Substituting these values first in equation 6-5 and 6-6 yields

$$F_{cx} = 35\,500 \, \left(\frac{t_1 \, t_2}{t_1 + t_2}\right)^2 \, \frac{E_x}{10^6} \, \frac{d^2}{\sqrt{\alpha}}$$
 (6-16)

for unequal face sheet thicknesses and

$$F_{cx} = 8860 \frac{E_x}{10^6} \frac{d^2}{\sqrt{\alpha}}$$
 (6-17)

for equal face sheet thicknesses.

Considering next the chordwise compressive allowable, recall equations 6-8 and 6-9. Again the chordwise dimension of the panel is 35 in. and an end fixity factor of 2 is assumed. Substituting gives

$$F_{cy} = 16110 \left(\frac{t_1 t_2}{(t_1 + t_2)} 2 \frac{d^2}{\lambda} \frac{E_y}{10^6} \right)$$
 (6-18)

for unequal face sheet thicknesses and

$$F_{cy} = 4030 \frac{d^2}{\lambda} \frac{E_y}{10^6}$$
 (6-19)

for equal face sheet thicknesses.

Now consider the inplane allowable shear stress from equations 6-11 and 6-12. For large panel aspect ratio, the buckling factor K_S equals 5.34. Substituting this and the value of 35 in. for b gives

$$F_{xy} = 86\ 000\ \left(\frac{t_1\ t_2}{t_1 + t_2}\right)^2\ \left(1 - \mu_e\right)\ \frac{G}{10^6}\ \frac{d^2}{\lambda}$$
 (6-20)

for unequal face sheet thicknesses and

$$F_{xy} = 21\ 500\ \left(1 + \mu_e\right) \frac{G}{10^6} \frac{d^2}{\lambda}$$
 (6-21)

for equal face sheet thicknesses.

Consider now a sandwich panel with the face sheets constructed of $[0/\pm45/90]_S$ laminates. The inner face sheet has 8 plies of 0.002 in. thickness, and the outer has 16 plies of 0.002 in. thick material. Thus,

$$T_1 = 8 (.002) = 0.016 \text{ in.}$$

 $T_2 = 16 (.002) = 0.032 \text{ in.}$
 $t = 24 (.002) = 0.048 \text{ in.}$
 $d = c + \frac{1}{2} (0.016 + 0.032) = c + 0.024$ (6-22)

where

 T_1 = the inner face sheet thickness

 T_2 = the outer face sheet thickness

d = distance between face sheet centroids

c = core height

Using the property values from above we obtain the following average values for the laminate

$$F_{cx} = \frac{1}{4} (290 + 16.4 + 74.8) = F_{cy} = 95.3 \text{ ksi}$$

$$E_{x} = \frac{1}{4} (20 + 1.13 + 5.16) = E_{y} = 6.57 \text{ msi}$$

$$F_{S} = \frac{1}{2} (20.8 + 148) = 84.4 \text{ ksi}$$

$$G = \frac{1}{2} (0.717 + 5.1) = 2.91 \text{ msi}$$

$$\mu_{x} = \frac{.31 (1.13) + .018 (20) + .80 (2.58)^{2}}{1.13 + 20. + 2.58 (2)} = \mu_{y} = 0.184$$

$$\alpha = Ex/Ey = 95.3/95.3 = 1$$

$$\mu_{e} = \left(\mu_{x} \mu_{y}\right)^{\frac{1}{2}} = 0.184$$

$$\lambda = 1 - \mu_{x} \mu_{y} = 1 - (0.184)^{2} = 0.966$$

$$\frac{t_{1} t_{2}}{(t_{1} + t_{2})} = \frac{.016 (.032)}{(.016 + .032)^{2}} = \frac{2}{9}$$

Substituting the above values in equations 6-16, 6-18 and 6-20 gives

$$F_{c_{X}} = 35 500 (2/9) 6.57d^{2} = 51 800d^{2}$$

$$F_{c_{Y}} = 16 110 (2/9) 6.57 (1/.966d^{2}) = 24 400d^{2}$$

$$F_{x_{Y}} = 86 000 (2/9) \frac{1.184}{6.966} (2.91)d^{2} = 68 200d^{2}$$
(6-24)

The allowable spanwise and chordwise compressive stresses and the allowable shear stress for the above panel are given in table 6-1 for a range of core thicknesses. Tables 6-1 through 6-10 show allowable stresses for a range of core thicknesses for other laminates (face sheets) of interest. Finally, table 6-11 shows a summary of the core thicknesses required to develop each of the allowable stresses for the laminates shown. Due to the limited scope of the study, only a single core thickness was selected although this parameter is known to effect optimum theoretical weight significantly. A core thickness of 1.50 in. was chosen since it develops the allowable spanwise compressive stress up to the material strength for all panels except those with thick face sheets and a preponderance of spanwise-oriented plies. It is more than sufficient to develop the allowable inplane shear strength. A core of nearly 2.00 in. thickness would be required to develop the chordwise compressive allowable stresses up to the material strength. Chordwise compression loads are small except near the side-of-body, near the landing trunnions and other such points with localized loads being introduced. The possible addition of some face sheet material over a very limited portion of the wing seemed advantageous compared to the relatively large increase in core thickness throughout the wing primary structure.

ALLOWABLES FOR STRUCTURAL RESIZING

Prior to performing the automated strength resizing, it was necessary to select a failure criterion and the associated material allowables. For 1976 advanced composites with their attendant matrix microcracking problems, the Tsai-Hill failure criterion correlates with test data better than other failure criteria (ref. 2-2). Since it was hypothesized that the 1986 high strength graphite/polyimide would permit design and fabrication of laminates that are truly fiber critical, an empirical data base with which to evaluate the various failure criteria was effectively lost. This, and the ease with which the maximum strain criterion can be physically interpreted, led to the choice of the latter as the failure criterion.

The titanium wing panels of Task II were replaced with high strength graphite/polyimide sandwich panels. However, since this phase of the contract was limited in scope, the spars and ribs in the wing primary structure remained of titanium structure as defined in Task II. However, it was assumed that the titanium alloy used in 1986 would, through development, have higher allowable stresses (strains) with no change in the elastic properties. The specific assumptions made for the titanium allowable properties are shown below:

Temperature °F	Modulus msi	Allowable Stress* ksi	Allowable Strain*
RT	16.4	164.0	10 000
250	15.5	139.5	9 000
450	14.6	116.8	8 000

^{*}Uniaxial Tension or Compression

The high strength graphite/polyimide properties are shown in table 2-1. The values for 250°F while not shown are identical to those at room temperature. It should be noted that the allowable strains for the high strength graphite/polyimide are significantly larger than those for the titanium alloy. To retain strain compatibility with the titanium spar and rib chords, the strains of the high strength graphite/polyimide have been limited to the allowable titanium strain. The mathematical model of the structure specifies a different material for the 0°, ±45° and 90° laminae on the upper surface and the lower. Thus, different strain limitations may be imposed on these laminae.

The 0° and 90° laminae allowable tensile strains were reduced to the allowable titanium tensile strain for the appropriate temperature. The allowable compressive strain for the 0° lamina (spanwise) was also reduced to these same strain limits. This, then, for uniaxial spanwise loading defines the maximum stress ratios as

$$R_{\text{spanwise}} = \frac{F_{\text{capplied}}}{F_{\text{callowable}}} = \frac{200 \text{ ksi}}{290 \text{ ksi}} = 0.69 @ \text{Room Temperature}$$

$$\frac{180 \text{ ksi}}{290 \text{ ksi}} = 0.621 @ 250^{\circ}\text{F}$$

$$\frac{160 \text{ ksi}}{260 \text{ ksi}} = 0.615 @ 450^{\circ}\text{F}$$

The interaction relationship used for buckling failure under combined biaxial compression and shear is shown in figure 6-4. This is used solely to establish the allowable strains. From figure 6-4 it can be seen that if $R_{\rm X}=0.69$, then $R_{\rm y}$ (chordwise) is limited to 0.767 in the absence of any shear loading. In the Initial Sizing Procedures paragraph above, a core thickness of 1.5 inches was selected. This core thickness develops only about 67% of the material allowable as an allowable buckling stress for chordwise compression loads. Thus for a chordwise-oriented ply, the allowable stress for the above biaxial compressive loading ($R_{\rm X}=0.69$ and $R_{\rm y}=0.767$) is

$$F_{c_V} = 0.767 (0.67) 290 = 149 \text{ ksi}$$

The decision was made to reduce the above chordwise compressive stress from 149 ksi to 134 ksi to permit some allowance for shear loading in conjunction with the biaxial compression. Thus, the maximum chordwise compressive stress ratio becomes

$$R_{y_{\text{max}}} = \frac{134}{0.67(290)} = 0.69$$

For spanwise compression and shear loading only the maximum shear stress ratio Rxy would be 0.55. For chordwise compression and shear loading only, the maximum shear stress ratio would be 0.76. With these conflicting values, a maximum diagonal stress of 200 ksi was selected which gives

$$R_{xy_{max}} = \frac{200 \text{ ksi}}{290 \text{ ksi}} = 0.69$$

Thus for room temperature, the allowable stress ratios are

$$R_{x_{max}} = 0.69$$

 $R_{y_{max}} = 0.69$
 $R_{xy_{max}} = 0.69$

Procedures similar to those above were followed with the 250°F properties to give

$$R_{x_{max}} = 0.621$$

 $R_{y_{max}} = 0.739$
 $R_{xy_{max}} = 0.721$

And, similarly for 450°F

$$R_{x_{max}} = 0.615$$
 $R_{y_{max}} = 0.744$
 $R_{xy_{max}} = 0.719$

For room temperature the preceding values redefined in terms of allowable strains in the individual lamina axes for the various laminae becomes

Tamina	Allowable Strain, in./in.			
Lamina	Tension	Compression	Shear	
0° —longitudinal 0° —transverse ±45° —longitudinal ±45° —transverse 90° —longitudinal 90° —transverse	0.01 0.01475 0.01475 0.01475 0.01 0.01475	-0.01 -0.0145 -0.01 -0.0145 -0.0067 -0.0145	±0.029 ±0.029 ±0.029 ±0.029 ±0.029	

For 250°F, the allowable strains in the individual lamina axes for the various laminae are

Lamina	Allowable Strain, in./in.		
	Tension	Compression	Shear
0°—longitudinal 0°—transverse ±45°—longitudinal ±45°—transverse 90°—longitudinal 90°—transverse	0.009 0.01475 0.01475 0.01475 0.009 0.01475	-0.009 -0.0145 -0.01045 -0.0145 -0.0072 -0.0145	±0.029 ±0.029 ±0.029 ±0.029 ±0.029 ±0.029

For 450°F, the allowable strains in the individual lamina axes for the various laminae are

Lamina	Allowable Strain, in./in.		
	Tension	Compression	Shear
0°—longitudinal	0.008	-0.008	±0.026
0°-transverse	0.0133	-0.013	±0.026
±45°—longitudinal	0.01325	-0.00935	±0.026
±45° – transverse	0.0133	-0.013	±0.026
90° —longitudinal 90° —transverse	0.008 0.0133	-0.0065 -0.013	±0.026 ±0.026

It should be noted that all laminates will be designed having a minimum of one lamina in each orientation.

For the ATLAS composite design module, the various laminate allowable strains had to be specified as allowable stresses. The reduced stiffnesses which transform strains to stresses in the individual lamina 1-2 coordinate axis system are given in terms of engineering constants by

$$Q_{11} = E_1 / (1 - \mu_{12} \mu_{21})$$

$$Q_{12} = \mu_{12} E_2 / (1 - \mu_{12} \mu_{21}) = \mu_{21} E_1 / (1 - \mu_{12} \mu_{21})$$

$$Q_{22} = E_2 / (1 - \mu_{12} \mu_{21})$$

$$Q_{66} = G_{12}$$
(6-26)

Thus for an individual lamina, the strain-stress relations are

$$\begin{cases}
\sigma_{1} \\
\sigma_{2} \\
\tau_{12}
\end{cases} = \begin{bmatrix}
Q_{11} & Q_{12} & 0 \\
Q_{22} & 0 \\
(\text{sym}) & Q_{66}
\end{bmatrix} \begin{cases}
\epsilon_{1} \\
\epsilon_{2} \\
\gamma_{12}
\end{cases} = \begin{bmatrix}
\frac{E_{1}}{1 - \mu_{12} \mu_{21}} & \frac{\mu_{12} E_{2}}{1 - \mu_{12} \mu_{21}} & 0 \\
\frac{E_{2}}{1 - \mu_{12} \mu_{21}} & 0 \\
(\text{sym}) & G_{12}
\end{bmatrix} \begin{cases}
\epsilon_{1} \\
\epsilon_{2} \\
\gamma_{12}
\end{cases} (6-27)$$

For high strength graphite/polyimide at room temperature:

$$E_1 = 20\ 000\ ksi$$
 $E_2 = 1130\ ksi$
 $G_{12} = 717\ ksi$
 $\mu_{12} = 0.31$
(6-28)

From the reciprocal relation

$$\frac{\mu_{12}}{E_1} = \frac{\mu_{21}}{E_2} \tag{6-29}$$

it follows that

$$\mu_{21} = \frac{E_2}{E_1} \quad \mu_{12} = \frac{1130}{20\,000} (0.31) = 0.0175$$
 (6-30)

Substituting these values in equation 6-27 gives

$$\begin{cases}
\sigma_{1} \\
\sigma_{2} \\
\tau_{12}
\end{cases} = \begin{bmatrix}
\frac{20\ 000}{1-0.31\ (0.0175)} & \frac{0.31\ (1130)}{1-0.31\ (0.0175)} & 0 \\
\frac{1130}{1-0.31\ (0.0175)} & 0 \\
\gamma_{17}
\end{bmatrix} \begin{cases}
\epsilon_{1} \\
\epsilon_{2} \\
\gamma_{12}
\end{cases} = \begin{bmatrix}
20\ 100 & 352 & 0 \\
1136 & 0 \\
(\text{sym}) & 717
\end{bmatrix} \begin{cases}
\epsilon_{1} \\
\epsilon_{2} \\
\gamma_{12}
\end{cases} (6-31)$$

Now substituting the allowable strains for room temperature in equation 6-31 provides the corresponding allowable stresses along the individual lamina axes.

Lamina	Allowable Stress, ksi		
Lannina	Tension	Compression	Shear
0°—longitudinal 0°—transverse ±45°—longitudinal ±45°—transverse 90°—longitudinal 90°—transverse	206.0 20.3 302.0 21.9 206.0 20.3	-206.0 - 19.99 -206.00 - 19.99 -139.80 - 18.83	±20.8 ±20.8 ±20.8 ±20.8 ±20.8 ±20.8

Similarly for 250°F, the allowable stresses for the various laminae along the individual lamina axes are

Lamina	Allowable Stress, ksi		
Lamma	Tension	Compression	Shear
0°—longitudinal 0°—transverse ±45°—longitudinal ±45°—transverse 90°—longitudinal 90°—transverse	186.10 19.92 302.00 21.90 186.10 19.92	-186.00 - 19.64 -215.00 - 20.20 -149.80 - 19.01	±20.8 ±20.8 ±20.8 ±20.8 ±20.8 ±20.8

For 450°F, the allowable stresses for the various laminae along the individual lamina axes are

Lamina	Allowable Stress, ksi		
	Tension	Compression	Shear
0°-longitudinal	164.30	-164.30	±12.01
0°-transverse	16.33	- 16.02	±12.01
±45°—longitudinal	269.00	-191.30	±12.01
±45°-transverse	18.02	- 16.46	±12.01
90°–longitudinal	164.30	-134.20	±12.01
90° – transverse	16.33	- 15.54	±12.01

The above allowables have been shown through use in the strength resizing to have adequately accomplished their purpose. That is, to provide allowance for panel stability under combined loading during strength resizing which had no explicit panel stability analysis. This is discussed further in Section 7.

REFERENCE

Robinson, James C.; Yates, E. Carson, Jr.; Turner, M. Jonathan; and Grande, Donald L.: "Application of an Advanced Computerized Structural Design System to an Arrow-Wing Supersonic Cruise Aircraft." AIAA Paper 75-1038, August 1975.

Table 6-1.—Allowable Buckling Stress Versus Core Thickness, Graphite/Polymide, [0/±45/90] S

 $F_{cx} = 95.3 \text{ ksi}$ $F_{cy} = 95.3 \text{ ksi}$ $F_{s} = 84.4 \text{ ksi}$

Minimum gage

 $t_1 = 0.016$ in. $t_2 = 0.032$ in. $\overline{t} = 0.048$ in.

c, in.	d, in.	F _x , ksi	F _y , ksi	F _{xy'} ksi
0.25	0.274	3.887	1.828	5.120
0.50	0.574	14.216	6.687	18.726
0.75	0.774	31.016	14.590	40.858
1.0884	1.1124	64.066	30.136	84.4
1.3327	1.3567	95.3	44.827	
1.9542	1.9782		95.3	

 $t_1 = 0.024$ in. $t_2 = 0.032$ in. $\overline{t} = 0.056$ in.

c,	d,	F _x ,	F _y ,	F _{xy'}
in.	in.	ksi	ksi	ksi
0.25 0.50 0.75 1.042 1.2775 1.875	0.278 0.528 0.778 1.070 1.3055 1.903	4.321 15.588 33.844 64.017 95.3	2.033 7.333 15.921 30.114 44.829 95.3	5.693 20.534 44.583 84.4

 $t_1 = t_2 = 0.032$ in. $\overline{t} = 0.064$ in.

c,	d,	F _X ,	F _y ,	F _{xy′}
in.	in.	ksi	ksi	ksi
0.25	0.282	4.631	2.179	6.102
0.50	0.532	16.484	7.753	21.716
0.75	0.782	35.617	16.752	46.92
1.017 1.247 1.833	1.049 1.279 1.865	64.091 _95.3	30.145 44.814 95.3	84.4

Table 6-2.—Allowable Buckling Stress Versus Core Thickness, Graphite/Polyimide, $[0/\pm45/90/90]_S$

$t_1 = 0.018 \text{ in.}$	
$t_2 = 0.036$ in.	
$\bar{t} = 0.054 \text{ in.}$	

 $F_{cx} = 86.5 \text{ ksi}$ $F_{cy} = 1,16.9 \text{ ksi}$ $F_{s} = 77.3 \text{ ksi}$

C,	d,	F _{x′}	F _y ,	F _{xy′} ksi
in.	in.	ksi	KSI	KSi
0.25	0,277	4,192	2.274	5.253
0.50	0.527	15.175	8.230	19.014
0.75	0.777	32.988	17.890	41.333
1.036	1.063	61.74	33,483	77.3
1.2312	1.2582	86.5	46.909	ļ
1.500	1.527		69.094	
1.600	1.627		78.439	
1.700	1.727		88.379	
1,8	1.827		98.910	
1.959	1.986		116.9	

Table 6-3.—Allowable Buckling Stress Versus Core Thickness, Graphite/Polyimide, $[0_3/\pm45/90]_S$

4 mil plies $\frac{t_1}{t} = t_2 = 0.048 \text{ in.}$ $\frac{t_1}{t} = 0.096 \text{ in.}$ $F_{cx} = 160.2 \text{ ksi}$ $F_{cy} = 69.0 \text{ ksi}$ $F_{s} = 63.2 \text{ ksi}$

0.25 0.298 5.708 1.73 4.77 0.50 0.548 19.3 5.85 16.1 0.75 0.798 40.9 12.4 34.2 1.0363 1.0843 75.57 22.9 63.2	c,	d,	F _{x′}	F _y ,	F _{xy'}
	in.	in.	ksi	ksi	ksi
1.3 1.348 116.8 35.4 1.4 1.448 134.8 40.9 1.5 1.548 154 46.7 1.5307 1.5787 160.2 48.562 1.8338 1.8818 69.0	0.25 0.50 0.75 1.0363 1.2 1.3 1.4 1.5	0.298 0.548 0.798 1.0843 1.248 1.348 1.448 1.548	5.708 19.3 40.9 75.57 100.1 116.8 134.8	1.73 5.85 12.4 22.9 30.3 35.4 40.9 46.7 48.562	4.77 16.1 34.2

Table 6-4.—Allowable Buckling Stress Versus Core Thickness, Graphite/Polyimide, $[0_4/\pm45/90]_S$

4 mil inner ply 4 mil outer ply $t_1 = t_2 = 0.056$ in. $t_1 = 0.112$ in. $F_{cx} = 178.7 \text{ ksi}$ $F_{cy} = 61.5 \text{ ksi}$ $F_{s} = 57.1 \text{ ksi}$

c,	d,	F _x ,	F _y ,	F _{xy′}
in.	in.	ksi	ksi	ksi
0.25	0.306	6.0	1.62	4.49
0.50	0.556	19.82	5.35	14.81
0.75	0.806	41.65	11.24	31.13
1.0356	1.0916	76.39	20.62	57.1_
1.2	1.256	101.13	27.3	
1.4	1.456	135.91	36.7	
1.5	1.556	155.2	41.9	
1.6136	1.6696	<u>178.7</u>	48.2	
1.829	1.885		61.5	

Table 6-5.—Allowable Buckling Stress Versus Core Thickness, Graphite/Polyimide, $[0_2/\pm45/90]_S$

4 mil inner ply 4 mil outer ply $t_1 = t_2 = 0.040$ in. $t_1 = 0.080$ in. $F_{cx} = 134.2 \text{ ksi}$ $F_{cy} = 79.5 \text{ ksi}$ $F_{s} = 71.7 \text{ ksi}$

F _{xy'} ksi
5.2
18.1
38.8
71.7

Table 6-6.—Allowable Buckling Stress Versus Core Thickness, Graphite/Polyimide, $[0_2/\pm 45_2/90]_S$

4 mil inner ply
4 mil outer ply
$t_1 = t_2 = 0.056$ in.
$\bar{t}' = 0.112 \text{ in.}$

 $F_{cx} = 106.6 \text{ ksi}$ $F_{cy} = 67.5 \text{ ksi}$ $F_{s} = 93.5 \text{ ksi}$

c,	d,	F _x ,	F _y ,	F _{xy'}
in.	in.	ksi	ksi	ksi
0.25	0.306	4.9	1.85	8.4
0.50	0.556	16.0	6.1	27.7
0.75	0.806	33.7	12.8	58.3
0.965	1.021	54.0	20.6	93.5
1.20	1.256	81.77	31.2	
1.378	1.434	106.6	40.6	
1.50	1.556		47.8	
1.792	1.848		67.5	

Table 6-7.—Allowable Buckling Stress Versus Core Thickness, Graphite/Polyimide, $[0/\pm45_2/90]_S$

$$\frac{t_1}{t} = t_2 = 0.048 \text{ in.}$$

 $F_{cx} = 76.0 \text{ ksi}$ $F_{cy} = 76.0 \text{ ksi}$ $F_{s} = 105.6 \text{ ksi}$

c,	d,	F _x ,	F _{y′}	F _{xy,}
in.	in.	ksi	ksi	ksi
0.25	0.298	4.125	2.040	5.410
0.50	0.548	13.950	6.897	18.295
0.75	0.798	29.581	14.625	38.795
1.0	1.048	51.020	25.225	66.911
1.23	1.278	75.87	37.512	99,503
1.27	1.318		39.897	105.829
1.50	1.548		55.036	
1.75	1.798		74.248	
1.77	1.818		75.909	

Table 6-8.—Allowable Buckling Stress Versus Core Thickness, Graphite/Polyimide, $[0_3/\pm 45_2/90]_S$

All 4 mil plies
$t_1 = t_2 = 0.064$ in.
$\bar{+}$ = 0.128 in

 $F_{cx} = 129.5 \text{ ksi}$ $F_{cy} = 61.1 \text{ ksi}$ $F_{s} = 84.4 \text{ ksi}$

c, in.	d, in.	F _{x′} ksi	F _{y'} ksi	F _{xy} , ksi
0.25	0.314	5.36	1.74	7.7
0.50	0.564	17.3	5.6	24.8
0.75	0.814	36.0	11.7	51.7
0.976	1.040	58.8	19.1	84.4
1.2	1.264	86.9	28.2	
1.479	1.543	129.5	42.0	
1.50	1.564		43.2	
1.797	1.861		61.1	

Table 6-9.—Allowable Buckling Stress Versus Core Thickness, Graphite/Polyimide, $[0_4/\pm 45_2/90]_S$

$$\frac{t_1}{t} = t_2 = 0.072 \text{ in.}$$

= 0.144 in.

$$F_{cx} = 147.3 \text{ ksi}$$

 $F_{cy} = 56.1 \text{ ksi}$
 $F_{s} = 77.3 \text{ ksi}$

C,	d,	F _x , ksi	F _{γ′} ksi	F _{xy'} ksi
in.	in.	KSI	Kai	1031
0.25	0.322	5.765	1.659	7.105
0.5	0.572	13.191	5.236	22.419
0.75	0.822	37.567	10.814	46.300
0.99	1.062	62.706	18.050	77.283
1.00	1.072	63.892	18.391	
1.25	1.322	97.168	27.970	
1.5	1.572	137.393	39.549	
1.56	1.632	148.081	42.625	
1.75	1.822		53.128	
1,80	1.872		56.084	

Table 6-10.—Allowable Buckling Stress Versus Core Thickness, Graphite/Polyimide, $[0_5/\pm45/90]_S$

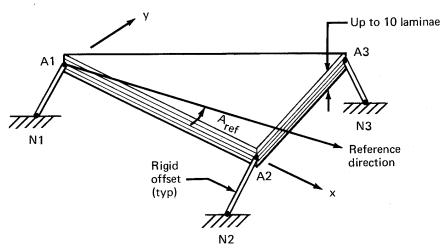
All 4 mil plies
$t_1 = t_2 = 0.064$
$\bar{t} = 0.128$

 $F_{cx} = 192.65 \text{ ksi}$ $F_{cy} = 55.85 \text{ ksi}$ $F_{s} = 52.6 \text{ ksi}$

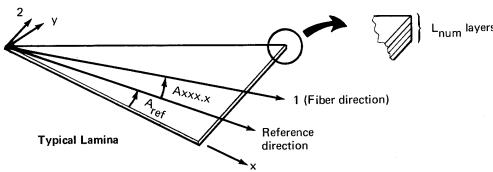
c,	d,	F _x ,	F _y ,	F _{xy} ,
in.	in.	ksi	ksi	ksi
0.25	0.314	6.25		
0.50	0.564	20.2		
0.75	0.814	42.0		
1.095	1.159	85.2		52.6
1.25	1.314	109.5		
1.50	1.564	155.1	38.4	
1.743	1.807	192.65		
1.886	1.950		55.85	

Table 6-11.—Core Thickness Required to Develop Buckling Allowables Equal to Material Strength

		ss of core requotes	, in .			
See table	F _{cx} ,	F _{cy′}	F _{s′}	Layup	t ₁ , in.	t ₂ , in.
6-1	1.33	1.95	1.09	[0/±45/90] _S	0.016	0.032
6-1	1.28	1.88	1.04	[0/±45/90] _S	0.024	0.032
6-1	1.25	1.83	1.02	[0/±45/90] _S	0.032	0.032
6-2	1.23	1.96	1.04	[0/±45/90/90] _S	0.018	0.036
6-3	1.53	1.83	1.04	[0 ₃ /±45/90] _S	0.048	0.048
6-4	1.61	1,83	1.04	[0 ₄ /±45/90] _S	0.056	0.056
6-5	1.42	1.84	1.03	[0 ₂ /±45/90] _S	0.040	0.040
6-6	1.38	1.79	0.97	[0 ₂ /±45 ₂ /90] _S	0.056	0.056
6-7	1.23	1.77	1.27	[0/±45 ₂ /90] _S	0.048	0.048
6-8	1.48	1.80	0.98	[0 ₃ /±45 ₂ /90] _S	0.064	0.064
6-9	1.56	1.80	0.99	[0 ₄ /±45 ₂ /90] _S	0.072	0.072
6-10	1.74	1.89	1.10	[0 ₅ /±45/90] _S	0.064	0.064



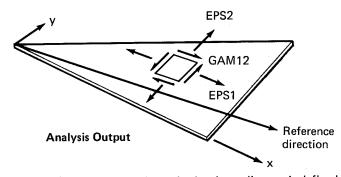
Triangular or quadrilateral laminated membrane plate element composed of up to 10 orthotropic laminae. The triangular CPLATE is a constant strain element. The quadrilateral CPLATE stiffness is generated from four constant strain triangles which intersect at a fifth internal node. This internal node is reduced by a static condensation. If warped, the quadrilateral CPLATE is equilibrated by transverse forces. The element may be offset from its structural nodes as shown above. A_{ref} defines the reference direction for the element.



The CPLATE is composed of 1 to 10 laminae, each of which is defined by four properties as shown below:

- ▼Axxx.x Defines the lamina fiber direction relative to the element reference direction
- ▼Axxx.x Defines the lamina temperature difference relative to the element reference direction

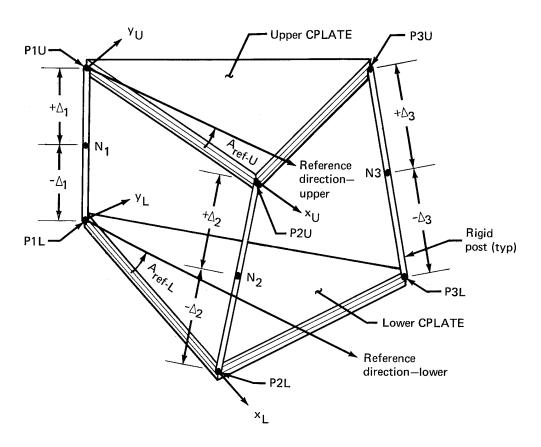
 ▼Txxxx Defines the lamina temperature difference relative to the element reference temperature
- ▼Lnum − Defines the number of layers (plies) of composite material within the lamina Identifies the composite material of the lamina



The CPLATE analysis output shown in the above diagram is defined below:

- ▼EPS1 -Lamina axial strain parallel to reference direction
- ▼EPS2 -Lamina axial strain perpendicular to reference direction
- ▼GAM12 Lamina shear strain

Figure 6-1.—Stiffness CPLATE Element



CCOVER element is composed of two triangular or quadrilateral ATLAS CPLATE elements separated by rigid posts. Eash CPLATE is as described in figure 6-1. One of the CPLATES may have zero properties. Mid-surface nodes (N1, N2, N3) are required. Addition of the respective Δ_Z coordinates to the input nodal Z coordinates defines the upper CPLATE corners, whereas subtraction defines the lower CPLATE corners. The directions of the rigid posts are defined by the nodal Z-axes which need not be parallel.

Figure 6-2.—Stiffness CCOVER Element

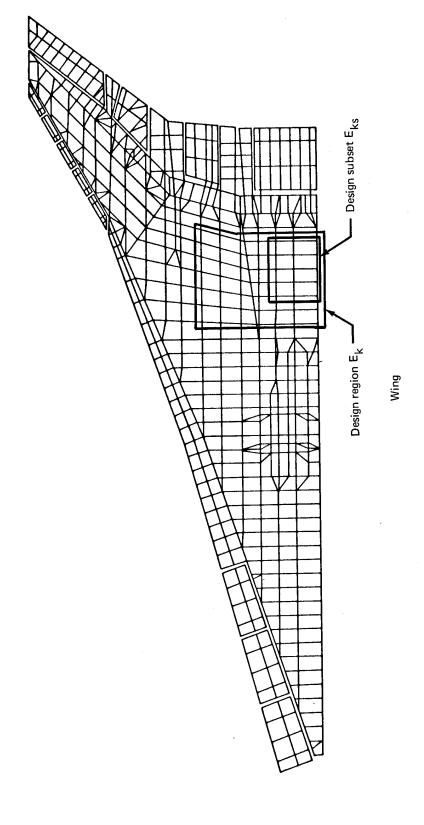


Figure 6-3.—ATLAS Composite Design Subsets (Illustrative Only.)

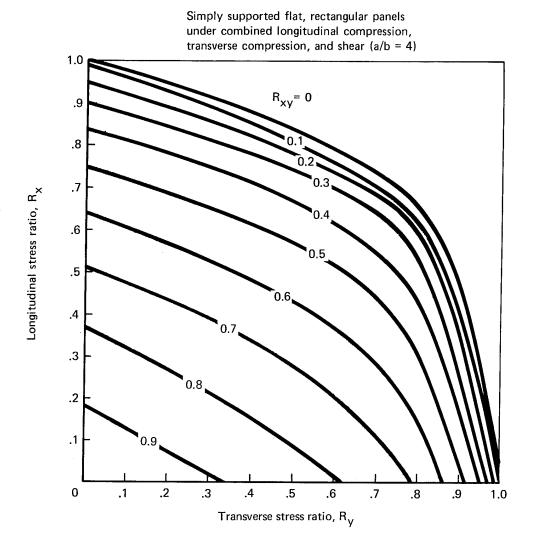


Figure 6-4.—Initial Buckling of Flat Rectangular Panels

SECTION 7

REVISION OF MATHEMATICAL MODEL

by

F. D. FLOOD

CONTENTS

																								Page
																								400
INTRODUCTION	•	•	٠	٠	•	•	•	•	•	•	•	•	•	•	٠	•	•	•	•	•	•	٠	•	192
MAIN WING BOX	•	•									•	•	•	•	•		•			•				192
WING TIP	•								•	•				•		•	•	•	•					193
WING MOUNTED FIN		•		•		•		•	•		•								•	•				193
LEADING AND TRAILING EDGES							•	•	•			•		•		•								194
FUSELAGE						•	•			•				•	•					•				194
STRENGTH RESIZING	•	•					•			•	•		•					•			•		•	195
PANEL STABILITY EVALUATION	•				•	•						•		•		•		•	•	•	•			197
REFERENCES																								198

TABLES

No.								Page
7-1	Material Designations and Number of Plies/Lamina to Initiate Model	Pr	eli	mi	na	ry		
	Sizing							199
7-2	Comparison of Titanium and Composite Fuselage, Station 1180.25							200
7-3	Comparison of Titanium and Composite Fuselage, Station 1775.26							201
7-4	Comparison of Titanium and Composite Fuselage, Station 2160.26							202
7-5	Comparison of Titanium and Composite Fuselage, Station 2930.26							203
7-6	Comparison of Titanium and Composite Fuselage, Station 3070.24							204
7-7	Summary, Comparison of Metal and Composite Fuselage Structure							205
7-8	Fuselage Stiffness Ratios							

FIGURES

No.		Page
7-1	Zones Used for Resize	208
7-2	Fuselage Stiffness Factor Distribution	209
7-3	Average Stiffness Factors	210
7-4	Sizing of Elements, First Strength Resize	211
7-5	Sizing of Elements, Second Strength Resize	225
7-6	Sizing of Elements, Third Strength Resize	239
7-7	Theoretical Wing Weight, Wing Box Primary Structure, ATLAS Resizing	253
7-8	Upper Surface Panels Checked for Stability After Resize Cycle 1	254
7-9	Lower Surface Panels Checked for Stability After Resize Cycle 1	255
7-10	Layup Changes Required for Stability After Resize Cycle 1 (Upper Surface)	256
7-11	Layup Changes Required for Stability After Resize Cycle 1 (Lower Surface)	257
7-12	Upper Surface Panel Stability Checks After Resize Cycle 2	
7-13	Lower Surface Panel Stability Checks After Resize Cycle 2	259

SYMBOLS

E	Modulus of elasticity
G	Modulus of rigidity (shear)
H/C	Honeycomb
K	Stiffness factor
t	Thickness
\overline{t}	Equivalent thickness
μ	Poisson ratio
ρ	Density
$V_{\mathbf{A}}$	Design maneuvering speed
$V_{\mathbf{f}}$	Design speed for deflected flaps

INTRODUCTION

The mathematical model used as the basis for the design of composite wing panels is the mathematical model resulting from the Task I and II configuration and analysis cycles, from reference 7-2. This original airframe concept consisted of all-titanium structure and was developed from the many trade studies and the experience accumulated during the National SST Program and the ensuing DOT funded follow-on program. The internal arrangement is based on the structure designed for the SCAT-15 configuration (ref. 7-2), with the member sizes based on allowables that reflect a current assessment of the available titanium technology.

The definition of the nodes used in the structural mathematical model was unchanged. The wing cover panels were revised to allow analysis and automated resize of advanced composite materials. The initial definition of the cover panels was estimated based on the loads from the reference 7-1 stress analysis. This initial sizing served to minimize the number of iterations necessary for convergence. The titanium internal structure of the wing was left unchanged because of the lack of sufficient budget to convert it to composite material.

Other structure such as the fuselage, empennage, and wing leading and trailing edges was sized by hand for the composite materials. These components were not resized in the subsequent analysis, but were modified to provide the elastic characteristics of a composite structure in terms of the stiffness and vibration modes. The following paragraphs describe in greater detail the revision of the components of the analytical model.

MAIN WING BOX

The cover panels of the main wing box were replaced using sandwich panels made up of graphite/polyimide composite surfaces and honeycomb core. The materials and the associated elastic and mechanical properties are described in Sections 1 and 2. Because of budget limitations, the internal structure consisting of titanium spars and ribs has not been replaced with composite structure. It has been assumed that the surfaces of the sandwich panels are laid up in a balanced symmetrical array of laminae to avoid the problems of anisotropic behavior during manufacture and under load. This results in somewhat conservative panel design as will be seen later.

The titanium panels were first replaced with representative composite panels having the approximate number of laminae necessary to carry the expected loads. A stress analysis was then performed on the finite element model and the panels resized for zero margin of safety at ultimate load, using the ATLAS composite design module.

The wing surface panels of the main wing box were divided into 16 zones for input for preliminary sizing. Each zone was picked to provide a number of panels that have similar layups and which would be subject to spanwise, chordwise and shear load components of similar proportions or which would be critical for constraint conditions such as minimum gage. These zones are shown in figure 7-1. Although zones 10 and 11 on the wing tip are in a region of minimum gage for strength, these zones

will be used for resizing this area for flutter purposes. As shown in the table 7-1, each zone has a ply orientation specified for the inner and outer skins of the upper and lower surface panels for the initial input. These layups were estimated based on the loads on the panels resulting from the reference 7-1 analysis, and were felt to be reasonable estimates of the panel thicknesses and orientation necessary to carry the loads. Also shown in the table is the material designator assigned to the laminae in each zone:

Minimum gage for the wing surfaces as defined in Section 3 are:

	Upper Surface	Lower Surface
	in.	in.
Inner Skin	.016	.016
Outer Skin	.024	.032

The ATLAS design module resizes the panels based only on the allowable material properties since there is no buckling analysis presently included. For this reason, the materials called out for the upper surface are separate from those called out for the lower surface, in order to permit the use of variations in the allowables to provide for the buckling requirement. The sizing of the panels that result from the resizing will be checked manually to determine if the panels are critical for buckling and if so, the allowables will be reduced appropriately to provide for that case.

In each zone, there is an individual material available for the 0°, ±45° and 90° laminae to permit selective stiffening for flutter.

WING TIP

The wing tip surface panels are replaced with composite sandwich covers as shown in table 7-1 (zones 10 and 11). The initial thickness was based on the loads in the tip skins, and this represents an estimate of strength requirements, although this area will likely be designed for stiffness due to flutter requirements. The initial sizing is based on the high strength graphite fiber.

As noted above, the wing tip is divided into two zones for the purpose of resizing. Zone 10 extends from the fin to the wing tip and includes the covers of the main wing box, and Zone 11 the region aft of the rear spar to the hinge line as shown in figure 7-1. The material designations are as shown in table 7-1. Each of the laminae $(0^{\circ}, \pm 45^{\circ})$ and (0°) are identified separately so that the type of fibers, lamina thickness, or strength of the individual lamina can be changed separately.

WING MOUNTED FIN

The structure of the wing mounted fin was not changed in this analysis except to substitute the equivalent properties of an equivalent quasi-isotropic layup of high strength fibers. Should it be necessary to stiffen the fin for flutter purposes, it may be more efficient to switch to fibers having a higher modulus and a lower strength.

LEADING AND TRAILING EDGES

The leading and trailing edge surfaces are modeled for graphite/polyimide sandwich construction. Since design loads are not available for these surfaces, the advanced composite surfaces will be designed to have the same inplane stiffnesses as the final reference 7-1 titanium structure. The majority of the leading edge panels will be miminum gage. The minimum gage areas are made of $[0/\pm45/90]$ which results in the following equivalent mechanical properties:

$$E_x = E_y = 7.635 \times 10^6 \text{ lbs/in}^2$$
 $G = 2.926 \times 10^6 \text{ lbs/in}^2$
 $\mu_X = \mu_y = .304$
 $\rho = .056 \text{ lbs/in}^3$

The panel sizes for the leading and trailing edges are based on keeping the Et's the same, i.e.,

Et
$$T_i = Et_{P/I}$$

Maintaining this ratio will result in surfaces having about 1.5 times the compressive strength and twice the shear strength as the titanium surfaces.

FUSELAGE

The fuselage for this analysis is based on the titanium fuselage from reference 7-1. This fuselage will be unchanged in-so-far as the internal arrangement is concerned, since the main purpose of modifying the fuselage is to provide the equivalent of a composite fuselage in its dynamic response in the vibration modes. It was also necessary that the strain under static load conditions be properly simulated in the regions where the wing and body share loads. The stringers and beams in the fuselage included area for the effective skin and the lumped stringers. Alternate frames were modeled with the equivalent area for two frames with effective skin, since the frame spacing in the model is 35 in. as compared to 17.5 in. in the airplane. Skins are idealized as "S" plates carrying shear, only.

The section properties of the titanium elements are not altered from those used on the Task II analysis. The change in stiffness was accounted for by altering the elastic properties in the material tables. This was the most economical way to make the appropriate changes in the fuselage elements.

Tables 7-2 through 7-6 present the comparison of the titanium and the composite skin gages, stringer areas and spacings, the appropriate effective moduli, and the t's for five stations along the fuselage. These results are summarized on table 7-7.

One of the basic considerations in modifying the fuselage skins for composite is the change in the structural concept and the effect that this has on the stiffness distribution around the cross section of the fuselage. The skin-stringer fuselage is generally designed by tension in the crown and by compression in the belly, resulting in fully effective skin panels for the compression in the belly, thereby lowering the effective stiffness. A typical comparison of the ratio of the Et in the crown and the belly for skin-stringer and sandwich is presented in table 7-8.

Another aspect of this consideration is the variation of the crown and belly stiffness distribution as a function of load factor. Because of the effect of buckling, as the load factor increases, the compression side of the skin-stringer fuselage becomes less effective. Generally the criteria for the National SST Prototype provided for no skin buckling up to a load factor of 1.1 for aerodynamic reasons. The sandwich panels, on the other hand, are sized for no buckling up to ultimate load, and therefore will be affected little if any by variations in load factor.

Based on these considerations, it is concluded that the stiffness characteristics of the skin-stringer fuselage is representative of the airplane in unaccelerated flight, but are somewhat high for load factor approaching limit load factor. On the other hand, the stiffness characteristics of the fuselage with sandwich panels is probably representative at all load factors up to limit.

Based on the analysis described earlier, factors are derived that account for the ratio between the modulus of elasticity of titanium and that necessary to maintain the same Et for the composite fuse-lage. These K factors are shown in table 7-7, and are presented in figure 7-2. Upon review of these factors and the associated labor and time involved in modifying the input for the mathematical model, it was decided to use a constant factor along the fuselage for these factors as shown in figure 7-3.

STRENGTH RESIZING

The strength resizing was performed considering mechanical loads only. The version of ATLAS that had been checked out for use on the large Arrow Wing mathematical model did not have the thermal loads capability. A significant schedule delay and an undetermined cost for unsuccessful runs would have been incurred had the thermal effects been included in the structural resizing.

Because of the difference in the coefficients of thermal expansion, temperature changes due to environmental conditions and aerodynamic heating will induce stresses in the skins, spar caps and splice plates. Since the critical flight conditions for structural loads are subsonic and transonic, the thermally induced stresses are relatively small compared to the stresses due to airloads. It should be noted, however, that the temperatures due to aerodynamic heating at cruise Mach number will induce local stresses of the order of 20 000 lb/in² and would need to be considered in the detail design of the spar caps and splice plates for a mixed titanium composite structure such as is being considered in this study.

During the strength resizing, some of the variables were constrained to be equal. These equality constraints followed from a prior assumption that each face sheet should be a balanced, symmetric laminate. To be balanced signifies that there is an equal number of +45°- and -45°-plies. To be symmetric implies that commonly oriented plies on opposite sides of the laminate symmetry plane are of equal number. Thus, the +45°-laminae were constrained to be equal in number to the -45°-laminae and each lamina on a given side of the laminate symmetry plane was constrained to be equal to the corresponding lamina on the opposite side of the symmetry plane. Further, with only mechanical loads being considered and with the finite element being used having only inplane (membrane) load-carrying capability, corresponding plies in the inner and outer face sheets of each panel were also constrained to be equal. Although internal pressures act on the wing panels, they are not significant when considered in conjunction with airloads and inertia loads.

For the first strength resize, it was considered technically feasible and financially advantageous to solve each wing panel (upper or lower CPLATE of a CCOVER element) as an individual problem. This certainly results in the most accurate theoretical weight result possible. It does not address the problem of practical layups from a manufacturing viewpoint but rather indicates the target theoretical weight of such a practical layup. The decision to resize each panel resulted in 750 optimization problems to be solved during the first resize. That this was accomplished for about 2/3 of the cost of the preceding stress analysis indicates the efficiency of the ATLAS composite design module. After the first strength resize, it was apparent that the entire strake area (wing forward of wheel well) was minimum gage. This region was excluded from resizing for the second resize.

The detailed results of the first resize are shown in figure 7-4. The zones identified in figure 7-4 correspond to those shown in figure 7-1. All of the final trends of the strength resize are evident in the first resize. This sometimes occurs with an extremely large change in the sizing from that originally specified. This indicates that the original sizing can be considerably different than the final with little effect. The detailed results of the second resize are shown in figure 7-5. For both the first and second resize, the lower bound constraint was solely that at least one layer (ply) must exist in each of the lamina orientations for the $[0/\pm45/90]$ layup. This lower bound approach was used since the ATLAS lower bound capability was such that lower bounds were imposed after the optimization problem was solved. The lower bounds for the third resize were determined manually since a decision had to be made between identical inner and outer face sheets or face sheets having similar layups with thicknesses in the proportion of the face sheet minimum gages. The decision was based on the lighter weight. Once the minimum gage layups were established, the finite element model was updated using the ATLAS composite design module. The above minimum gage determination for the total laminate is a development capability that should be accomplished in the future.

It is apparent from a review of figures 7-4, 7-5 and 7-6 that the regions outboard and forward of the wheel well and outboard of the wing-mounted fin are sized by the minimum gage constraints. With the exception of the lower surface just inboard of the outboard engine beams, the panels adjacent to the rear spar are predominantly unidirectional laminates oriented parallel to the rear spar. Along the side-of-body on the wing lower surface, the body bending induces chordwise loads that peak inboard of the wheel well where up to six chordwise plies are required. The largest strength requirement for ±45° laminae occurs six spars forward of the rear spar midway between the engine beams on the upper surface. Note that the corresponding lower panel does not require these ±45° plies. It is also worth noting the relative sizing of these latter lower surface panels and those located immediately aft. These panels were input in two different zones and had different original sizing occurring as a step function across the zone boundary. With two resizes, the relative sizing appears more disparate than the initial sizing. This leads to the conclusion that a preferred approach would be to input a uniform sizing (uniformly varying would require too much input) over the entire wing and let the ATLAS composite design module determine the varying sizing requirements. This approach should result in a more realistic sizing distribution.

Figure 7-7 illustrates the relative theoretical weight for each cycle of resize. The relatively small theoretical weight increment between the first and second resize indicates that for weighing purposes, the resizing has acceptably converged. The relatively larger increment of weight added from the second to the third resize indicates that the minimum gages selected have a significant weight impact.

PANEL STABILITY EVALUATION

After each cycle of strength sizing, the resized wing panels were evaluated regarding instability failure. The Boeing-developed COOPB, Laminated Composite Analysis Program, was used for this purpose. An orthotropic plate buckling analysis for simply supported plates subjected to inplane biaxial compression and shear loads was performed. This analysis includes the effect of core shear stiffnesses.

After the first resize, panels for the stability checks were selected based on 1) the layups of the panels after the strength optimization and 2) an assessment of the loads and change of loads in that region. For example, on the wing upper surface near the rear spar and side-of-body where high spanwise compressive stresses exist, if adjacent panels were several layers different in 0° (spanwise) layers, the lighter panel was selected for a stability check. In this manner a total of 86 upper and lower surface panels were selected and checked. When a panel was found to be unstable for the design loads, additional panels in the immediate region were also evaluated. This resulted in another eighteen panels being checked. The result of this investigation was that nine panels were found which were unstable for the design loads as a consequence of insufficient stiffness. The location of these panels and the critical design load case(s) are shown in figures 7-8 and 7-9. For six of the unstable panels, sufficient stiffness to render them stable for the critical load was achieved by adding one 0.002 in.-thick layer to each of the face sheet laminates. Two 0.002 in.-thick layers per face sheet were required for the other three panels. However, further examination of these latter three panels revealed that the rounding scheme within the ATLAS composite design module for converting the lamina thicknesses from real values to an integer number of plies (layers) had produced thicknesses less than the theoretical optimum in the laminae critical for panel stability. To explain further, a theoretical lamina thickness of 0.0049 in. is sized to two 0.002 in.-thick layers since as noted previously a simple arithmetic rounding scheme is used for the real value-to-integer number conversion. The layup changes required for the unstable strength-sized upper and lower surface panels to become stable are presented in figures 7-10 and 7-11, respectively.

After the second cycle of stress analysis and strength-optimized resize, panel stability was again evaluated using the first cycle results as a guide for selecting panels for evaluation. One upper surface panel near the rear spar at the side of body lacked sufficient stiffness as strength sized to preclude instability failure. Figures 7-12 and 7-13 summarize the panel stability evaluation and results performed after the second strength resize.

The third strength resize enforced the actual minimum gage constraints on the various face sheets as opposed to the single layer minimum constraints in the first and second resize cycles. Thus, each face sheet layup had the same or increased stiffnesses which precluded the necessity for further panel stability evaluation.

REFERENCES

- 7-1 Boeing Staff: Study of Structural Design Concepts for an Arrow Wing Supersonic Transport Configuration. NASA CR 132576-1 and -2, 1976.
- 7-2 Boeing Staff: Mach 2.7 Fixed Wing SST Model 969-336C (SCAT 15F). D6A11666-1, The Boeing Company, 1969.

Table 7-1.—Material Designations and Number of Plies/Lamina to Initiate Model Preliminary Sizing

			Material designation and number of plies/lamina						
				surface		er surface			
	Zone	Lamina	Outer skin	Inner skin	Inner skin	Outer skin			
	1a, 1b	0 +45, -45 90	C07 (3) C09 (3) C11 (3)	C01 (2) C03 (2) C05 (2)	C02 (2) C04 (2) C06 (2)	C14 (4) C16 (4) C18 (4)			
	1c, 1d, 1e	0 +45, -45 90	C07 (3) C09 (3) C11 (3)	C01 (2) C03 (2) C05 (2)					
	2	0 +45, -45 90	C07 (3) C09 (3) C11 (3)	C01 (2) C03 (2) C05 (2)	C02 (2) C04 (2) C06 (4)	C14 (4) C16 (4) C18 (8)			
	3	0 +45, -45 90	C07 (3) C09 (3) C11 (3)	C01 (2) C03 (2) C05 (2)	C08 (3) C10 (3) C12 (6)	C14 (4) C16 (4) C18 (8)			
ng box	0 C07 (3)		C09 (3)	C07 (3) C09 (3) C11 (3)	C08 (3) C10 (3) C12 (3)	C14 (4) C16 (4) C18 (4)			
Main wing box	0 C13 (4) 5 +45, -45 C15 (4) 90 C17 (4)		C15 (4)	C13 (4) C15 (4) C17 (4)	C14 (4) C16 (4) C18 (4)	C14 (4) C16 (4) C18 (4)			
	6	0 +45, -45 90	C13 (12) C15 (8) C17 (8)	C13 (12) C15 (8) C17 (8)	C14 (12) C16 (8) C18 (8)	C14 (12) C16 (8) C18 (8)			
	7	0 +45, -45 90	C13 (16) C15 (4) C17 (4)	C13 (16) C15 (4) C17 (4)	C14 (16) C16 (4) C18 (4)	C14 (16) C16 (4) C18 (4)			
	8	0 +45, -45 90	C13 (16) C15 (8) C17 (8)	C13 (16) C15 (8) C17 (8)	C14 (16) C16 (8) C18 (8)	C14 (16) C16 (8) C18 (8)			
	9a, 9b,	0 +45, -45 90	C13 (20) C15 (4) C17 (4)	C13 (20) C15 (4) C17 (4)	C14 (20) C16 (4) C18 (4)	C14 (20) C16 (4) C18 (4)			
Wing tip	10	0 +45, -45 90	C19 (4) C20 (4) C21 (4)	C19 (4) C20 (4) C21 (4)	C19 (4) C20 (4) C21 (4)	C19 (4) C20 (4) C21 (4)			
Win	11	0 +45, -45 90	C22 (4) C23 (4) C24 (4)	C22 (4) C23 (4) C24 (4)	C22 (4) C23 (4) C24 (4)	C22 (4) C23 (4) C24 (4)			

Note: Parenthesized values are the number of 0.002-in. plies per lamina.

Table 7-2.—Comparison of Titanium and Composite Fuselage, Station 1180.25

Titanium (ref. resize following first analysis)	Advanced composite honeycomb
Crown Skin gage = 0.030 in. Stringer area = 0.1176 in. ² (including padup) Stringer spacing = 5.4 in. $\bar{t} = 0.0518 \text{ in}^2/\text{in}$.	Crown $[0_{2}/\pm 45/90]_{S}$ 4 mil each skin $\bar{\tau} = 0.080 \text{ in}^{2}/\text{in}.$ $E_{axial} = 9.26 \times 10^{6} \text{ lb/in}^{2}$ $E_{circular} = 5.48 \times 10^{6} \text{ lb/in}^{2}$ $G = 2.91 \times 10^{6} \text{ lb/in}^{2}$
Side Skin gage = 0.030 in. Stringer area = 0.1176 in ² Stringer spacing = 5.0 in. $\bar{t} = 0.0535 \text{ in}^2/\text{in}.$	Side $[0/\pm 45/90]_{S}$ 4 mil each skin $\bar{t} = 0.064 \text{ in}^{2}/\text{in}.$ $E_{axial} = E_{circular} = 6.57 \times 10^{6} \text{lb/in}^{2}$ $G = 2.91 \times 10^{6} \text{lb/in}^{2}$
Belly Skin gage = 0.034 in. Stringer area = 0.265 in ² Stringer spacing = 5.4 in. $\bar{t} = 0.083$ in ² /in.	Belly Same as crown
B/C = 1.602	B/C = 1.0

Table 7-3.—Comparison of Titanium and Composite Fuselage, Station 1775.26

Titanium (ref. resize following first analysis)	Advanced composite honeycomb
Crown Skin gage = 0.035 in. Stringer area = 0.17 in ² Stringer spacing = 5.0 in. $\bar{t} = 0.069 \text{ in}^2/\text{in}$.	Crown $[0_{3}/\pm 45/90]_{S}$ 4 mil each skin $\bar{t} = 0.096 \text{ in}^{2}/\text{in}.$ $E_{axial} = 11.05 \times 10^{6} \text{ lb/in}^{2}$ $E_{circular} = 4.76 \times 10^{6} \text{ lb/in}^{2}$ $G = 2.18 \times 10^{6} \text{ lb/in}^{2}$
Side Skin gage = 0.030 in. Stringer area = 0.1176 in ² Stringer spacing = 5.0 in. $\bar{t} = 0.0535 \text{ in}^2/\text{in}$.	Side $[0/\pm 45/90]_S$ 4 mil each skin $\bar{t} = 0.064 \text{ in}^2/\text{in}$. $E_{\text{axial}} = E_{\text{circula}} = 6.57 \times 10^6 \text{ lb/in}^2$ $G = 2.91 \times 10^6 \text{ lb/in}^2$
Belly Skin gage = 0.050 in. Stringer area = 0.46 in ² Stringer spacing = 4.4 in. $\bar{t} = 0.155 \text{ in}^2/\text{in}$.	Belly Same as crown
B/C = 2.246	B/C = 1.0

Table 7-4.—Comparison of Titanium and Composite Fuselage, Station 2160.26

Titanium (ref. resize following first analysis)	Advanced composite honeycomb
Crown Skin gage - 0.048 in. Stringer area = 0.34 in ² Stringer spacing = 4.7 in. $\bar{t} = 0.12 \text{ in}^2/\text{in}$.	Crown $[0_4/\pm 45/90]_S$ 4 mil each skin $\bar{t} = 0.112 \text{ in}^2/\text{in}.$ $E_{axial} = 12.33 \times 10^6 \text{ lb/in}.^2$ $E_{circular} = 4.24 \times 10^6 \text{ lb/in}.^2$ $G = 1.97 \times 10^6 \text{ lb/in}.^2$
Side Skin gage = 0.035 in. Stringer area = 0.14 in ² Stringer spacing = 5.0 in. $\bar{t} = 0.063 \text{ in}^2/\text{in}$.	Side $[0/\pm 45/90]_S$ 4 mil each skin $\bar{t} = 0.064 \text{ in}^2/\text{in}$. $E_{axial} = E_{circular} = 6.57 \times 10^6 \text{ lb/in}^2$ $G = 2.91 \times 10^6 \text{ lb/in}^2$
Belly Skin gage = 0.070 in. Stringer area = 0.56 in ² Stringer spacing = 4.4 in. $\bar{t} = 0.197 \text{ in}^2/\text{in}$.	Belly $[0_5/\pm 45/90]_S$ $\bar{t} = 0.128 \text{ in}^2/\text{in}.$ $E_{axial} = 13.29 \times 10^6 \text{lb/in}^2$ $E_{circular} = 3.85 \times 10^6 \text{lb/in}^2$ $G = 1.813 \times 10^6 \text{lb/in}^2$
B/C = 1.64	B/C = 1.142

Table 7-5.—Comparison of Titanium and Composite Fuselage, Station 2930.26

Titanium (ref. resize following first analysis)	Advanced composite honeycomb		
Crown Skin gage = 0.066 in. Stringer area = 0.53 in ² Stringer spacing = 4.4 in. $\bar{t} = 0.186 \text{ in}^2/\text{in}$. Side of body Skin gage = 0.066 in. $\bar{t}_{axial} = 0.099 \text{ in}^2/\text{in}$.	Crown $[0_8/\pm 45/90]_S$ 4 mil each skin $\bar{t} = 0.176 \text{ in}^2/\text{in}.$ $E_{axial} = 15.12 \times 10^6 \text{lb/ft}^2$ Side of body Assume: K_G same as side $K_E \text{ same as belly}$		
Side Skin gage = 0.066 in. Stringer area = 0.45 in ² Stringer spacing = 5.0 in. $\bar{t} = 0.156 \text{ in}^2/\text{in}$.	Side $[0_4/\pm 45_2/90]_S$ 4 mil each skin $\bar{t} = .144 \text{ in}^2/\text{in}$ $E = 10.16 \times 10^6 \text{lb/in}^2$ $G = 2.67 \times 10^6 \text{lb/in}^2$		
Belly Skin gage = 0.10 in. Stringer area = 0.62 in ² Stringer spacing = 4.6 in. $\bar{t}_{axial} = 0.235 \text{ in}^2/\text{in.}$ $\bar{t}_{spanwise} = 0.130 \text{ in}^2/\text{in.}$	Belly $[0_7/\pm 45/90_4]$ S $\bar{t} = 0.208 \text{ in}^2/\text{in}$. $E_{axial} = 11.911 \times 10^6 \text{lb/in}^2$ $E_{spanwise} = 7.159 \times 10^6 \text{lb/in}^2$		
B _{axial} /C = 1.263	B _{axial} /C = 1.182		

Table 7-6.—Comparison of Titanium and Composite Fuselage, Station 3070.24

Titanium (ref. resize following first analysis)	Advanced composite honeycomb
Crown Skin gage = 0.60 in. Stringer area = 0.44 in ² Stringer spacing = 4.4 in. $\bar{t} = 0.16 \text{ in}^2/\text{in}$. Side of body Skin gage = 0.06 in. $\bar{t} = 0.09 \text{ in}^2/\text{in}$.	Crown $[0_{6}/\pm \ 45/90]_{S}$ 4 mil each skin $\bar{t} = 0.144 \text{ in}^{2}/\text{in}.$ $E_{axial} = 14.03 \times 10^{6} \text{lb/in}^{2}$ $E_{circular} = 3.55 \times 10^{6} \text{lb/in}^{2}$
Side Skin gage = 0.06 in. Stringer area = 0.43 in ² Stringer spacing = 5.0 in. $\bar{\tau} = 0.146 \text{ in}^2/\text{in}$.	Side $[0_5/\pm 45/90]_S$ 4 mil each skin $\bar{t} = 0.16 \text{ in}^2/\text{in}$. $E_{axial} = 11.145 \times 10^6 \text{lb/in}^2$ $G = 2.4702 \times 10^6 \text{lb/in}^2$
Belly Skin gage = 0.10 in. Stringer area = 0.60 in ² Stringer spacing = 4.6 in. $\bar{t} = 0.23 \text{ in}^2/\text{in}$.	Belly Same as crown
B/C = 1.44	B/C = 1.0

Table 7-7.—Summary, Comparison of Metal and Composite Fuselage Structure

Crown

	Titanium		EŧH/C	Advanced composite H/C			
Station	t	E	Εī	EtTi	ŧ	E _{axial}	Ετ
1180.25	0.0518	16.4	0.8495	0.872	0.080	9.26	0.7408
1775.26	0.069	16.4	1.1316	0.937	0.096	11.05	1.0608
2160.26	0.120	16.4	1.9680	0.702	0.112	12.33	1.3810
2930.26	0.186	16.4	3.0504	0.872	0.176	15.12	2.6610
3070.24	0.160	16.4	2.6240	0.770	0.144	14.03	2.0200

Belly

Station		Titanium		Et _{H/C}	Advanced composite H/C		
Station	ŧ	E	Eŧ	EtTi	ŧ	E _{axial}	Ε τ
1180.25	0.083	16.4	1.3612	0.544	0.080	9.26	0.7408
1775.26	0.155	16.4	2.5420	0.417	0.096	11.05	1.0608
2160.26	0.197	16.4	3.2310	0.526	0.128	13.29	1.7011
2930.26	0.235	16.4	3.8540	0.643	0.208	11.91	2.4772
3070,24	0.230	16.4	3.7720	0.536	0.144	14.03	2.0200

Axial Stiffness

Station	K _{crown}	K _{belly}	K _{avg}
1180.25	0.872	0.544	0.708
1775.26	0.937	0.417	0.677
2160.26	0.702	0.526	0.614
2930.26	0.872	0.643	0.758
3070.24	0.770	0.536	0.653
	avg = 0.8306	avg = 0.5332	avg = 0.682

Table 7-7.—(Concluded)

Side Axial Stiffness

Station	Titanium			K _{axial}	Advanced composite H/C		
Cution	ŧ	E	Eŧ	side	ŧ	E _{axial}	Et
1180.25	0.0535	16.4	0.8774	0.4792	0.064	6.570	0.4205
1775.26	0.0535	16.4	0.8774	0.4792	0.064	6.570	0.4205
2160.26	0.0630	16.4	1.0332	0.4070	0.064	6.570	0.4205
2930.26	0.1560	16.4	2.5584	0.5719	0.114	10.160	1.4632
3070.24	0.1460	16.4	2.3944	0.7440	0.160	11.145	1.7832

Side Shear Stiffness

Station	t	G	Gt	K _{Gside}	t = t	G	Gt
1180.25	0.030	6.2	0.1860	1.0013	0.064	2.91	0.18624
1775.26	0.030	6.2	0.1860	1.0013	0.064	2.91	0.18624
2160.26	0.035	6.2	0.2170	0.8582	0.064	2.91	0.18624
2930.26	0.066	6.2	0.4092	0.9396	0.144	2.67	0.38448
3070.24	0.060	6.2	0.3720	1.0620	0.160	2.47	0.39520

Table 7-8.—Fuselage Stiffness Ratios

Station	Et _{crown}	E _{tbelly}	Et _{belly}
1180.25	0.8495	1.3612	1.602
1775.26	1.1316	2.5420	2.246
2160.26	1.9680	3.2310	1.642
2930.26	3.0504	3.8540	1.263
3070.24	2.6240	3.7720	1.438
			avg = 1.638

Etbelly E_{tbelly} Et_{crown} Et_{crown} Station 0.7408 1.000 1180.25 0.7408 1775.26 1.0608 1.0608 1.000 2160.26 1.3810 1.7011 1.233 2930.26 0.931 2.6610 2.4772 3070.24 1.000 2,0200 2.0200 avg = 1.033

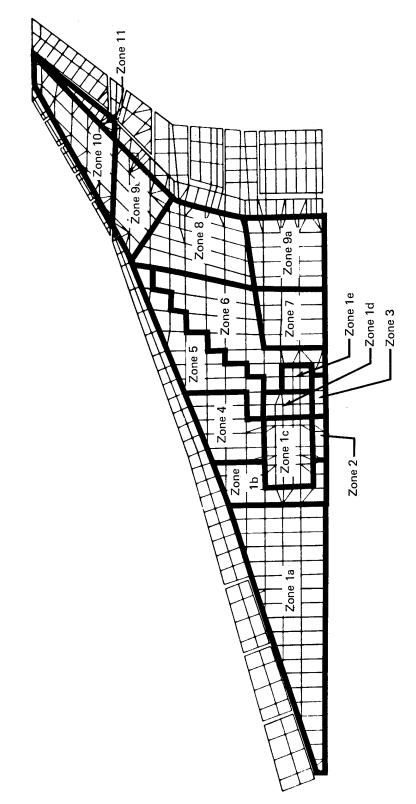


Figure 7-1.—Zones Used for Resize

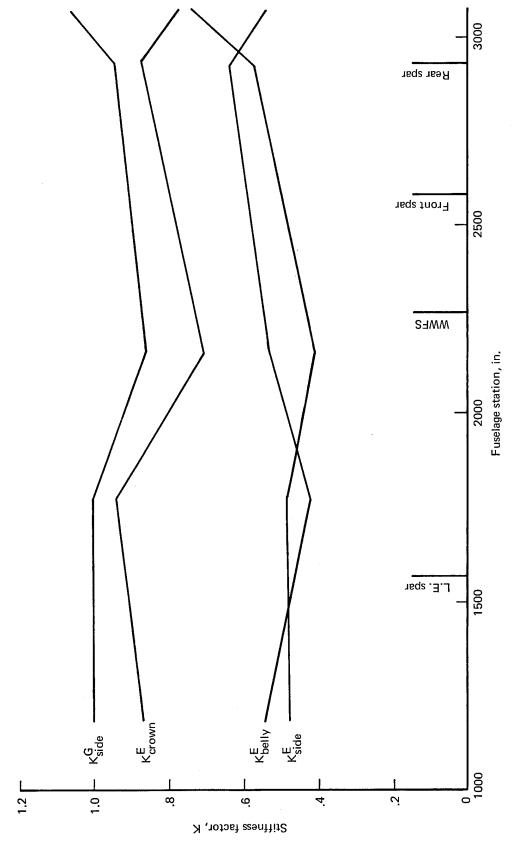


Figure 7-2.—Fuselage Stiffness Factor Distribution

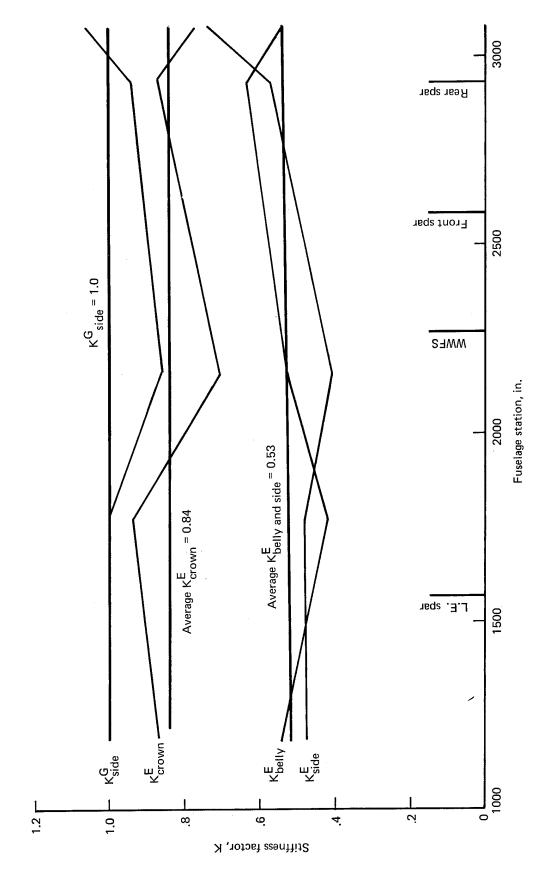


Figure 7-3.—Average Stiffness Factors

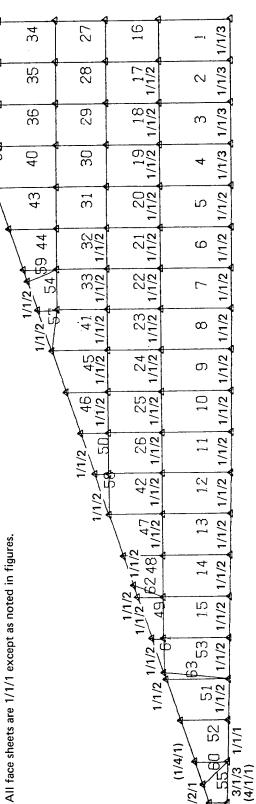
Sizing values i/j/k define the subscripts in the standard laminate code for a $[0; \pm 45; 90_k]$ | laminate parentheses. If a single set of sizing values is shown for either an upper or lower panel, it applies equally to the sandwich inner and outer face sheets. Otherwise, the two sets of values are shown composed of 0.002-in.-thick plies. The lower (upper) panel sizing is shown without (within) within a brace with the thinner laminate being the inner face sheet. NOTE:

37

38

39

'n



Zone 1a

Figure 7-4.—Sizing of Elements, First Strength Resize

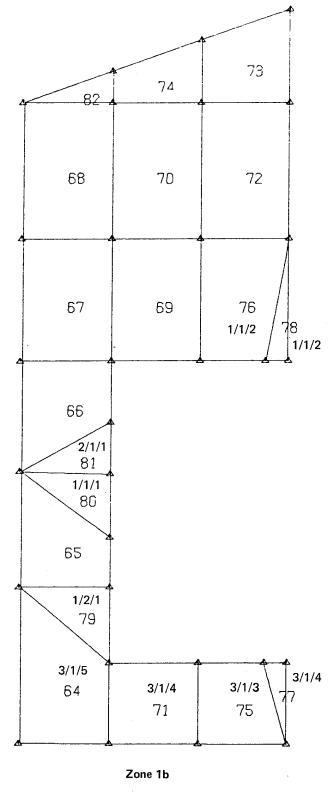


Figure 7-4.—(Continued)

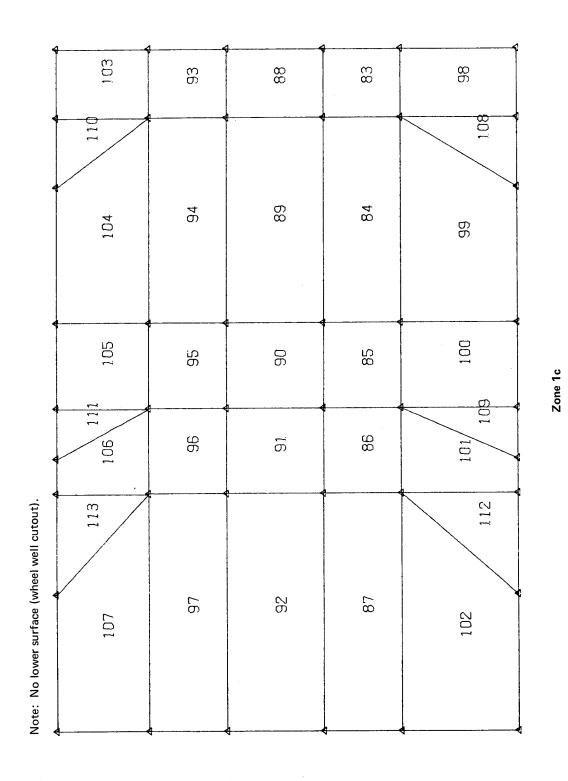


Figure 7-4.—(Continued)

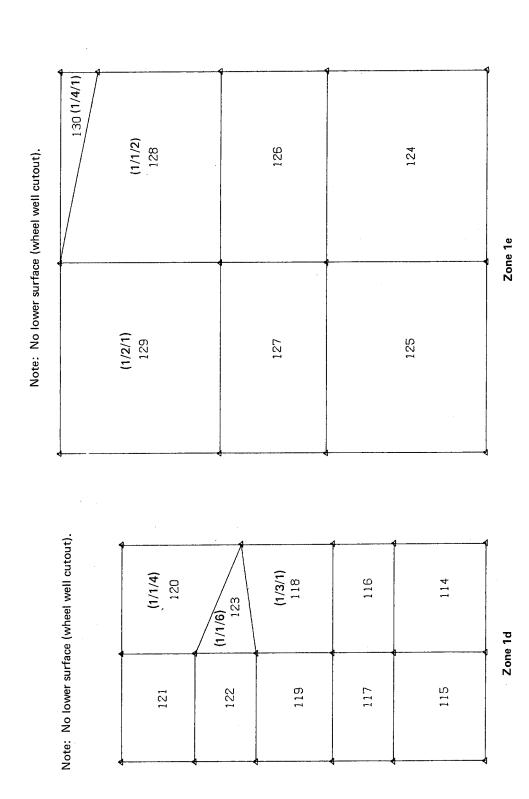


Figure 7-4.—(Continued)

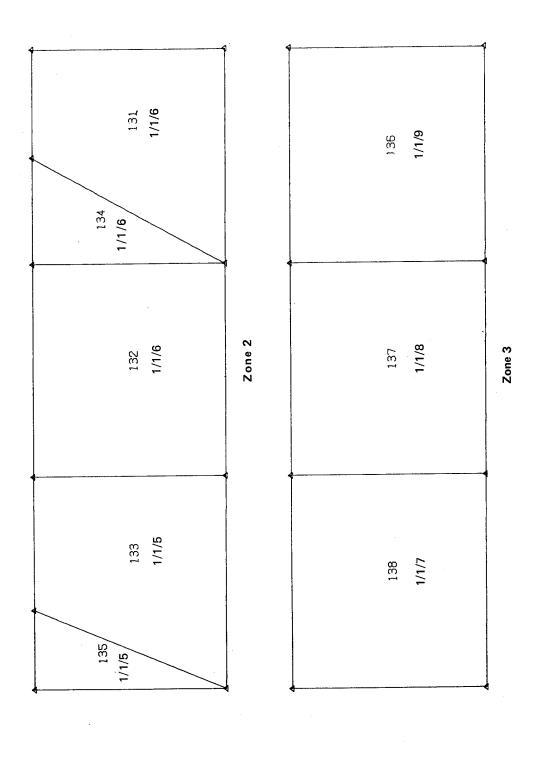


Figure 7-4.—(Continued)

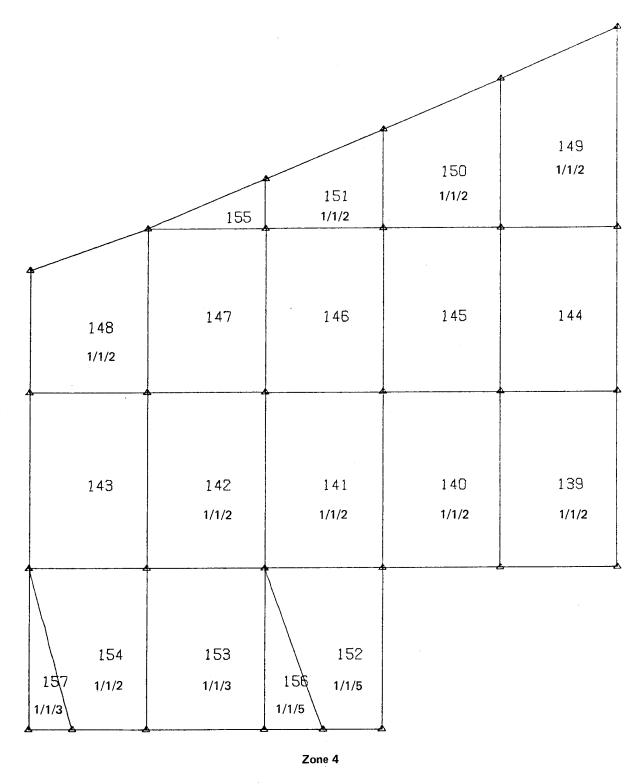
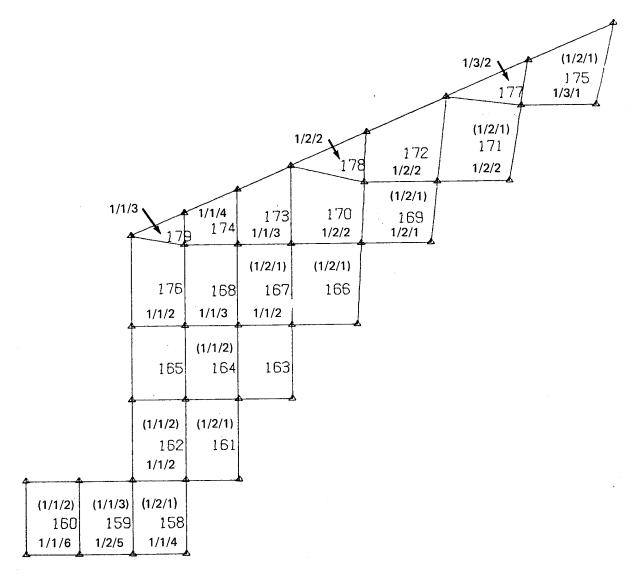
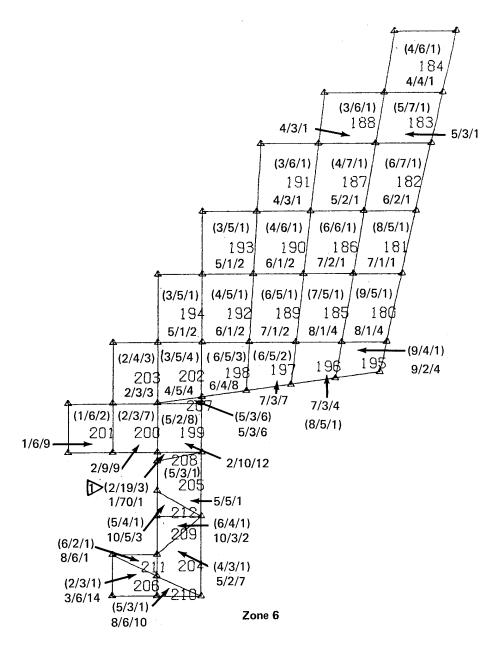


Figure 7-4.—(Continued)



Zone 5

Figure 7-4.—(Continued)



Element 208 sizing modified to $\frac{(5/4/4)}{6/8/5}$ prior to second cycle analysis.

Figure 7-4.—(Continued)

7/4/7 228 (8/2/4)	(6/3/1) 5/5/3 227	(7/3/1) 226 6/3/3	(8/3/1) 225 6/3/2
11411 228			
(6/3/1)	(6/3/1)	(7/3/1)	(8/3/1)
224	223	222	221
10/2/8	8/3/7	7/2/5	7/1/4
(6/3/1)	(6/3/1)	(7/3/1)	(8/3/1)
220	219	218	217
4/32/4 🄀	5/4/5	2/2/54	7/1/5
(5/3/1)	(6/3/1)	(7/3/1)	(8/3/1)
216	215	214	213
6/2/4	7/2/3	7/1/5	7/1/5

Element 220 lower surface sizing modified to 5/7/2 (based on COOPB analysis) prior to second cycle analysis.

Figure 7-4.—(Continued)

Element 218 lower surface sizing modified to 7/1/5 (based on COOPB analysis) prior to second cycle analysis.

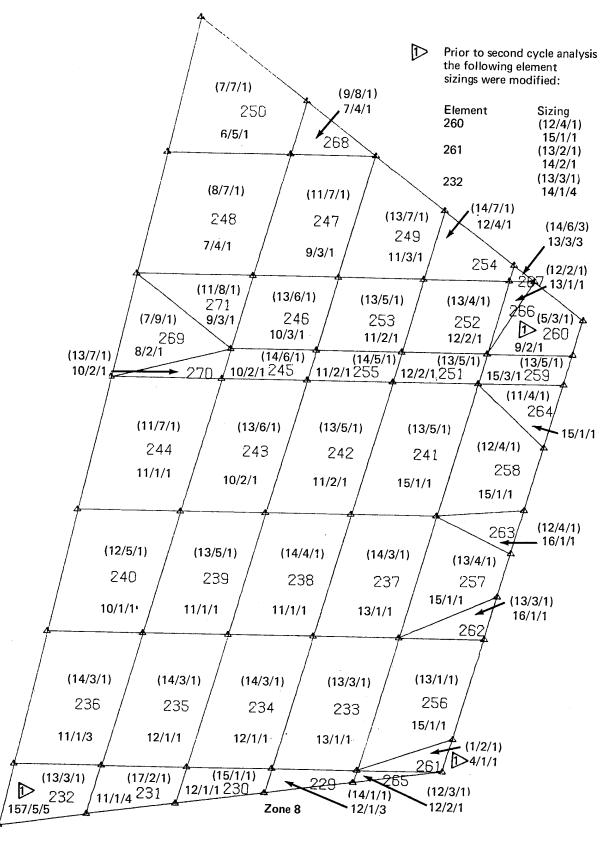


Figure 7-4.—(Continued)

(11/3/1)	(12/3/1) 286	(12/3/1) 285	(13/2/1) 284	(1/1/1) 4/1/1 (12/2/1) 291 13/1/1
287 9/2/1		11/1/1	12/1/1	(15/3/1) 15/1/1 299
				14/1/1
(11/3/1)	(12/3/1)	(13/2/1)	(14/2/1)	(14/3/1
283	282	281	280	290
9/1/3	10/1/2	11/1/1	11/1/1	(15/2/1) 14/2/1 297
				(15/1/1) 296 13/2/1
(12/2/1)	(13/2/1)	(13/2/1)	(14/1/1)	(15/1/
279	278	277	276	289
9/1/3	10/1/3	11/1/1	12/1/1	(15/1/1) 14/2/1 295
				(15/1/1) 14/2/1
(11/2/1)	(13/2/1)	(13/2/1)	(14/2/1)	(15/1/
275	274	273	272	288
9/1/5	9/2/4	10/2/4	12/1/4 (12/3/1 17/2/2	15/1/1

Figure 7-4.—(Continued)

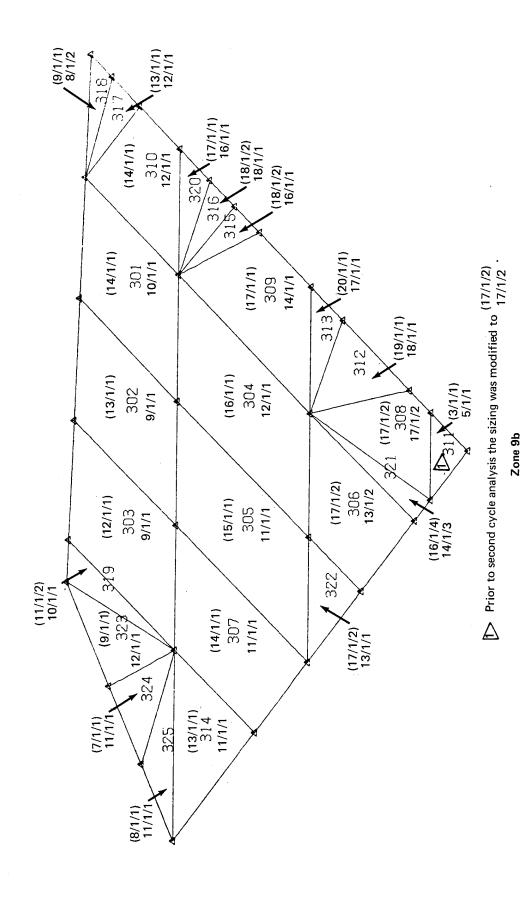


Figure 7-4.—(Continued)

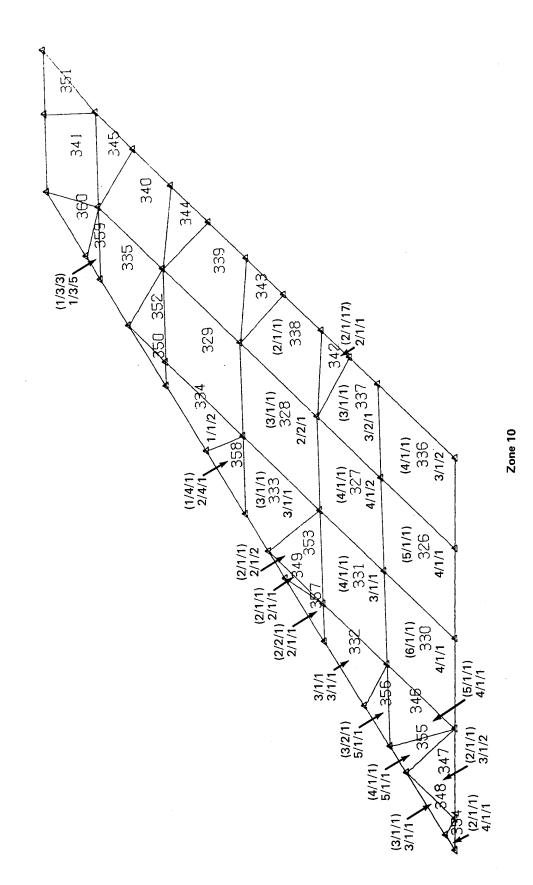


Figure 7-4.—(Continued)

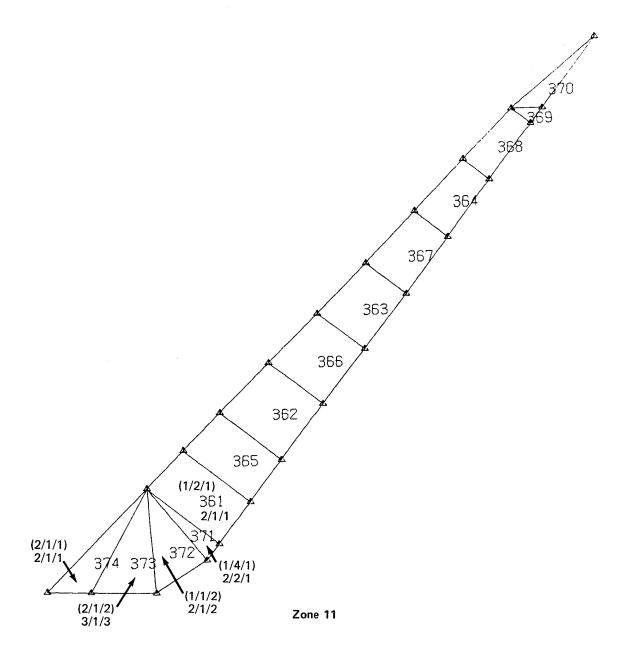


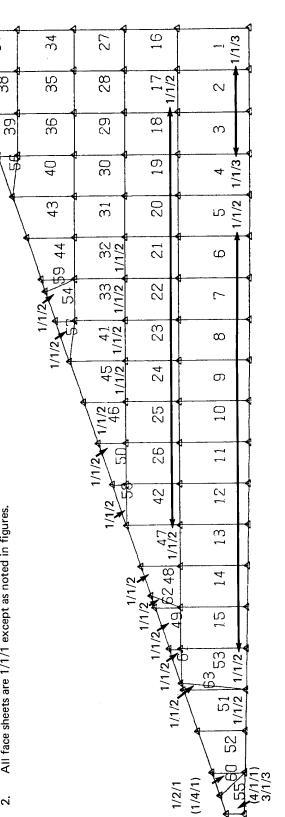
Figure 7-4.—(Concluded)

Note:

- Sizing values i/j/k define the subscripts in the standard laminate code for a $[0_i/45_i/90_k]_T$ laminate composed of 0.002 in, thick plies. The lower (upper) panel sizing is shown without (within) parentheses. If a single set of sizing values is shown for either an upper or lower panel, it applies equally to the sandwich inner and outer face sheets. Otherwise, the two sets of values are shown within a brace with the thinner laminate being the inner face
- All face sheets are 1/1/1 except as noted in figures. 2

37

38



Subsection E101 was restrained from resizing in this (2nd) resize.

Zone 1a

Figure 7-5.—Sizing of Elements, Second Strength Resize

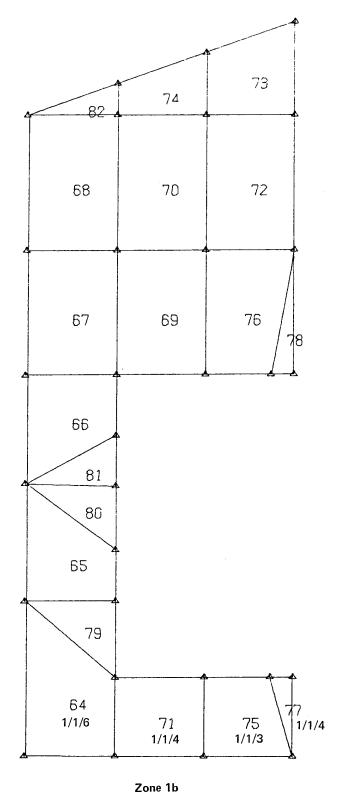
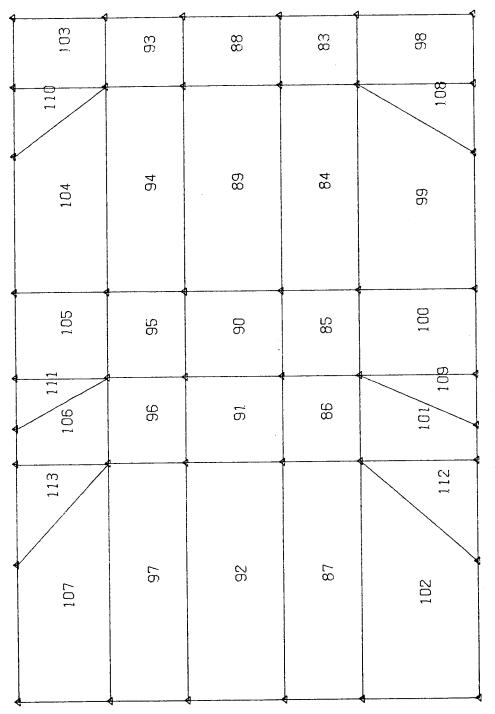


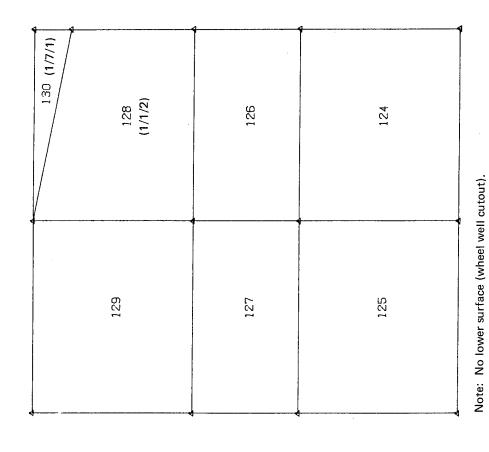
Figure 7-5.—(Continued)



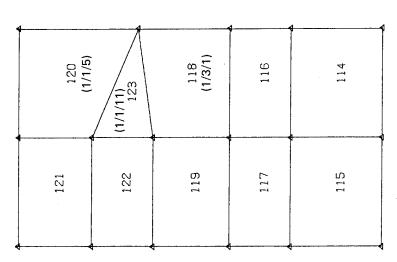
Note: No lower surface (wheel well cutout).

Zone 1c

Figure 7-5.—(Continued)



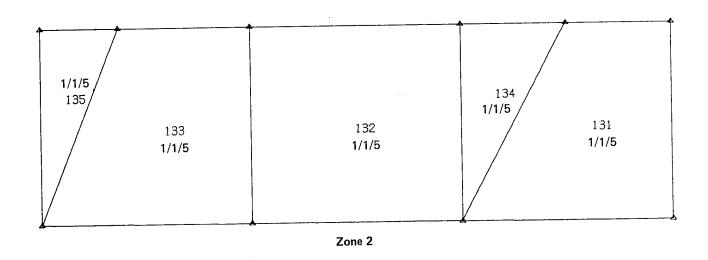
Zone 1e



Note: No lower surface (wheel well cutout).

Zone 1d

Figure 7-5.—(Continued)



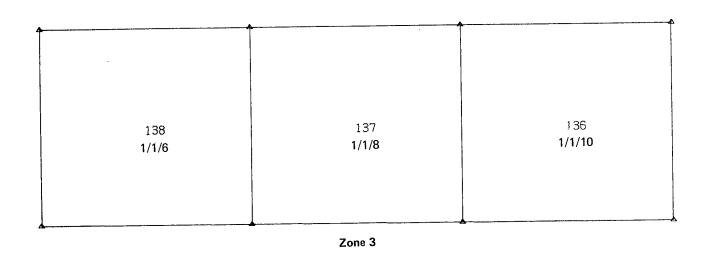


Figure 7-5.—(Continued)

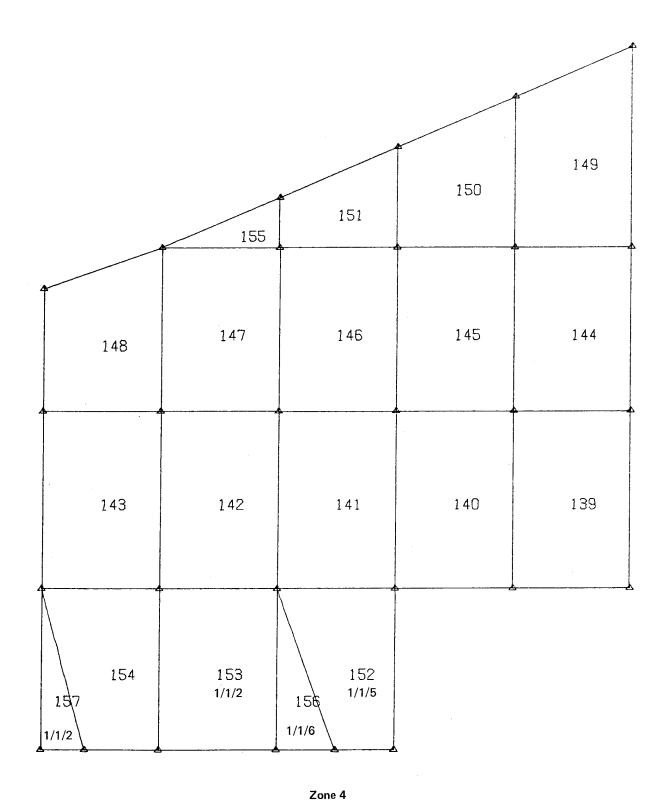


Figure 7-5.—(Continued)

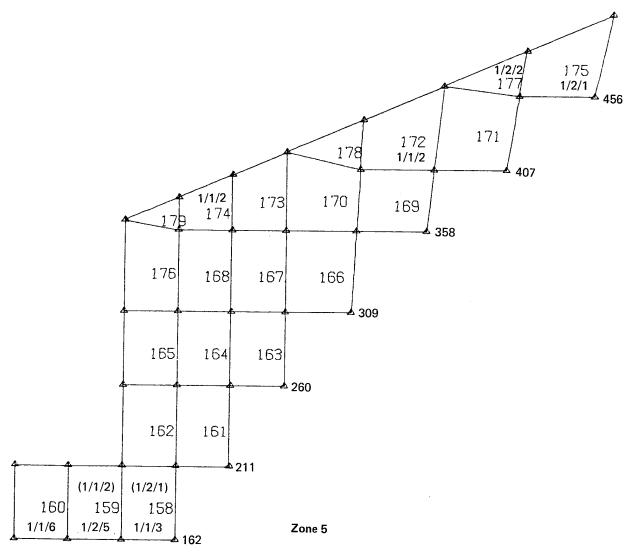


Figure 7-5.—(Continued)

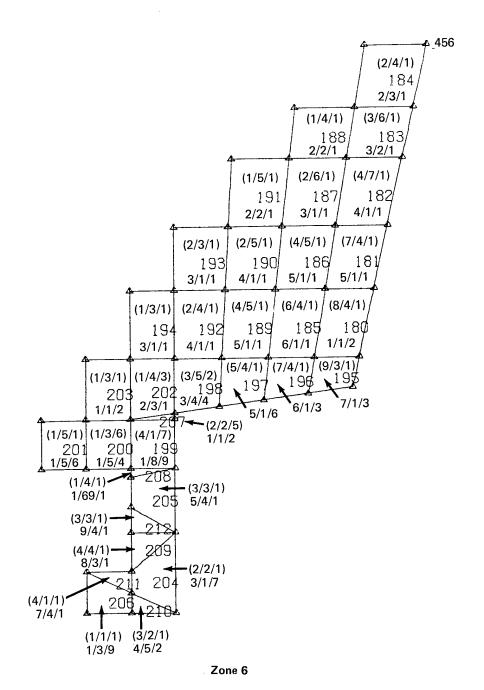
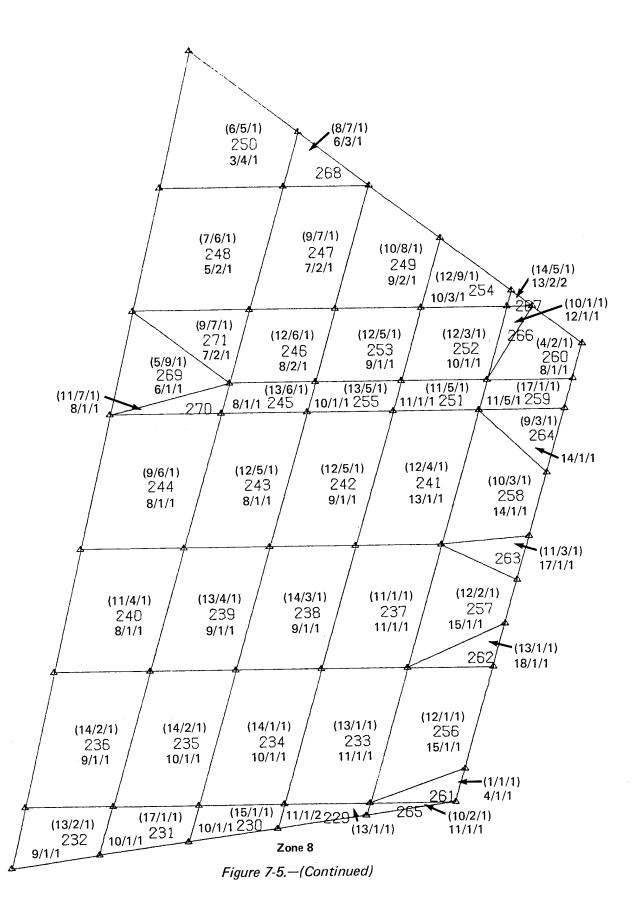


Figure 7-5.—(Continued)

(6/1/5) 228 2 /6/8	(4/3/1) 227 3/4/3	(6/3/1) 226 4/4/2	(7/3/1) 225 4/3/1
(4/2/1)	(4/3/1)	(6/3/1)	(7/3/1)
224	223	222	221
6/1/3	5/2/9	5/1/6	5/1/4
(4/2/1)	(4/2/1)	(6/2/1)	(7/2/1)
220	219	218	217
1/9/1	3/3/5	5/1/5	5/1/5
(3/3/1)	(5/3/1)	(6/2/1)	(7/2/1)
216	215	21 4	213
4/1/3	5/1/3	5/1/4	5/1/4

Zone 7

Figure 7-5.—(Continued)



			4	4/1/1 (1/1/1) 300
(10/3/1) 287 7/2/1	(11/3/1) 286 8/1/1	(12/2/1) 285 9/1/1	(13/1/1) 284 11/1/1	(11/2/1) 291 13/1/1 14/1/1 (17/3/1) 299
(10/3/1) 283 7/1/2	(12/2/1) 282 8/1/1	(13/1/1) 281 9/1/1	(14/1/1) 280 10/1/1	298 (18/3/1) 14/1/1 (15/2/1) 290 14/1/1 (16/1/1) 14/2/1 297
(11/2/1) 279 7/1/3	(13/1/1) 278 8/1/2	(13/1/1) 277 9/1/1	(14/1/1) 276 11/1/1	(16/1/1) 13/1/1 (15/1/1) 289 13/1/1 (16/1/1) 14/1/1 295
(10/2/1) 275 6/4/1	(13/1/1) 274 7/1/4	(13/1/1) 273 9/1/3	(14/1/1) 272 11/1/3	(15/1/1) 294 14/1/1 (16/1/1) 288 13/1/3 16/1/1 (8/3/1) 298 (11/3/1) 299 20/1/1

Zone 9a

Figure 7-5.—(Continued)

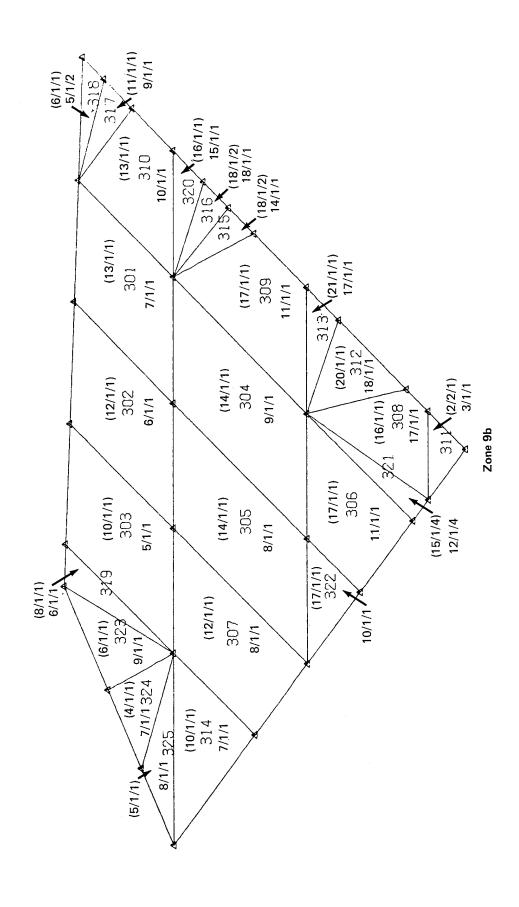


Figure 7-5.—(Continued)

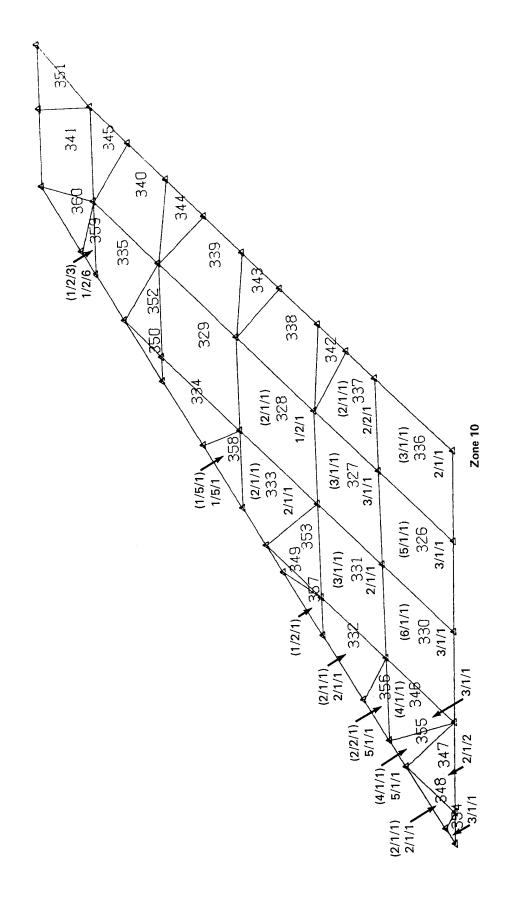
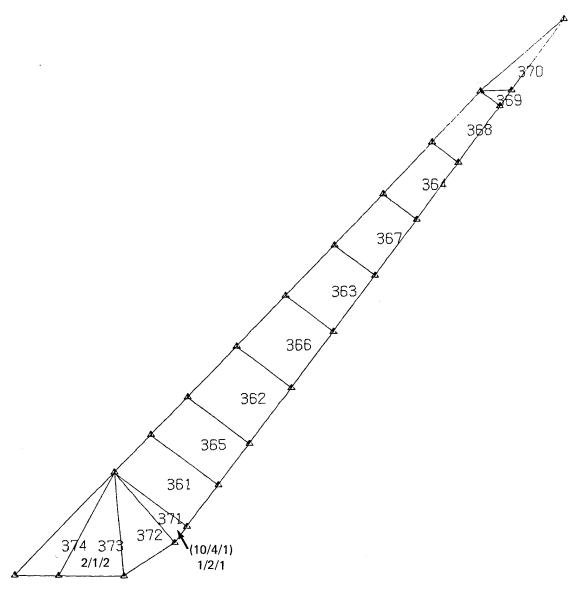


Figure 7-5.—(Continued)



Zone 11

Figure 7-5.—(Concluded)

Note:

Sizing values i/j/k define the subscripts in the standard laminate code for a $[0_i/45_i/90_k]$ Taminate composed of 0.002 inch-thick plies. The lower (upper) panel sizing is shown without (within) parentheses. If a single set of sizing values is shown for either an upper or lower panel, it applies equally to the sandwish inner and outer face sheets. Otherwise, the two sets of values are shown within a brace with the thinner laminate being the inner face sheet.

37

38

39

2. Except as noted on the figures all face sheet sizing is:

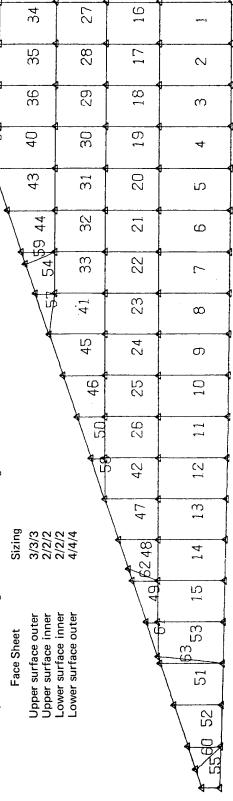


Figure 7-6.—Sizing of Elements, Third Strength Resize

Zone 1a

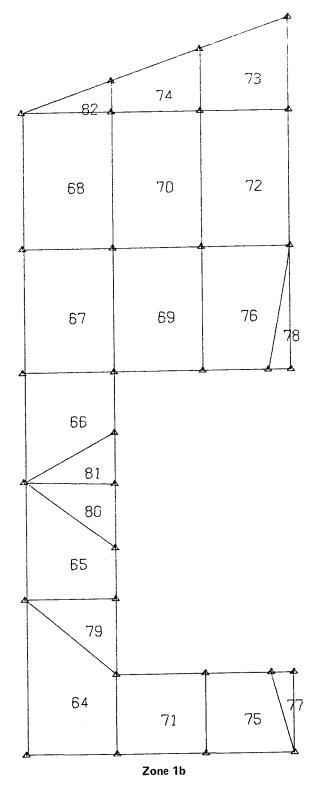
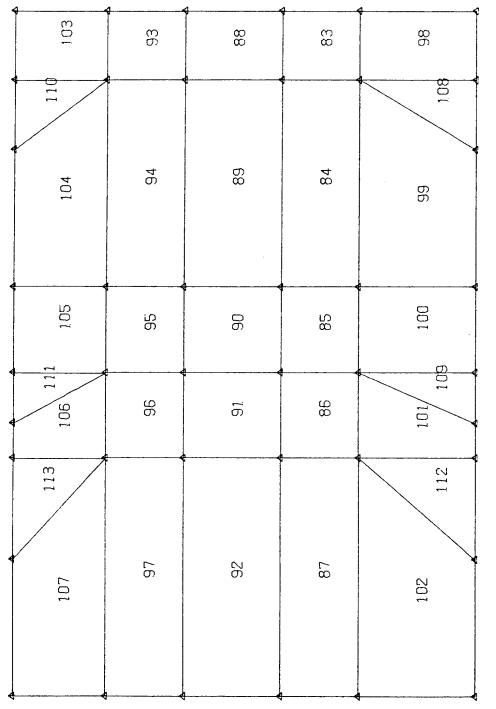


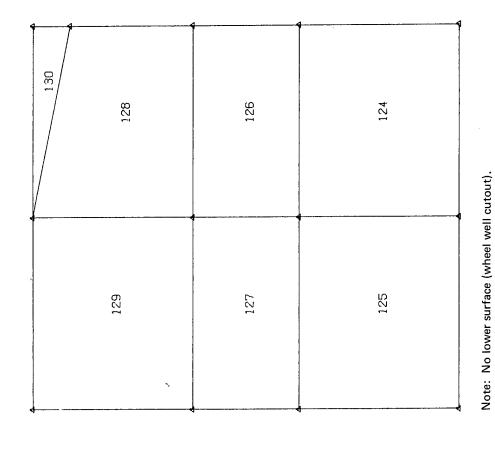
Figure 7-6.—(Continued)



Note: No lower surfaces (wheel well cutout).

Figure 7-6.—(Continued)

Zone 1c

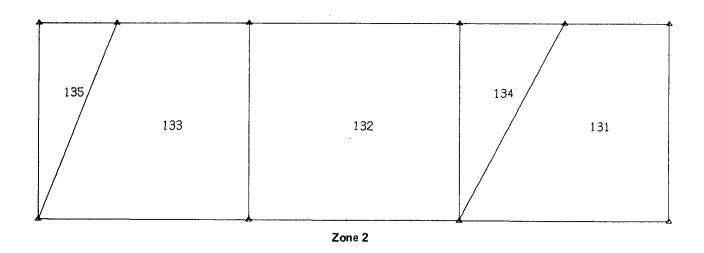


Note: No lower surface (wheel well cutout).

Zone 1d

Zone 1e

Figure 7-6.—(Continued)



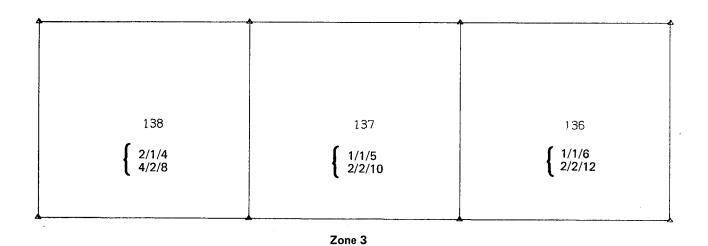


Figure 7-6.—(Continued)

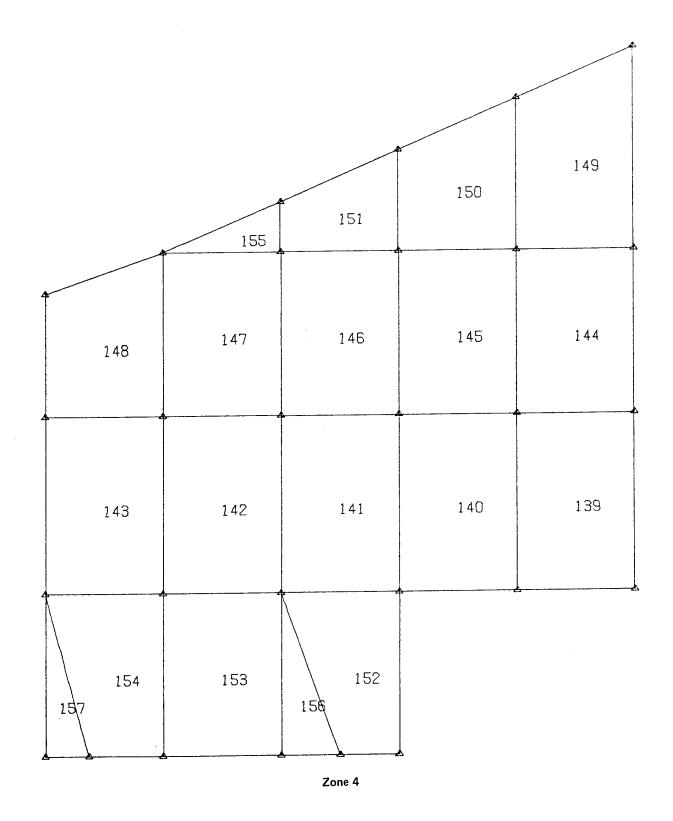
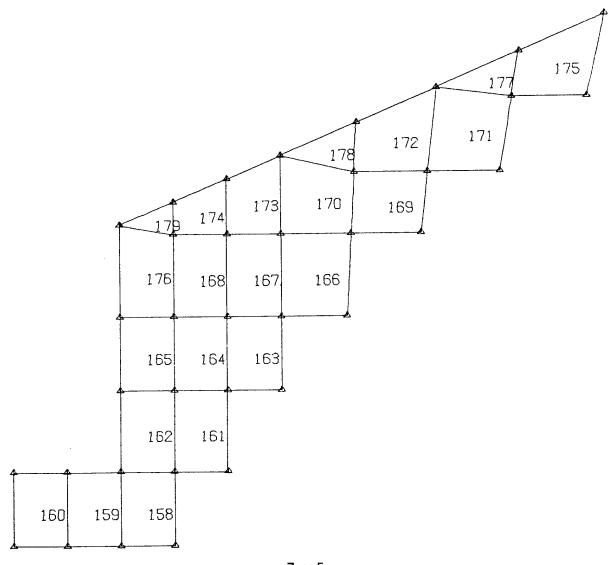


Figure 7-6.—(Continued)



Zone 5

Figure 7-6.—(Continued)

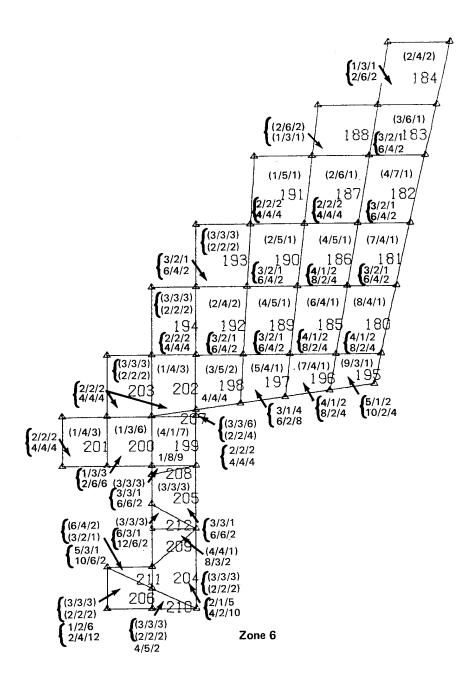
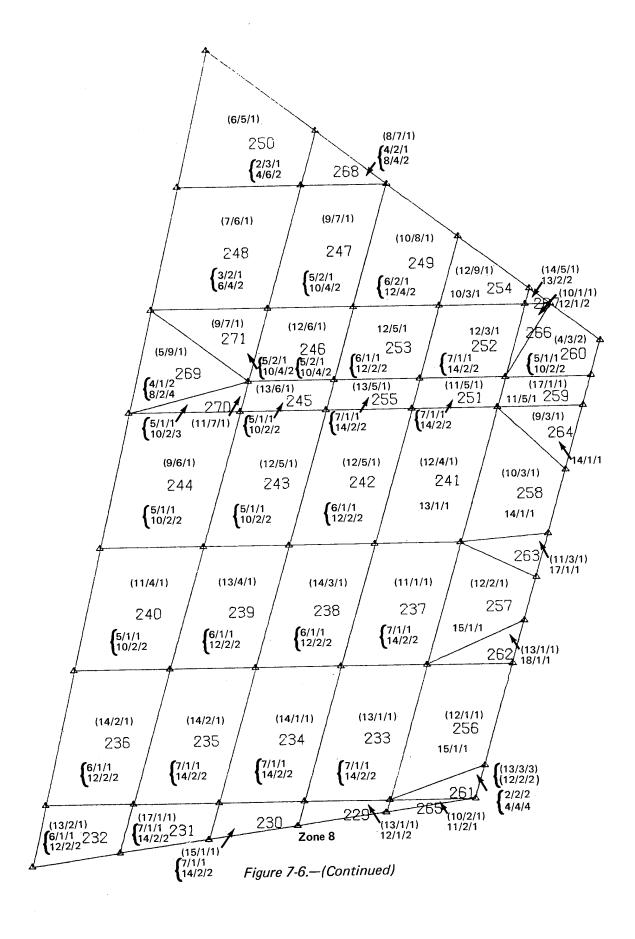


Figure 7-6.—(Continued)

(6/1/5) 228 2 /6/8	(4/3/2) 227 { 2/3/2 4 /6/4	(6/3/1) 226 (3/3/1 (6/6/2	(7/3/1) 225 { 3/2/1 6/4/2
(4/3/2) 224 { 4/1/2 8 /2/4	(4/3/2) 223 5/2/9	(6/3/1) 222 {3/1/4 6/2/8	(7/3/1) 221 { 3/1/3 6/2/6
(4/3/2) 220 1/9/1	(4/3/2) 219 {2/2/4 4/4/8	(7/2/1) 218 { 4/1/4 { 8/2/8	(7/2/1) 217 { 4/1/4 8/2/8
(3/3/3) 216 {3/1/3 6/2/6	(5/3/1) 215 { 4/1/2 8 /2/4	(6/2/2) 214 {3/1/3 6/2/6	(7/2/1) 213 {3/1/3 6/2/6

Zone 7

Figure 7-6.—(Continued)



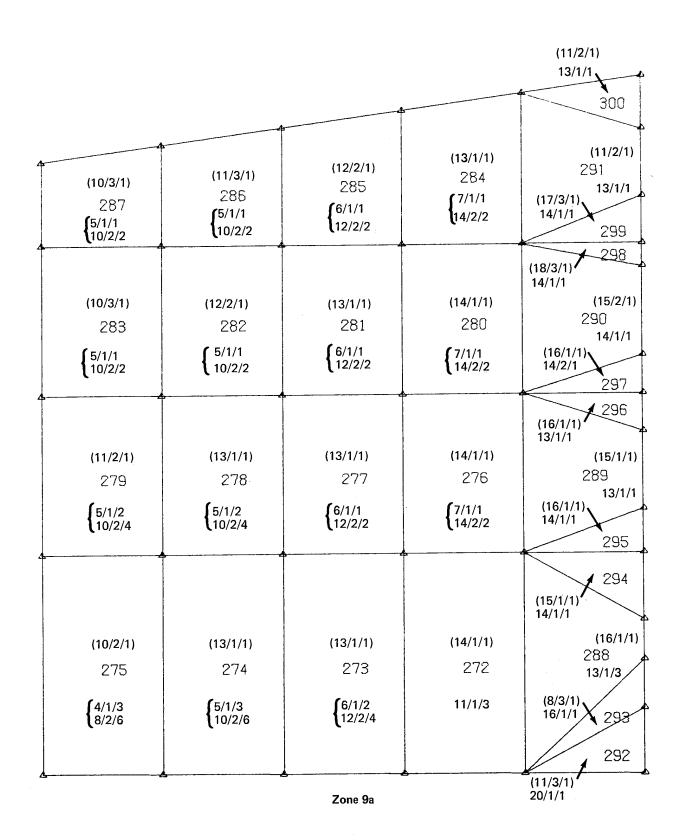


Figure 7-6.—(Continued)

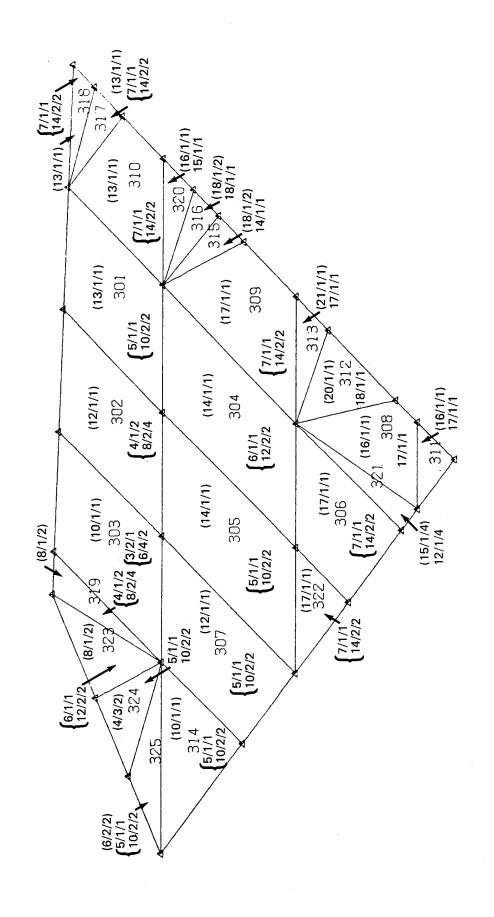


Figure 7-6.—(Continued)

Zone 9b

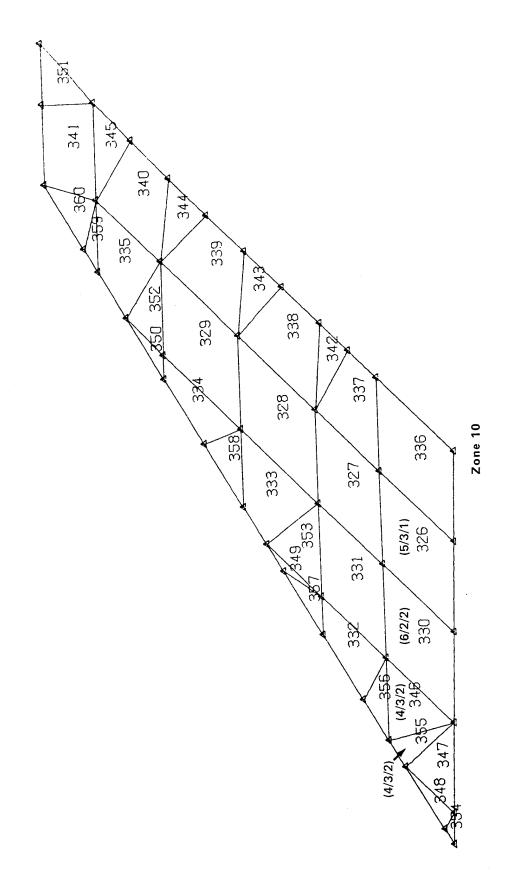
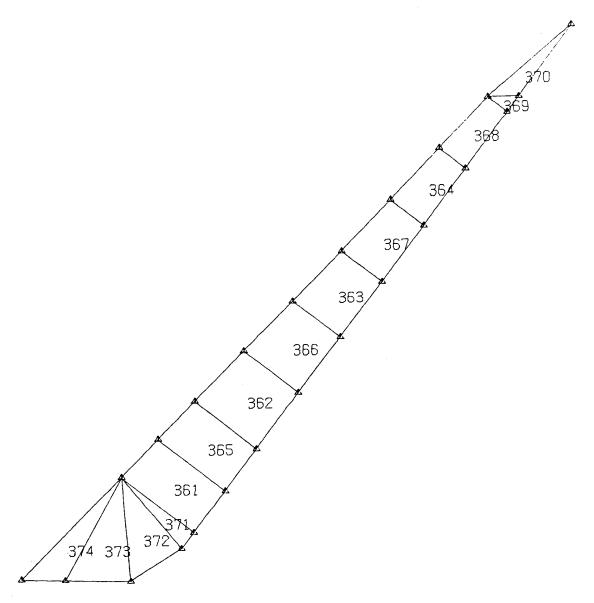


Figure 7-6.—(Continued)



Zone 11

Figure 7-6.—(Concluded)

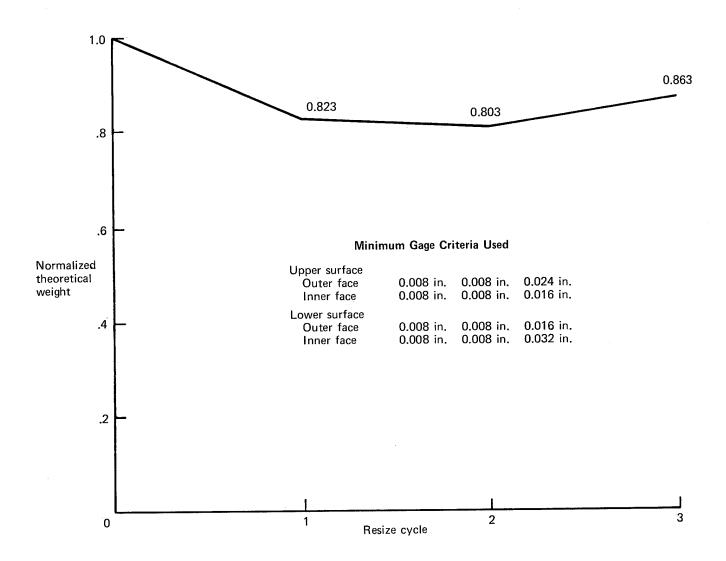


Figure 7-7.—Theoretical Wing Weight, Wing Box Primary Structure, ATLAS Resizing

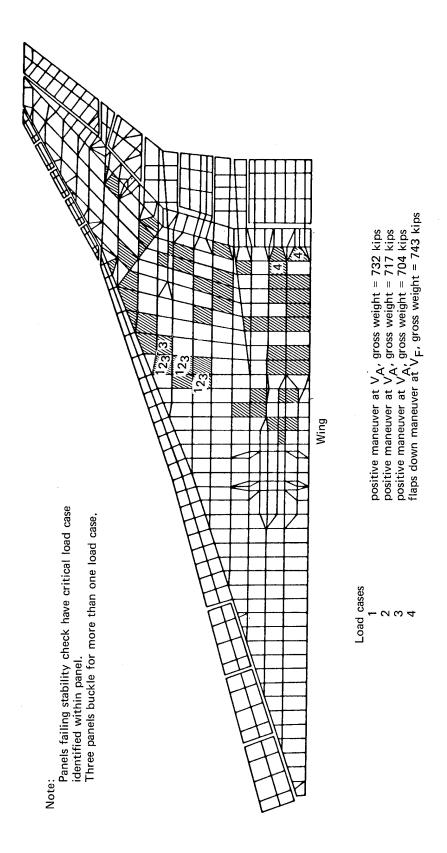


Figure 7-8.—Upper Surface Panels Checked for Stability After Resize Cycle 1

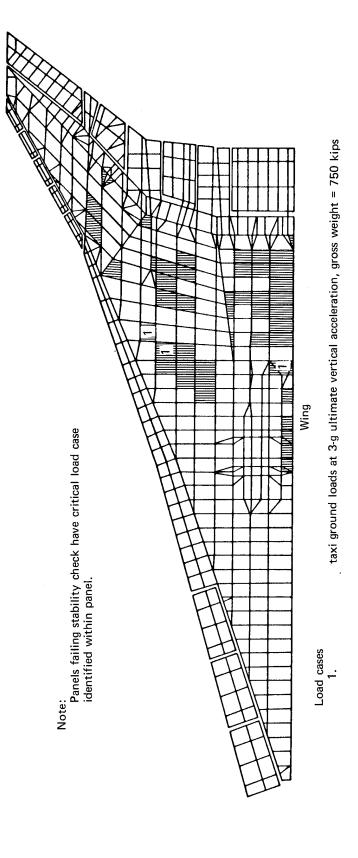


Figure 7-9.—Lower Surface Panels Checked for Stability After Resize Cycle 1

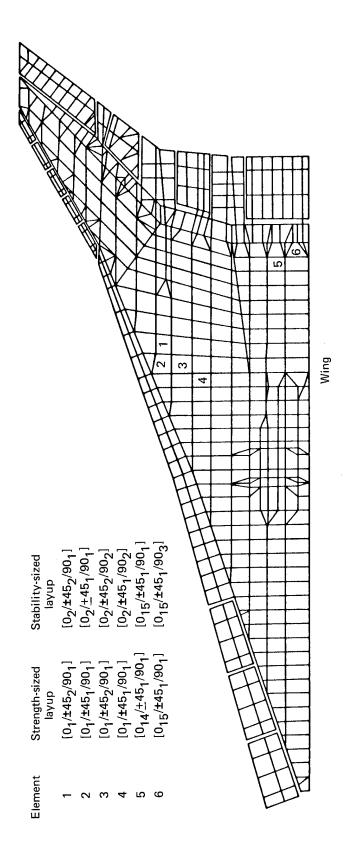


Figure 7-10.—Layup Changes Required for Stability After Resize Cycle 1 (Upper Surface)

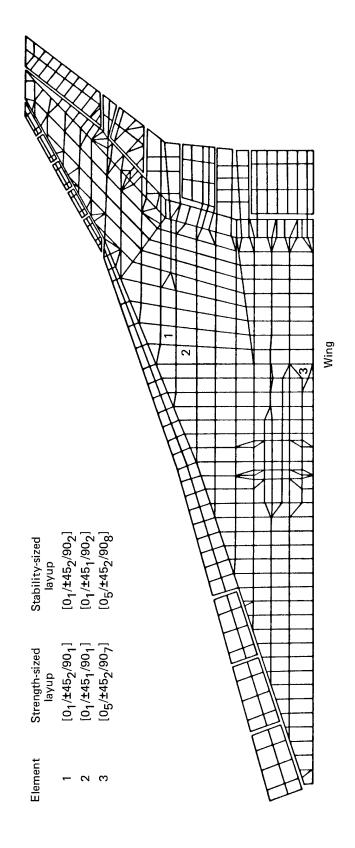


Figure 7-11.—Layup Changes Required for Stability After Resize Cycle 1 (Lower Surface)

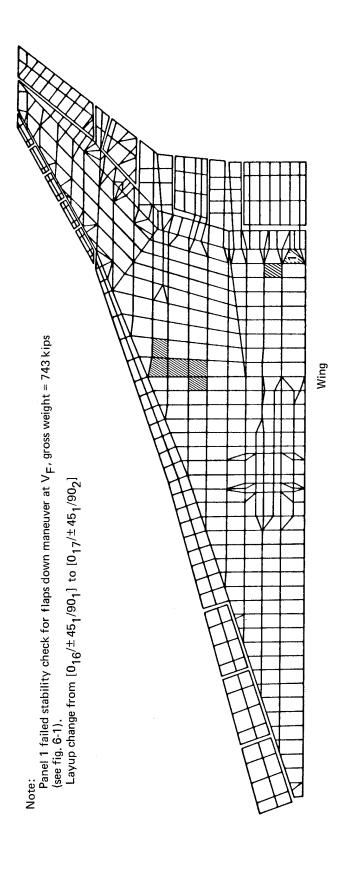


Figure 7-12.—Upper Surface Panel Stability Check After Resize Cycle 2

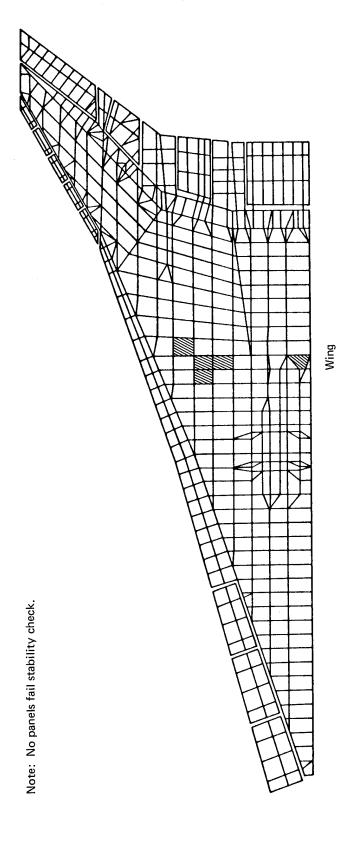


Figure 7-13.—Lower Surface Panel Stability Check After Resize Cycle 2

SECTION 8

FLUTTER ANALYSIS

by

C. R. PRATT-BARLOW J. G. LELONG

CONTENTS

	Page
FLUTTER APPRAISAL AND REDESIGN PROCEDURE	266
FLUTTER ANALYSIS OF STRENGTH DESIGNED HYBRID STRUCTURE	266
STIFFNESS REDESIGN OF ADVANCED COMPOSITE COVER PANELS	267
STIFFNESS DESIGN OF HYBRID STRUCTURE	268
REFERENCES	269

TABLES

Page
270
271
271
272
273

FIGURES

No.		Page
8-1	Stiffness Constraints on Hybrid Structure "Strength Design" from Use of	
	Titanium Design Internal Structure	298
8-2	Effect of Stiffness Design Changes on Flutter Speed for M = 0.9, Symmetric,	
0 2	High Cross Weight Condition	299
8-3	Comparison of Wing Mode Shapes 1 through 6. Hybrid Structure, Strength Design	300
8-4	Anisotropic Coupling Trends High Strength Graphite/Polyimide	301
8-5	Stiffness Designed Composite Cover Panels, Medium Modulus Graphite/Polyimide	302
8-6	Tailoring of Fiber Properties for Medium Modulus Graphite/Polyimide	303
8-7	Airplane Vibration Mode 1. Hybrid Structure Stiffness Design	304
8-8	Airplane Vibration Mode 2. Hybrid Structure Stiffness Design	305
8-9	Airplane Vibration Mode 3. Hybrid Structure Stiffness Design	306
8-10	Airplane Vibration Mode 4. Hybrid Structure Stiffness Design	307
8-11	Airplane Vibration Mode 5. Hybrid Structure Stiffness Design	308
8-12	Airplane Vibration Mode 6 Hybrid Structure Stiffness Design	309
8-13	Airplane Vibration Mode 7. Hybrid Structure Stiffness Design	310
8-14	Airplane Vibration Mode 8. Hybrid Structure Stiffness Design	311
8-15	Airplane Vibration Mode 9, Hybrid Structure Stiffness Design	312
8-16	Airplane Vibration Mode 10, Hybrid Structure Stiffness Design	313
8-17	Airplane Vibration Mode 11, Hybrid Structure Stiffness Design	314
8-18	Airplane Vibration Mode 12, Hybrid Structure Stiffness Design	315
8-19	Airplane Vibration Mode 13, Hybrid Structure Stiffness Design	316
8-20	Airplane Vibration Mode 14, Hybrid Structure Stiffness Design	317
8-21	Airplane Vibration Mode 15, Hybrid Structure Stiffness Design	318
8-22	Airplane Vibration Mode 16, Hybrid Structure Stiffness Design	319
8-23	Airplane Vibration Mode 17, Hybrid Structure Stiffness Design	32U 321
8-24	Airplane Vibration Mode 18, Hybrid Structure Stiffness Design	<i>J</i> <u>L</u> I

SYMBOLS

E_1	Young's modulus in spanwise direction
E_2	Young's modulus in transverse direction
G_{12}	Shear modulus
μ_{12}	Poisson's ratio for strain in the 2-direction due to normal stress in the 1-direction
μ_{21}	Poisson's ratio for strain in the l-direction due to normal stress in the 2-direction
F_1^{tu}	Ultimate tensile strength in direction of fibers
t	Thickness of layup for a cover panel
E' ₁	$= E_1/(1-\mu_{12} \mu_{21})$
E'2	$= E_2/(1-\mu_{12}\mu_{21})$
V_{D}	Dive speed
DOF	Degree of freedom
(N/M/P)	: Code for panel face layup
	N plies at 0°
	M plies at +45°
	M plies at -45°
	P plies at 90°

FLUTTER APPRAISAL AND REDESIGN PROCEDURE

The same flutter appraisal technique used for the titanium airplane study (fig. 11-4 of ref. 8-1) was used for the hybrid structure airplane with advanced composite cover panels. Budget constraints limited analysis to only the M=0.9 symmetric, high gross weight condition which was critical for the titanium airplane of Task II (ref. 8-1).

All variations of the hybrid structural model, including the strength design, had the stiffened wing fin, thickened wing tip with stiffened spars, stiff engine beams with diffusion ribs and spar and rib structure developed for the final titanium stiffness design but without its added wing tip ribs, figure 8-1. The body was modified to be the equivalent strength design in high strength graphite/polyimide as discussed in Section 7, with roughly seventy percent of the stiffness of the titanium strength design.

The effect of the stowed landing gear on the airplane vibration modes, inadvertently omitted during the final flutter analysis of the titanium airplane study, was included here. The landing gear resonance couples into the 5.0 Hz airplane mode, but has practically no effect on flutter.

The revised flutter clearance placard of Section 11 (ref. 8-1) was used to evolve a valid weight comparison with the titanium stiffness design. Airplane performance changes for both thickened wing tip and placard change apply to all hybrid structure designs.

FLUTTER ANALYSIS OF STRENGTH DESIGNED HYBRID STRUCTURE

Flutter analysis of the strength designed hybrid structure yielded a relatively low frequency critical flutter mode, 287 KEAS, 1.52 Hz, well below the requirement of 444 KEAS at M = 0.9 (figures 8-2 and 8-3). A comparison of front and rear spar deflections at the wing fin station and the wing tip showed that the hybrid strength design structure had excessive flexibility in torsion and in wing tip bending. This was confirmed by comparing stiffness levels of typical cover panels in the heavily loaded aft wing box and the wing tip with those for the stiffness designed titanium airplane as shown in table 8-1. A comparison of modal frequencies and relative contributions to the energy balance at flutter for the hybrid strength designed structure are shown in table 8-2. The substantial amount of wing tip torsion in mode 6 (see fig. 8-3) is believed to be a major factor in the large positive contribution of that mode to the energy balance at neutral stability.

STIFFNESS REDESIGN OF ADVANCED COMPOSITE COVER PANELS

Four stiffness redesign cycles, with modifications to the advanced composite cover panels, were conducted before achieving a hybrid structure stiffness design which meets the M = 0.9 flutter requirement. The typical composite panel layups and stiffness levels in the lower half of table 8-1 summarize the stiffness design development.

In Stiffness Redesign 1, the balanced, symmetric (orthotropic) composite panel layup philosophy used in the strength design was maintained but $\pm 45^{\circ}$ plies were restored to increase wing torsional stiffness in the heavily loaded aft wing box such that the effective shear stiffness of a typical composite panel layup was roughly half that of the titanium strength design. This resulted in a 13/9/1 layup for the typical panel (using the same coding scheme adopted in Section 6). The effective spanwise bending stiffness in the aft wing box of the hybrid structure strength design was already roughly half that of the titanium strength design. The strength design distribution of 0° and 90° plies in the aft wing box was preserved when adding a uniform number of $\pm 45^{\circ}$ plies. In addition, five 90° plies near the engine beam diffusion ribs were used to obtain effective load diffusion into the cover panels. Finally, both bending and torsional stiffnesses of the wing tip were increased to roughly half those of the titanium stiffness design by using a uniform 12/8/8 layup. Figure 8-2 shows the improvement in flutter characteristics for the stiffness redesign cycles. Stiffness Redesign 1 raised the critical flutter mode to 337 KEAS, 1.62 Hz and the second flutter mode to roughly the $1.2V_D$ requirement.

Stiffness Redesign 2 crudely exploited the potential anisotropic behavior of the composite layup in the wing tip. The findings of Austin and others (ref. 8-3), were confirmed for an isolated composite cover panel (fig. 8-4) in that unbalancing the ±45° plies lowers the effective shear modulus unduly whereas limited reorienting of the spanwise plies of an otherwise balanced layup provides favorable anisotropic behavior in terms of both increased effective shear modulus and changed twist coupling parameter. However, favorable twist coupling parameter trends for static aeroelastic tailoring of a sweptback wing appear to be more readily obtained than for increased flutter speed. Nevertheless, compared with the 12/8/8 wing tip layup of Stiffness Redesign 1, limited experiment yielded a 15/10/1 layup with spanwise fibers reoriented 15° aft, with the same overall thickness but 35% greater shear stiffness from a 22% more effective shear modulus together with a 15% decrease in the twist coupling parameter. This Stiffness Redesign 2 strategy was effective in raising the speed of the third flutter mode by 7% without any weight increase over Stiffness Redesign 1, but the critical flutter mode was raised by only 4 KEAS to 341 KEAS, 1.62 Hz, while the second flutter mode was similarly unaffected, as shown in figure 8-2. No further anisotropic effects were studied.

Table 8-1 shows that compared with the second stiffness modification, Stiffness Redesign 3 had twice the ±45° plies in the aft wing box typical 13/18/1 layup and twice the 0° and ±45° plies in the wing tip 30/20/1 layup, without sparwise fibers reoriented aft. Additionally, the 90° plies near the engine beam diffusion ribs were doubled to 10 plies. This raised wing stiffness levels to roughly the values for the titanium stiffness design. However, the critical flutter mode was raised to only 382 KEAS, 1.64 Hz. This is probably a direct consequence of a lower wing bending/torsion stiffness ratio from the reduced body stiffness and relatively lower bending stiffness in the aft wing box.

STIFFNESS DESIGN OF HYBRID STRUCTURE

For the hybrid structure final stiffness design, medium modulus graphite/polyimide cover panels were used, replacing the high strength material. With minimum weight increment this increased the stiffness level over stiffness redesign 3 by roughly 50% in shear and 80% in spanwise bending because 20% more spanwise plies were required to maintain adequate strength. The stiffness designed composite cover panels are shown in figure 8-5. Material suppliers have indicated that for the 1986 time period fibers with strength and moduli intermediate to values for T600 and T90 fibers could be provided, as indicated by the dashed line in figure 8-6. The medium modulus material selected had a moderate decrease in tensile strength, corresponding to the fiber properties at the intersection of the radial and dashed lines. This was regarded as a favorable choice for the hybrid structure from considerations of strain compatibility between the titanium and composite materials. Table 8-3 compares material properties considered.

Figure 8-2 shows M = 0.9 flutter clearance with the 450 KEAS, 1.75 Hz critical flutter mode of the hybrid structure stiffness design, for the symmetric, high gross weight condition. Table 8-4 compares the titanium and hybrid structure stiffness design vibration mode frequencies and energy balance at flutter. Higher frequency modes have less effect for the hybrid structure stiffness design flutter. Table 8-5 details the hybrid structure stiffness design mode shapes, which are shown in figures 8-7 through 8-24.

The stiffness redesign mass increment to the hybrid structure "strength design" to satisfy flutter criteria is 8702 lb as detailed in Section 9. Despite limitations imposed on the optimization of the stiffness design by budget limitation and technical approach, Section 9 weights analysis shows the hybrid structure stiffness design wing primary structure outboard of the center section to be 6730 lb lighter than the titanium stiffness design which has about the same M = 0.9 flutter speed, 453 KEAS, 1.91 Hz, for the symmetric, high gross weight condition. The hybrid structure stiffness design has a higher bending/torsion stiffness ratio than the titanium stiffness design, particularly in the wing tips. In fact, the wing tips are so stiff that moderate weight saving would result from changing cover panels to equivalent stiffness T90 high modulus graphite/polyimide layups outboard of the wing mounted fins. Conversely, table 8-1 shows that typical cover panels of the equivalent hybrid structure stiffness design in T600 high strength graphite/polyimide would be theoretically 47% heavier than with the selected medium modulus material.

REFERENCES

- 8-1 Boeing Staff: Study of Structural Design Concepts for an Arrow Wing Supersonic Transport Configuration. NASA CR 132576-2, 1976.
- 8-2 Gordon, C. K.; and Visor, O.E.: SCAR Arrow-Wing Active Flutter Suppression System. NASA CR 145147, 1977.
- 8-3 Austin, F.; et al.: Aeroelastic Tailoring of Advanced Composite Lifting Surfaces in Preliminary Design, AIAA/ASME/SAE 17th Structures, Structural Dynamics and Material Conference, King of Prussia, Pennsylvania, 1976.

Table 8-1.—Stiffness Redesign, Typical Advanced Composite Honeycomb Wing Cover Panels

					Typica	Typical wing honeycomb panel	d qmoo.	anel					
				Aft w	Aft wing box					M	Wing tip		
		Panel	Face layup,	Theo. weight,	Sti	Stiffness ratios		Panel	Face lavub.	Theo.		Stiffness ratios ²	
	Structure	plies	in.	lb/ft2	Sparwise	Transverse	Shear	plies		lb/ft2	Sparwi	Transverse	Shear
	Stiffness design	1	0.065	3.0	1.0	1.0	1.0		0.08 in.	3.68	1.0	1.0	1.0
(009	Strength design	32	13/1/1	0.52	0.48	0.08	0.10	80	1/1/1	0.13	0.05	0.05	0.05
9T) At	Stiffness mod 1	64	13/9/1	1.03	0.66	0.26	0.51	72	12/8/8	1.16	0.51	0.40	0.39
voo etia grente r or etid	ਤੂਰ ਤੁਹਾਤੀ ਜ਼ਿਲਤ mod 2	64	13/9/1	1.03	0.66	0.26	0.51	72	15 ^a /10/1	1.16	09.0	0.24	0.53
1giH	Stiffness mod 3	100	13/18/1	1.61	0.85	0.45	0.98	142	30/20/1	2.29	1.25	0.44	0.93
٥	Stiffness design	106	16/18/1	1.74	1.41	0.65	1.45	154	36/20/1	2.53	2.11	0.64	1.37
T6C stiff	T600 equivalent stiffness design	158	24/27/1	2.55	1.38	0.65	1.42	230	54/30/1	3.71	2.14	0.66	1.41
					E11 t	E22 t	G ₁₂ t				E ₁₁ 't	E ₂₂ 't	G ₁₂ t
Uni	Unit panel stiffness for stiffness ratio = 1.0	iffness ra	atio = 1.0	1	2.28	10 ⁶ lb/in. 2.28	0.80		² Unit Panel – Stiffnesses	inel	2.73	10 ⁶ lb/in. 2.73	0.98

Ply thickness = 0.002 in.

^aWingtip sparwise fibers rotated 15° aft

^bMedium modulus graphite polyimide on entire wing structure

Table 8-2.—Comparison of Flutter Energy Balance for Strength Designed Hybrid Structure

Mode	Airplane natural frequency, Hz	Energy contribution at neutral stability (source positive)
Plunge	0.0	-0.075
Pitch	0.0	-0.138
1	0.80	-1.0
2	0.97	-0.415
3	1.82	0.637
4	2.00	-0.551
5	2.69	-0.152
6	2.89	0.606
7	2.99	0.438
8	3.30	0.016
9	3.55	0.142
10	3.86	0.061
11	4.63	-0.041
12	5.04	0.267
13	5.43	-0.006
14	5.66	0.066
15	5.78	0.170
16	6.51	-0.008
17	7.36	-0.009
18	7.40	-0.010

Table 8-3.—Advanced Composite Material Properties, 1986

			yimide (unidirecti 6 fiber volume	onal)	
Com	posite type		T600 high strength	T90 high modulus	Medium modulus
Density '	ρ	lb/in ³	0.056	0.058	0.057
Elastic	E ₁₁	10 ⁶ psi	20.0	40.0	30.0
properties	E ₂₂	10 ⁶ psi	1.13	1.8	1.4
(relative to	G ₁₂	10 ⁶ psi	0.717	0.98	0.8
material axes,	ν ₁₂	_	0.31	0.29	0.3
RT)	ν ₂₁	_	0.018	0.013	0.014
Longitudinal tensile ultimate	F ₁ ^{tu}	ksi	295.0	148.0	234.0

Table 8-4.—Comparison of Flutter Energy Balance for Stiffness Designs

		vibration mode quency, Hz	0,	tribution at neutral (source positive)
Mode	Titanium	Hybrid structure	Titanium	Hybrid structure
Di	0.0	0.0	0.007	0.000
Plunge	0.0	0.0	-0.097	-0.069
Pitch	0.0	0.0	-0.111	-0.046
1	0.97	0.87	-0.744	-0.104
2	1.18	1.14	-1.0	-1.0
3	2.18	1.92	0.524	0.511
4	2.43	2.49	0.467	0.027
5	2.79	2.93	0.035	0.012
6	3.00	3.39	0.040	0.137
7	3.37	3.53	0.377	0.225
8	3.63	3.56	0.003	0.137
9	3.81	4.23	0.110	0.067
10	4.00	4.36	-0.051	-0.001
11	4.41	5.09	0.200	0.050
12	4.68	5.78	-0.002	-0.006
13	6.22	5.97	0.112	0.037
14	6.35	6.06	0.036	-0.008
15	6.75	6.91	0.005	0.000
16	7.21	7.50	0.105	0.031
17	8.03	7.84	0.015	-0.000
18	8.62	8.15	-0.024	0.000

Table 8-5.—Airplane Vibration Mode Shapes*, Hybrid Structure Stiffness Design

Row	Node	DOF	Mode 1	Mode 2	Mode 3	Mode 4
1	1020	1	0.0000000	01763017	.01414464	00246597
2	1020	2	0.00000000	0.00000000	.00681722	.01617304
3	1020	3	1.00000000	27853248	.09156377	02265588
4	1020	4	0.00000000	0.00000000	.00017145	.00043833
5	1020	5	0.00000000	.00048709	00044882	.00002246
6	1027	6	0.000000000	6.66696699	.06666657	.0(600030
7	1070	1	0.00000000	00906330	.01481598	.01781366
. 8	1070	2	0.00000000	0.00000000	.01205193	.02888156
9	1070	3	1.00000000	28654505	.17294126	.15549984
10	1070	4	6,000000000	6.000000000	.00C34178	.00087914
11	1070	5	0.00000000	.0048739	000667659	00047996
12	1070	6	0.00000000	C.00000000	•00000284	.00000509
13	670	3	1.00000000	.44827772	00840345	.02174310
14	663	3	1.00000000	.31732466	11544393	.03254357
15	652	. 3	1.00000000	.14392205	16982519	.02042128
16	644	3	1.00000000	.00656381	14243762	.01.694331
17	637	3	1.000000000	14085763	06(50285	.08144992
∴ 18	7 92	3	1.00300000	22380793	.13286036	.22625777
19	784	3	1.00000000	28787966	.28116864	.43380687
20	779	3	1.00000000	33807874	.40358779	.61701612
21	775	3	1.000000000	37191661	.48857390	.74656916
22	627	3	1.00166606	.44135136	01413543	.02233175
23	618	3	1.00000000	.39468852	05716620	.02753816
24	615	3	1.00000000	.35823988	08717904	.03061794
25	613	3	1.00000000	.31158191	11756858	.03231718
26	610	3	1.000000000	.27720826	13606580	.03227871
27	608	- 3	1.00000000	.23055029	15362895	.02988652
28	605	3	1.00000000	.19099891	16301013	.02605792
29	603	3	1.00000000	.15661064	16685256	.02182523
30	600	3	1.00000000	•10502824	16792587	.01517961
31	597	3	1.00000000	.05423491	15993703	.00936259
32	692	3	1.00000000	.43414736	02016384	.02296141
33	693	3	1.000,00000	.38784983	06215528	.02793042
34	694	3	1.00000000	.35168857	09023115	.03051827
35	562	3	1.00000000	.30539105	11980759	.03205908
36	560	3	_1.00000000	.27129503	13680295	.03171866
37	6 9 5	3	1.00000000	.22499751	15359512	.02925151
38	555	3	1.00000000	.18605499	16189523	.02542289
39	553	3	1.00000000	.15195897	16536889	.02110606
40	550	3	1.00000000	.10081494	16563283	.01409369
41	547	3	1.00000000	.04967092	15706856	.00800838
42	544	3	1.00000000	00147311	13566238	.06436159
43	5.41	3	1.60006000	05251714	16116570	.00875037
44	539	3	1.00000000	69389768	06203774	.02683914
45	537	3	1.00000000	14552879	.00251767	.07633097
46	536	3	1.00000000	17280560	.04361189	.11587648

^{*}Elastic modes start at Mode 3.

Table 8-5.—(Continued)

Row	Node	DOF	Mode 1	Mode 2	Mode 3	Mode 4
47	534	3	1.00000000	20251785	.09263493	.16839137
48	476	3	1.00000000	22239583	.12834145	.20992259
49	716	3	1.00000000	24263425	.16976796	.26448513
50	713	3	1.00000000	26014986	.20721133	.31545239
51	712	3	1.00000000	27702252	.24472833	.36802795
52	709	3	1.00000000	29347628	.28249344	.42216696
53	708	3	1.00000000	31034894	.32210998	.47988662
54	705	3	1.00000000	32679783	.36200907	.53933873
55	704	3	1.00000000	34367049	.40410724	.60323592
56	701	3	1.00000000	35948617	.44431486	.66497891
57	700	3	1.00000000	37750835	.49030568	.73575986
58	533	3	1.00000000	39429334	.53276704	.80074112
59	85	3	1.00000000	.35653508	08644390	.03015331
60	82	3 3	1.00000000	.30539105 .25424702	11886552 14155929	.03071707
61	79	3	1.00000000	.25424702	14262818	.03093491
62	129	<u></u>	1.0000000	.20310300	15437532	.02692139
63 64	76 176	3	1.00000000	.20310300	15747515	.02721362
65	73	. 3	1.000000000	.15195897	15862167	.02162621
66	173	3	1.00000000	.15195897	16203486	.02106533
67	50	3	1.00060000	.10081494	15217667	.01276558
68	120	3	1.00000000	.10081494	15574254	.01222094
69	220	3	1.00000000	.10081494	16190736	.01276377
70	. 67	3	1.00000000	.04957092	14913895	.00161046
71	167	3	1.06000000	.04957092	14886663_	.00261785
72	267	3	1.00000000	.04967092	15497544	.0654386
73	44	3	1.00000000	00147311	11954793	00760874
74	114	3	1.00000000	00147311	12795300	06962076
75	214	3	1.60000000	00147311	12978656	00386481
76	314	3	1.00000000	00147311	13378844	.00167190
77	41	3	1.00000000	05261714	09498684	01942564 01746680
78	111	3	1.00000000	05261714 05261714	09616530 09803070	0174666
79 80	211 311	3 3	1.00000000	05261714	099996446	00206396
81	<u> </u>	3	1.00000000	10376117	065(2756	03099185
82	158	3	1.00000000	10376117	06335210	02333582
83	209	3	1.00000000	08776039	07462843	01652320
-84	309	3	1.00000000	09050756	06991578	00078742
85	409	3	1.00000000	09342579	06428651	.01912062
86.	207	3	1.00000000	12319590	04712888	01837505
87	307	3	1.00000000	13152507	03288993	.00619332
88	407	3	1.00000000	13917719	01508087	.04060548
8 9 .	55	3	1.0000000	15490519	02953383	04415418
90	155	3	1.00000000	15490519	02464686	03006415
91	205	3	1.06000000	15754520	01856452	01939564
92	305	_3	1.00000000	17142228	.00715438	.01751608

^{*}Elastic modes start at Mode 3.

Table 8-5.—(Continued)

Row	Node [OOF	Mode 1	Mode 2	Mode 3	Mode 4
93	405	3	1.00000000	18416445	.03711991	.06734237
94	385	3	1.00000000	19360417	.06562104	.11919767
95	454	3	1.00000000	20716465	.07970692	.12057412
96	464	3	1.00000000	23328223	.13369861	.19419653
97	474	3	1.00000000	25348652	.18018387	.26218465
98	484	3	1.00000000	27656863	.22208521	.32591017
99	493	3	1.00000000	31059735	.30825575	. 44256795
100	502	3	1.00000000	35406491	.40960724	.58862689
101	512	3	1.00000000	37367012	.46518332	.68040726
102	522	3	1.000000000	39004595	.51202006	.75810024
103	52	3	1.00000000	20604922	.00918915	05878685
104	152	3	1.00000000	20604922	.01744830	03801308
105	202	3	1.00000000	20671166	.02529950	01995674
106	302	3	1.00000000	22064232	.06002544	.03509024
107	382	3	1.00000000	23426559	.10607651	.11854741
108	452	3	1.00000000	25489907	.15024359	.17937382
109	462	3	1.00000000	28101662	. 21227457	.27147466
110	482	3	1.00000000	31830305	.31037126	.42668609
111	492	3	1.00000000	33446457	.35477660	.49873627
112	179	3	1.00000000	24566392	.03558677	07905532
113	146	3	1.00000000	24566392	.04063567	06884985
1114	1.92	3	1.00000000	24556392	.04975813	04740084
115	200	3	1.00000000	24556392	.06089287	02175822
116	298	3	1.00000000	25596092	.09080256	.02770046
117	350	3	1.00000000	26525939	.12066953	.09297847
118	398	3	_1.000000000		.15025342	.13828432
119	819	3	1.00000000	29975482	.21943764	.23986895
120	816	3	1.00000000	32357332	.28264755	.34009068
121	470	3	1.00000000	34366075	.33766622	•42909271
122	810	3	1.00000000	35590122	.36917828	.47797049
123	808	3	1.00000000	36817579	.40743441	•54438526
124	806	3_	1.00000000	38464903	. 45918681	.63458567
125	8 04	3	1.00000000	40112228	.51142307	.72603426
126	8 0 3	3	1.00000000	40935403	•53769204	.77215886
127	801	3_	1.00000000	41987509		.83108729
128	531	3	1.00000000	43023054	.60407802	.88855405
129	899	3	1.00000000	28142577	.06508683	08529287
130	887	3_	1.00000000	28142577	.07522009	06373749
131	940	3	1.00000000	31308636	.08888791	09601778
132	937	3	1.00000000	31308636	.09985076	07309280
133	1023	3_	1.00000000	29603835	.10611959	027(6270_
134	878	3	1.000003300	28860542	.12665725	.03817241
:135	876	3	1.00000000	29250211	.14808058	.08003377 .05056845
136	928	3_	1.00000000	31468888	.15731534	The second section of the second section is a second section of the second section of the second section is a second section of the second section sec
137	926	3		31714379	.17721897	.09209456 .18226105
138	1063	3	1.00000000	30334464	.20024074	TOTE OTON

^{*}Elastic modes start at Mode 3.

Table 8-5.—(Continued)

Row	Node	DOF	Mode 1	Mode 2	Mode 3	Mode 4
139	91.6	3	1.00000000	34137632	.29789735	.33142171
140	915	3	1.00000000	35958846	.35318609	.42597783
141	908	3	1.0000000	38530173	.42636102	.54707160
142	906	3	1.00000000	40146811	.47880039	.63974469
143	904	3	1.00000000	41762962	.53168416	.73362228
144	902	3	1.00000000	43379601	.58535470	.82948860
145	920	3	1.00000000	44575884	.62655044	.90412453
146	900	3	1.00000000	45586742	.66023373	.96451856
147	1021	3	1.00000000	32648123	.13501884	02688445
148	1061	3	1.00000000	33891653	.24930054	.21634887
149	965	3	1.00000000	37528237	.37862249	.44878533
150	957	3	1.009000000	40130250	.46144689	.59492032
151	954	3	1.00000000	42548145	.54130582	.73718513
152	951	3	1.00000000	44961169	.62336523	.88517397
153	953	3	1.00000000	46818428	.68689403	1.00000000
154	767	3	1.00000000	22277575	.13408407	.22414456
155	766	3	1.00000000	23901033	.16778363	.26907379
156	763	3	1.00060000	25652594	.21566383	.32116563
157	762	3	1.000000000	27339860	.24351429	.37462266
158	759	3	1.00000000	28984749	.28163212	.42970813
159	758	3	1.00000000	30672015	.32161382	.48837926
160	755	3	1.00000000	32317391	.36175586	•5484588 Q
161	754	3	1.0(000000	34004657	.40377237	.61217171
162	751	3	1.00000000	35586225	.44362022	.67303370
163	750	3	1.00000000	37388443	.48917950	.74275680
164	237	2	0.0000000	0.0000000	00466627	01316444
165	235	2	0.00000000	0.00000000	01585457	04371027
166	232	2	_0.00000000	6.00036003	03497496	095 90053
167	227	2	0.00000000	0.06000500	04865246	13541237
168	227	2	0.00000000	0.00000000	05996807	16867408
169	226	2	c.0 0000000	0.00000000	07172626	20361984
170	475	2	0.00000000	0.00000000	00050551	00216068
171	285	2	0.00000000	6.00000000	01099463	03094947
172	282	2	0.00000000	0.00000000	02935067	08126730
173	472	2	0.00000000	0.0000000	00106137	00584409
174	332		_0.0000000	0.00000000	01781127	05123939
175	329	2	0.00000000	0.0000000	03960832	11193838
176	277	2	0.00000000	0.00000000	05529603	15652582
177	862	_2_	<u>u.0000000</u>	6.00000000	.0CCC2570	0(558441
178	379	2	0.00000000	000000000000000000000000000000000000000	02048162	06224712 11995438
179	377	2	C.00000000	0.60000000	04124489	16353199
180_	376	2	0.00000000	0.00000000	05680166 07267725	2(8(8399
181	375	2	0.00000000	0.00000000 0.0000000	00218234	01648920
182	428	2	0.00000000	6. 66636636	01825490	060(3274
183	427	2 .	_^.000000000 	0.00000000	04540845	13389517
184	426	2	0.0000000	0.03030000	-,07740047	- • 1330371

^{*}Elastic modes start at Mode 3.

Table 8-5.—(Continued)

Row	Node	DOF	Mode 1	Mode 2	Mode 3	Mode 4
				0.0000000	05749812	16678365
185	424 417	2	0.00000000	0.0000000	00281138	01969827
186	416	2	~~.00000000 ~~.000000000	(.6.0000000	02999804	09373515
187		2	0.000000000	0.6000000	05844826	17122436
188	415	2	0.000000000	0.00000000	07372627	21301914
189	414		1.00000000	37530185	.40363978	.51397447
190	374	3	0.00000000	.03895704	05263124	02914391
191	374	1 5	0.00000000	.03045704	00688279	00098070
192	471	3	1.600000000	1.60000000	1.0060060	18464158
193	3189	3	1.000000000	.91437629	.81293666	14326017
195	3187	3	1.000000000	.84252511	.66036566	10982347
196	3185	3_	1.00000000	.77277439	.51968748	07956954
197	3181	3	1.00000000	.65310711	.29882154	03446162
198	2038	3	1.09000000	.61225521	.22436865	01943523
199	2098	3	1.00066990	.26111119	.14469570	00450610
200	2158	3	1.000000000	.50996716	.07138792	.06854683
201	2218	3 .	1.00000000	.45882313	.00688704	.01903789
202	2278	<u>-</u>	1.00000000	.40767910	04486726	.02597470
203	2338	3	1.00000000	.35653508	08581149	.02993111
204	2398	- 3	1.00000000	.30539165	11763927	.03138474
205	2458	3	1.00000000	.25424702	13995638	.03025327
20€	2518	3 .	1.00000000	.20310300	15271289	.02663158
207	2578	3	1.00000000	.15195897	15639994	.02076657
208	2638	3	1.00000000	.10031494	15125473	.01295248
209	2698	3	1.00060000	.04967092	13812576	.00352092
210	27 58	3	1.00000000	(0147311	11885687	00742094
211	2818	3	1.00000000	05261714	09451730	01973499
212	2878	3	1.00000000	10376117	06522286	03356966
213	2938	3	1.00000000	15490519	03168865	04905609
214	2998	3	1.00000000	26634922	.00592160	06639837
215	3058	3	1.00000000	25719325	.04313547	08864692
216	3201	3	1.00000000	31581404	.08964431	12344657
217	3205	3	1.00000000	45502321	.20879640	21826520
218	3208	.3	1.00000000	52633260	.27443774	27478171
219	3212	_3_	1.00000000	60412023	.34762324	338(6562
550	3253	5	0.000000000	.00048709.	00045682	.00046065
221	3250	3	1.00900000	55848627	.30511942	30210315
222	3225	3	1.00000000	52813482	.27602973	27669566
223	3225	5	0.00000000	.00048709	00045120	.00039066
224	3183	3	1.00000000	.70248789	.38602359	05195556 - 36859982
1225	3203	3	1.00000000	38722.85	.14875627	16859982 .0000437
226	410	4	0.00000000	0.60606000	00060578 00025747	.00009521
227	410	5	0.00000000	.09048709	13286260	00550557
228	410	3	1.00000000	.01596457	13200200	

^{*}Elastic modes start at Mode 3.

Table 8-5.—(Continued)

Row	Node	DOF	Mode 5	Mode 6	Mode 7	Mode 8
1	1020	1	00313472	04093259	.01294485	.01446483
2	1020	2	.00180415	00012027	00327211	00007031
3	1020	3	.12822397	21356674	.00108648	01173859
4	1020	4	.00022307	00029479	00004739	00000115
5	1020	5	: .00018325	.00095228	00003854	00008433
6	1027	6	00000527	.00001547	00000265	00000172
7	1070	1	01127640	04024554	.01685384	.03411850
8	1070	2	02721228	.05774231	00816101	00737947
9	1070	3	.08743667	22275891	00863547	.03569257
10	1070	4	00029031	.00083772	00015742	00016836
11	1070	5	.00055216	.00104633	00069238	00052805
12	1070	6	00000930	.00001676	000003369	000000096
13	670	3	39058935	11976175	00799195	03849764
14	663	3	32363369	06955588	.00016683	.00439703
15	652	3	02901628	.06677184	.00620518	.04249152
16	644	3	.23258980	.13906362	00433060	00086252
17	637	_	. 25876717	.04206434	03710098	07889191
18	792	3	.13276215	.05094774	05946078	07964125
19	784	3	09323872	.24002073	08538935	07147441
20	779	3	31565104	.47682908	12038140	07863470
21	775	3	47885041	.66016623	14934868	08481591
22	627	3	38731007	11736323	00767022	03674525
· 23	618	3	37357697	10269125	00479163	02228817
24	615	3	35535889	08884264	00249245	01019640
25	613	3	31588803	06659694	.00032143	.03513203
26	610	3	27381658	04537131	•00231570	.01645221
27	608	3	20007074	01187266	.00444577	.02874180
28	605	3	12700035	.02100493	.00572244	.03673826
29	603	3	06010510	.04962773	.00611119	.04004922
30	600	3	.04788459	•09431555	•00516144	.03843651
31	597	3	.15059493	•12743284	.00185165	.02448729
32	692	3	38398417	11487460	00733419	03490249
33	693	3	35873355	09987655	00445211	02053596
34	694	3	34726700	08543966	00225489	00901586
35	562	3	30741850	06338585	.00048357	.00589689
36	560	3	26408445	04264229	.00231833	.01617760
37	6 95	3	19118985	01014130	.00435233	.02781768
38	555	3	12082365	.02030557	.00552452	.03494490
39	553	3	05536004	.04806389	.00598412	.03850504
40	550	3	.04936078	.09083808	.00509565	.03687736
41	547	3	.15090219	.12339450	.00183807	.02294021
42	544	3:	.22412726	.12686276	00390469	00241575
43	541	3	.26437630	•1)419069 07250722	01223243 02087368	03189824 05344825
44	539	3	.27215994	.07259732		07236540
45	537	_3	.24870577	.03203280	03405633	07748768
. 46	5,36	3	.22001708	.01862944	04181125	01146166

Table 8-5.—(Continued)

Row	Node	DOF	Mode 5	Mode 6	Mode 7	Mode 8
	F 2/	2	.17436518	.01916430	04913767	07567356
47	534 476	3	.13411029	.03035843	05373524	07178100
48		3	.07943424	.06369086	05888108	06681405
49 50	716 713	3	.02601696	.10214232	06410146	06258991
51	712	3	03128649	.14901733	07013656	05895072
52	709	3	09237744	.20377208	07701106	05593082
53	708	3	15936601	.26791600	08533877	05363384
54	705	3	23103378	.34255451	09569701	05377498
55	704	3	31054323	.43036013	10839777	05645885
56	701	3	38910298	.52011116	12182901	06078240
57	700	3	47976707	.62448123	13831690	06581913
58	533	3	56266952	.71845843	15329906	06888044
59	85	3	34965819	08726377	00258676	01074655
60	82	3	30609070	06367297	.00029376	.00489325 .01833996
61	7 9	3	23794093	03354955	.00276166	.01833440
62	129	3_	24020853	03302991	.00297052 .06430758	.02578674
63	76	3	15363134	00209187	•00483367	.02576674
64	176	3	15390350	.00335844	.00525895	.02961105
65	73	3	06896423	.02615908	.00580145	.03527969
66	173	3	06370183	.04079064	.00482212	.02241834
67	50	3	.01028224 .02007999	.05504665	.00505395	.02723637
68	120	3	.03589972	.07754463	.00535819	.03509758
69	220	3 3	.10726556	.08691337	.00601921	.02834354
70	- 67	3	.10881157	.08752399	.00367175	.02112496
71	167	3	.13997994	.11618298	.00265261	.02451759
72 73	267 44	3	.11652435	.04638120	.00282516	.00445934
74	114	3	.15506654	.08135406	.00289718	.00732101
75	214	3	.17736404	. 09564330	.06029723	.00353785
76	314	· 3	.20958364	.11774904	00255409	00034078
77	41	3	.14968976	.04187521	.00140896	00548750
78	111	3	.16378831	.05069469	.00028857	00773657
79	211	3	.19236471	.06638828	00238897	01353015
80	311	3	.23344622	.08658423	00716740	02260436
81	58	3	.16647919	.02865820	00046343	01672420
82	158	3	.18295672	.03077142	00303452	02199620
83	209	3	·19652543 ~		00433467	02325246
84	309	3	.23060365	.05507606	01040189	03473756
85	409	3	.26134812	.05788945	01786857	04786127
- 86	207	3	.19269383	.01804181	00582720	02894976
87	307	3	.21851364	.31263520	01293554	04100510
88	407	3	.23691014	.01743534	02256297	05473445
89	. 55	3_	.15504209	.00534766	00148139	02314141
90	155	3	.17159605	03464274	00414427	02738286 02993357
91	295	3 .	.17993671	01217756	00616141	03933690
92	305	3	.19699756	03515672	01361702	03733070

Table 8-5.—(Continued)

Row	Node	DOF	Mode 5	Mode 6	Mode 7	Mode 8
93	405	3	.20228337	03259607	02544869	05489522
94	385	3	.19074067	01166673	03652148	06358798
95	454	3	.17224684	03539336	03180382	05131676
96	464	3	.11838500	00690070	04115304	04999850
97	474	3	.05993481	.04078851	04983109	04950776
98	484	3	.00034044	.09880448	05935592	05015042
99	493	3	14104863	.20859613	06635499	03534986
100	502	3	32579366	. 38802838	09044728	02886658
101	512	3	43177697	.52379534	11507286	04127897
102	522	3	52097043	.64174707	13654729	05278766
103	52	3	.12295049	02545657	00123317	02306924
104	152	3	.14475752	05715456	00262762	02428836
105	202	3	.15546277	07608782	00427856	02375976
106	302	3	.16394277	11377954	01616657	02186430
107	382	3	•14225172	09994565	02091621	02190434
108	452	3	.39718314	08272050	02494908	01439175
109	462	3	.01431883	01375936	03167956	00975585
110	482	3	14656854	.16498914	05298070	01293955
111	492	3	22514144	.26080486	06826911	01869872
112	179	3	.08081687	02706589	00031644	02695635
113	146	3		05743325	00011673	02047954
114	1.92	3	.12272834	11106249	00003986	01917167
115	200	3_	.13938092	14651678	00147142	01716601
116	298	3	•14252315	18929570	00370314	00462712
117	350	3	.12752515	20817234	00775896	.01351436
118	398	3	10567774	18846723	01143350	.01803091
119	819	3	.01916293	13368553	01072009	.03461071
120	816	3	08567470	01939532	/01351347	.03774978
121	470	3	18310195	•09694802	02403534	.03178080
122	810	3	24016505	.16016656	03269836	.03240011
123	808	3	31297865	.26215230	05191613	.01963978
124_	806	3_	41308340	•40395475	07914276	.00267863
125	8 04	3	51588234	.55124785	10808604	01403368
126	803	3	56815207	•62668648	12310378	02238474
127	801	3	63494379	.72310762	14229184	03309219
128	531	3	69945788	81571725	16057153	04347791
129 130	8 9) 8 8 7	3	.06647859	06943019	.00(81617	02077644
131		3	.09696126	13671101	.00169122	01866231
132	940 937	3 3	04676375 07978449	09407740 16964116	.00186727 .00310966	02060386 01783643
133	1023	3	.11977439	24369707	.00275606	00883271
134	878	3	.12325971	26755176	.00273000	.01716985
135	876	3	.11618993	28613605	00134977	.03149569
136	928	3	.10841751	33839458	.00457522	.03742861
137	926	3	.10200721	35371622	.00437322	.05113095
138	1063	3	.06281516	24483260	66657578	.05145109
		•	- TUCKULIZO	TE TTOSEON		**************************************

Table 8-5.—(Continued)

Row	Node	DOF	Mode 5	Mode 6	Mode 7	Mode 8
139	916	. 3	%10193090 ·	08969149		.07622631
140	915	7 3	23025829	. 03638873	.00049043	.07376715
141	908	3	33897999	.21667162	03296145	.05762985
142	906	3	44376350	.36858186	06301117	.03837971
143	904	3	55155386	.52702504	09466156	.01854007
			66423419	.69493479	12881140	00162337
144	902	3	75639277	.83552074	15857995	01627290
145	920	3_	Accessed to the control of the contr	.94350614	18694921	02808423
146	900	3	82839031	30741459	.00495806	00410710
147	1021	3	.11017945		.00024749	.09133642
148	1061	3_	.02398718	32591695	.01343978	.10434416
149	965	3	24060447	.02704272	* * * * * * * * * * * * * * * * * * * *	.06526718
150	957	3	40389308	.27234617	03943374	.03413260
151	954	3	56843959	.51525068	08818790	.00248272
152	951	3	74762443	.78673263	14454223	
153	950	3	88789402	1.0000000	18947211	02009252
154	767	3_	•12968641	.04563503	05778187	07652399
155	766	3	.08424590	•07545535	06243691	07318545
156	763	3	.02900351	.11771565	06815704	06984456
157	762	3_	02991632	.16817112	07470178	06729694
158	759	3	09292738	.22725923	08244264	06600472
159	758	3	16184140	.29564818	09176173	06572307
160	755	3_	23470405	.37304556	10310421	06761422
161	754	3	31385922	•46049732	11617852	07684586
162	751	3	39062913	.54710167	12948892	07443965
163	750	3	47915212	.64758286	14547411	07811410
164	237	2	00947229	.01119128	.00041267	.00045976
165	235	2	.00210893	02820491	.00953926	.01186027
166	232	2	.04157675	14024194	.04562217	.06858440
167	229	2	.07150849	26043647	.12256842	.26911378
168	227	2	.09765875	37345432	.19887739	.48649467
169	226	2	.12567585	49987912	.28713881	.74693119
170	475	2	01278621	.02397795	00289760	00353654
171	285	2	00448652	00852026	.00387691	.00235223
172	282	2	.02900562	10935117	•03866563	.05940477
173	472	Ž	02399786	.03651723	00189127	00022426
174	332	2	.00323209	04587446	.02424550	.04003922
175	329	2	.05064145	20901105	.11077718	.2521950C
176	277	2	. 48684587	34661599	.19258284	.47748842
177	862	2	03962725	.05599082	.00046657	.00511215
178	379	2	.00637713	09926202	.08504134	.21401585
179	377	2	.05424130	26513353	.17295643	.44797207
180_	376	2	.09093922	39728183	.24628118	.65082235
181	375	2	.12872189	53451176	.32309169	.86537698
182	428	2	03661491	01464773	.08841286	.26724018
183	427	2	.00069940	12993470	.13903741	.39315282
L		<u>Z</u>	.06451354	33156816	.23082853	.62869699
184	426	۷,	**********	, , , , , , , , , , , , , , , , , , , ,	• = 	

Table 8-5.—(Continued)

Row	Node	DOF	Mode 5	Mode 6	Mode 7	Mode 8
185	424	2	.09296291	42145093	.27167987	.73344944
186	417	2	03540412	03736658	.11432299	.34938437
187	416	2	.02858985	24105461	.20844307	.59340855
188	415	2	.09577176	45474572	.30663663	.84749177
189	414	2	.13240091	57416081	.36361531	1.00000000
190	374	3	30532829	.17651172	.71082004	00708493
191	374	1	.05443909	.03777696	1.00000000	10325103
192	471	5	.00143078	00050502	00012601	00045318
193	3191	3	1.00000000	.29020919	.02519929	.14083102
194	3189	3	.65052179	.16908037	.01311640	.06664468
195	3187	3	.38933317	.07763930	.00419717	.01347851
196	3185	3	.16097816	.00352012	00275057	02561978
197	3181	3	13977472	08284764	01006937	06057392
198	2038	3	23043973	10502234	01142375	06426834
199	2098	3	30488271	11908631	01180223	06244678
200	2158	3	35732176	12469571	01079049	05497704
201	2218	3	38224691	12022842	00871219	04223899
202	2278	3	37610773	10643549	00574587	02679124
203	2338	3	34630503	08617381	00265628	01094132
204	2398	3	29764405	06122644	.00013768	.00390070
205	2458	3	23069807	03276347	.00242982	.01587758
30£	2518	3	15167554	00419938	.00398814	.02312886
207	2578	3	06978930	•02053452	.00475139	.02516061
208	2638	3	.00595514	.03699733	.00462679	.02122016
209	269 8	3	.06692933	.34370552	.00389202	.01357164
210	2758	3	.11479524	.04422220	•00279832	.00420146
211	2818	3	.14620491	.03936700	.00158881	00521305
212	2878	3	.15609578	.02694934	.00049784	01359554
213	2938	3	.14264268	.00927541	00030285	01905104
214	2998	3	.10883527	00817617	000586LC	02083991
215	3058	3	.05483149	01119123	00052763	02072496
216	3201	3	05464648	.00866919	00033660	01702054
217	3205	3	40654178	.03718458	.00082816	.00738025
218	3208	3	64181039	•14954234	.00181372	.02866661
219	3212	3	91136014	•22297646	.00299267	.05448411
220	3253	5	.00172140	00047442	00000767	00016961
221	3250	3	76166924	•18334956	.00236339	.04081416
222	3225	3	64688998	.15075243	.00183174	.02903428
223	3225	5	.00164417	00044141	00000703	00015285
224	3183	3	03000169	05340933	00775164	05078462
225	3203	3	21215143	.03982257	.00010614	00782300
226	410	4	.00005080	.00004510	00000422	0000399
227	410	5	00021769	.00021441	.00002327	.00016544
228	410	3	.13004857	.07828306	.00422565	.01673362

Table 8-5.—(Continued)

Row	Node	DOF	Mode 9	Mode 10	Mode 11	Mode 12
1	1023	1	.02696501	01455468	06899450	.12440528
2	1020	2	02736661	.00479122	.01666985	03229600
3	1020	3	.09242949	02160619	.06643277	.31707276
4	1020	4	00057012	.00005091	.00039127	.00030372
5	1020	5	00049777	.00017127	00004410	00224764
6	1020	6	00001375	.00000533	.00000568	00006958
7	1070	1	.00244060	01376413	11145402	04502133
8	1070	2	01494618	.01007554	.05614457	04381302
9	1070	3	11025247	.00164039	06443409	13615634
10	1070	4	00066252	.00018465	.00131962	00616168
11	1970	5	.00002690	.00014413	.00206900	.00145710
12	1070	6	00000110	.00000338	.00601044	00001722
13	670	3	.00671467	.01470718	03279601	00075034
14	663	3	.00291601	00635653	.14163868	03805343
15	652	3	03693978	01376479	02244829	.21982228
16	644	3	12223243	.01869808	16667947	.51225267
17	637	3	20478976	.04556601	.35192205	.19775155
18	792	3	23318605	.04209220	.47267363	.13307459
19	784		11929708	.03115366	.40441419	.15334882
20	779	3	.04404779	.00738559	.29410943	.22406282
21	775	3	.18061468	31170636	.19752585	.29649534
22	620	3	.00655110	.01388465	02696401	00205676
23	618	3	.00538422	.00663149	.03669976	01647993
24	615	3	.00439625	.00065124	.08756589	02810829
25	613	3	.00283687	00656380	.13937501	03778223
26	610	3	.00065140	01130494	.15591466	03234327
27	698	3	00425931	01527504	.13514580	00015473
28	605	3	01341069	01631638	.08111834	.06668386
29	603	3	02499809	01491043	.01813640	•14492139
30	600	3	05319783	00829767	09743813	.31058197
31	597	3	08759067	.00369434	1783C815	.45714756
32	6 92	3	.00637733	.01301786	02675582	06344716
33	693	3	.00521586	.00583859	.04126899	01742606
34	694	3	.00425295	.00023074	.08669108	02786017
35	562	3	.00275346	00676964	.13667849	03744789
36	560	3	.00090634	01100503	.14930342	03352345
37	695	3	00357028	01475463	.12931465	00452059
38	555	3	01117307	01571109	.08138613	.05095306
39	553	3	02144122	01462561	.02161530	.12217988
40	550	3	04684414	00832944	09225101	.27587742
41	547		; 08949403	.00358703	17411305	.42145761
42	544	- 10 T	10376602	.01709526	14416937	.42680389
43	541		12295135	.0293G180	01668520	.33801080
44	539		14558253	.03668895	.12994060	.25399132
45	537		18619663	.04192859	.31907387	.17411162
46	5.36	3	20846098	.04267549	.39903879	.14803571

Table 8-5.—(Continued)

Row	Node	DOF	Mode 9	Mode 10	Mode 11	Mode 12
47	534	3	21902757	.04107010	• 42953353	.12975055
48	476	3	21577742	.03934373	.42880963	.11718670
49	716	3	19828210	.03727683	.41382140	.11054212
50	713	3	17547302	.03539605	.39605807	.10878411
51	712	3	14566373	.03326360	.37576969	.11243709
52	709	3	10867904	03068061	.35226287	•12169133
53	708	3	06349743	.02728022	.32454784	.13750635
54	705	3	01014999	•02172457	•29164733	.16089356
55	704	3_	•05362855	.01299250	.24758091	.19026151
56	701	3	.11976785	.00232120	.19693930	.22057527
57	700	3	.19791470	01030635	.13617190	.25729984
58	5 3 3	3	. 27043953	02078783	.67978659	.291(5164
59	85	3	.00437701	.00110936	.07866446	02601742
60	82	3	.00304906	00624902	•13239245	03859827
61	79	3	.00149985	01172197	.14555783	03996853
62	129	3	.00065352	61240728	.15134142	03526716
63	76	3	.00045380	01363323	.11137271	03618316
54	176	3	06438272	01512867	.11114765	.00227867
65	73	3	.00041319	01391052	.06752972	02120351
66 67	<u>173</u> 50	3 3	00986436 .00876467	- 01000108	•04988113	05582163
68	120	3	00283124	01038758 01014935	.01698961 01737207	.01854715
69	220	3	02708041	01017245	06699442	.17084925
70	67	3	.01661006	C0918296	18509636	11443594
71	167	3	01881439	00318594	11169661	.11160441
72	267	3	06581600	.00131725	17542406	.36797614
73	44	3	.02573460	00259912	02014048	11799415
74	114	3	.00935510	.00062902	12311111	04986498
75	214	3	03543699	• ₩0689729	12436100	.15448287
76	314	3	08357573	.01404074	14169150	.35221852
77	41	3	.03217162	.00119518	02754927	13246747
7 8	111	3	.01714023	.00419424	03785411	08688710
79	211	3	01621015	.01078970	04692760	.01716052
80	311	3	07130781	·62650960	03927392	.19118136
81	58	3	.03806902	•00501665	00982939	15117978
82	158	3	.01329010	.06956607	.06826153	10239502
83	209	3	00771793	.01239615	.00415933	04612752
84	309	3	06401003	.02281555	.04268930	.09179039
85	409	3	12352878	.03294159	.10174588	.21538448
86 97	207	3	00358607 06002708	.61336423	.04366851 .11467777	07663177 .02953437
87	307 407	<u>3</u>	12402603	.03201351	.20493255	.11568850
88 89	407 55	3	.04823218	****	. 20493299 5 • 01084842.	15825340
90	155	3	.02077801	.00935009	.03846418	11748627
91	205	3	.00126880	.61157757	.06669115	08165597
95	305	3	05640786	.01837247	.14735361	.02150233
()		-	2.2.2.2.7			

Table 8-5.—(Continued)

Row	Node	DOF	Mode 9	Mode 10	Mode 11	Mode 12
93	405	·3	12657988	.02874848	.27408033	.09076134
94	385	3	17733557	.03560153	.34677459	.10813858
95	454	3	15568492	.03040753	.29400964	.07945727
96	464	3	17094460	.03151022	.31858350	.07410538
97	474	3	16455684	.03146190	.32692972	.07427432
98	484	3	14618370	.03162312	.33476322	.085715 73
99	493	3	04703197	.02250231	.23135728	.08765189
100	502	3	.10228789	.00601232	.10537018	.13141801
101	512	3	.17896805	00478590	.08195461	.19241585
102	522	3	.24750961	61568674	.05425427	.24467469
103	52	3	.06543899	.00182537	.01859785	11339963
104	152	-3	.04504679	.00162850	.04277308	03875166
105	202	3	.02295312	.00259867	.05962422	.00152925
106	302	3	04343298	.00803081	.10550591	.03937296
107	382	3	11899720	.01900464	.166(8078	.01360572
108	452	3	12941125	.02027538	.15715214	01200519
109	462	3	10868504	.02097422	.14565336	01739655
110	482	- 3	01801318	.01814573	.12768293	.03672135
111	492	3	.03283204	.01409308	.12041918	.07591431
112	179	3	.07546870	00035744	.01107056	10456939
113	1.46	3	.07918811	00339987	.02699687	04123835
114	192	3	.07824640	00858654	.04167278	.08314627
115	200	3	.05741556	00957435	.06033482	.15253116
116	298	3	00504305	00599520	.03985524	.09407735
117	350	3	07859775	.00048920	.00087778	03375289
118	398	3	10713749	.0613493	.06389312	08481360
119	819	3	09531618	.01251569	02978648	13637586
120	816	3	02920609	.01569387	04702350	10823985
121	470	3	.03511709	.01041831	06881574	07005518
122	810	3	.07974678	.00811931	09179981	04734281
123	808	3	.12844585	00610420	09815288	00192640
124	8 0 5	3	.19974235	01050674	10521304	.06762213
125	804		.27762910	02016873	11076790	.14645712
126	803		.31864272	02486069	11334779	.18868574
127	801	3 .	.37103284	03086727	11649512	.24275628
128	5 3 1	3_	.41994116	03650103	11764064	.29371677
129	890		.09947427	00664297	.02052353	02646425
130	887		.11113164	01469562	.04094899	
131	940		.12086471	01115452	.02349475	.01624676
132	937		.13712593	02072496	.04441873	.19111867
133	1023		.11304273	02765453	.06437489	.38649960
134_	8 7 8		.00765985	61737374	03(99424	.11345759
135	876		04488840	01344141	07193588	.01431858
136	928		.01099755	02656170	10063630	.12013385
137	926		04190705	02245682	13998452	.01789472
138	1063		11333246	00113364	12015112	18279352
						*

Table 8-5.—(Continued)

Row	Node	DO	F Mode 9	Mode 10	Mode 11	Mode 12
139	916	3	.00314998	.01308642	19478216	19534844
140	915	3	.07166144	•01693226	18968464	14477641
141	908	3	.17406231		21766632	06102653
142	906	3	.25269348	00939596	23224429	.01382218
143	904	3	•33880933	02235159	24748533	.09900016
144	902	3	.43735311	03611048	27095315	.19617423
145	920	3	•53267233	04719990	30468346	.26789778
146	900	3	.60001449	65521423	32116280	• 35455274
147	1021	3	•14574489	03905943	.07367052	.55093888
148	1061	3	11731177	01223312	27788509	29470940
149	965	3	•11863067	•01949052	30209776	20205999
150	957	3	.23481128	66192784	28233361	05191205
151	954	3	•36785050	02338929	313(3252	•67595329
152	951	3_	•53982519	04686374	36894664	.24184054
153.	950	· -	•68122754	06332557	41414297	.37962126
154	767	3	22612504	.04131022	•45643131	•12691914
155	766	3_	21107069	.03979333	• 44631593	•12277899
156	763	3	18629464	.03762366	•42995196	.12361675
157	762	3	15460580	.03490930	•41044488	.13009976
158	759	3_	11557810	.03099526	.38611753	•14222199_
159	7 58	3	06886167	.02581251	•35646988	•15973268
160	755	3	01514894	.01855995	.32144812	•18339692
161	754	3	.04740722	.06935329	.27778733	.21219628
162	751 750	3	.11098383	06630182	.23131512	.24208725
163	750 237	3 2	.18668241	01117630	.17611030	.27889646
164			.01489073	00029051	00908614	02685010
165 166	235 232	2	•02565942	00405485 .02946368	07010550	06775234
167	229	2	•23133024	• 22986457	11707622	13423611
168	227	2	• 45024954	.45293238	.08194793	.06346337
169	2 26	2	.71687699	.72325150	.63640242	•31071878 •62520749
170	475	2	.00676098	.00154200	.01347207	01867002
171	285	2	.01592305	00785646	05451899	06454984
172	282	2	.04077959	.02693187	09966505	11531673
173	472	2	.026 91 846	.00245961	00535647	02926399
174	332	2	.04784444	.02116424	06460291	07723823
175	329	2	. 23608077	.22376051	.10831631	.09193227
176	277	2	•45264179	.44961502	.34106567	.32592999
177	862	2	•05419573	·C0574172	02503574	 03465691
178	379	_2_	· 24380024	.20840687	. 16169411	•14969746
179	377	2	• 45 7229 21	•43701390	.37991876	. 368 21145
180	376	2	.64750611	.63866429	•58503695	•57566318
181	375	2	.84969376	.85272845	•805E2590	.79955444
182	428	2	.35626012	.29301582	.34356645	.33793208
183	427	2^	.45755795	.40922391	.43378430	•42723344
184	426	2	.65341025	.63051968	.61971017	•61329793

Table 8-5.—(Continued)

Row	Node	DOF	Mode 9	Mode 10	Mode 11	Mode 12
185	424	2	.74029030	.72885456	.70202506	.69566066
186	417	2	.44981738	.38280696	.45906791	.45545241
187	416	2	.65559889	.61365989	.65891162	.65615088
188	415	2	.86836699	.85341670	.86411508	.86206817
189	414	2	1.00000000	1.00000000	1.00000000	1.00000000
190	374	3	.08065251	00127883	16354826	10769690
191	374		10238079	00656725	.17068535	.09241676
192	471	5	00128350	.00010492	.00228163	.00067993
193	3191	3	01900631	06499356	.56061164	-:11998229
194	3189	<u>3</u>	00861470	02948636	.21591984	04470191
195	3187	3	00121672	00430622	02209605	.00584873
196	3185	3	.00415884	.01383030	17846312	.03822247
197	3181	3	.00884774	.02899830	26937783	.05440681
198	2038	3	.00924768	.02986204	24489165	.04777968
199	2030	3	.00924700	.02811975	20026334	.03662142
200	2158	3	.00835186	.02305018	13023532	.02207322
201	2218	3	.00705135	.01681082	05829278	.06479477
202	2278	3	.00566767	.00898470	.01393052	01110965
	2338	3	.00431943	.00133715	.07331068	02474227
203	2398		.00308618	60541251	.11462563	03528011
204		3 3	.00228381	01027455	.12552568	04041949
205	2458		To the second se	01253864	.10547454	04232463
206	2518	3	· 00257610 • 00486437	01239153	.06801686	04815480
207	2578	3 .		00996035	.02773622	06657062
208	2638	3	.01028524	00998039	.02773022	09516946
209	2698	3	.01823565		01536575	12130298
210	2758	3 3	.02673168	00282338 .00061464	02307595	14005183
211	2818		.03500539	.00282388	01526939	15499373
212	2878	3	.04521454	•00329848	00279593	15433453
213	2938	3	.05610543	.00327676	.00581415	13530975
214	2993	3	.06593695	manufacture and the second sec	.00567062	12466181
215	3058	3	.06880566	.0(11961) .00120865	.00878628	11838874
216	3201	3	.05713976		00148781	02243154
217	3205	3_	01724455	.00030958	01389458	.06823029
218	3208	3	08349637	00027695 00097151	02970378	.18236615
219	3212	3	16429262	•00097131	.06016634	00076685
220	3250	5	.00053239		02166935	.123(6370
221	3250	3	12166944	00058912	01405230	.06952302
222	3225	3	08461175	00028866	.00009109	00066245
223	3225	5	.00047697	.00000417	25588565	.05300599
224	3183	3	.00754794	.02501746	.00612253	08292393
225	3203	3	.02948282	.00078267	00006226	.00027214
226	410	4	00006826	.00001164	00006226	.00027214
227	410	5	00007177	00005166	14618089	10036550
228	410	3	.01778722	00463054	11010003	- • 10030330

Table 8-5.—(Continued)

Row	Node	DOF	Mode 13	Mode 14	Mode 15	Mode 16
1	1023	3	.01590217	.24937640	46133774	14191312
2	1020	2	.02138088	02613737	.01940364	.01085639
3	1020	3	.14656150	00080717	.08210176	.07628983
4	1020	4	.03068161	.00027250	.00061561	.60083097
5	1020	5	00129631	00004402	.00020445	.00022593
6	1020	6	00002025	00005827	.00005252	00000212
7	1070	1	13545088	.29164768	44031146	12912678
8	1070	2	•07349995	11941160	20584382	17436383
9	1070	3	01892490	03586309	.03102852	00233484
10	1070	4	.00178691	00151359	00322023	00228516
11	1070	5	.00165859	00034079	00012446	.00047648
12	1070	6	.00001173	00003659	00005798	00006199
13	670	3	04002423	.12618319	•19130598	30676141
14	663	3	08590493	.14008655	.12427102	25157295
15	652	3	13526117	40553773	16561629	.16320659
16_	644	3	46721819	.10212800	.19213940	45037489
17	637	3	.20179725	.17977472	23581538	11064149
18	792	3	.54747084	07527248	72354611	24850149
19	784	3	.51407914	07117452	84277127	30286805
20	779	3	.34779247	.07780150	74517924	21002160
21	775	3	.17683988	.24445289	59565517	08646439
22	620	3	04056678	.12424398	.18715957	29961645
23	618	3	05970498	.15048175	•17955872	31845378
24	615	3	07326724	.15921394	•16459418	30977148
25	613	3	08247062	.13415259	•11794653	23739241
26	610	3	07781155	.15668363	.04251221	10071198
27	608	3	06277360	09701215	07288973	.10766350
28	605	3	06665335	25142775	15310193	.22344207
29	603	3	09057172	34467146	17262414	.21969993
30	600	3	19176602	38731793	09549213	.01267956
31	597	3	35022878	20862468	.06918661	30031573
32	692	3	04115950	•12220073	.18279207	29204566
33	693	3	05938535	.14660417	.17244818	30692410
34	694	3	07001086	.15103799	.15523137	29108228
35	562	3	07860459	.12761568	.11105529	22181126
36	560		07103643	.05721436	.04047580	09046415
37	695	3	05526430	08577062	06838114	.10832697
38	555	3	05481334	22160572	14353922	.22313198
39	553	3	07179528	32143191	17367126	.24287631
40	550	3_	15636774	36640166	09738997	.03635647
41	547	3	31529864	18420713	.07214710 .17387803	38211582
42	544		39509414	.12765631 .33833283	.15978566	28687348
43	541	3_	32824177	•34725006	.05099666	10163367
44	539		15374335 .17220438	.17581318	20368463	08766376
45	5.37	3	.34814282	.04715524	37319296	10628303
46	5 36	3	• 57017202	• V T 1 I J J & T	131317670	

Table 8-5.—(Continued)

TI JUT D TOTAL STATE OF THE STA	665479
	3843460
49 716 3 .49951474088542406760494523	3802164
50 713 3 .49491811096789767088856925	886481
51 712 3 .48182002095558707339708727	7322642
	7751375
	967658
	469573
	9470748
701 3	2736535
	3802170
20 733 3 7575 2 7576 2 7	032892
11011242 = 20	2974907
01 02 01 01 01 01 01 01 01 01 01 01 01 01 01	2971859
	2858302
	586773
	3656464
	3324234
	4337661
67 50 3 .079558780673950010876276 .27	7037708
68 120 3 .059540641550038010741895 .21	L419517
07 220 3	1017219
70 67 3 1.00000000 .04185944 .1740336350	9704214
11 101 3 103032721	3985387
72 20, 3	7775025
15	2751493
11, 3	0110758
	4918555
	2602360 7997186
	2388525
	2952920
	4104262
00.	7404176
	5965547
83 209 312676720 .21489515 .02793445 .13	2895752
	0145111
	2314558
86 277 310471216 .14560180 .02851899 .1	5154543
87 307 305876197 .19020970 .0376180509	9255052
88 407 3 .03102485 .2043999004866465 .0	0192991
89 55 312445708 .0100030602686704 .0	9233859
90 155 311191875 .04863353 .03565025 .1	3194427
91 20) 3	3894744
92 305 3 .03081047 .06816129 .05089101 .1	2057282

Table 8-5.—(Continued)

Row	Node	DOF	Mode 13	Mode 14	Mode 15	Mode 16
93	405	3	.21459385	00495265	06835633	.04959947
94	385	3	.32545458	01907759	28029439	05812641
95	454	3	. 28241535	04244356	20134326	02962700
96	464	3	.35895702	07350559	38104470	11746271
97	474	3	.39667515	09120624	50249176	17957968
98	484	3	.42351320	09891570	59983679	22495233
99	493	3	.29724785	06435976	47246962	17858428
100	502	3	.10695336	.05487701	27208438	06402368
101	512	3	.04739162	.16562031	27776066	01779187
102	522	3	01991505	.27172347	25068556	.03851281
103	52	3	12363494	08215957	01964793	04204001
104	152	3	07839731	02710076	.05842242	.05484296
105	202	3	03513900	.00086980	.09887273	.10649304
106	302		.05689519	.00267531	.11200045	.12595644
107	382	3	.16940798	06601805	03970414	.01867570
108	452	3	.19002411	09586202	11781134	04231786
100	462	<u>3</u>	.19657458	11903529	17428769	09079667
110	482		.16653629	07862111	21308030	09871429
		3	.14673245	03081337	24320495	09020804
111	492	<u>3</u> 3	12959133	13249571	05451726	15806327
112	179		09149046	10489276	01200118	09220692
113	1.46	3	01276552	04881904	.05534805	.01505602
114	192	3_	.05041689		.09728799	.08768022
115	200	3		00761593	.17047962	.13847148
116	298	3	.04854809	.00053945		.09233183
117	350	3	• 32204827	01357051 04810566	•12591652 •03476092	.01738383
118	398	3	.03575207			04667652
119_	819	3	.01923804	13466213	.05144788	01782858
120	816	3	01784782	15997055	.16658244	
121	470	3	06385698	12879706	•22720319	.01602978
122	810	3	10788879	09104178	.27201068	. 04673463
123	808	3	13756644	02187758	•26089465	.07354700
124	8 0 5	3.	18103623	.09146276	.23548655	•11603053 •16617925
125	804	3	22879852	.22678926	.20049343	.19432890
126	803	3	25456781	.30159612	.18143167	.23002607
127	801	3	28718616	.39730912	.15605924	.25833757
128	531	_ 3	31337517	.48317270	.12344674	23269072
129	890	3	11402739	19064620	04512319 .03060034	10913487
130	887	3	01742587	13557228		32435326
131_	940	3	11524450	25389473	05421977	19199917
132	937	3	00569103	19566600	.02436412	.06243006
133	1023	3	.18238121	00516321	.07556574	
134	87 8	_3_	.03545081	00568157	.25627113	.16473184
135	876	3	00098898	01017987	.27528148	.21009401
136	928	3	.01811060	01125684	.36998394	
137	926	_ 3	01742388	01554512	.38655739	.20809610
138	1063	3	05850051	04247857	•02479944	03039929

Table 8-5.—(Continued)

139 916 3 178871J4 23571588 .47480266 140 915 3 20634975 19919865 .54775514 141 908 3 28236461 04946303 .53424341 142 906 3 34510433 .08321714 .53945961 143 904 3 41751699 .24589952 .54308477	.05706309 .08515249 .14646718 .20905212 .28643447 .40(75095 .55213062 .64003448 .05133770 06481671
140 915 3 20634975 19919865 .54775514 141 908 3 28236461 04946303 .53424341 142 906 3 34510433 .08321714 .53945961 143 904 3 41751699 .24589952 .54308477	.14646718 .20905212 .28643447 .40(75095 .55213062 .64003448 .05133770 06481671
141 908 32823646104946303 .53424341 142 906 334510433 .08321714 .53945961 143 904 341751699 .24589952 .54308477	.20905212 .28643447 .40(75095 .55213062 .64003448 .05133770 06481671
142 906 334510433 .08321714 .53945961 143 904 341751699 .24589952 .54308477	.28643447 .40(75095 .55213062 .64003448 .05133770 06481671
143 904 341751699 .24589952 .54308477	.40(75095 .55213062 .64003448 .05133770 06481671
170	.55213062 .64003448 .05133776 06481671
144 902 351885955 .45572660 .58350851	.64003448 .05133770 06481671
145 920 364732918 .69062410 .68867465	.05133770 06481671
146 900 372260330 .84361874 .72894279	06481671
147 1021 3 .28142753 .00493308 .05489410	
148 1061 31869903000828048 .02866859	77
149 965 33564295627232991 .91674528	.16762169
173 02445	.21397285
150 957 338400692 .00333081 .67163665 151 954 350814259 .25446598 .70890739	.34433771
152 951 372326362 .65567504 .86248982	.59224598
153 950 390567692 1.00000000 1.00000000	.80812993
154 767 3 .529070240747294069363328	23657218
155 766 3 .537423850907535174083624	26337096
156 763 3 .533896660972097577712148	28358805
157 762 3 .520654050929032280201006	29517465
158 759 3 .494569650754007180880154	29403306
159 758 3 .455957770443005279998096	28091487
160 755 3 .40329189 .0039505977269988	25258975
161 754 3 .33101874 .0700192771467945	20473236
152 751 3 .24990084 .1447483563856902	14605776
163 750 3 .15013182 .2408062554355128	07129998
164 237 2012666670290352402391732	03291976
165 235 20903519404201457 .11575796	.00278865
166 232 21501027913179288 .27435798	00377340
167 229 20445544507087593 .19617423	.02142699
168 227 2 .10088888 .02711546 .04706272	.05063994
169 226 2 .29230981 .1637589516656816	.08872054
170 475 2 .016624610329973307738317	05578317
171 285 20668971004775793 .06440616	02117931
172 282 21341139911426405 23083528	00996888
173 472 2019256150385216303523697	05496888
174 332 21015800507860914 .14178428	02279363
175 329 20192904104269644 .11979549	.00779115
176 277 2 .11462121 .04269220 .00481663	.04317102
177 862 20637309803825548 .02584057	
178 379 2 .03310995 .0165794904328920	02227680
179 377 2 .15374334 .0878834312020989	.05962368
180 376 2 .27420415 .1662917421604898	
181 375 2 .40590024 .2536320232369979	.10360425
182 428 2 .16734592 .1386514932909622	05138320 01996535
183 427 2 .21086419 .1561995231622485	.04088308
184 426 2 .30836023 .2052262032188333	• 0400000

Figure 8-5.—(Continued)

Row	Node	DOF	Mode 13	Mode 14	Mode 15	Mode 16
			(A companie)			.06846787
185	424	2	.35144341	.22660058	32281773 43609072	04792090
186	417	2	•24142314 •34920973	•19528592 •25367766	45922296	.61379764
187	416	2		A MANAGEMENT AND A STATE OF THE		.08110165
188	415	2	.45901382	•31099548 35067775	47205682 50542148	.12455367
189	414	2	•53859339	.35967775		
190	374	3	17828794	26317410	.68518598	.13731578
191	374	. 1	.17244498	.13174555	42322331	08101973 06149332
192	471	5	.00290381	. 30005904	00498126	66928167
193	3191	3	17955264	.24651244	.58932502	12346889
194	3189	3	05128146 .03081711	.05109845 06813932	.11887436 16162028	.20130496
195 196	3187 3185	3	.07793900	12874811	29328659	.35396242
197	3181	3	.08777368	12127411	23909920	.29667197
198	2038	3	.06369512	06668724	10679330	.13224041
190	2035	3	.03675480	01502127	.01139453	01239671
200	2158	3	.00426401	•04719317	.10584405	15458765
201	2218	3	02762078	.10044140	.17027385	25956192
202	2278	3	05082759		.17754949	29784319
203	2338	3 	A photograph for a contract of the contract of	•13382366 •13863004	.14962921	27098374
203	2398	3	06250881	.10986807	•09790052	17957963
205	2458	3	06028537 03877159	.04543321	.01970580	02205019
206	2518	3	00287003	02569569	05709826	.14239036
207	2578	3	.03720848	06872212	10578645	• 25670623
208	2638	3	.05720040	05120092	10530663	.27689290
209	2698	 3	.07284887	0120072	09130435	.26882891
210	2758	3	.04931028	.03489721	07333478	.24139917
211	2818	3	.00830457	.36027264	05676146	.19384123
212	2878	3	05337189	.04547464	05381825	.14317697
213	2938	3	10110914	01302872	05322039	.04683089
214	2993	3	12458760	08671029	05696500	08676862
215	3058	3	15060331	15397638	08160342	22983502
216	3201	3	18416561	24209501	13437624	45716645
217	3205	3	05333384	11370757	06903447	25425789
218	3208	3	.12816852	.14375191	.06569917	.26217085
219	3212	3	.36939602	.50323490	.25603937	1.00000000
220	3250	5 :	00166304	00254184	00135529	00527733
221	3250	3	.24930868	•32966533	.16449935	.64867219
222	3225	3	.12970510	.14436201	.06580711	.26174327
223	3225	5	00135705	00196264	00103146	00397007
224.	3183	3	.09274320	13785742	29324192	.35697196
225	3203	3	15466787	23596574	13135565	47909433
226	410	4	00030266	•00006484	.00010380	00015613
227	410	5	.00423859	00035936	.00095892	00336652
228	410	3	.62447487	.05687475	.10929934	32130819

Table 8-5.—(Continued)

Row	Node	DOF	Mode 17	Mode 18	Mode 19	Mode 20
1	1020	1	02314168	.04478124	03951053	04928244
2	1020	2	.01575665	.01438686	.00120003	02248158
3	1020	3	02276216	00370230	.01073736	• 01544605
4	1020	4	.00046649	•00045998	.00000512	00049870
5_	1020	5	.00045798_	•00001492	00041502	00035788
6	1020	6	.00001332	.00000054	06060298	00001028
7	1070	1	.01258850	.00809172	04396339	03846238
8	1070	2	13712158	03123729	00099305	.08143452
9	1070	3	.02015366	03405190	.01849936	.02956109
10	·1070	4	00192479	00013747	00008309	.00092424
11	1070	5	00000350	.00080869	00040358	00076047
12	1070	6	00004246	00002376	.00000781	.00004538
13	672	3	01957339	18369989	35196679	05718703
14	663	3	00392009	.02504426	.005C5913	.02039269
15	652	3	.03423388	04503851	08954375	05963992
16	644	3	00072927	.10585896	02197266	.05695571
17	637	3	.06671431	.17524311	02468738	04650415
18	792	3	•03100599	17204478	.03475469	01549524
19	784	3	.00996895	29862127	.06492232	.00000205
20	779	3	.11758510	40304965	.10277053	.06280362
21	775	3	.25908314	48905080	.14269749	.16530387
22	620	3	01892095	17590867	04954884	05439336
23	618	3	01657661	12869158	03724262	03703169
24	615	3	01264585	07103760	02107053	01497763
25	613	3	00388726	.02454393	.00567053	.01987076
26	610	3	.00735638	.09569898	.02098589	.03711995
27	608	3	.02120934	.11813924	.01209141	.02364172
28	605	3	.03053944	.07018697	02459979	01375762
29	603	3	.03238965	.00165837	06007179	04334397
30	600	3	.02339508	11526088	10575856	06191079
31	597	3	.00377929	09703767	07950427	00939242
32	692	3	01821320	16739078	04689937	05130991
33	6 93	3	01574500	11993951	03460255	03416121
34	694	3	01268652	06751432	01958341	01438150
35	562	3	00387915	.02354446	.00625817	.01915614
36	560	3	.00590624	.08758648	.02146453	.03508088
37	695		.01862881	.10961484	.01445828	.02342526
38	555		.02693711	•07229967	01500658	00794677
39	553		.02993570	.00883210	04920214	03920867
40	550	and the real control	•02065950	11737024	09723691	06247849
41	547		00010957	10051682	06677618	00633977
42	544	and the latest and th	00653826	.10141387	.00204731	.05831355
43	541	3	.01451502	.28200897	.01016914	•05597476
44	539		.04279940	.30947807	01321151	.01023262
45	537		.06316822	.16813690	02684190	04541400
46	536	and the second	.05803698	.04070987	01460850	05182945

Table 8-5.—(Concluded)

Row	Node	DOF	Mode 17	Mode 18	Mode 19	Mode 20
47	534	3	.04704685	07521295	.01053099	03729131
48	476	3	.03277506	14217048	.02633744	02417640
49	716	3	.01280241	17147276	.03260668	02481128
50	713	3	00218542	19529333	.03772610	02519672
51	7.12	3	01155143	22112582	.04368134	02283390
52	709	3	01213692	24850578	.05081452	01627044
53	7.08	3	.00066910	28055112	.06056607	00376078
54	705	3	.03211017	31767708	.07349002	.01675592
55	704	3	. 08330629	34924467	.08725514	.04746624
56	701	3_	.14595625	37603201	•99982766	.08548393
57	700	3	.23047380	40044947	.11824884	.14395401
58	, 533	3	• 31363622	43078660	.13741391	.20955462
59	.85	3	01272855	07709415	02213656	01817337
60	82	3	00586951	.01182673	.00515035	.01666129
61	79	3	.00613033	.10633447	.03464464	.04439944
62	129	3	·00881825	.11847674	.03366610	.04662740
63	76	3	.01105629	•09208550	.02861365	.02396634
64	176	3	.02017791	.10215992	.01271499	.01576865
65	73	3	01322219	.06302799	.02116973	.00088405
66	173	3	·0256854W	.45132249	01221402	02345622
67	50	3	00418344	00618056	.02165570	•06196040
86	120	3	.00158361	04384866	00314621	01935008
69	220	3	.01609800	12471033	07780291	07115745
70	67	3	.06918307	.16786183	.00015161	08017127
71	167	3	01293836	08751595	.02267785	00989969
72	267	3	00598396	16505605	06685801	01640827
73	44	3	02259471	04850885	.02369531	.0(812358
74	114	3	08729028	21881570	1.00000000	42066354
75	214	3	03468139	.00594604	.10323190	.05545586
76	314	3_	01546465	.07793524	.02990067	.06202030
77 78	41	3	02734361	66142715	.01455117	.0(877466
79	111 211	3 3	02606613	02795274	.03239479	.01085666
80	311	3	02407637 00470186	•06948519	.05166797	.03455093
81	511 58	3	02525702	.20357301 06863112	•03276654 ••02345279	.05320158
-		_				.00542483
82	158 209	<u>3</u> 3	00989067	.00014026	02514#37	00229734
84	309	3	00895481 -01584046	.06801361 .20836581	GC870325 01036528	.00732736 .01105452
85	409	3	.03567001	.29109192	01219235	.01224001
86	207	3		Andreas and the second	transfer of the second	and the second s
87	307	3	.01365425 .04090211	.03965221 .13989558	04966261 05113199	02402328 04263004
88	407	3 .	.05601383	.18532711	04246260	04684652
89	55	3	00520185	08025298	07615169	01459713
90	155	3	.02273709	02379395	07504920	03575273
91	205	3	.03652762	.01348661	06930129	-:04499690°
92	305	3	•05477346	.08357541	06930129	07125362
	رود	,	•\V\T\T\T\T\T\T\T\T\T\T\T\T\T\T\T\T\T\T\	•003777T	- • 00012101	- OLTENDO

Table 8-5.—(Continued)

Row	Node	DOF	Mode 17	Mode 18	Mode 19	Mode 20
93	405	3	.04943518	.08476835	0//32000	00001700
94	385	3	.04153172	•62566135	04412089 01969190	08286793
95	454	3	• (2995352	.03136798	02285730	05975964
96	464	3	• 01384980	04556889	06103869	06669654
97	474	3	00690847	10108077		05235055
98	484	3	02050913	15123268	.01362373	04262314
99	493	3	03093804	12624831	•02491092	03552650
100	502	3	.03358324	12035919	.01815375 .02174872	04316890
101	512	3	•14065381	23651832	•06533929	02819984 .06124298
102	522	3	.24482552	32897421	.10336367	15229917
103	52	3	00311401	06575598	05248584	00068108
104	152	3	.02258459	03038686	05767907	02171911
105	202	3	.03683993	00081990	04660694	03271543
106	302	3	.06422342	.04595413	03657516	06428578
107	382	3	.01369901	•04039434	02146026	04422853
108	452	3	02491742	.03421439	01975497	04853637
109	462	3	07523351	.05206244	02900422	07750271
110	482	3	07915311	.03234099	02808410	103CC1C5
111	492	3	04333,754	02214106	011661C8	08441470
112	179	3	00634560	04503022	02280625	.01039762
113	146	3	00719866	04403810	02598870	.01083724
114	192	3	00388385	02995496	02464586	.00768187
115	200	3	.01035961	00411435	01740841	00863843
116	298	3	.06609987	.01134395	00427153	03258396
117	350	3	.07522431	00871447	•01111487	01363498
118 119	398	3	.02051598	00576535	.00523963	•00306903
120	819 816	3	11990128	•12423265	04223689	05869107
		3	19333078	•27004640	09406688	16263000
121	470 810	3	18800469	•29470218	16148274	18635041
123	878	_3	16826261 10720557	•30131451	10270909	17872523
124	806		•00347833	•24373651	08248784	14010893
125	804	3	•14450076	•12873141 - •02413450	04657580	05561924
126	803	_3	.22499736	11191456	.01631698	.06294697
127	801	3	•32825228	22538786	.04948324	.13386657
128	531	3	•41948375	33152368	.13169089	.22497116 .30277751
129	8 90	3	01601958	06841026	02598131	.03792002
130	887	3	02420429	07034362	02614968	•04726245
131	940	3	02627670	09176550	02713632	.06435632
132_	937_	_3	03912744	119808932	02589195	.67839694
133	1023	3	03927682	00800315	.02449093	.03012464
134	878	3	.09482280	C3979848	.05364738	02665009
135	876	3	.13559093	07855344	.09217564	.05350108
136	928	3	.14870891	10926209	.13483130	.09054382
137	926	3	•19033249	14905768	•17406809	.12451577
<u> 138</u>	1063	_3	00050147	04580522	02571578	.04931068

Table 8-5.—(Continued)

Row	Node	DOF	Mode 17	Mode 18	Mode 19	Mode 20
		•	20007422	• 48966425	16162875	25997984
139	916	3	28997833 32427618	.57214724	19078599	31663536
140	915	3	18096525	.42134510	13540188	20555098
141	903	3 3	05297249	.31231688	09329804	11621031
142	906 904	3	.11947787	.15335381	02959467	.03944295
143	904	3	.35863325	05005848	.05950055	.27723069
144	921	3_	.64430356	25884476	.16281610	.59646445
146	900	3	.82523386	40670733	.23052487	.78876679
147	1021	3	07341456	00522457	.05225559	.05298655
148	1061	3	.00844017	11487935	.05848050	.11017304
149	965		51436128	1.600000000	34112141	57073698
150	957	3	15437790	.45878255	14220646	19364556
151	954		.10650512	.24096967	05241367	.02724216
152	951	3	.58143513	11975140	.11927801	.53377257
153	950	3	1.00000000	43568701	.27285945	1.00000000
154	757	3	.03022781	16364940	.03224973	01856259
155	766	3	.01424025	19424312	.03890163	01541849
156	763	3	.00182663	22314886	.04527527	014(1032
157	762		00337600	25217150	.05215317	01163349
158	759	3	.00217718	28139007	.05998169	00572375
159	758	3	.01978824	31291784	.06984774	.06593477
160	755	3	.75436470	34977285	.68285326	.02653347
161	754	3	.10556555	38435257	.09737472	.05744167
162	751	3_	.16660254	41563534	.11265814	
163	750	- 3	.24914758	45854643	.13429090	. 15799354
164	237	2	01715902	01888406	.00316538	.01390542
165_	2 3 5	2	04224314	.05591195	01812872	06394735
166	232		17529498	.24106145	07941677	08042674 09342177
167	229		13021148	.22335079	07463164 04340557	07764824
168	227		03107078	.12989157	.0(923195	04295068
169	226		.11859368	02446824	.00809554	.01892200
170	475		01887811	03688283	01353785	.00298563
171_	285		04718319	.03651357	06798144	06392910
172	282		15308297 03831178	00852605	00216047	.01573454
173	472			.12783700	04455292	03017210
174	332		10775177	.15226310	05238826	05895068
175	329		09258789 00960469	.08873154	03036948	05726320
176	277		05813044	.03520250	01641618	.06742169
177	862		01227308	00230515	0C388851	.01705786
178	379		.05320152	03416659	.00851736	.00445081
179 180	377 376		.13436385	09091242	.02961188	.00152029
181	375		.22706152	15708067	.05431685	00139981
182	428		.13976213	25997368	.07819058	.13476393
183	427		.14891646	22827528	.06965653	.1(420034
184	426		.18860847	19567175	.06292083	.05383063

Table 8-5.—(Continued)

Row	Node	DOF	Mode 17	Mode 18	Mode 19	Mode 20
185	424	2	. 205'56002	17890608	.05919977	.02977350
186	417	2	.20429656	34719018	.16675035	.16707168
187	416	2	.25697771	33347562	.16656407	.12468651
199	415	2	.30603545	30326870	.10116178	.06973196
189	414	2	.35859961	31342328	.10838376	.04373202
190	374	3	20836632	.33744639	08449058	14694884
191	374	1	.17457126	29051306	.08203183	$.132183 \epsilon 1$
192	471	5	.00109917	00307096	.00091851	.00121018
193	3191	3	03327703	30191872	07222179	086777719
194	3189	3	00334647	U1244852	06613820	.00227586
195	3187	3	.01323388	.13981335	.03679567	.04357733
196	3185	3	.01929994	.18404839	.04625371	.05232131
197	3181	3	.01183681	.08891571	.02117467	.02035800
198	2038	3	.00039796	035J2521	01225201	01960256
199	2098	3	00831449	11955722	03359763	04390803
200	2158	3	01508515	17327063	04854976	05886387
201	2218	3	01811740	17950024	04987517	05662801
202	2278	3	01676957	14092109	03977982	04164325
203	2338	3	01225640	07613953	02114297	01835892
234	2398	3	00547834	.0021385	.06296217	.06846713
205	2458	3	.00198519	.06137398	.02373287	.02578962
206	2518	3	.00564854	.07264844	.03039212	.02278849
207	25.78	3	.00369114	.64759358	.02916722	.01220391
208	2638	3	00491938	.00527993	.02610828	.00722699
209	2698	3	01444759	02498635	.02441217	.00791194
210	2758	3	02288657	05066208	.01935289	.0(891518
211	2818	3	C2706717	66705636	.06795715	.00891809
212	2878	3	02547601	07792089	01560027	.00769764
213	2939	3	01810417	07549984	03316472	.00429311
214	2998	3	00995906	05575194	02837054	•005 96 99 6
215	30.58	3	.00211946	02272860	01286192	.00490785
216	3271	3	.02769356	.04951242	.62376450	0(235026
217	3205	3	•02452364	.06347590	.03363735	00526710
218	3208	3	01273365	01942437	00591734	.06067567
219	3212	3	07015243	15544539	07309517	.01123896
220	3250	5	.00042652	.60114136	.30052310	00048385
221	3250	3	04389225	09511351	04363739	.06671732
222	3225	3	01224493	01730905	06459675	.00040977
223	3225	5	.00029355	.00066409	.00031907	00004836
224	3183	3	.01674699	.14398768	.03514700	.03738089
225	3203	3	.03615621	.08084515	.04013058	00572378
226	410	4	00002151	.00000421	•00C1U996	600,00761
227	410	5	.011038482	•C0069612	00047823	06663572
228	410	3	·02277987	.04342973	03894199	.00989365

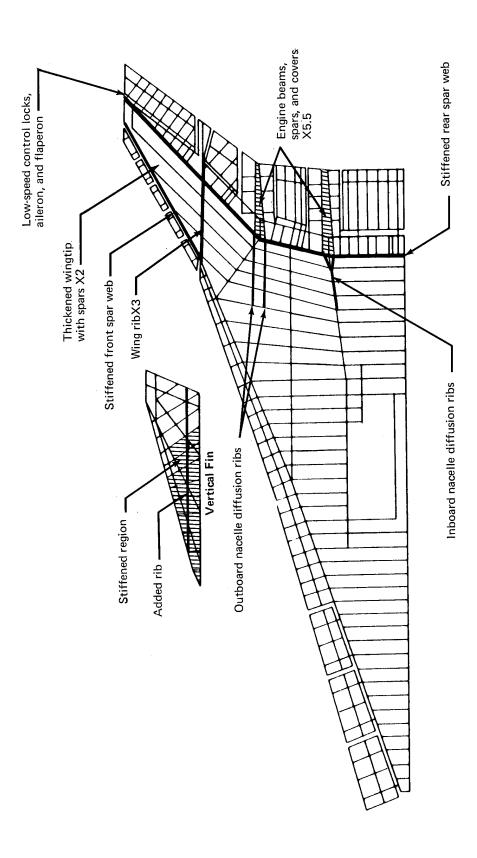
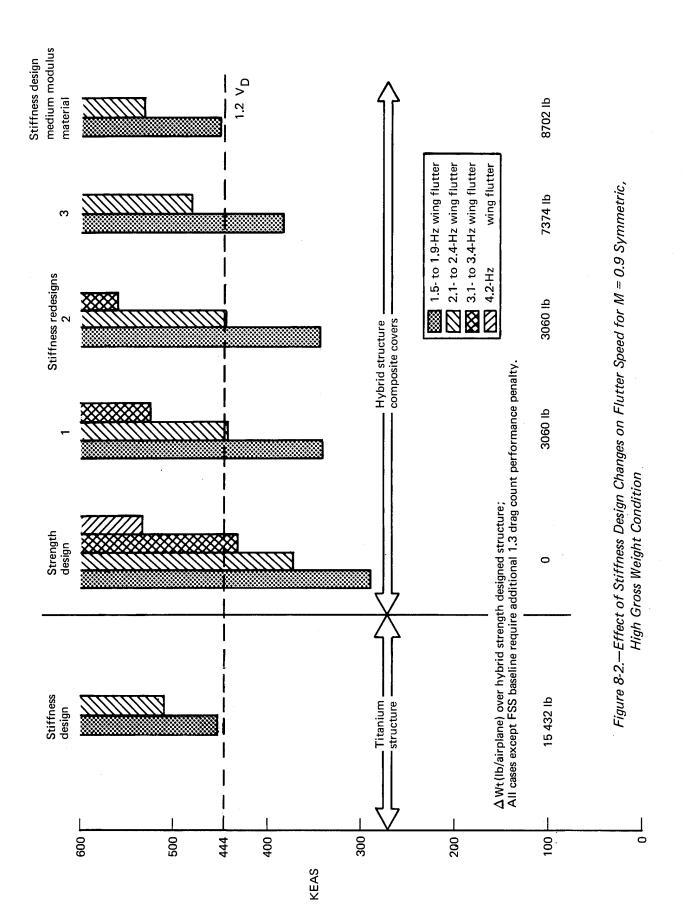


Figure 8-1.—Stiffness Constraints on Hybrid Structure "Strength-Design" from Use of Titanium Design Internal Structure



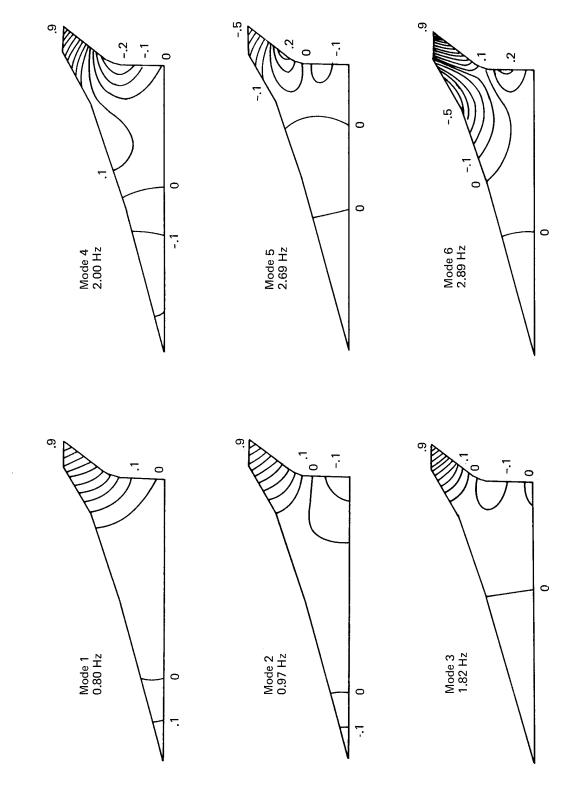


Figure 8-3.—Comparison of Wing Mode Shapes 1 Through 6, Hybrid Structure, Strength Design

C₁₁ = Spanwise normal strain induced by unit normal spanwise stress

 C_{16} = Shear strain induced by unit normal spanwise stress

 C_{66} = Shear strain induced by unit shear stress

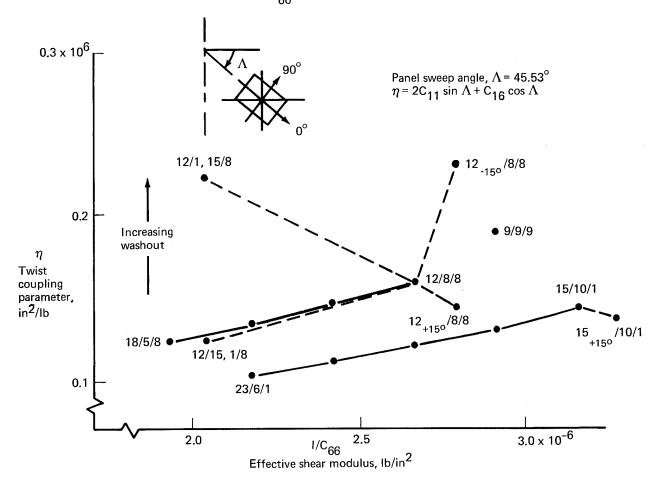


Figure 8-4.—Anisotropic Coupling Trends, High-Strength Graphite / Polyimide

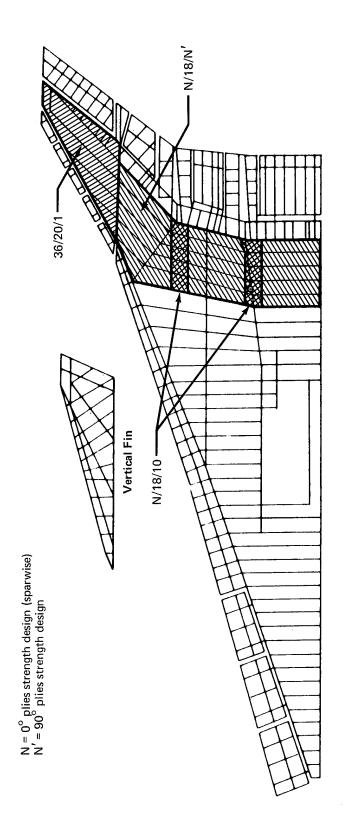


Figure 8-5.—Stiffness Designed Composite Cover Panels, Medium Modulus Graphite/Polyimide

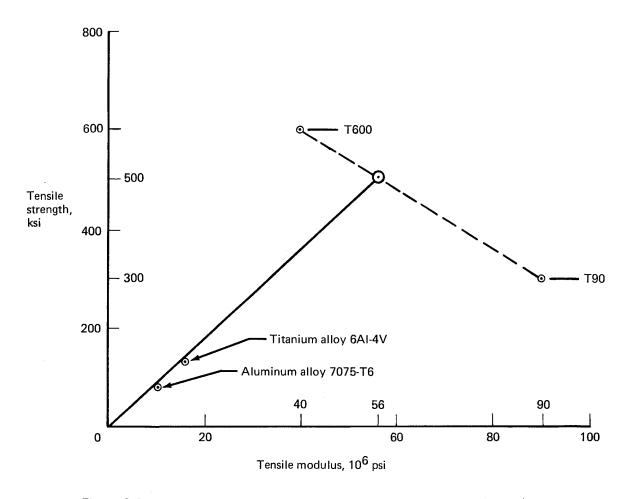


Figure 8-6.—Tailoring of Fiber Properties for Medium Modulus Graphite/Polyimide

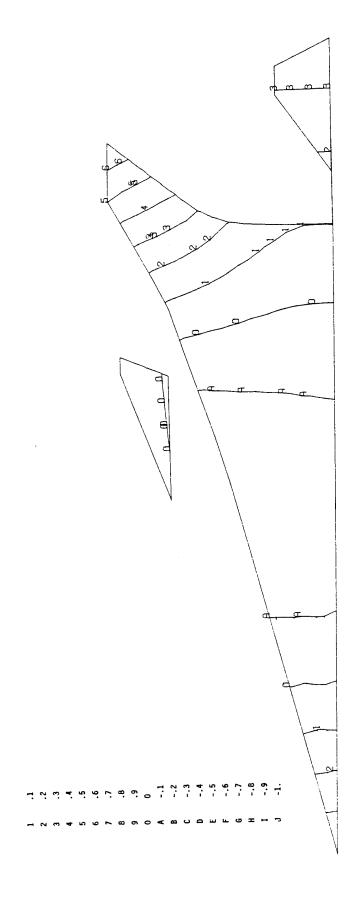


Figure 8-7.—Airplane Vibration Mode 1, Hybrid Structure Stiffness Design; Symmetric, High Gross Weight Condition, 0.867 Hz

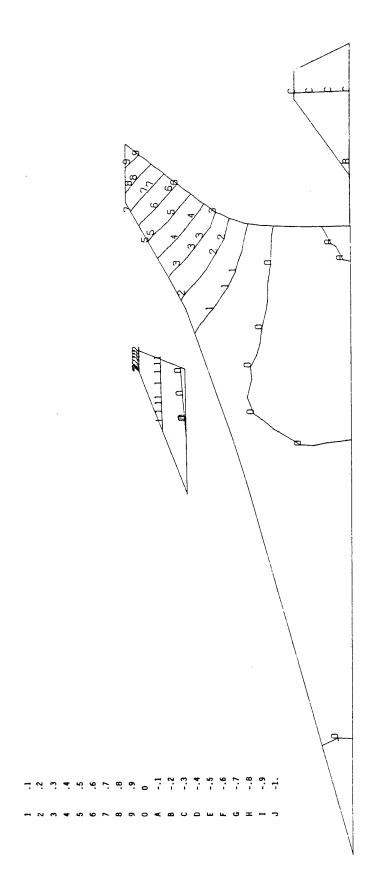


Figure 8-8.—Airplane Vibration Mode 2, Hybrid Structure Stiffness Design; Symmetric, High Gross Weight Condition, 1.141 Hz

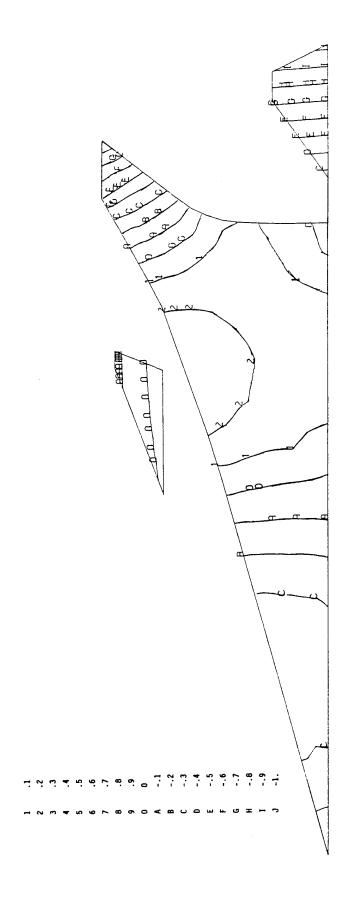


Figure 8-9.—Airplane Vibration Mode 3, Hybrid Structure Stiffness Design; Symmetric, High Gross Weight Condition, 1.915 Hz

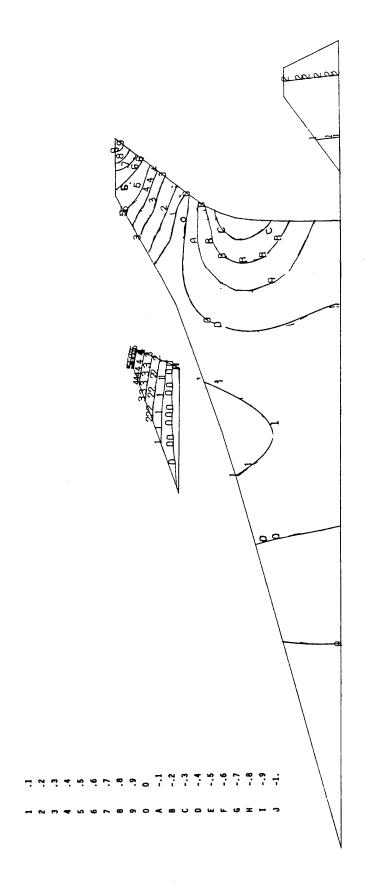


Figure 8-10.—Airplane Vibration Mode 4, Hybrid Structure Stiffness Design; Symmetric, High Gross Weight Condition, 2.487 Hz

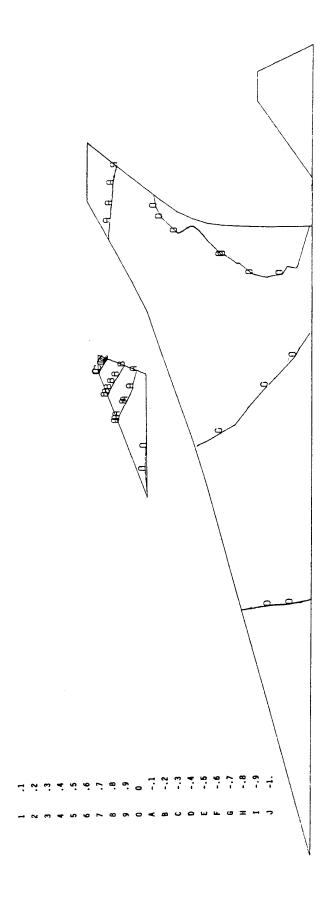


Figure 8-11.—Airplane Vibration Mode 5, Hybrid Structure Stiffness Design; Symmetric, High Gross Weight Condition, 2.929 Hz

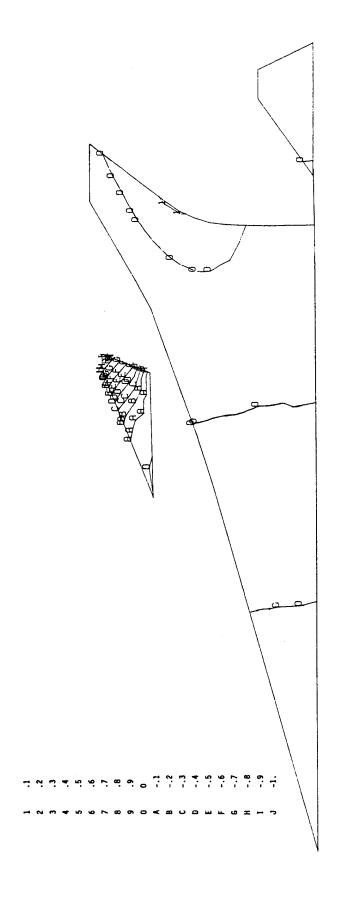


Figure 8-12.—Airplane Vibration Mode 6, Hybrid Structure Stiffness Design; Symmetric, High Gross Weight Condition, 3.391 Hz

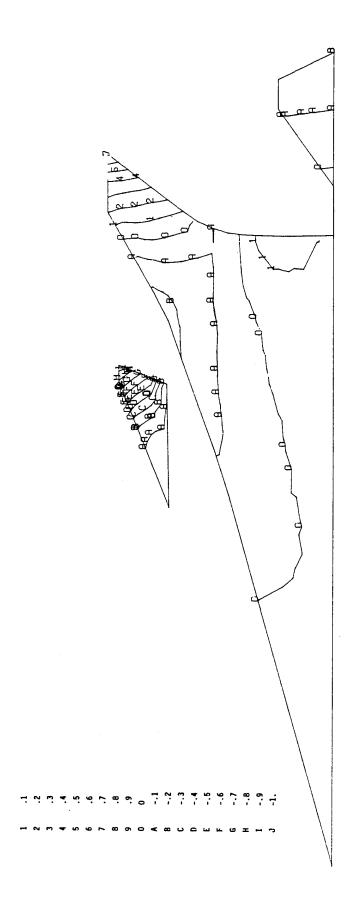


Figure 8-13.—Airplane Vibration Mode 7, Hybrid Structure Stiffness Design; Symmetric, High Gross Weight Condition, 3.525 Hz

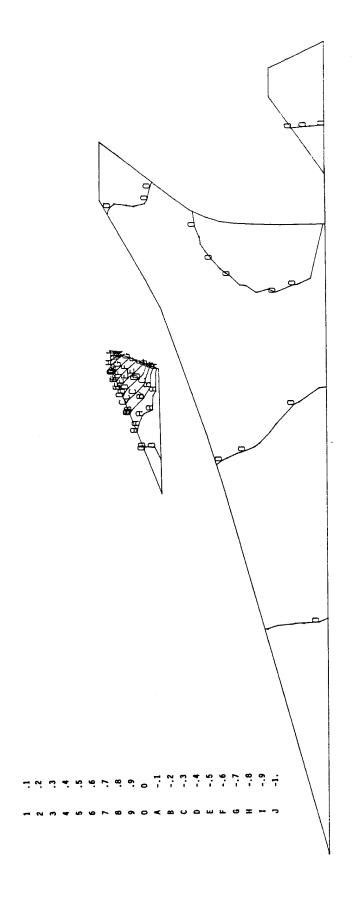


Figure 8-14.—Airplane Vibration Mode 8, Hybrid Structure Stiffness Design; Symmetric, High Gross Weight Condition, 3.561 Hz

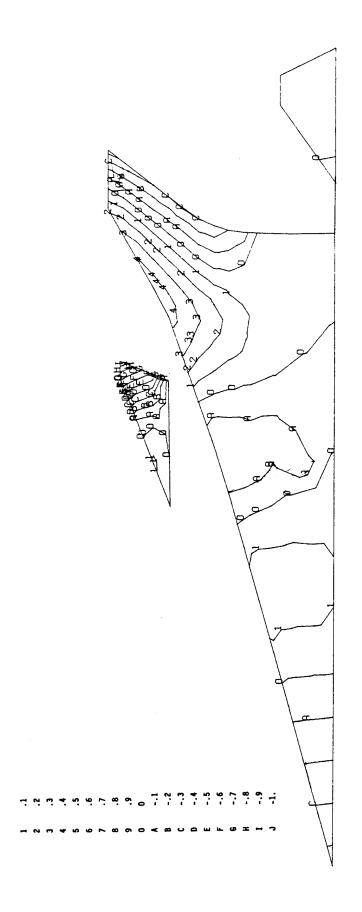


Figure 8-15.—Airplane Vibration Mode 9, Hybrid Structure Stiffness Design; Symmetric High Gross Weight Condition, 4.229 Hz

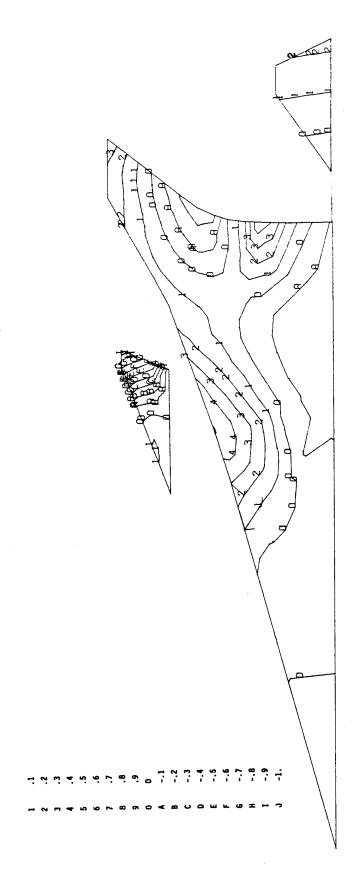


Figure 8-16.—Airplane Vibration Mode 10, Hybrid Structure Stiffness Design; Symmetric, High Gross Weight Condition, 4.355 Hz

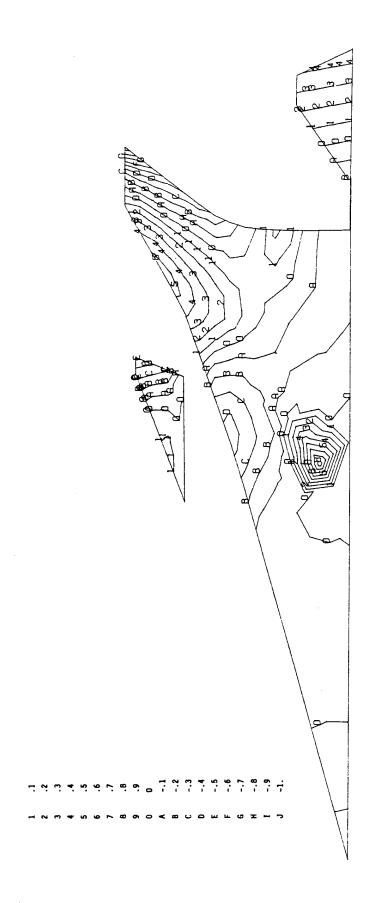


Figure 8-17.—Airplane Vibration Mode 11, Hybrid Structure Stiffness Design; Symmetric, High Gross Weight Condition, 5.090 Hz

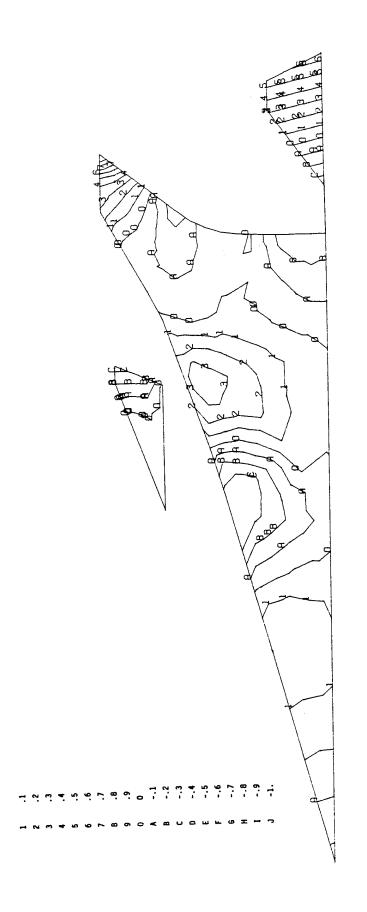


Figure 8-18.—Airplane Vibration Mode 12, Hybrid Structure Stiffness Design; Symmetric, High Gross Weight Condition, 5.777 Hz

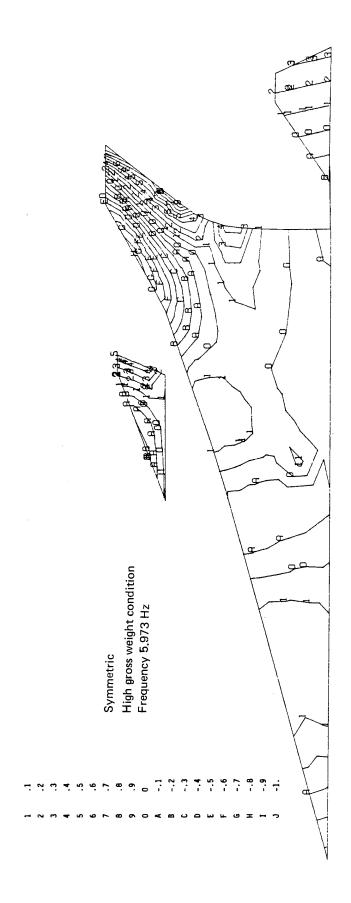


Figure 8-19.—Airplane Vibration Mode 13, Hybrid Structure Stiffness Design; Symmetric, High Gross Weight Condition, 5.973 Hz

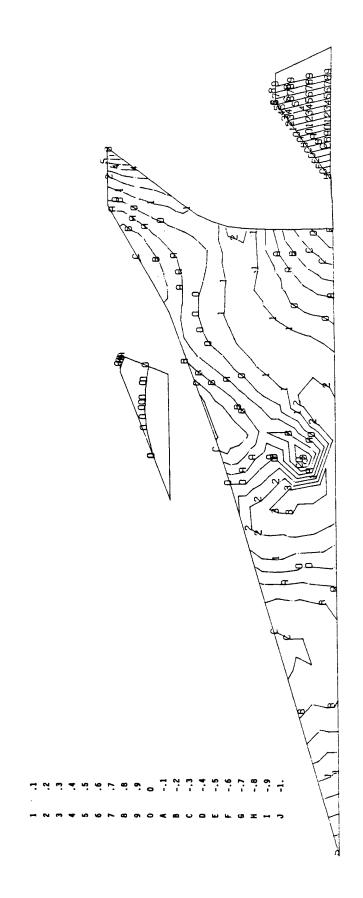


Figure 8-20.—Airplane Vibration Mode 14, Hybrid Structure Stiffness Design; Symmetric, High Gross Weight Condition, 6.058 Hz

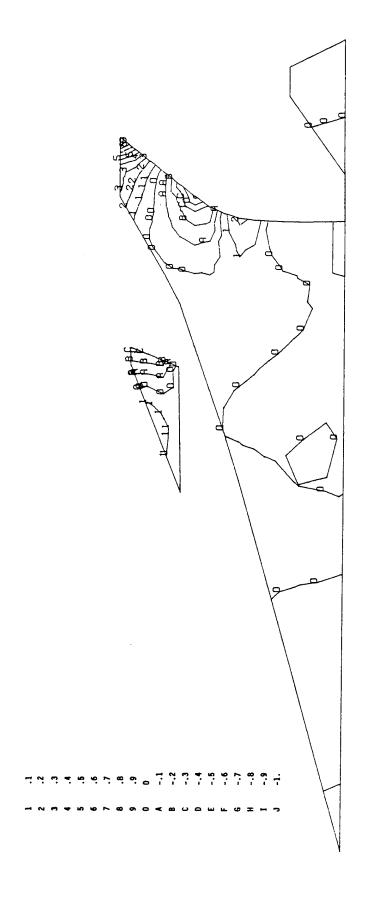


Figure 8-21.—Airplane Vibration Mode 15, Hybrid Structure Stiffness Design; Symmetric, High Gross Weight Condition, 6.911 Hz

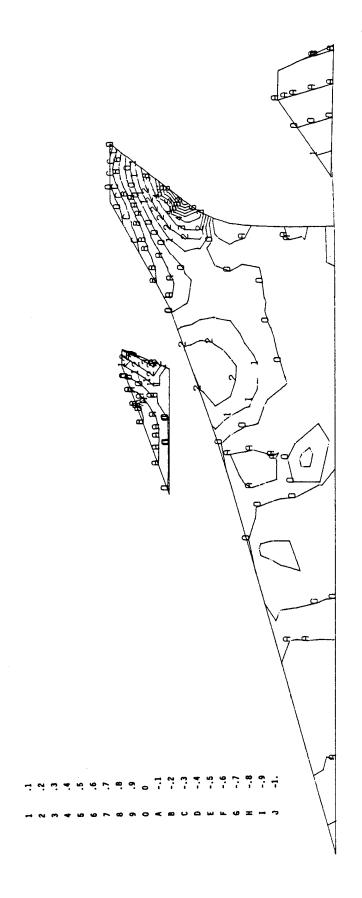


Figure 8-22.—Airplane Vibration Mode 16, Hybrid Structure Stiffness Design; Symmetric, High Gross Weight Condition, 7.504 Hz

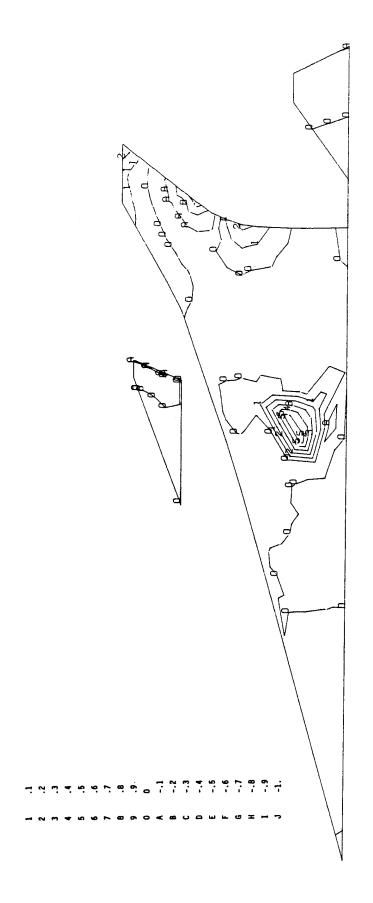


Figure 8-23.—Airplane Vibration Mode 17, Hybrid Structure Stiffness Design; Symmetric, High Gross Weight Condition, 7.840 Hz

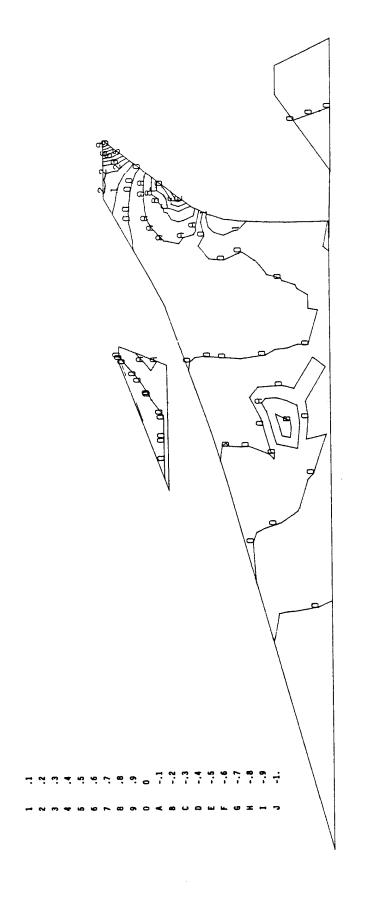


Figure 8-24.—Airplane Vibration Mode 18, Hybrid Structure Stiffness Design; Symmetric, High Gross Weight Condition, 8.154 Hz

SECTION 9

FINAL WEIGHT ANALYSIS

by

K. J. DEBORD M. D. HALVORSEN

CONTENTS

	Page
	220
INTRODUCTION	
REVISED TASK II TITANIUM WING WEIGHT	328
WEIGHT ANALYSIS OF ADVANCED COMPOSITE COVERED WING	328
WING WEIGHT COMPARISON SUMMARY	328
WING SECTION WEIGHT COMPARISON	329
GROUP WEIGHT AND BALANCE STATEMENT	329
REFERENCES	330

TABLES

No.									Page
9-1	Revised Task II Titanium Wing Weight, Model 969-512B								331
9-2	Wing Weight Comparison Summary, Model 969-512B							•	332
9-3	Group Weight and Balance Statement, Model 969-512B.		•			•			333

FIGURES

No.		Page
9-1	Wing Section Weight Comparison, Upper Surface Cover,	
	Stiffness Design, Model 969-512B	334
9-2	Wing Section Weight Comparison, Lower Surface Cover, Stiffness	
	Design, Model 569-512B	335
9-3	Total Wing Section Weight Comparison, Total Wing, Stiffness Design,	
	Model 969-512B	336

SYMBOLS

△ Increment

GR/PI Graphite/Polyimide

lb Pounds

TI Titanium

INTRODUCTION

This section provides the operational empty weight of the configuration developed in reference 1 utilizing advanced composite structural material. The weight of the structural wing box outboard of the side of body was derived from the ATLAS finite structural analysis. This analysis showed that there was a 6730 lb or 10.4% weight reduction of the wing box outboard of the center section utilizing advanced composite cover panels but retaining titanium substructure compared to an all titanium wing box. The remainder of structural component weight changes from titanium to advanced composite were based on a previous NASA study as described in a later paragraph.

REVISED TASK II TITANIUM WING WEIGHT

It was necessary to make a number of revisions to the Task II titanium wing weight in order to have a valid base from which to assess the advantages of composite construction. Table 9-1 lists the weight changes to the final stiffness titanium wing presented in reference 9-1, table 12-6. These revisions increase the titanium wing weight from 95 760 lb to 97 812 lb. Most of these changes result from corrections to the weight of the structural model. All weights and weight savings are quoted per airplane.

Table 9-2 also tabulates the revised final stiffness all titanium wing.

ADVANCED COMPOSITE COVERED WING WEIGHT ANALYSIS

Combining the non-optimum weight factors outlined in Section 5 with the weight of the modeled structure from the ATLAS finite element analysis, produces the weight of the wing primary structural elements. To this must be added the weight of the honeycomb core and bond, landing gear doors, the wing center section, the leading and trailing edge secondary structure and miscellaneous items.

Table 9-2 presents the weight build-up of the Model 969-512B wing with five combinations of advanced composite covers: the strength design, three stiffness redesigns and the final stiffness design. All five wings have identical titanium internal structure. The final stiffness design wing weighs 88 572 lbs, which is 8702 lb more than the strength design. Section 8 describes the additional cover material added over strength design.

WING WEIGHT COMPARISON SUMMARY

The last two columns of table 9-2 show the weight increment between the final stiffness all titanium wing from Task II and the final stiffness advanced composite covered wing from the Task III analysis. As can be seen, the theoretical composite covers are 9504 lb or 48.6% lighter than the titanium. However, when this is combined with the higher non-optimum factors, and core and bond weight, the weight saving is reduced to 17.8%. The considerably higher core and bond weight with the composite wing cover compared to core and braze weight of the titanium cover is due in part to a difference in honeycomb area. The titanium covered wing has a portion of the lower surface which is integral skin stiffener construction where no honeycomb is used. Four outboard wing tip ribs which were added in

the titanium wing for stiffness have been eliminated in the composite cover wings. Otherwise, the substructure is identical in the two wings. A hand calculation was made of the weight reduction for composite landing gear door covers. This was small, compared to the total weight of the door hinges and mechanism and shows a 5% reduction of the total door weight. The wing center section weight reduction of 12 percent for the composite panel was derived from the adjacent outboard wing panel weight reduction.

In summary, the total weight reduction of the theoretical structural elements of the composite wing is 8284 lb or 15.7%; the weight reduction for the total outboard wing box is 6730 lb or 10.4%; and the reduction for the total wing including the center section, leading and trailing edge is 9240 lb or 9.4%.

WING SECTION WEIGHT COMPARISON

Figures 9-1 and 9-2 show a section weight comparison of the titanium wing upper and lower cover panels from Task II and the graphite/polyimide covers used in Task III for the stiffness designed wings. In figure 9-1, the forward strake upper panel T9 with minimum skin gage shows a 13.9% weight reduction when changing from titanium to advanced composite. As would be expected in the more highly loaded area, aft, the weight reduction increases to 35.3% in section T6. However, in sections T1, T2, T3 and T4, there is a significant reduction in the weight improvement in changing to a composite cover. This is due to the large increase in the thickness of the cover skins to satisfy the stiffness requirements shown in figure 8-24. The same pattern of weight reduction is shown on the lower surface in figure 9-2. However, sections T2, T3 and T4 show high percent weight reductions because the titanium design was integral skin, stringer construction. These sections would have been lighter if they had originally been designed as titanium honeycomb sandwich. With the lighter titanium sections; T2, T3 and T4, the weight reductions due to changing to composite structure would then be similar to the upper surface for these sections.

The total upper surface cover weight reduction for composite design was 13.9% while the lower surface showed 21.5% reduction. The combined upper and lower surface cover weight reduction was 17.8%.

Figure 9-3 provides a weight comparison of the Task II titanium wing with the Task III advanced composite wing by sections combining all structural elements. These are the weights shown in table 9-2 for the stiffness designed wing but they are shown as weight per side rather than weight per airplane.

While the cover weight reduction for changing from titanium to composite amounted to 17.8%, the total wing structural weight reduction was 9.4%.

GROUP WEIGHT AND BALANCE STATEMENT

Table 9-3 presents a group weight and balance comparison of the Task II titanium airplane with the Task III advanced composite structure. The wing weights are taken from table 9-2. The weight reduction shown for the remainder of the structure on Task III using advanced composite was based on the NASA study, reference 9-2.

The total structural weight reduction for advanced composite compared to titanium is 10.5%. This is reduced to 6.6% when related to the total operational empty weight.

REFERENCES

9-1 Boeing Staff: Study of Structural Design Concepts for an Arrow Wing Supersonic Transport Configuration. NASA CR-132576-1 and -2, 1976.

Table 9-1.—Revised Task II Titanium Wing Weight, Model 969-512B

		Wt, lb
Wing weight — final stiffness design (ref. 9-1, table 12-6)		95 760
Delete skin over lower surface wheel well	,	-590
Revised cover material non optimum factors		+2 137
Add spar web stiffeners		+1 035
Add rib web stiffeners		+1 028
Change element designation from spars to ribs	(Spars) (Ribs)	-406 +414
Delete core and braze in lower surface integral stiffened cover area		-1 244
Correct landing gear door area		-864
Incorporate outboard fixed T.E. panel into wing structural box		+542
Revised wing weight—final stiffness design	3.2.0° 5.0° 5.0° 5.0° 5.0° 5.0° 5.0° 5.0° 5	97 812

Table 9-2.—Wing Weight Comparison Summary, Model 969-512B

Item Fi	Titanium		Advance	Advanced composite covers	e covers		VVT change Titanium	nge um	
stif	Final	Strength	Stiff	Stiffness redesigns	SL	Final	t		
	stiffness,	design,	1,	2,	3,	stiffness,	composite,	site,	_
	<u>q</u>	q	q	<u>a</u>	g	ql	qı	%	
Theoretical cover material 19	999 6	4 650	989 9	989 9	9 344	10 062	-9 504	-48.6	
rial	7 028	5 350	6 374	6 374	8 030	8 640	+1 612	+22.9	
	14 094	14 094	14 094	14 094	14 094	14 094			
Nonoptimum spar material									
(incl. web stiffeners) 3	3 152	3 152	3.152	3 152	3 152	3 152			
Theoretical rib material 5	5 952	5 654	5 654	5 654	5 654	5 654	- 298	- 5.0	
Nonoptimum rib material									
(incl. web stiffeners) 2	2 128	2 034	2 034	2 034	2 034	2 034	- 94	- 4.4	
Theoretical beam material	654	654	654	654	654	654			
Nonoptimum beam material	86	86	86	86	86	86			
Total structural element weight 52	52 672	35 686	38 746	38 746	43 060	44 388	-8 284	-15.7	1
Core and braze/bond 8	8 050	9 7 66	9926	9 766	9976	9 766	+1 716	+21.3	
Landing gear doors and mech.	3 236	3 0 7 4	3 074	3 074	3 074	3 074	- 162	- 5.0	
Fairing, fence, and misc	096	960	960	960	096	960			
Total wing box									
ion)	64 918	49 486	52 546	52 546	26 860	58 188	-6 730	-10.4	
Wing center section 8	8 560	7 530	7 530	7 530	083 2	7 530	-1 030	-12.0	
-	8 460	7 868	7 868	7 868	2 898	7 868	- 592	- 7.0	
dge .	5 770	5 482	5 482	5 482	5 482	5 482	- 288	- 5.0	
	4 864	4 474	4 4 7 4	4 474	4 474	4 474	- 390	- 8.0	
Moveable trailing edge	5 240	5 030	5 030	5 030	5 030	5 030	- 210	- 4.0	
Total wing structure 97	97 812	79 870	82 930	82 930	87 244	88 572	-9 240	5 '6 -	

Table 9-3.—Group Weight and Balance Statement, Model 969-512B

	Revised	Task II	Weight	change	Task	: 111
Group	Weight, Ib	Arm, in.	lb	%	Weight, Ib	Arm, in.
Wing	97 812	2604.0	- 9 240	- 9.4	88 572	2604.0
Horizontal tail	6 530	3623.0	- 914	-14.0	5 616	3623.0
Vertical tail (body and wing mounted)	5 850	3406.0	- 585	-10.0	5 265	3406.0
Body	56 140	2117.0	- 8 421	-15.0	47 719	2117.0
Main gear	37 320	2548.0	- 3 172	- 8.5	34 148	2548.0
Nose gear	3 760	1178.0	- 320	- 8.5	3 440	1178.0
Nacelle	19 080	2949.0	- 1 049	- 5.5	18 031	2949.0
Total structure	226 492	2529.5	-23 701	-10.5	202 791	2535.5
Engine (incl T/R, S/S and nozzle)	45 200	3076.0			45 200	3076.0
Engine accessories	1 350	2944.0			1 350	2944.0
Engine controls	780	2308.0			780	2308.0
Starting system	300	2919.0			300	2919.0
Fuel system	9 110	2495.0			9 110	2495.0
Total propulsion	56 740	2968.2			56 740	2968.2
Instruments	1 865	1710.0			1 865	1710.0
Flight controls	14 700	2679.0			14 700	2679.0
Hydraulics	5 795	2854.0			5 795	2854.0
Electrical	5 160	2092.0			5 160	2092.0
Electronics	2 885	1282.0			2 885	1282.0
Furnishings	19 010	1817.0			19 010	1817.0
ECS	8 430	2440.0			8 430	2440.0
Anti-icing	135	558.0			135	558.0
APU ·	250	2978.0			250	2978.0
Insulation	2 900	1913.0			2 900	1913.0
Total systems and equipment	61 130	2209.7			61 130	2209.7
Options	2 500	2491.0			2 500	2491.0
Manufacturer's empty weight	346 862	2544.6	-23 701	- 6.8	323 161	2549.5
Standard items	8 200	2193.0			8 200	2193.0
Operational items	5 260	1716.0			5 260	1716.0
Operational empty weight	360 322	2524.5	-23 701	- 6.6	336 621	2527.8
Payload	48 906	1882.0			48 906	1882.0
Zero fuel weight	409 228	2447.7	-23 701	- 5.8	385 527	2445.9

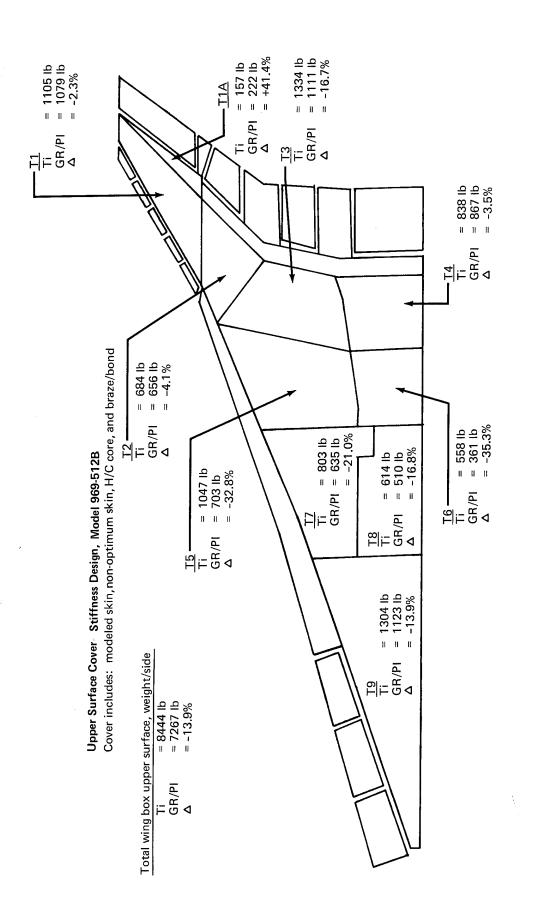


Figure 9-1.—Wing Upper Surface Section Weight Comparison, Upper Surface Cover^a, Stiffness Design, Model 969-512B

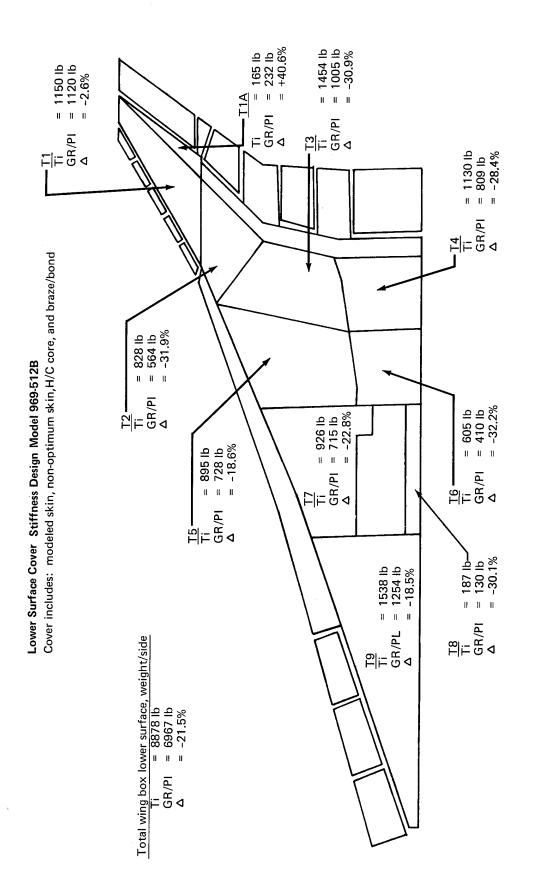


Figure 9-2.—Wing Lower Surface Section Weight Comparison, Lower Surface Cover^a, Stiffness Design, Model 969-512B

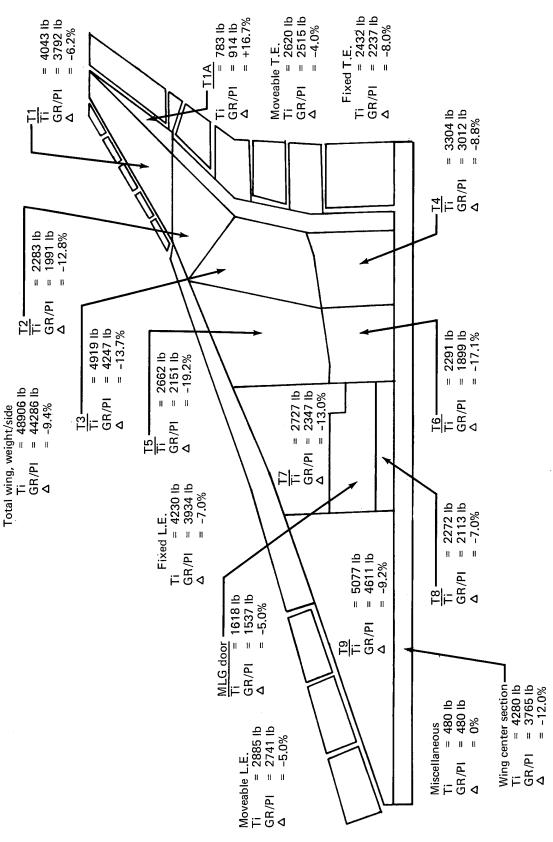


Figure 9-3.—Total Wing Section Weight Comparison, Total Wing, Stiffness Design, Model 969-512B

SECTION 10

AERODYNAMIC HEATING ANALYSIS

by

V. DERIUGIN

CONTENTS

	Page
SUMMARY	341
INVESTIGATION OF TEMPERATURE DISTRIBUTIONS IN COMPOSITE LAMINATES .	341
METHODOLOGY FOR DETERMINING AVERAGE CONDUCTIVITIES	342
METHODOLOGY FOR THERMAL ANALYSIS USING SIMPLIFIED MODEL	342
MODELING OF LIGHT GAGE AND HEAVY GAGE CROSS SECTIONS	343
DETERMINATION OF TEMPERATURE DISTRIBUTION FOR MISSION PROFILE	343
REFERENCES	344

TABLES

No.		Page
10-1	Node Plan for Advanced Composite Model	345
10-2	Conductors in Composite Model	345
10-3	Layups of Honeycomb Panels for Wing Structural Sections	346
10-4	Properties Used for Thermal Analysis	347

FIGURES

No.		Page
10-1	Layup Model Breakdown	
10-2	Node Arrangement, Layup Direction [0]	349
10-3	Node Arrangement, Layup Direction [+45]	350
10-4	Node Arrangement, Layup Direction [-45]	351
10-5	Node Arrangement, Layup Direction [90]	352
10-6	Basic Material Conductivities and Sample Layup, Average Conductivity	353
10-7	Light Gage Structural Section	354
10-8	Heavy Gage Structural Section	355
10-9	Average Thermal Conductivities for Light and Heavy Gage Designs (Dimensions A,	
	B. C. and D)	356
10-10	Fuel Tank Temperatures, Light Gage, Wet Upper Panel: T1, T2, T24, T25	357
10-11	Fuel Tank Temperatures, Light Gage, Wet Upper Panel: T5, T6, T20, T21	358
10-12		359
10-13	Fuel Tank Temperatures, Light Gage, Wet Upper Panel: T14, T16, T18	360
10-14	Fuel Temperature, Light Gage, Wet Upper Panel: T35	361
10-15	Fuel Tank Thermal Gradients, Light Gage, Wet Upper Panel: T1, T2, T5-7,	
	T19-T21, T24-T25	362
10-16	Fuel Tank Thermal Gradients, Light Gage, Wet Upper Panel: T7, T8, T8-10, T8-T13	363
10-17	Fuel Tank Thermal Gradients, Light Gage, Dry Upper Panel: T1, T2, T24, T25	364
10-18	Fuel Tank Temperatures, Light Gage, Dry Upper Panel: T5, T6, T20, T21	365
10-19	Fuel Tank Temperatures, Light Gage, Dry Upper Panel: T8, T10, T12	366
10-20		367
10-21	Fuel Temperatures, Light Gage, Dry Upper Panel: T35	368
10-22		
	T19-T21, T24-T25	369
10-23	Fuel Tank Thermal Gradients, Light Gage, Dry Upper Panel: T7-T8, T8-T10,	
	T8-T13	370
10-24	Fuel Tank Temperatures, Heavy Gage, Dry Upper Panel: T1, T2, T24, T25	3/1
10-25	Fuel Tank Temperatures, Heavy Gage, Dry Upper Panel: T5, T6, T20, T21	372
10-26	Fuel Tank Temperatures, Heavy Gage, Dry Upper Panel: T14, T16, T18	373
10-27	Fuel Temperature, Heavy Gage, Dry Upper Panel: T35	374
10-28	Fuel Tank Temperatures, Heavy Gage, Wet Upper Panel: T1, T2, T24, T25	375
10-29	Fuel Tank Temperatures, Heavy Gage, Wet Upper Panel: T5, T6, T20, T21	376
10-30	Fuel Tank Temperatures, Heavy Gage, Wet Upper Panel: T8, T10, T12	377
10-31	C 777 D 1 TO 5	378

SUMMARY

The structural thermal analysis for Task III was performed using the same methods as those employed during the Task II study (ref. 10-1). The analysis consisted of determining the external thermal environment as well as the resulting structural temperature distributions. Whereas the external environments were identical to those of reference 10-1 due to the same vehicle mission profile, the temperatures and temperature distributions throughout the structure were different due to the introduction of graphite/polyimide material in the honeycomb sandwich skin panels instead of the titanium previously used. In order to be able to apply the same methodology as in Task II, a study was made of the effects of laminations and their thermal properties on structural temperature distributions. Because of very pronounced directionality of the thermal conductivity, particular attention was focused on local temperature gradients which might conceivably introduce differential thermal stresses and, thus, delaminations between laminae if appropriate stress levels were reached. None of these effects were observed, and it was therefore possible to avoid excessively detailed modeling and to work with averaged and lumped properties and geometric arrangements.

The results showed that the temperatures were predominantly lower than those obtained in the titanium airframe at the same time exhibiting similar time and spatial characteristics. The differences in magnitudes are largely due to the differences in surface emissivities and absorptivities as well as in the material conductivities. The gradients through the graphite/polyimide honeycomb sandwich panels were generally somewhat larger than for titanium of similar configuration.

INVESTIGATION OF TEMPERATURE DISTRIBUTIONS IN COMPOSITE LAMINATES

Representative arrays of material layups were examined with respect to possible analytical approaches that would yield a manageable model with acceptable accuracy. A 24 lamina layup of 0.1 mm (.004 in.) thick laminae was selected and grouped into 7 layers having different layup directions as shown in figure 10-1. A 3x3 basic node arrangement was selected for the 0° and 90° layup directions whereas for the ±45° layup directions the same basic node array was augmented by intermediate nodes for modeling convenience. The node plan is shown in table 10-1. The basic model covered an area of 76.2 cm x 76.2 cm (30x30 in.). The arrangement of the nodes is shown in figures 10-2 through 10-5. Each node, shown in figures 10-2 through 10-5 represents a capacitor and is also connected with adjacent nodes by appropriate conductors as listed in table 10-2. Aerodynamic heating representative of a typical supersonic cruise environment exhibiting a sharp temperature rise at approximately 30 minutes into the mission profile was also simulated by conductors. The resulting temperature rise of 194K (350°F) over a period of 14 minutes resulted in a maximum temperature difference of approximately .89K (1.6°F) between the upper (Layer 1) and lower (Layer 7) layers and is insignificant from the point of view of generating delaminating differential stresses. It was therefore decided to treat graphite/polyimide laminate layups as lumped nodes with appropriately averaged conductivities.

METHODOLOGY FOR DETERMINING AVERAGE CONDUCTIVITIES

The average conductivities in the streamwise direction were obtained by averaging the directional conductivities weighted by the associated layup layer thicknesses. Thus the average conductivity can be expressed as:

$$K_{avg} = \frac{\sum K_i \delta_i}{\sum \delta_i}$$

where

K_i = directional conductivity of basic material

 δ_i = layer thickness.

The basic material conductivities and the average conductivity of the sample layup as functions of temperature are shown in figure 10-6. For comparison, the figure also shows the thermal conductivity of 6Al-4V titanium.

METHODOLOGY FOR THERMAL ANALYSIS USING SIMPLIFIED MODEL

The methodology of the thermal analysis was identical to that employed in reference 10-1 with regard to use of the Boeing Engineering Thermal Analyzer (BETA) program. However, averaged conductivities were used as inputs to this program utilizing the experience of the preliminary investigation. The average conductivities of layups intended for the actual design (see table 10-3) were determined as discussed above. The longitudinal conductivities are considerably larger and show more variation with temperature than transverse conductivities. Therefore, emphasis was placed on obtaining average longitudinal conductivity values whereas for transverse conductivity a single value of

$$1.44 \frac{\text{W}}{\text{mK}} (1.93 \times 10^{-5} \frac{\text{Btu in.}}{\text{in.}^2 \text{ sec }^{\circ}\text{F}})$$

was used for the selected high strength graphite/polyimide material. Furthermore, since the honeycomb core of this material consists of layers with fiber directions of $\pm 45^{\circ}$, appropriate conductivity values had to be used in determining analytically the conductances through the respective honeycomb panels. These conductances are shown in table 10-4. In addition, radiation between the honeycomb face sheets was accounted for using radiation exchange factors as described in reference 10-2. These radiation exchange factors were computed as:

.178 for 56.1 Kg/m³ (3.5 lb/ft³) Graphite/Polyimide Honeycomb .178 for 112.1 Kg/m³ (7.0 lb/ft³) Graphite/Polyimide Honeycomb .148 for 224.2 Kg/m³ (14.0 lb/ft³) Graphite/Polyimide Honeycomb

Accounting for radiation interchange between the honeycomb face sheets improves the accuracy of predicting effective honeycomb conductance by having the program include the effects of changing face sheet temperatures on actual honeycomb conductance.

MODELING OF LIGHT GAGE AND HEAVY GAGE CROSS SECTIONS

The wing cross section selected for analysis was geometrically similar to that analyzed in reference 10-1. The same node arrangement was used. All layups were treated as one compound layer with averaged properties. The titanium spar was identical to that in reference 10-1. The analysis was performed on light gage and on heavy gage honeycomb sandwich panel designs each with wet and dry upper panels. The structural cross section model with the light gage is shown in figure 10-7. The heavy gage model is shown in figure 10-8. The layups for the respective dimensions shown in figures 10-7 and 10-8 are presented in table 10-3. The average thermal conductivities, shown in figure 10-9, were computed using the methodology discussed above using the basic material conductivities, the layup direction and the thicknesses of the respective layers.

DETERMINATION OF TEMPERATURE DISTRIBUTION FOR MISSION PROFILE

The aerodynamic heating rates were calculated using a 6190 km (3340nm) mission profile as in reference 10-1. Solar heating and radiation to space were also included. As shown in table 10-4, the painted graphite/polyimide solar absorptance was assumed to be 0.3 and the emittance to space 0.8. For the internal radiation exchange 0.2 was assumed for the titanium emittance and 0.8 for the graphite/polyimide. Honeycomb panel conductances were used as described in table 10-4. The fuel management scheme as well as the conductance between fuel and structure, were assumed identical to those of reference 10-1.

The initial temperature before flight was assumed as 289K (60°F). Temperature distributions, thermal gradients, and fuel temperatures for both light and heavy gage designs with wet and dry upper panels are shown in figures 10-10 through 10-31. The node designations are shown in figures 10-7 and 10-8, respectively.

Most of the temperatures obtained in the present analysis are lower than those obtained in reference 10-1 but exhibit the same general characteristics. The lower temperatures can be partially explained by the lower absorptance-emittance ratio of the surface of the graphite/polyimide material (see table 10-4). The largest temperature difference of 67K (120°F) occurs at Node 2 due to a combination of higher emittance during the internal radiation exchange with internal structure and fuel, and a lower conductance assumed for the upper panel (see table 10-4). The temperatures of the outer lower surface skin are nearly the same as in reference 10-1. However, over the lower spar they are approximately 44K (80°F) higher which is caused by the significantly lower panel conductance assumed for the lower panel as compared with Task II.

The thermal gradients are generally somewhat higher but show similar characteristics to those of the titanium airframe. They are generally consistent with the differences in conductances, emittances and lower density-specific heat product of the graphite/polyimide material. Very little difference in temperatures and thermal gradients is observed between light gage and heavy gage designs. The similarity of temperatures and thermal gradients with those of reference 10-1 can be explained by comparable conductivities of some of the graphite polyimide layups with the thermal conductivity of titanium, particularly in the heavy gage design (see fig. 10-9).

REFERENCES

- 10-1 Boeing Staff: Study of Structural Design Concepts for an Arrow Wing Supersonic Transport Configuration. NASA CR 132576-1 and -2, 1976.
- 10-2 Swan, R. T.; and Pittman, C. M.: Analysis of Effective Conductivities of Honeycomb-Core and Corrugated-Core Sandwich Panels. NASA TN D-714.

Table 10-1.—Node Plan for Advanced Composite Model

Sample Model Layup Order: Total 24 Layers $[0_5/\pm45_3/90]_S$

Number of layers	Layup direction Node numbers		Number of nod	
5	0	1-9	9	
3	+45	11-35	25	
3	-45	41-65	25	
2	90	71-79	9	
3	-45	81-105	25	
3	+45	111-135	25	
5	0	141-149	9	
	127			

Table 10-2.—Conductors in Composite Model

	Number of conductors
Nodes 1-9	12
Nodes 11-35	36
Nodes 41-65	36
Nodes 71-79	12
Nodes 81-105	36
Nodes 111-135	36
Nodes 141-149	12
Layers 1, 2	45
Layers 2, 3	25
Layers 3, 4	45
Layers 4, 5	45
Layers 5, 6	25
Layers 6, 7	45
Aeroheating	9
Total conductors	419

Table 10-3.—Layups of Honeycomb Panels for Wing Structural Sections

Light gage				ŀ	leavy gage		
Gage				Gage			
Dimension (fig. 10-7)	Total	Titanium	Layup	Dimension (fig. 10-7)	Total	Titanium	Layup
Α	0.081 (0.032)		[0/+45/90/-45] _S	А	0.183 (0.072)		[0/+45/0/-45/90/ 0/±45/0] _S
В	0.041 (0.016)		Same as A	В	0.183 (0.072)		Same as A
С	0.234 (0.092)	0.081 (0.032)	[0/Ti/+45/90/ Ti/-45] _S	С	0.396 (0.156)	0.107 (0.042)	[0/Ti/+45/0/Ti/ -45/90/0/+45/ Ti/-45/0] _S
D	0.229 (0.090)	0.041 (0.016)	Same as C plus 0.076 (0.03) thick (±45) GR/PI shim	D	0.498 (0.196)	0.107 (0.042)	Same as C plus 0.102 (0.04) thick (±45) GR/PI shim
Center core ρ_{CC} = 56.1 (3.5) Edge core ρ_{EC} = 112.1 (7.0)					ore ρ _{CC} = 56. e ρ _{EC} = 224.		

GR/PI = Graphite polyimide Dimensions: cm (in.) ρ = density, kg/m³ (lbm/ft³) Titanium interleaves are 0.02 (0.008) and 0.01 (0.004), respectively. They are bonded in place with 0.009 (0.0035) thick layer of polyimide adhesive.

Dimensions are given in figures 10-7 and 10-8.

Table 10-4.—Properties Used for Thermal Analysis

		Titanium	Graphite polyimide	
Solar absorptance Upper panel Lower panel (Assuming 10% of solar energy reflected from ground)	$lpha_{ m upper}$	0.7 0.07	0.3 0.03	
Emittance	ϵ	0.2	0.8	
Ratio	$lpha \epsilon_{ m upper} \ lpha \epsilon_{ m lower}$	3.5 0.35	0.375 0.0375	
(Density) (Specific heat) $\frac{MJ}{m^3K} \left(\frac{Btu}{in.^3 ^{\circ}F} \right)$	$ ho C_p$	2.41 (0.0208) at 283 K (50° F) 3.65 (0.0229) at 505 K (450° F	1.42 (0.0123)	
Thermal conductivity		See figures 10	-6 and 10-9.	
Honeycomb panel conductance $\frac{W}{m^2K}\left(\frac{Btu}{ft^2hr^\circ F}\right)$		Effective	Pure conductance with radiation component accounted for by program	
Center core		34 (6.0) (Task II)	14.98 (2.64) — light and heavy gage	
Edge core		216 (38.0) (Task II)	29.96 (5.28) — light gage 59.92 (10.56) — heavy gage	

Lam	ina	L ayup direction	Layer direction
Lam	IIIa		
1			
2			
3	_ ⊙	0	1
4			
5	4 Laminae		
6			2
7	_ _	+45	2
8	3 Laminae		
9		45	3
10		-45	3
11	2.5 Laminae		4
12	_ + 0	90	
13	2.5 Laminae	90	
14	_	45	5
15		-45	9
16	3 Laminae		
17	_ \	. 45	6
18		+45	0
19	_		
20	4 Laminae		
21		0	7
22	<u> </u>	0	,
23			
24			

Material: High strength graphite/polyimide, 0.1 mm (0.004 in.) thick

Figure 10-1.—Layup Model Breakdown

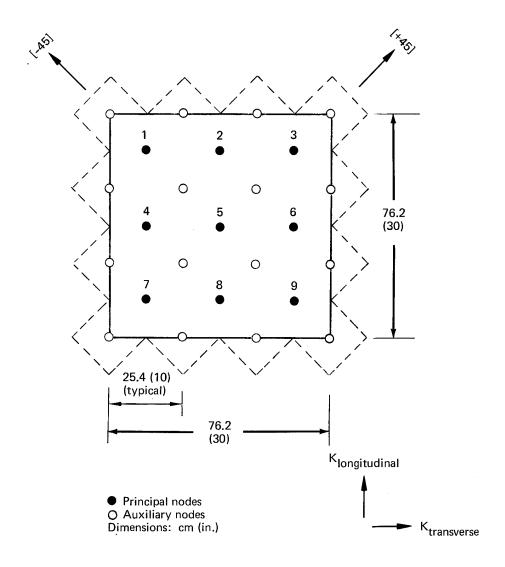


Figure 10-2.—Node Arrangement, Layup Direction [0]

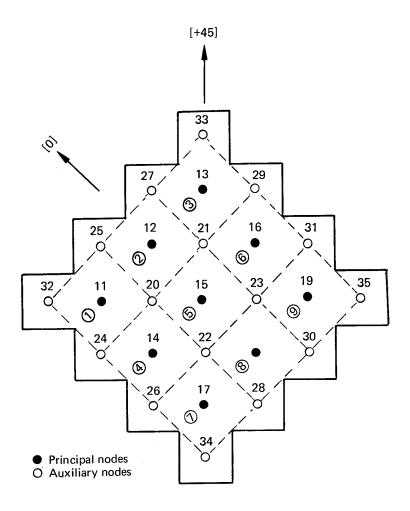


Figure 10-3.—Node Arrangement, Layup Direction [+45]

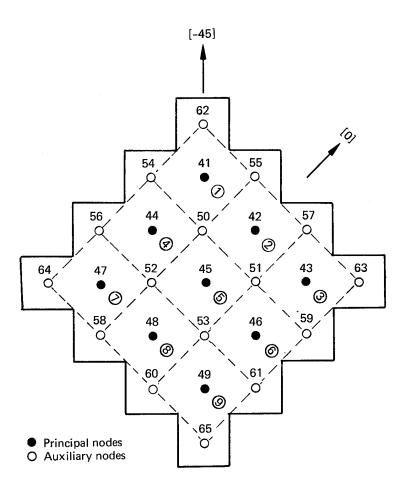


Figure 10-4.—Node Arrangement, Layup Direction [-45]

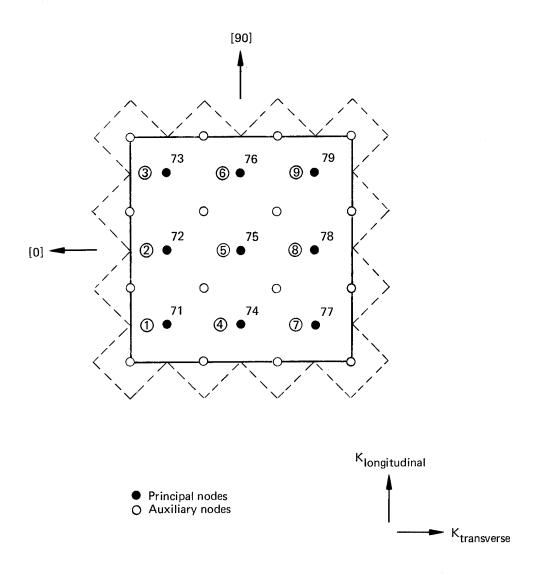


Figure 10-5.—Node Arrangement, Layup Direction [90]

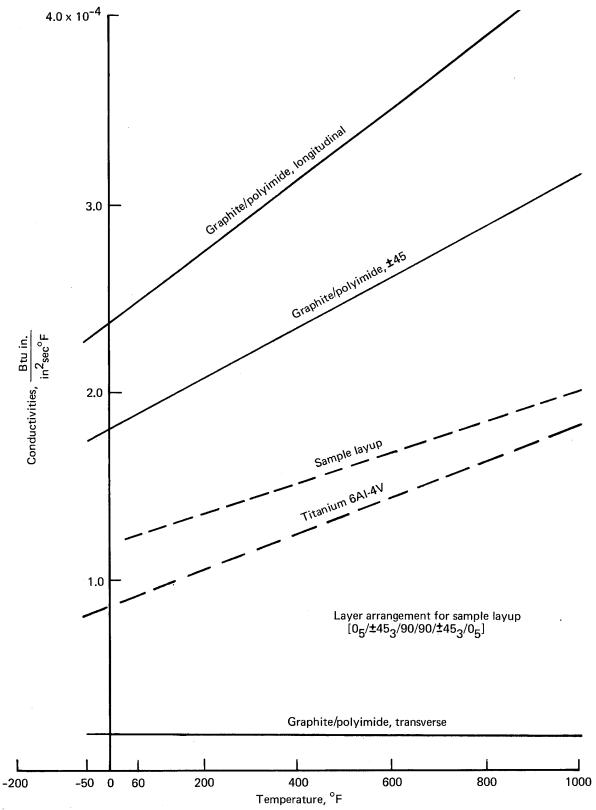


Figure 10-6.—Basic Material Conductivities and Sample Layup, Average Conductivity

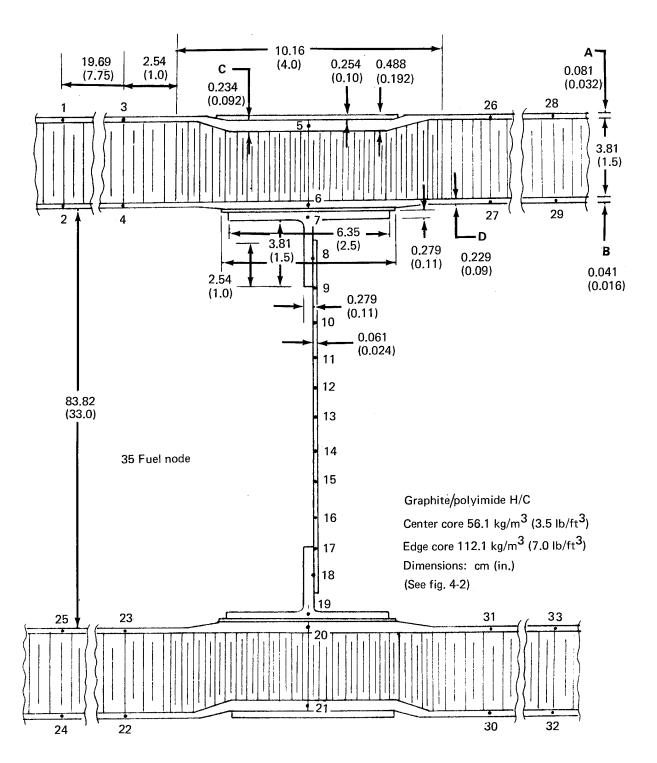


Figure 10-7.—Light Gage Structural Section

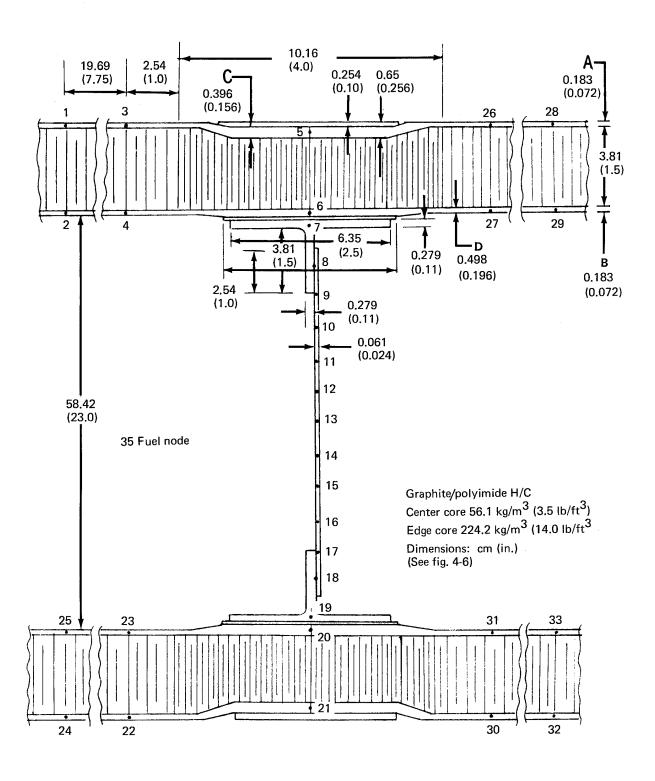


Figure 10-8.—Heavy Gage Structural Section

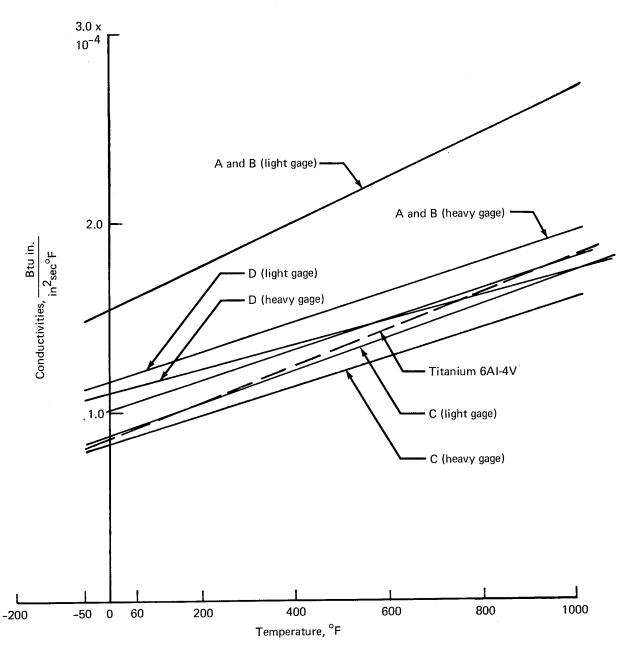


Figure 10-9.—Average Thermal Conductivities for Light and Heavy Gage Designs (Dimensions A, B, C, and D)

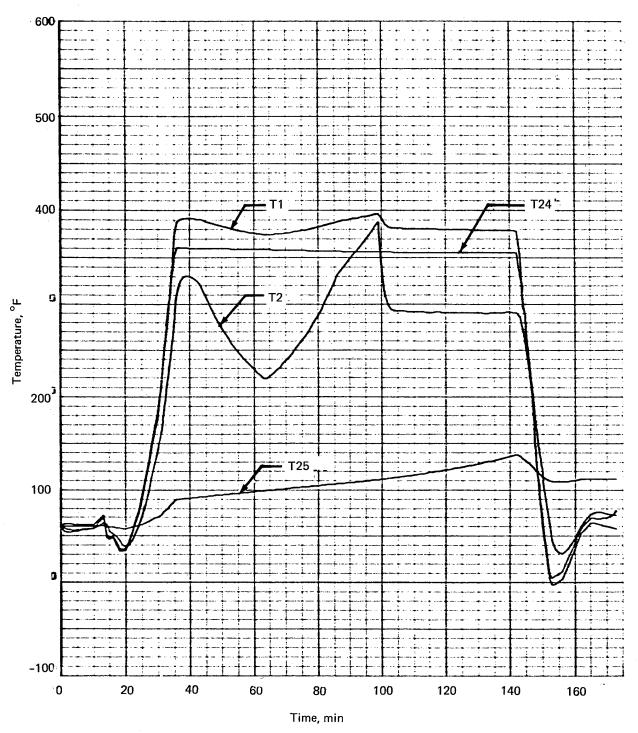


Figure 10-10.—Fuel Tank Temperatures, Light Gage, Wet Upper Panel: T1, T2, T24, T25

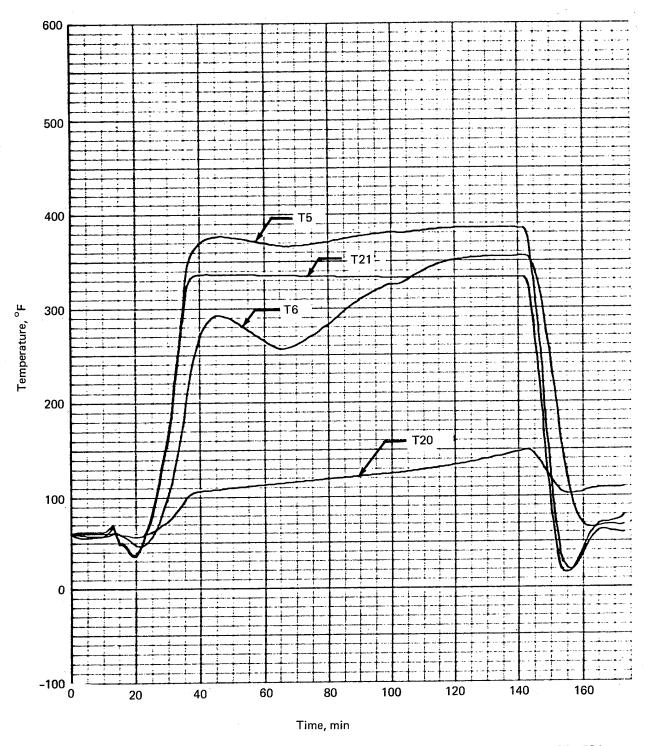


Figure 10-11.—Fuel Tank Temperatures, Light Gage, Wet Upper Panel: T5, T6, T20, T21

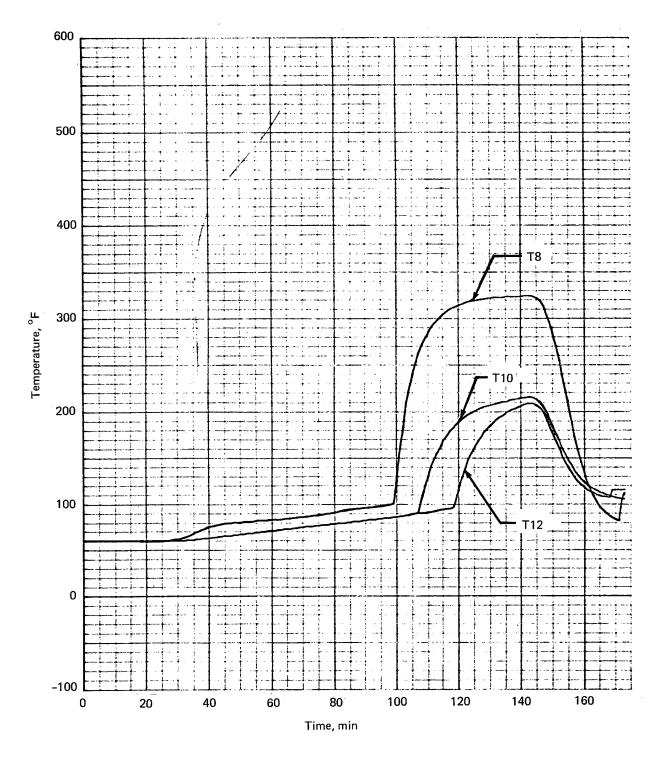


Figure 10-12.—Fuel Tank Temperatures, Light Gage, Wet Upper Panel: T8, T10, T12

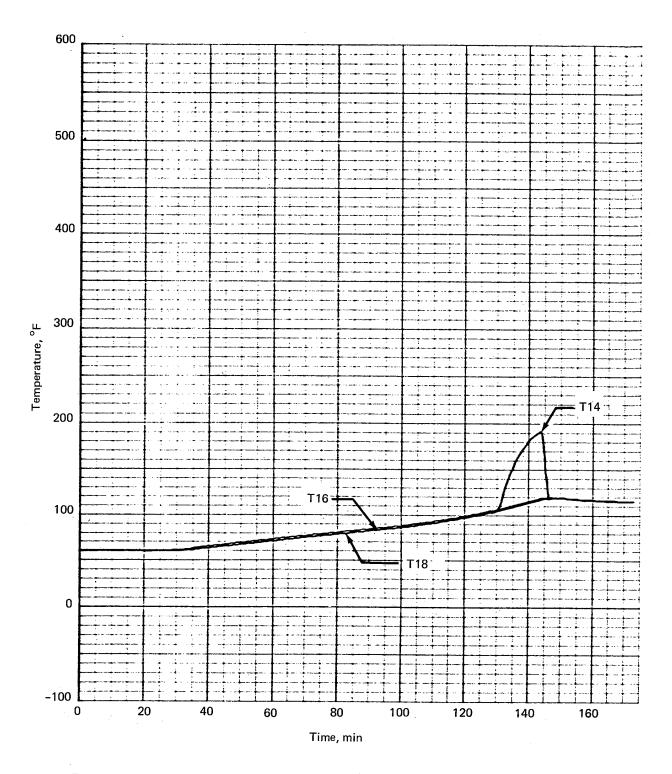


Figure 10-13.—Fuel Tank Temperatures, Light Gage, Wet Upper Panel: T14, T16, T18

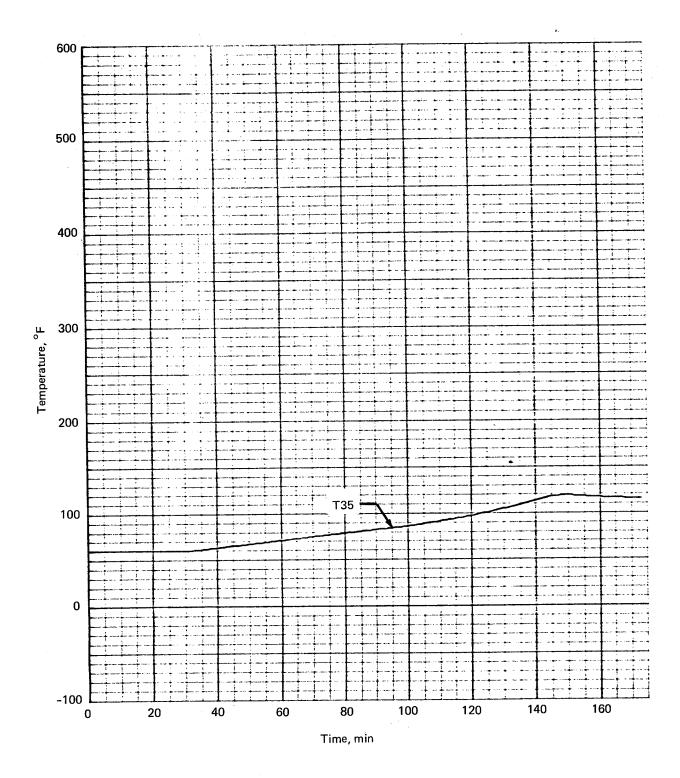


Figure 10-14.—Fuel Temperatures, Light Gage, Wet Upper Panel: T35

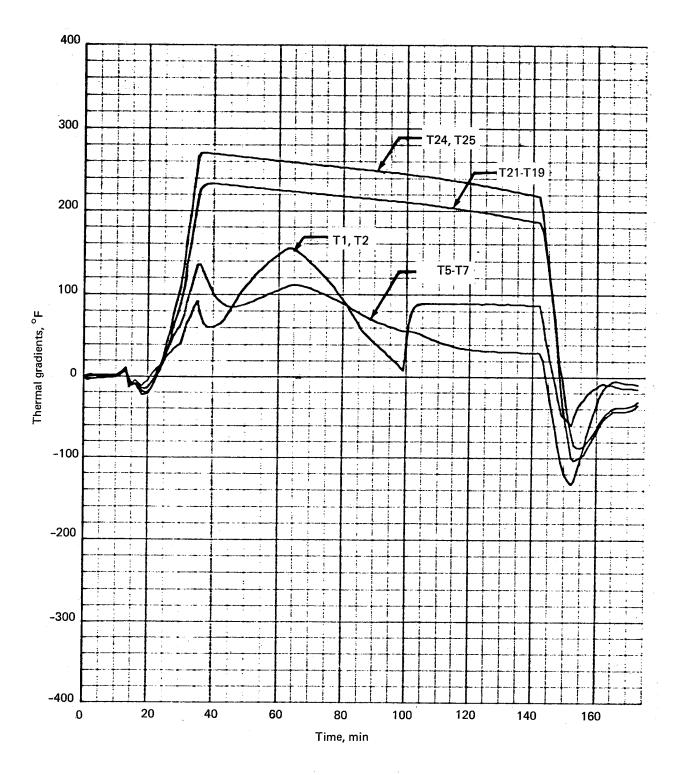


Figure 10-15.—Fuel Tank Thermal Gradients, Light Gage, Wet Upper Panel: T1, T2; T5-T7, T21-T19; T24, T25

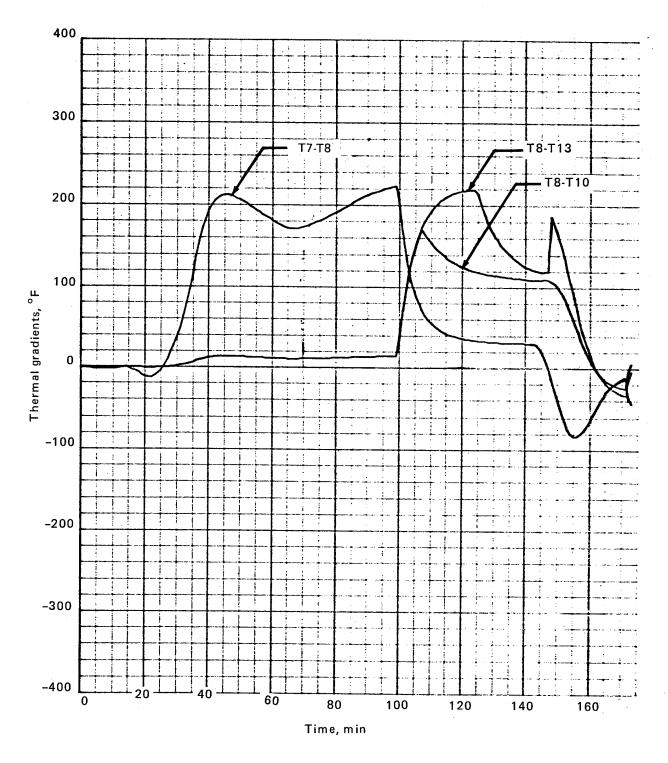


Figure 10-16.—Fuel Tank Thermal Gradients, Light Gage, Wet Upper Panel: T7-T8; T8-T10; T8-T13

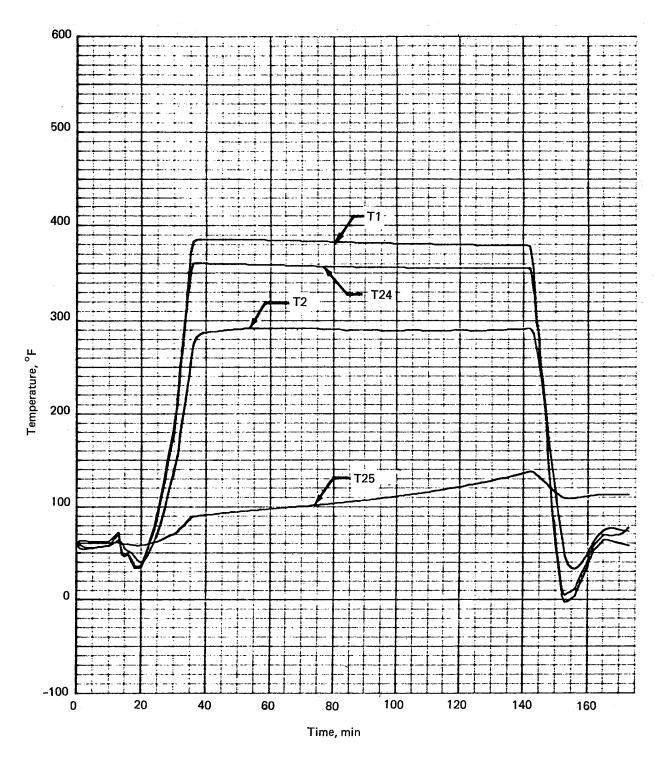


Figure 10-17.—Fuel Tank Temperatures, Light Gage, Dry Upper Panel: T1, T2, T24, T25

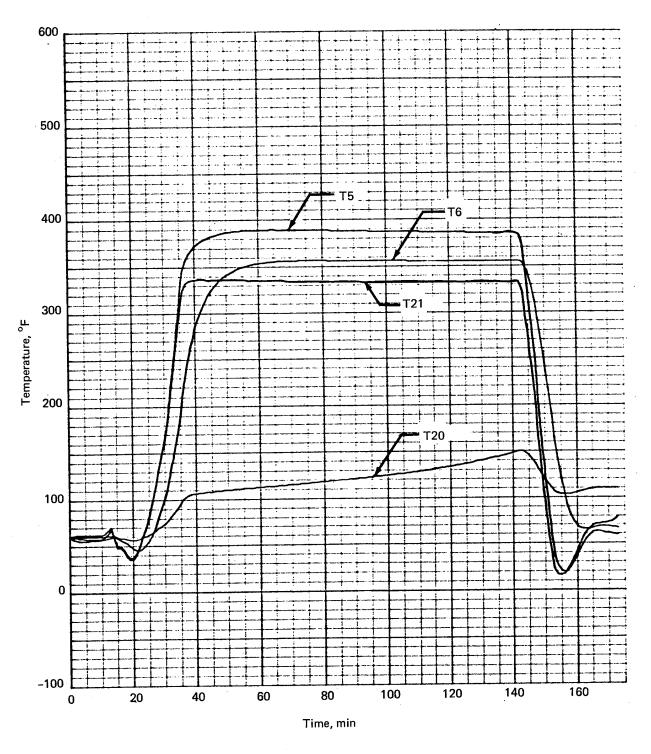


Figure 10-18.—Fuel Tank Temperatures, Light Gage, Dry Upper Panel: T5, T6, T20, T21

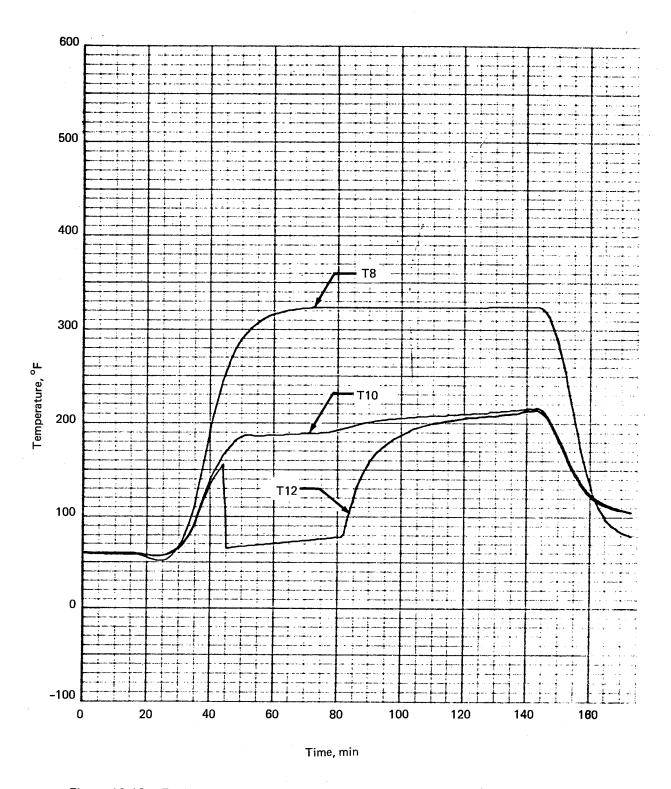


Figure 10-19.—Fuel Tank Temperatures, Light Gage, Dry Upper Panel: T8, T10, T12

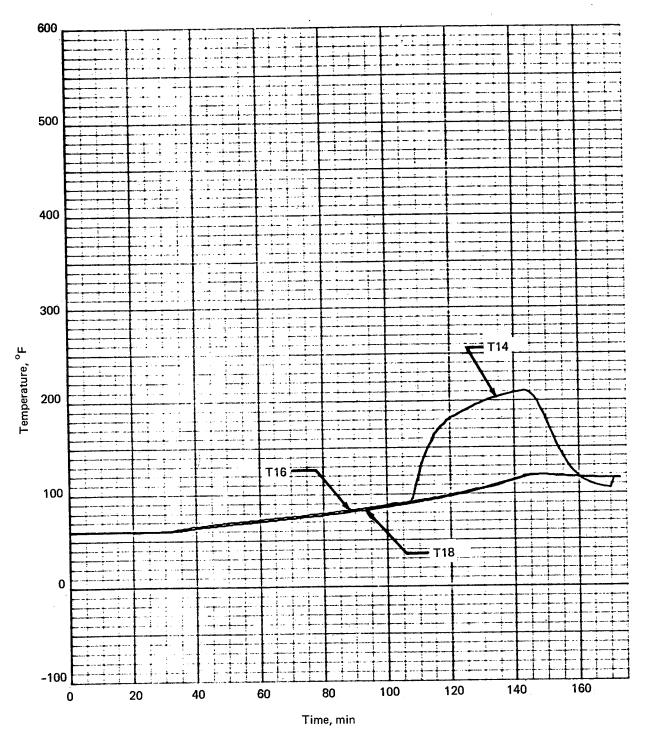


Figure 10-20.—Fuel Tank Temperatures, Light Gage, Dry Upper Panel: T14, T16, T18

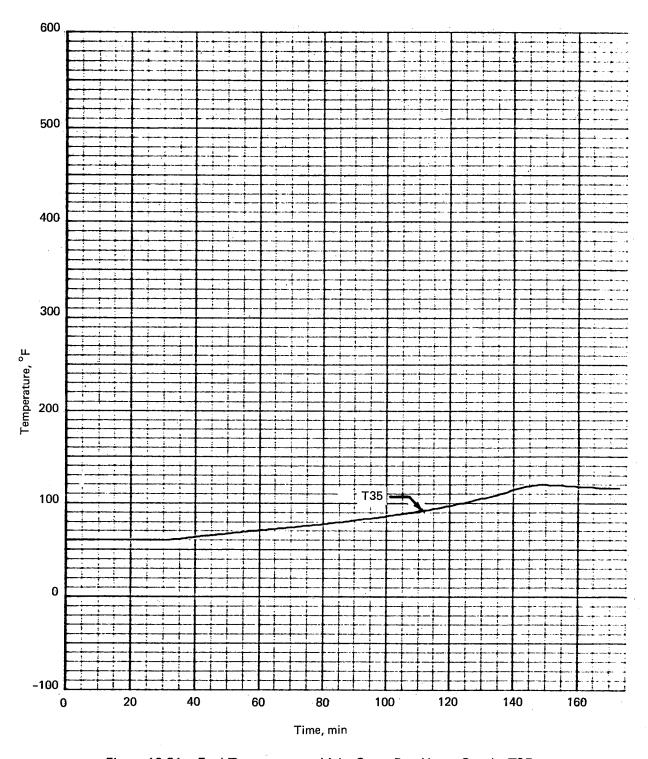


Figure 10-21.—Fuel Temperatures, Light Gage, Dry Upper Panel: T35

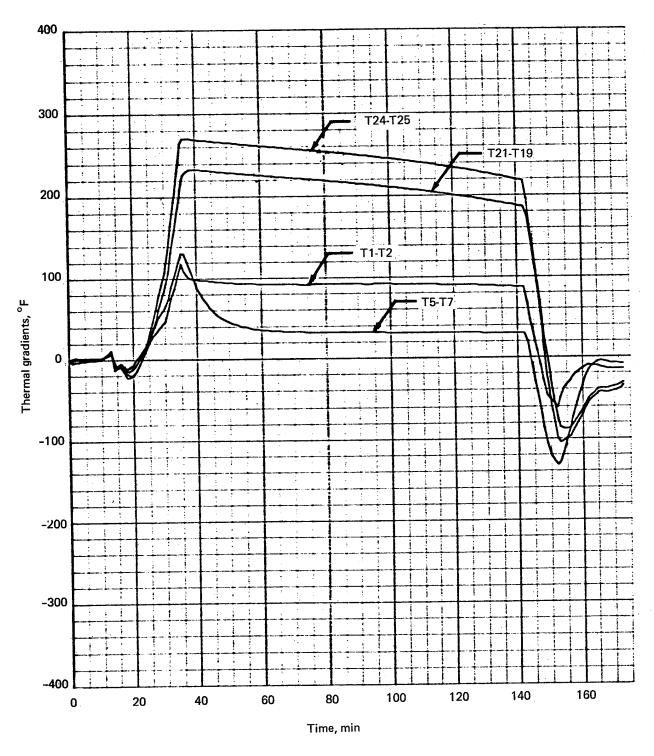


Figure 10-22.—Fuel Tank Thermal Gradients. Light Gage, Dry Upper Panel: T1-T2; T5-T7; T21-T19: T24-T25

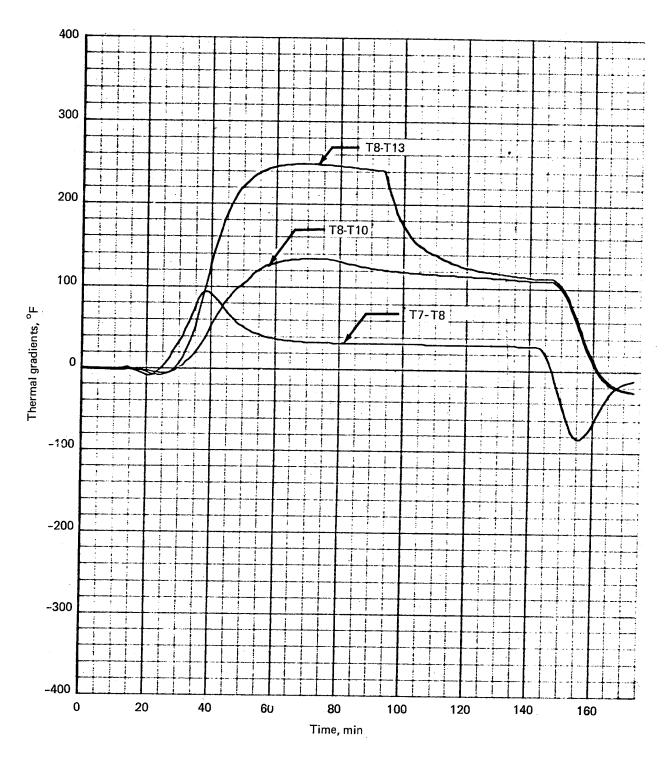


Figure 10-23.—Fuel Tank Thermal Gradients, Light Gage, Dry Upper Panel: T7, T8; T8-T10; T8-T13

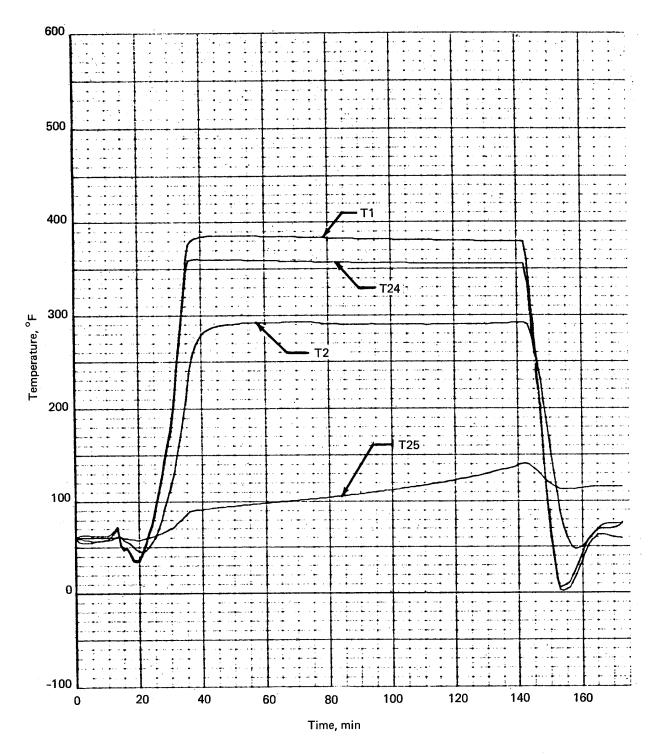


Figure 10-24.—Fuel Tank Temperatures, Heavy Gage, Dry Upper Panel: T1, T2, T24, T25

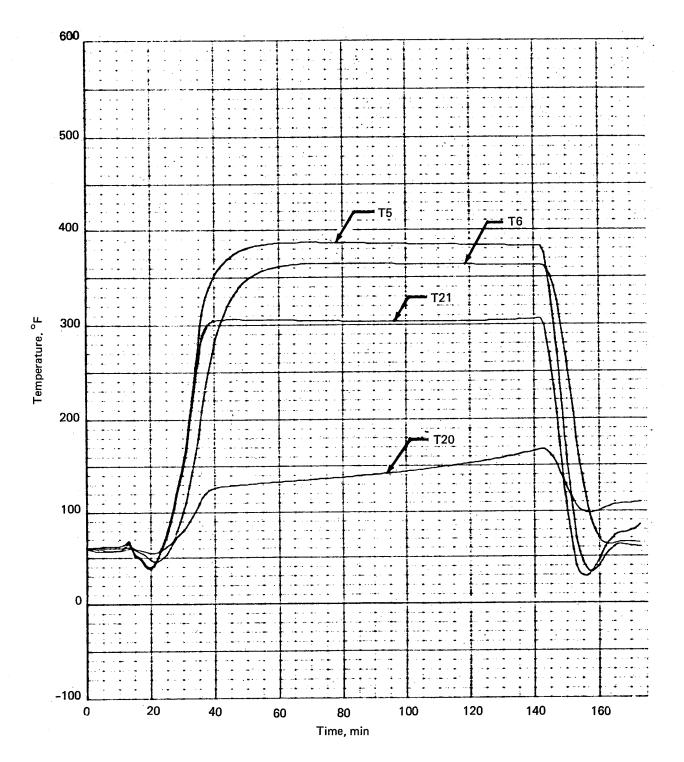


Figure 10-25.—Fuel Tank Temperatures, Heavy Gage, Dry Upper Panel: T5, T6, T20, T21

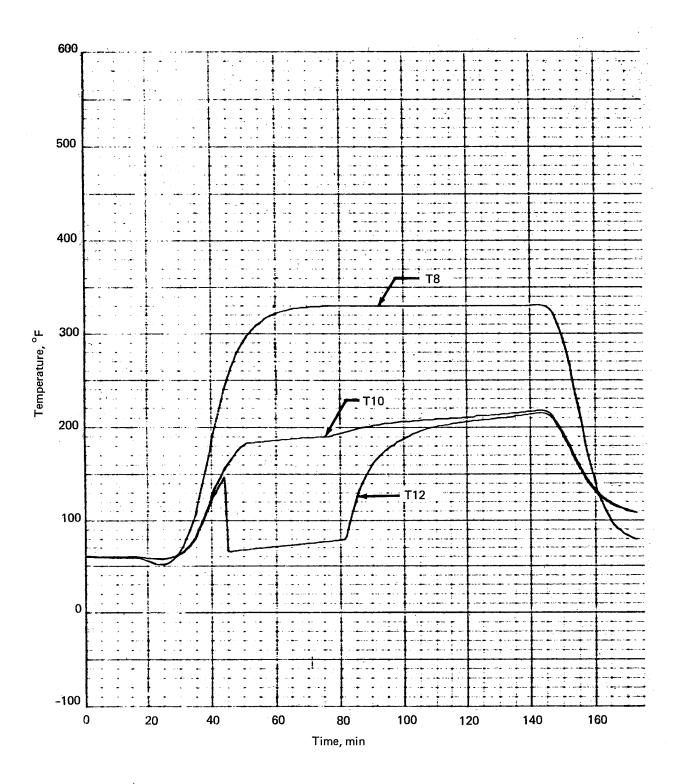


Figure 10-26.—Fuel Tank Temperatures, Heavy Gage, Dry Upper Panel: T14, T16, T18

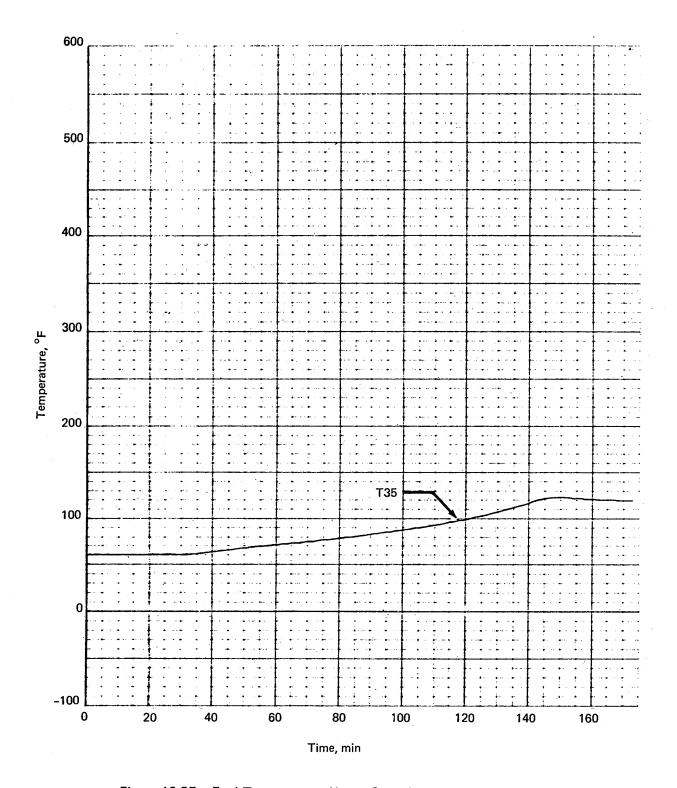


Figure 10-27.—Fuel Temperature, Heavy Gage, Dry Upper Panel: T35

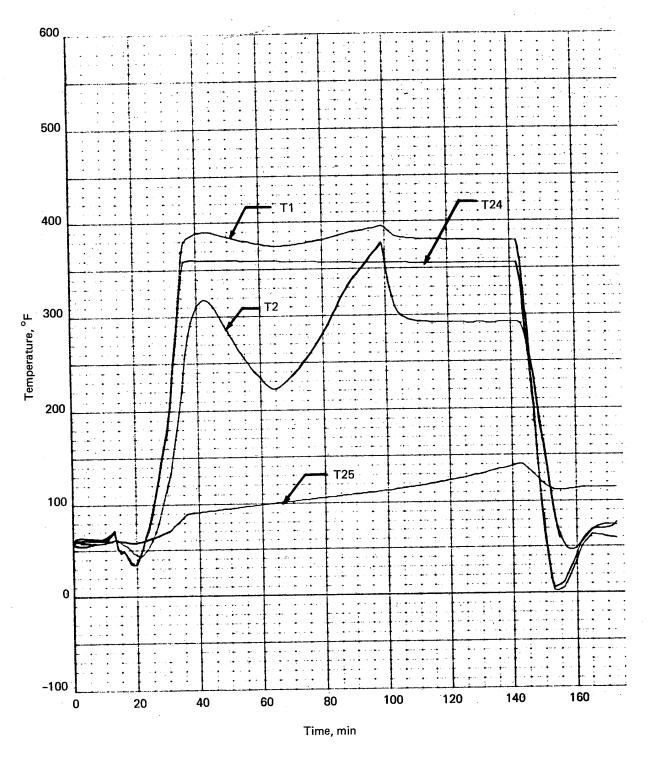


Figure 10-28.—Fuel Tank Temperatures, Heavy Gage, Wet Upper Panel: T1, T2, T24, T25



Figure 10-29.—Fuel Tank Temperatures, Heavy Gage, Wet Upper Panel: T5, T6, T20, T21

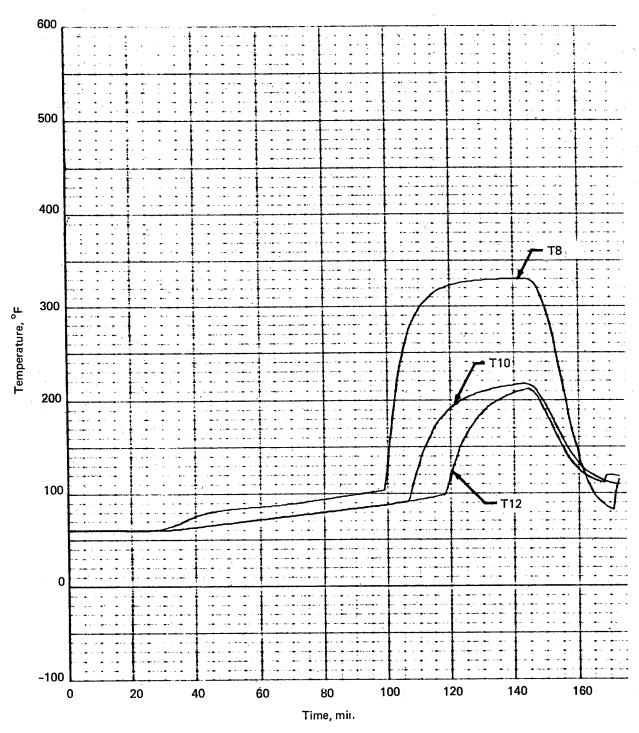


Figure 10-30.—Fuel Tank Temperatures, Heavy Gage, Wet Upper Panel: T8, T10, T12

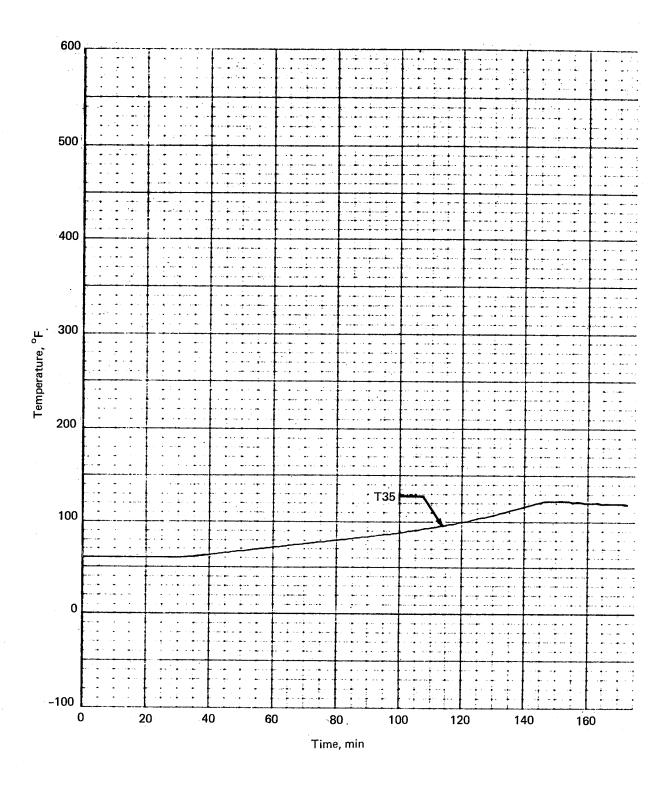


Figure 10-31.—Fuel Temperature, Heavy Gage, Wet Upper Panel: T35